



**Epidemiology and genetic analysis of praziquantel treatment response of
Schistosoma mansoni in preschool-aged children in Uganda**

SHANNAN STAR SUMMERS

**Thesis submitted in accordance with the requirements for the degree of
Doctor of Philosophy
of the
University of London**

April 2025

Department of Clinical Research

Faculty of Infectious and Tropical Diseases

LONDON SCHOOL OF HYGIENE & TROPICAL MEDICINE

Funded by MRC LID Doctoral Training Programme

Research group affiliation(s): Schistosomiasis Clinical Research Group
Webster Schistosomiasis Group
Helminth Genomics Group

Declaration

I, Shannan Star Summers, confirm that the work presented in this thesis is my own. Where information has been derived from other sources, I confirm that this has been indicated in the thesis. This thesis does not exceed the maximum permitted word length, it contains less than 100,000 words.

Supervisory team and advisory committee:

Supervisors: Amaya Bustinduy (London School of Hygiene and Tropical Medicine, UK), Bonnie Webster (Natural History Museum, UK) and Michael Miles (London School of Hygiene and Tropical Medicine, UK).

Advisory committee: Stephen Doyle (Wellcome Sanger Institute, UK), Fiona Allan (Natural History Museum, UK), Tapan Bhattacharyya (London School of Hygiene and Tropical Medicine), Russell Stothard (Liverpool School of Tropical Medicine, UK), Emily Webb (London School of Hygiene and Tropical Medicine) and Susana Campino (London School of Hygiene and Tropical Medicine).

Preface

Grants and additional funding secured during PhD studentship

1. **2023:** Royal Society of Tropical Medicine and Hygiene Early Career Grant (£4973) to fund my project entitled “Anthelmintic drug resistance monitoring in *Schistosoma japonicum*”.
2. **2023:** Hamish Ogston Foundation Platinum Jubilee Grant (£4985) to fund my project entitled “Population genomics of *Schistosoma mansoni* in response to drug treatment”.
3. **2023:** London Centre for Neglected Tropical Disease Research Travel Grant Scheme (£650).
4. **2023:** American Society of Tropical Medicine and Hygiene travel award (\$2150).
5. **2022:** Best poster award (£100) at Royal Society of Tropical Medicine and Hygiene Research in Progress Meeting.
6. **2022:** World Federation of Parasitologists Scholarship award for attendance at ICOPA 2022 (\$430)
7. **2022:** LSHTM Doctoral Project Travelling Scholarship (£3150) to fund post-treatment follow-up sample collection in Uganda.
8. **2022:** Awarded MRC funding to undertake training modules in population genetics (\$1200).

Publications during the PhD studentship

1. **Summers, S.**, Pennance, T., Archer, J., Stothard, R., Tian-Bi, Y.-N. T., Webster, J. P., Garba, A., Ame, S., Senghor, B., Rollinson, D., Emery, A., & Webster, B. (in review at PLOS NTDs). Phylogeography of *Schistosoma bovis*, *S. curassoni* and associated *S. haematobium* group hybrids across sub-Saharan Africa revealed by mitochondrial *cox1* analyses.
2. **Summers, S** “Schistosomiasis and praziquantel resistance” (2022). [BugBitten BMC blog available](#).
3. **Summers , S.**, Bhattacharyya, T., Allan, F., Stothard, J. R., Edielu, A., Webster, B. L., Miles, M. A., & Bustinduy, A. L. (2022). A review of the genetic determinants of praziquantel resistance in *Schistosoma mansoni*: is praziquantel and intestinal schistosomiasis a perfect match? *Frontiers in Tropical Diseases*, 3, Article 933097. <https://doi.org/10.3389/ftd.2022.933097>

Journal manuscripts reviewed during the PhD studentship

Reviewed published manuscripts for the following academic journals: Parasites & Vectors and Parasitology Research.

Presentations delivered during the PhD studentship

1. **2023:** ASTMH annual meeting, Chicago USA. Poster presentation.
2. **2023:** Parasitic Helminths: New Perspectives in Biology and Infection, Hydra, Greece. Oral and poster presentation.
3. **2023:** Natural History Museum Student Conference, London, UK. Oral presentation.
4. **2023:** LSHTM Research Degree Student Conference, London, UK. Poster presentation.
5. **2022:** British Society for Parasitology Spring Meeting, York, UK. Poster presentation.

Placement undertaken during the PhD studentship

I undertook a project entitled “Investigating the genetic relationships among hundreds of admixed *Haemonchus contortus* larvae from a controlled genetic cross population” at the Wellcome Sanger Institute. I gained analytical and bioinformatics skills, including proficiency in writing scripts using R and Bash. I developed proficiency working with the Sanger HPC for processing and analysing large genomic sequencing datasets.

Courses completed during the PhD studentship

1. FutureLearn training course for using Nextflow in genomic datasets.
2. Undertaken courses entitled “Fundamentals of Population Genetics, Applications of Population Genetics, Genetic Epidemiology and Statistical Genetics” at the University of Washington.
3. Undertaken additional Master’s modules during PhD study in genomics and epidemiology.
4. Attended several training courses in creating conceptual frameworks, writing and literature searching.

Outreach and public engagement during the PhD studentship

1. **2024:** Interviewed live at the Natural History Museum “Meet the Scientist”.
2. **2022-2024:** Hosted 1-4 work experience students per year in laboratories at the London School of Hygiene and Tropical Medicine.
3. **2022-2024:** Given several career journey talks to secondary school students.
4. **2022:** Selected to be a Social Media Ambassador at ICOPA 2022.
5. **2022:** Co-organised and delivered MRC Disease Outbreak Control workshops to schools.

Teaching, training and student supervision delivered throughout the PhD studentship

Teaching

Provided teaching for Masters modules at the London School of Hygiene and Tropical Medicine in pathogen genomics and on laboratory modules including those in molecular

biology, parasitology and entomology. I was a tutor and marked examinations for MSc Neglected Tropical Diseases module and for MSc infectious disease (distance learning).

Student supervision

- Co-supervised LSHTM MSc Medical Parasitology student, Abigail Hitchcock “The mapping of *Bulinus spp* snails for the understanding of the transmission of urinary schistosomiasis, female genital schistosomiasis and associated increased HIV risk in Zambia”. **2023**.
- Provided advisory support to Dominic Lee, Germain Lam and Ciara Cunningham undertaking MSc research projects in Uganda related to the Praziquantel In Preschoolers trial.

Acknowledgements

Firstly, I would like to thank my supervisors Amaya, Bonnie and Michael, for all the help and support they have provided over the course of the PhD. I would also like to thank Fiona for your support within the lab, field work and for the many cups of tea to talk over things. Thank you to Steve for your invaluable mentorship and feedback throughout my final year, you gave me the confidence to “do a little bit of pop gen” and made me feel part of your team at the Sanger Institute. I would also like to thank Duncan, our chat at ICOPA gave me the push and drive to apply for funding to incorporate genomic analyses into my PhD work.

This work would not have been possible without the study participants and amazing field team from the Praziquantel in Preschoolers clinical trial. I am extremely grateful.

I would like to thank the Helminth Genomics group at the Sanger Institute for providing really useful feedback during lab meetings and presentations and for all of your moral support. I would also like to thank the schistosomiasis group at the LSHTM and the Natural History Museum for your support regarding laboratory and field work.

I am very grateful to Marina for your friendship, humour and our many hiking adventures together, your encouragement has kept me motivated in my final year. I would like to also thank Sophia aka my work wife for your support, many pumpkin bars and “humour” over the years. A few more thank yous to the team at LSHTM: Niamh, Rich, Luke, Olimpia, Brownyn, Morgan and Lucy.

To my partner Tim, I would like to express my appreciation to you for supporting me through this academic journey from undergrad to this PhD. You’ve always taken an interest in the wormy work I do and it inspires me to continue what I do.

I would like to thank my Mum, Dad and my brother Paul for all of your endless love and unwavering support you’ve given me over the past 27 years. You are my biggest cheerleaders even if you don’t have a clue what I’m on about, I appreciate you always being there.

Finally, I would like to acknowledge the financial assistance throughout my PhD which has allowed me to undertake this research, attend conferences and training courses and placements. In particular, the MRC-LID for awarding me studentship funding. I would also

like to acknowledge the Hamish Ogston foundation and the LSHTM travel award for supporting additional collection of field samples and for undertaking whole genome sequencing of the samples collected.

I would like to thank everyone who has contributed to the completion of this thesis, I am extremely grateful and thankful. The support network has been an essential part of this journey and I thank you all for being part of it.

Table of Contents

Declaration	2
Supervisory team and advisory committee:	2
Preface	3
Grants and additional funding secured during PhD studentship.....	3
Publications during the PhD studentship.....	3
Journal manuscripts reviewed during the PhD studentship.....	3
Presentations delivered during the PhD studentship.....	4
Placement undertaken during the PhD studentship.....	4
Courses completed during the PhD studentship.....	4
Outreach and public engagement during the PhD studentship.....	4
Teaching, training and student supervision delivered throughout the PhD studentship.....	4
Teaching.....	4
Student supervision.....	5
Acknowledgements	6
Table of Contents	8
List of Figures	11
List of Tables	13
List of Appendices	14
Abbreviations	16
1. Introduction	19
1.1 Schistosomiasis background.....	19
1.2 Life cycle of schistosomiasis.....	19
1.3 The Schistosoma genus.....	20
1.4 Epidemiology.....	21
1.5 Pathology of schistosomiasis.....	23
1.5.1 Intestinal schistosomiasis.....	23
1.5.2 Hepatic schistosomiasis.....	23
1.5.3 Urogenital schistosomiasis.....	24
1.6 Control of schistosomiasis.....	24
1.6.1 Snail control.....	24
1.6.2 WASH and health education.....	25
1.6.3 Treatment / Chemotherapy.....	25
1.6.3.1 History of anti-schistosomal chemotherapy.....	25
1.6.3.2 Mass drug administration of praziquantel.....	26
1.6.3.2 The praziquantel treatment gap.....	28
Thesis structure	30
Aim and objectives	32
Aim:.....	32
Objectives:.....	32
3.1 Introduction	60
3.2 Methods	63

3.2.1 Ethics statement.....	63
3.2.2 Study design.....	63
3.2.3 Pharmacokinetic sampling and analysis.....	64
3.2.4 Parasitological detection and clearance.....	64
3.2.5 Data analysis.....	65
3.3 Results.....	67
3.3.1 Baseline characteristics of the sub-study cohort.....	67
3.3.2 Population parasitological clearance.....	69
3.2.3 Individual parasite clearance by Kato-Katz.....	70
3.2.3 Individual antigen clearance.....	71
3.2.4 Impact of demographic and pharmacokinetic factors on cure rate.....	74
3.4 Discussion.....	77
4.1 Introduction.....	82
4.2 Methods.....	85
4.2.1 Ethics statement.....	85
4.2.2 Sample collection.....	85
4.2.3 DNA extraction.....	86
4.2.4 Optimisation of sequencing library preparation.....	86
4.2.5 Library preparation.....	87
4.2.6 Sequence quality control and mapping.....	88
4.2.8 Sample geographical distribution.....	88
4.2.9 Sex determination.....	89
4.2.10 Variant calling and filtering.....	89
4.2.11 Sample relatedness.....	90
4.2.12 Population structuring.....	90
4.2.13 Within population diversity.....	90
4.2.14 Between population diversity.....	91
4.3 Results.....	92
4.3.1 Whole genome sequencing of miracidia.....	92
4.3.2 Broad-scale genetic diversity of Ugandan <i>Schistosoma mansoni</i>	94
4.3.3 Within-population genetic diversity.....	98
4.3.4 Between population genetic diversity.....	99
4.4 Discussion.....	104
5.1 Introduction.....	110
5.2 Methods.....	113
5.2.1 Ethics statement.....	113
5.2.2 Genomic methods.....	113
5.2.2.1 Whole genome sequence analyses of <i>Schistosoma mansoni</i> miracidia collected from study participants from Lake Albert, pre- and post-treatment.....	113
5.2.2.2 Preparation of whole genome sequencing data and variant calling.....	114
5.2.2.3 Population structuring.....	114
5.2.2.4 Sample relatedness.....	115
5.2.2.5 Genomic diversity.....	115
5.2.2.6 Between population differentiation and selection.....	115

5.2.2.7 Analysis of the SmTRPMPZQ genomic region.....	116
5.2.3 Amplicon sequencing of the transmembrane region of SmTRPMPZQ.....	116
5.2.3.1 Sample Information.....	116
5.2.3.2 Primer design.....	117
5.2.3.3 PCR reactions and generation of the barcoded TRP amplicons from each miracidia.....	118
5.2.3.4 Pooling of amplicons and multiplex amplicon sequencing.....	118
5.2.3.5 Bioinformatic analysis of amplicon data.....	119
5.3 Results.....	120
5.3.1 Population structure of <i>Schistosoma mansoni</i> populations in Lake Albert pre and post-treatment.....	120
5.3.2 The effect of praziquantel treatment on pre- and post-treatment populations.....	122
5.3.3 Genetic differentiation between pre-treatment and post-treatment stratified by treatment arms.....	125
5.3.4 Selection between pre-and post-treatment populations.....	127
5.3.5 Genetic diversity of SmTRPMPZQ.....	130
5.4 Discussion.....	133
6.1 Recapitulation and directions for future work.....	137
6.1.1 Future directions.....	139
6.2 Conclusion.....	142
References.....	206

List of Figures

Figure 1.1: Life cycle of schistosomiasis.

Figure 1.2 Summary of the phylogeny of the *Schistosoma* genus

Figure 3.1: Study design and data availability.

Figure 3.2: Study flow chart showing the data completeness at baseline, week four and month 12 follow-up.

Figure 3.3: *Schistosoma mansoni* clearance outcomes comparing baseline 40 mg/kg PZQ vs 80 mg/kg PZQ at four-week post treatment.

Figure 3.4: Distribution of log egg counts at three time points: baseline, week four and month 12 follow-up stratified by treatment regimen.

Figure 3.5: A & B) distribution of CAA antigen concentration measured in urine (pg/mL) at baseline and week 4 follow-up, stratified by treatment regimen.

Figure 3.6: Individual PZQ plasma levels from 14 children, stratified by baseline treatment received and PZQ enantiomer.

Figure 4.1: Map displaying the geographical location from which the samples originated.

Figure 4.2: Kinship network of 246 miracidial samples.

Figure 4.3: Population structure of the *Schistosoma mansoni* samples.

Figure 4.4: Autosomal nucleotide diversity (π) of Ugandan *Schistosoma mansoni* populations.

Figure 4.5: Genome-wide genetic differentiation (F_{st}) between different Ugandan districts.

Figure 4.6: Between-population diversity.

Figure 5.1: Map displaying the geographical distribution of villages bordering Lake Albert, Uganda, where *S. mansoni* miracidia were selected for whole genome sequencing (indicated with *) and amplicon sequencing.

Figure 5.2: Population structure of Lake Albert *Schistosoma mansoni* miracidia.

Figure 5.3: Nucleotide diversity comparisons for each time point (pre- and post-treatment) and between treatment regimens.

Figure 5.4: Genome-wide genetic differentiation (F_{st}) between standard and intensive treatment populations.

Figure 5.5: Genome-wide XP-EHH comparisons between pre and post-treatment groups, stratified by treatment regimen.

Figure 5.6: Distribution and frequency of genetic variation in SmTRPM_{pZQ}.

List of Tables

Table 1.1: The definitive host range, distribution and pathology of *Schistosoma* species infecting humans.

Table 1.2: History of drugs used to treat schistosomiasis, the mode of action, species active and disadvantages.

Table 3.1: Descriptive characteristics of study participants.

Table 3.2: Effect of infection intensity, sex, weight, age, treatment regimen, anaemia and village on cure by Kato-Katz. Testing for association was undertaken using the Wald test.

Table 4.1: The total number of variants, SNPs, indels and individuals detailed for each dataset before and after filtering.

Table 5.1: Number of *Schistosoma mansoni* miracidia with whole genome sequence data generated per village, sampling time point, and treatment arm (40mg/kg and 80 mg/kg PZQ).

Table 5.2: Number of *Schistosoma mansoni* miracidia that passed quality control and were used in the analysis.

Table 5.3: Sample information for miracidia that successfully amplified all four amplicon targets for amplicon sequencing.

Table 6.1: Summary of major findings in each chapter of the thesis.

List of Appendices

Appendix Table 3.1: Effect of 80 mg/kg versus 40 mg/kg praziquantel on cure rates based on three diagnostic tests: KK, CCA and CAA.

Appendix Table 3.2: Effects of 80 mg/kg versus 40 mg/kg PZQ on egg reduction rate (ERR).

Appendix Table 3.3: Comparison of mean pharmacokinetic parameters between two treatment regimens (40 mg/kg PZQ vs 80 mg/kg PZQ).

Appendix Table 4.1: Sample information, including the accession number, country, and district of the published whole genome sequencing data used.

Appendix Figure 4.1: Protocol for collection of miracidia on Whatman FTA cards.

Appendix Figure 4.2: A selection of images from fieldwork in Uganda in November 2021.

Appendix Figure 4.3: Distribution and density of nuclear variant quality metrics (QUAL, DP, MQ, SOR, FS, QD, MQRankSum, and ReadPosRankSum).

Appendix Figure 4.4: Distribution and density of mitochondrial variant quality metrics (QUAL, DP, MQ, SOR, FS, QD, MQRankSum, and ReadPosRankSum).

Appendix Figure 4.5: Bioanalyzer results generated from Novogene for the pooled library.

Appendix Table 4.2: Quality control measures for 96 miracidia whole genome sequenced.

Appendix Table 4.3: Miracidia sex determination for *S. mansoni* miracidia.

Appendix Table 4.4: Genome-wide mean π for each Ugandan district.

Appendix Figure 4.6: Population structure of *Schistosoma mansoni*.

Appendix Figure 4.7: Individual sampling missingness of *Schistosoma mansoni* samples.

Appendix Figure 4.8: Cross-validation error (CV) values generated using ADMIXTURE with K values ranging from 1-10.

Appendix Figure 4.9: Admixture plots depicting the ancestry proportions using ADMIXTURE. Theoretical K values (K=5-10) are displayed.

Appendix Figure 4.10: Material Transfer Agreement between LSHTM and the Medical Research Council/ Uganda Virus Research Institute and LSHTM Research Unit.

Appendix Figure 5.1: Primer design for amplifying the PZQ binding site in SmTRPM_{PZQ} (Smp_246790.1).

Appendix Table 5.1: Primers designed for amplification of the exons encoding the PZQ binding site in SmTRPM_{PZQ} (Smp_246790.1).

Appendix Table 5.2: Primer sequences plus barcodes for amplicon sequencing.

Appendix Figure 5.2: Overview of amplicon pooling process.

Appendix Figure 5.3: Population structure of Lake Albert miracidia.

Appendix Table 5.3: Genome-wide mean nucleotide diversity (π) for each treatment time point stratified by treatment group.

Appendix Table 5.4: Genome-wide mean genetic differentiation (F_{st}) comparisons between time point and treatment group.

Appendix Table 5.5: Genes encoding proteins present in the candidate regions of differentiation using genome-wide F_{st} .

Appendix Table 5.6: Genes encoding proteins present in the candidate regions of selection using genome-wide XP-EHH.

Appendix Table 5.7: The mean coverage and distribution of SNPs and (indels) detected in each amplicon.

Appendix Table 5.8: The position and frequency of intronic SNPs.

Appendix Table 5.9: The position and frequency of intronic indels. *associated with a homopolymer region.

Appendix Table 5.10: The position and frequency of non-synonymous and synonymous SNPs in the transmembrane region of SmTRPM_{PZQ} (Smp_246790.1).

Abbreviations

Absolute divergence	Dxy
Area under the curve	AUC
Basepair	bp
Circulating anodic antigen	CAA
Circulating cathodic antigen	CCA
Confidence interval	CI
Cross population extended haplotype heterozygosity	XP-EHH
Cross-validation error	CV
Cure rate	CR
Cytochrome oxidase subunit 1	cox1
Disability-adjusted life years	DALYs
Depth	DP
Egg reduction rate	ERR
Egg per gram	epg
Female genital schistosomiasis	FGS
FisherStrand	FS
Fixation index	Fst
Genome-wide association study	GWAS
G protein-coupled receptor	GPCR
Kato-Katz	KK
Kilobase	Kb
Linkage-disequilibrium	LD
MappingQualityRankSumTest	MQRanksum
Mass drug administration	MDA
Maximum likelihood	ML
Maximum plasma concentration	C _{max}

Minor allele frequency	MAF
Mitochondrial DNA	mtDNA
Neglected tropical disease	NTD
Nucleotide diversity	π
Odds ratio	OR
Pharmacogenetics	PG
Pharmacokinetics	PK
Pharmacokinetic/pharmacodynamic	PK/PD
Point of care	POC
Praziquantel	PZQ
Praziquantel in preschoolers clinical trial	PIP
Preschool-aged children	PSAC
Principal component analysis	PCA
Pseudoautosomal region	PAR
Quality	QUAL
QualByDepth	QD
Quantitative trait locus	QTL
Rapid diagnostic test	RDT
ReadPosRankSumTest	ReadsPosRankSum
RMSMappingQuality	MQ
<i>Schistosoma mansoni</i> Transient Receptor Melastatin Ion channel PZQ	SmTRPM _{PZQ}
Schistosomiasis control initiative	SCI
Schistosomiasis in Mothers and Infants	SIMI
School-aged children	SAC
Schistosome and snail resource	SSR
Single nucleotide polymorphism	SNP
Standard deviation	SD
StrandOddsRatio	SOR

Tartar Emetic	TE
Time to reach peak drug concentration	T_{max}
Up-converting phosphor labels lateral flow	UCP-LF
Water, sanitation and hygiene	WASH
Whole genome amplification	WGA
Whole genome sequencing	WGS
World Health Organisation	WHO
Z-specific region	ZSR

1. Introduction

1.1 Schistosomiasis background

Schistosomiasis is a neglected tropical disease (NTD) caused by parasitic digenetic trematodes belonging to the genus *Schistosoma*. Over 240 million people are infected, and an additional 700 million are at risk in endemic regions (1). The disease is present in 78 countries with major foci across Africa, Asia and South America (2) and more recently in southern Europe (3). The majority of the disease burden (> 90%) occurs in sub-Saharan Africa, where the disease is responsible for at least 1.4 million disability-adjusted life years (DALYs) and 24,000 deaths annually (2,4–7).

1.2 Life cycle of schistosomiasis

Schistosoma blood flukes have a complex life cycle which involves two hosts: an intermediate freshwater snail host and a definitive mammalian host (Figure 1.1). Within the intermediate snail host, the miracidium develops into a mother sporocyst, then through asexual reproduction, produces daughter sporocysts, which produce infective cercariae. Hundreds to thousands of cercariae are released from the snail host into the water. During water contact, cercariae, the infectious stage, penetrate the skin of the mammalian host. Cercariae shed their forked tails and transform into schistosomulae, which migrate within the circulatory system to the lungs, to the heart, and then the liver to develop where they exit via the portal vein system when mature. Male and female adult stages migrate and reside in copula in the mesenteric veins of either the intestine (intestinal schistosomiasis) or the vesical plexus (urogenital schistosomiasis) of the definitive host (Table 1.1). Adult schistosomes can live in copulation within their human hosts for up to 40 years (4,8). Eggs are released and traverse the intestinal or bladder wall to reach the lumen and then are excreted in either faeces or urine, respectively (3–5). When exposed to water, eggs hatch into miracidia, ciliated larval stages, which infect the intermediate snail host (9). However, a proportion of the eggs unable to exit the body become trapped in tissues, most commonly in the liver and urogenital system, triggering an inflammatory immune response which causes chronic schistosomiasis (10,11).

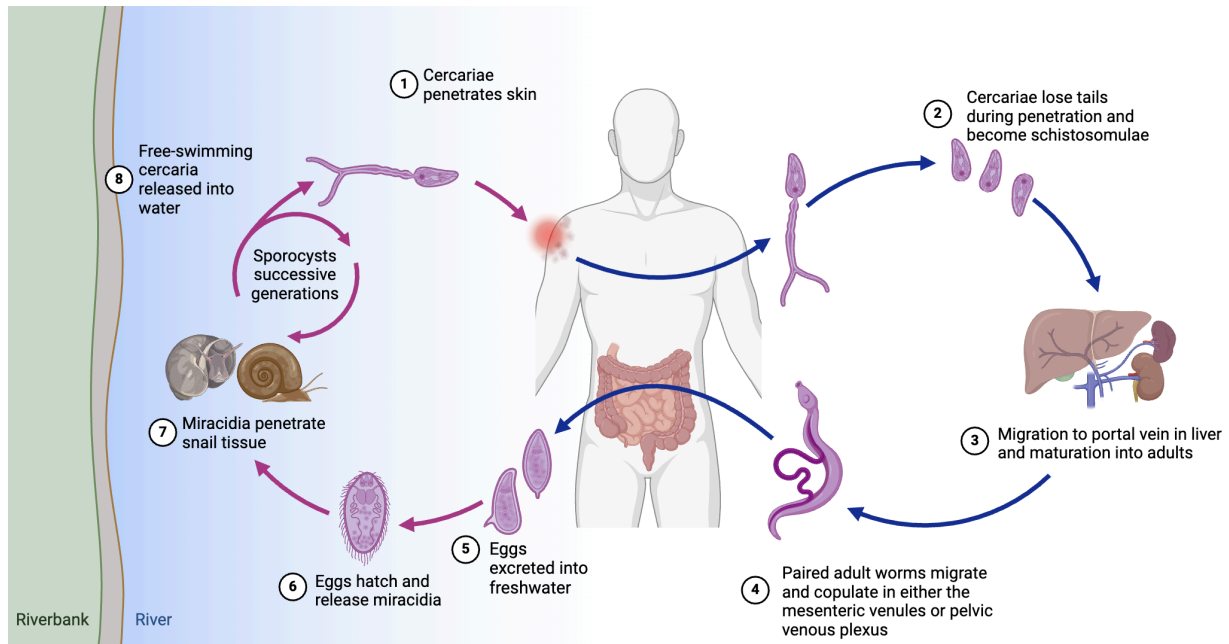


Figure 1.1: Life Cycle of schistosomiasis. Adapted from (12). Figure created using Biorender.com.

1.3 The *Schistosoma* genus

The *Schistosoma* genus comprises 23 species, six of which are responsible for human schistosomiasis (13) (Table 1.1). Among these, the most medically important species are *S. mansoni*, *S. haematobium* and *S. japonicum*, whilst *S. mekongi*, *S. intercalatum* and *S. guineensis* are comparatively less prevalent (14). Historically, schistosomes have been arranged into four groups: *S. japonicum*, *S. indicum*, *S. mansoni* and *S. haematobium*, based on egg morphology and the intermediate snail host they utilise for development (15). However, in recent years, the phylogeny of the *Schistosoma* genus has undergone much change due to the use of molecular techniques to compile robust phylogenies of schistosomes. Phylogenetic and phylogeographic studies have extensively used a range of genetic markers, the nuclear marker ribosomal RNA gene unit and several mitochondrial genes to construct *Schistosoma* phylogenies (15–22). A standard phylogeny using mitochondrial markers has recently been produced and widely referenced in the literature (18,19,22).

Despite the genus appearing monophyletic, the *Schistosoma* phylogeny is divided into six major clades, which correlate to their geographical distributions (Figure 1.2) (18). The *S. japonicum* complex appears basal on the phylogenetic tree (Figure 1.2), suggesting an oriental origin of the *Schistosoma* genus (13,17,23,24). Three clades contain species from Africa, where the hippo-infecting *S. hippopotami* clade is the most basal. The *S.*

haematobium clade and the *S. mansoni* clade represent the two major African schistosomes, separated by the *S. indicum* group, which are found in western and southern Asia, suggesting that these were derived from the re-invasion of Asia (16–19,23).

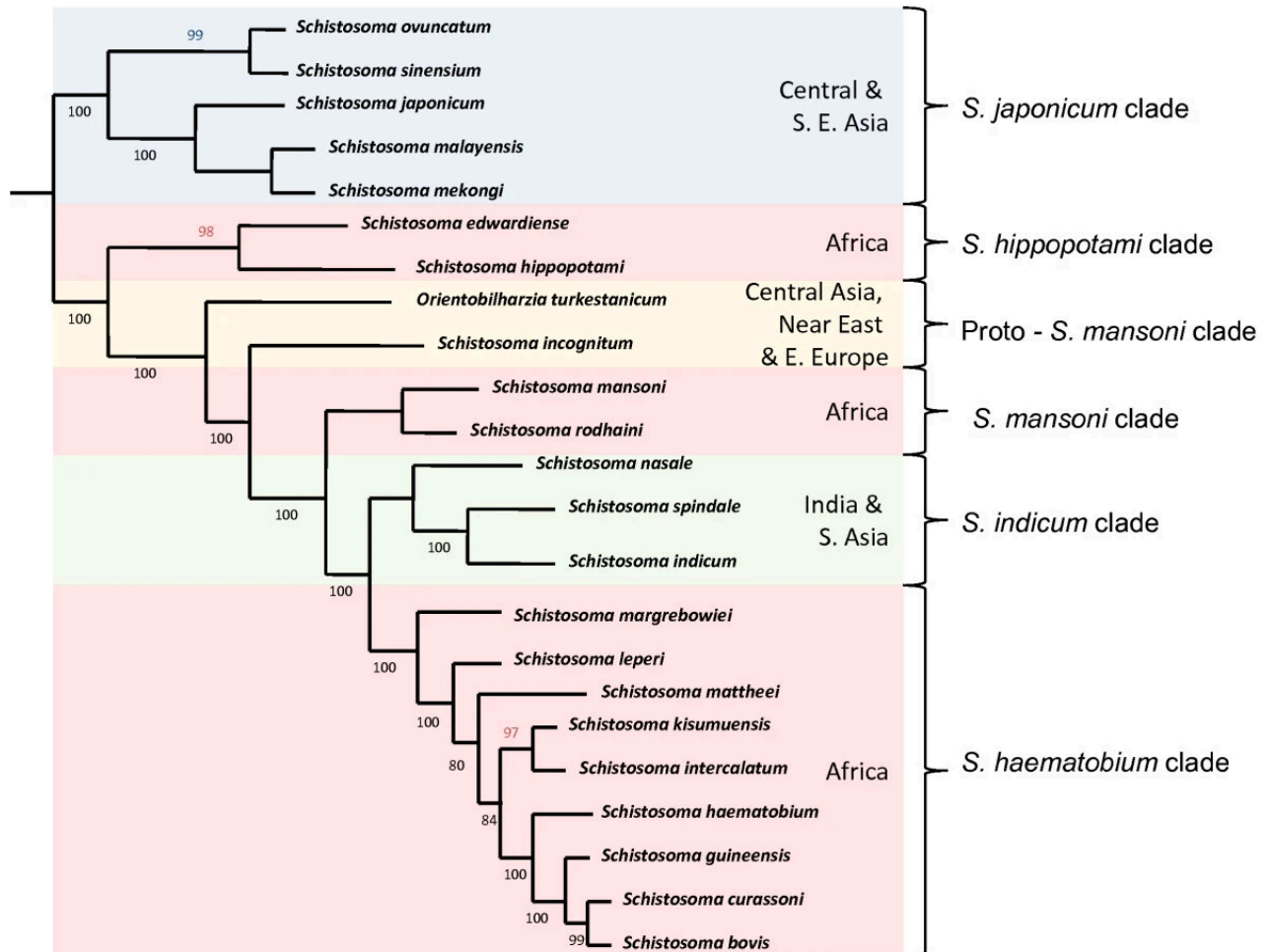


Figure 1.2: Summary of the phylogeny of the *Schistosoma* genus using partial *cox1* and *lsrDNA*, and complete *ssrDNA* sequences. Figure from Lawton *et al.* (15).

1.4 Epidemiology

Schistosomiasis has a focal epidemiology governed by human water-contact patterns and the intermediate snail hosts (25). Infection within endemic settings often occurs within two years of age, when the intensity of infection increases during the next ten years. The prevalence and infection intensities peak in young adolescents, which declines in adulthood. However, elevated prevalence persists within subgroups of adults who regularly interact with water as part of their daily routines (laundry, fishing and car washing) (4).

Table 1.1: The definitive host range, distribution and pathology of *Schistosoma* species infecting humans.

	Species	Definitive host range	Intermediate host range (genus)	Global distribution	Site in the definitive host	Pathology	Zoonotic?
Urogenital	<i>S. haematobium</i>	Humans	<i>Bulinus</i>	Africa, Southern Europe (Corsica) & Middle East	Venous plexus of the bladder	Haematuria, polyposis, bladder thickening, hydronephrosis, bladder fibrosis, female/ male genital schistosomiasis & bladder cancer	No
Intestinal	<i>S. mansoni</i>	Humans, rodents, baboons & primates	<i>Biomphalaria</i>	Africa, South America, Middle East & Caribbean	Inferior mesenteric veins draining the large intestine	Periportal fibrosis, hepatosplenomegaly, intestinal inflammation, blood in stool, diarrhoea & central nervous system complications.	*
	<i>S. japonicum</i>	Humans, livestock & domesticated animals such as horses and dogs	<i>Oncomelania</i>	China & Southeast Asia	Superior mesenteric veins draining the small intestine		Yes
	<i>S. mekongi</i>	Humans, dogs, pigs & livestock	<i>Tricula</i>	Cambodia & Laos	Venules of the small intestine		Yes
	<i>S. intercalatum</i>	Humans	<i>Bulinus</i>	Central Africa	Venules of the colon		No
	<i>S. guineensis</i>	Humans	<i>Bulinus</i>	Central Africa	Rectal veins		No

(*) indicates zoonotic reservoirs exist, but the *Schistosoma* sp is not considered zoonotic (9,26,27).

1.5 Pathology of schistosomiasis

The pathologies associated with schistosomiasis are not caused directly by the adult worms but instead by the copious number of eggs which become permanently trapped within the host liver or intestines (*S. mansoni*, *S. mekongi* and *S. japonicum*) or the urogenital system and bladder (*S. haematobium*). Trapped eggs induce a host granulomatous immune response characterised by eosinophils, lymphocytes, and alternatively activated macrophages (4,28,29). Consequently, the sequelae of chronic infections are primarily associated with the species-specific oviposition site of the adult worms (Table 1.1) (6).

There are three disease phases of schistosomiasis, beginning with a localised dermatitis reaction following cercarial skin penetration. Four to six weeks post-infection, it can then progress to acute schistosomiasis (Katayama fever), an immune complex reaction leading to systemic effects such as weight loss, vomiting, fever, urticarial rash and diarrhoea (10,30,31). Acute schistosomiasis is rarely reported in individuals residing in endemic regions for *S. haematobium* or *S. mansoni*. Still, it most commonly occurs in travellers exposed to schistosome antigens for the first time (4,32).

1.5.1 Intestinal schistosomiasis

Over time, most individuals experience a reduction in the granulomatous response to eggs through various mechanisms, resulting in the progression to chronic intestinal schistosomiasis for *S. mansoni* (4). *Schistosoma mansoni* eggs migrating through the intestinal wall instigate bleeding, pseudopolyposis, ulcerations and mucosal granulomatous inflammation (33,34). Lesions are typically located in the rectum and large bowel. Clinical manifestations present as rectal bleeding, intermittent abdominal pain and diarrhoea, with the severity of symptoms related to the intensity of infection (35).

1.5.2 Hepatic schistosomiasis

Inflammatory hepatic schistosomiasis is an initial response to *S. mansoni* eggs trapped in the liver's presinusoidal periportal spaces. This condition predominantly contributes to schistosomal hepatomegaly in children and adolescents (10,36,37).

Chronic hepatic schistosomiasis typically emerges several years after the infection has progressed, affecting adults with prolonged and intense infections, possibly influenced by an immunogenetic predisposition (38,39). Some individuals with hepatic schistosomiasis have

poor immunoregulatory responses to parasite egg antigens and develop considerable fibrosis, leading to periportal fibrosis with hepatosplenic disease (4,34). This fibrosis results in the gradual narrowing of portal veins, leading to portal hypertension, splenomegaly and gastrointestinal varices. The most serious complication of fibrotic hepatic schistosomiasis is bleeding from the gastro-oesophageal varices caused by increased portal hypertension, which can rupture and is usually fatal (10).

1.5.3 Urogenital schistosomiasis

Urogenital schistosomiasis is caused mainly by *S. haematobium* and can affect both urinary and genital systems, each with its cadre of symptoms. The eggs of *S. haematobium* incite granulomatous inflammation, leading to ulceration of the ureteral walls and bladder. Early signs of urinary schistosomiasis include dysuria, especially haematuria, characteristic of an infection with *S. haematobium* (40,41). Similar to chronic intestinal schistosomiasis, chronic urogenital schistosomiasis results from poor regulation of immunoregulatory responses to *Schistosoma* eggs which results in chronic fibrosis of the urogenital tract (42,43). This fibrosis can manifest as obstructive uropathy when compounded by bacterial superinfection and renal dysfunction and can lead to fatal outcomes. Additionally, infection with *S. haematobium* is strongly linked to squamous-cell carcinoma of the bladder, which often presents as multifocal tumours (42).

Furthermore, female genital schistosomiasis (FGS) is a chronic gynaecological condition caused by *S. haematobium* and is estimated to affect 30-56 million girls and women mostly within sub-Saharan Africa (44). The clinical pathologies associated with FGS include abdominal pain, vaginal itching, discharge and post-coital bleeding (45). Evidence has emerged which suggests that women with FGS have an increased risk of HIV and HPV that can result in cervical cancer (44,46,47).

1.6 Control of schistosomiasis

1.6.1 Snail control

The control of schistosomiasis requires disrupting a complex life cycle involving multiple life stages and hosts. The intermediate snail hosts are important for determining the distribution of schistosomiasis and are responsible for the focal epidemiology of the disease. In Africa, two genera of freshwater snails (*Biomphalaria* and *Bulinus*) are responsible for transmission and have been an important focus of schistosomiasis control efforts involving the use of

molluscicides and environmental modification (intended to destroy snail habitats) (32,48,49). Molluscicides were used extensively in Asia, Africa and South America from the 1950s to 1970s until chemotherapy for humans contributed to the decline (48,50,51). Niclosamide was most commonly used as it is efficacious against all snail life cycle stages and is effective in elimination programs in Africa, such as Morocco (48,52). However, molluscicides are labour intensive, non-specific, and can have detrimental environmental consequences, such as being toxic to marine organisms other than snails, such as fish (53,54).

1.6.2 WASH and health education

Poverty, poor health education and lack of clean water, sanitation and hygiene (WASH) are important drivers in maintaining transmission of schistosomiasis in endemic areas. The risk of exposure to contaminated water sources and infection can be considerably reduced through improved access to WASH and education (55). Ensuring access to WASH is crucial for infection prevention, especially re-infection. Initiatives involving WASH aim to minimise environmental contamination and transmission of *Schistosoma* larval stages by safely disposing of human waste and promoting hygiene. For example, a 77% median reduction in the prevalence of schistosomiasis was found in a meta analysis of 12 studies examining the implementation of WASH facilities with rates of schistosomiasis (56).

In endemic areas, poor knowledge of the disease can present a barrier to control programs; for example, a study in Malawi found that children refused praziquantel (PZQ) treatment due to its appearance and smell and reports from class members who felt dizzy after taking the drug (57). This distrust was also felt at the community level, leading to children missing school during treatment days as schistosomiasis was considered normal, therefore failing to understand the need for treatment. However, following community education and involvement in the treatment program, compliance improved which highlights the pivotal role health education can play in positively influencing behaviour (58).

1.6.3 Treatment / Chemotherapy

1.6.3.1 History of anti-schistosomal chemotherapy

Table 1.2 details the history of drugs used to treat schistosomiasis (59,60). The first group of compounds used for schistosomiasis chemotherapy were antimonial compounds, including tartar emetic (TE), which was introduced in 1918 and used for around 50 years. The anti-schistosomal properties of TE were discovered through the observation that Berber tribesmen who were treated for leishmaniasis also experienced an interruption in haematuria

caused by *S. haematobium* infection (61). However, TE required treatment with multiple doses administered over the course of a month via intravenous administration. Although the drug appeared promising, the efficacy was very limited and those treated reported severe side effects (62).

Antimonial compounds were the only available treatment for schistosomiasis until after World War II when lucanthone was introduced into clinical practice (59). Lucanthone was a promising alternative to antimonials as it could be administered orally and side effects were typically limited to nausea and vomiting. Furthermore, significant progress began in the 1960s with the introduction of drugs such as hycanthone, niridazole, oxamniquine, and metrifonate. The discovery that hycanthone, a metabolite of lucanthone, is significantly more biologically active and effective *in vitro* led to lucanthone being replaced in clinical practice (63,64). Even though hycanthone could be administered orally, it gave frequent side effects, therefore intramuscular administration of a single dose became the standard treatment for schistosomiasis (65). Another drug used during this time was oxamniquine which was the front-line treatment for *S. mansoni* infection in South America where only *S. mansoni* is present (66). In contrast, oxamniquine was used minimally in Africa where *S. mansoni* and *S. haematobium* are present (67). Both oxamniquine and hycanthone share the same mode of action which requires pro-drug activation via a sulfotransferase (Table 1.2). Studies have demonstrated cross-resistance between hycanthone and oxamniquine (68–70). The use of oxamniquine was discontinued due to several factors, including widespread drug resistance and the availability of PZQ, whose patent had expired, making it considerably cheaper (59).

Merck initially explored the pyrazino-isoquinoline ring system as potential animal tranquillisers. In the early 1970s, Bayer discovered that these compounds had anthelmintic properties and the compounds were further investigated (71). Amongst these compounds was PZQ which was first marketed as a veterinary cestocide (72). Praziquantel's antischistosomal properties were initially evaluated in animal studies, followed by toxicological and pharmacological assessment in animals and humans (73). The WHO and Bayer then collaborated to conduct large-scale clinical trials in Africa, Japan, the Philippines, and Brazil (74). With positive outcomes and toxicology studies showing no major short- or long-term side effects (75), PZQ quickly became the mainstay of schistosomiasis treatment and remains so.

1.6.3.2 Mass drug administration of praziquantel

In the absence of an effective anti-schistosome vaccine, the cornerstone of schistosomiasis control programmes is regular treatment with PZQ. Since 1984, PZQ has become the drug

of choice to treat schistosomiasis and displaced all past drugs which are no longer used due to cost, side effects and drug resistance (76,77). Dose finding studies in the 1970s and 1980s indicated that a single 40 mg/kg dose of PZQ was safe and sufficiently effective for treating *S. mansoni* and *S. haematobium* (74,78,79). However, repeated dosing is likely required for optimal effect in highly endemic areas (80).

The WHO currently recommends annual preventive chemotherapy, with a single dose of PZQ, which is efficacious against all *Schistosoma* species with minimal adverse effects (81). Praziquantel is currently delivered through annual mass drug administration (MDA) programmes, usually targeting school-aged children (SAC), a high-risk group which are shown to have the highest infection intensity, prevalence and morbidity risk (57). Schools are often used as delivery points for the administration of praziquantel as they provide a convenient and efficient way to reach a large number of children.

Prior to the early 2000s, the use of PZQ for preventive chemotherapy was limited in sub-Saharan Africa which changed in 2005 when Merck committed to donating 250 million doses of praziquantel annually (82). In 2002, the Schistosomiasis Control Initiative (SCI) was established to facilitate the implementation of MDA control programmes in several African countries (Mali, Burkina Faso, Niger, Zambia, Tanzania, Rwanda, Burundi and Uganda) (83) where Uganda was the first country to begin MDA in 2003. The primary objective of the MDA programmes was to achieve a reduction in schistosome-related morbidity from PZQ chemotherapeutic intervention (84). By 2013, SCI had assisted in the delivery of over 100 million PZQ treatments, resulting in a significant reduction in prevalence and morbidity in endemic regions (83–86). Scaling up of the distribution of PZQ has been successful, where the number of people treated increased dramatically from 7 million in 2006 to 57 million in 2015 (87). A study compared 2000-2010 geolocated schistosomiasis survey data (before most sub-Saharan African countries had scaled up schistosomiasis control programmes) with 2011-2014 and 2015-2019 data. A considerable reduction in schistosomiasis was found where the prevalence amongst school-aged children reduced from 23% in 2000-2010 to 9.6% in 2015-2019 (82). Due to the early successes from MDA programmes, the WHO has shifted its focus from morbidity control to the elimination of schistosomiasis as a public health problem by 2023 (49). As part of this control strategy, the new WHO treatment guidelines for schistosomiasis recommend extending treatment access to include at-risk populations above the age of two, including pregnant and lactating women. In Chapter 2, I provide a detailed overview of the new WHO treatment guidelines for schistosomiasis.

Chemotherapy alone appears to be insufficient to interrupt transmission and achieve elimination of schistosomiasis. Within this paradigm shift from control to elimination, an integrated control approach incorporating snail control, improved WASH, chemotherapy and public health education is recommended, using several integrated measures to interrupt several parts of the parasite's life cycle (88).

1.6.3.2 The praziquantel treatment gap

Schistosomiasis affects around 123 million children (89,90) which represents a significant proportion of the disease burden. Whilst SAC have long been the focus of MDA programmes due to their high infection risk, preschool-aged children (PSAC), those aged five years or younger, were largely overlooked in these efforts. This neglect was partly based on the incorrect assumption that younger children had minimal exposure to schistosomal cercariae-infested water and, thus, were considered low risk for infection (91). However, growing evidence suggests that PSAC are at significant risk, particularly in high-transmission areas. Recent estimates indicate that as many as 50 million PSAC in Africa alone may be infected with schistosomiasis (92).

Paediatric schistosomiasis is of particular concern for at least two reasons. Firstly, regular water contact reported in PSAC will likely result in a progressive increase in individual worm burden. These untreated infections acquired during early life likely contribute to the worsening of the morbidity of the disease within the individual (93). Secondly, this age group plays a role in maintaining local disease transmission with regular water contact leading to contamination of water bodies. In addition, washing children's soiled clothes in water bodies contributes to hidden environmental contamination and transmission (94).

Factors contributing to the treatment gap in PSAC include: PZQ is only approved for use in children aged four years and above (95) and the lack of a paediatric formulation which has been developed but has yet to be widely available (96). Despite this, PZQ has been used in off-label settings, for example, in the Schistosomiasis in Mothers and Infants (SIMI) project conducted in villages on the lakeshore of Albert and Victoria in Uganda (97). The aim of the study was to assess the need for and performance of PZQ in under seven year olds in *S. mansoni* endemic areas. The study found few reported side effects which were resolved by the 21 day follow-up. However, this study found that the dose of 40 mg/kg PZQ gave suboptimal cure rates for *S. mansoni* amongst the PSAC (97). A pharmacokinetic/ pharmacodynamic study conducted within the same area of Uganda found that the standard

40 mg/kg PZQ dose was insufficient for treating PSAC and that higher doses are needed (80).

Table 1.2: History of drugs used to treat schistosomiasis, the mode of action, species active and disadvantages.

Drug	Mode of action	Species active	Disadvantages
Antimonials	Inhibition of phosphofructokinase (PFK) is essential for converting fructose-6-phosphate to fructose-1,6-diphosphate in schistosomes. Parasite PFK is 80x more sensitive to the drug than mammalian PFK.	<i>S. mansoni</i> & <i>S. haematobium</i> & <i>S. japonicum</i>	Side effects such as thrombocytopenia intravenous administration. Mass treatment facilitated widespread Hepatitis C infection in Egypt (98).
Niridazole	Inhibition of schistosome cholinesterase activity resulting in flaccid muscle paralysis of adult worms. This may cause the detachment of worms and result in the hepatic shift of worms.	<i>S. mansoni</i> & <i>S. haematobium</i> & <i>S. japonicum</i>	Requires repeated dosing, side effects such as vomiting and seizures.
Hycanthone	Pro drug activated by <i>Schistosoma</i> sulfotransferase. Pro-drug metabolite binds to worm DNA and macromolecules, resulting in worm death.	<i>S. mansoni</i> & <i>S. haematobium</i> & <i>S. japonicum</i>	Mutagenic, toxicity, intramuscular administration, drug resistance.
Oxamniquine	Pro drug activated by <i>S. mansoni</i> sulfotransferase. Pro drug metabolite (OXA-SO ₃) binds to worm DNA and macromolecules, resulting in worm death.	<i>S. mansoni</i>	Widespread drug resistance, cost, active only against one <i>Schistosoma</i> species.
Metrifonate	Inhibition of cholinesterase resulting in flaccid paralysis in schistosomes.	<i>S. haematobium</i>	Poor compliance due to need for repeated doses, efficacious against one <i>Schistosoma</i> species.

Thesis structure

The primary aim of this PhD was to investigate the epidemiology and genetic basis of praziquantel treatment response of *Schistosoma mansoni* in preschool-aged children in Uganda. This is addressed through several key objectives, and each is explored in the respective chapters of the thesis.

In **Chapter 2**, I reviewed the literature on the genetic determinants of praziquantel resistance in *Schistosoma mansoni*. The review discusses the recent advances in understanding the molecular basis of praziquantel action in *S. mansoni* and the genetic basis of drug resistance. Praziquantel resistance is discussed in the context of potentially confounding factors that may decrease efficacy within endemic settings and the most recent treatment guidelines recommended by the WHO.

In **Chapter 3**, I conducted a secondary data analysis on a subset of 96 participants from the Praziquantel in Preschoolers (PIP) clinical trial in Uganda. The main aim was to investigate *S. mansoni* clearance using different diagnostics (Kato-Katz, urine circulating cathodic antigen (CCA) and urine circulating anodic antigen (CAA) detection) to determine the cure rates and egg reduction rates for each treatment dose (40 mg/kg vs 80 mg/kg praziquantel). I then explored the impact of demographic and pharmacokinetic factors on cure rate.

In **Chapter 4**, I applied a low-input library methodology to generate whole genome sequence data from 96 single *S. mansoni* miracidia collected from preschool-aged children participating in a clinical trial in Lake Albert. Using publicly available genomic data from other regions of Uganda, several African countries and Guadeloupe, I explored the geographical population structuring of *S. mansoni*. With a more in depth focus on the Ugandan *S. mansoni* populations from Lake Albert and Lake Victoria I investigated the extent of gene flow and population dynamics between the two endemic foci. Before the start of my PhD, only a few genomes were publicly available from *S. mansoni* miracidia collected from Lake Albert, an area endemic for intestinal schistosomiasis in Uganda. This is partly due to the challenge in obtaining enough DNA from accessible *S. mansoni* larval stages from human hosts and the costs associated with generating whole genome sequence datasets.

In **Chapter 5**, I analysed the genomic data generated in Chapter 4 from *S. mansoni* miracidia collected at pre- and post-praziquantel treatment from a cohort of preschool-aged children. The main aim of this chapter was to investigate the genetic impact of praziquantel treatment on *S. mansoni* populations and determine if there was a differential impact

between treatment regimens (40 mg/kg vs 80 mg/kg PZQ). A particular focus was analysing the genetic diversity of a proposed candidate gene in praziquantel resistance, named the *Schistosoma mansoni* Transient Receptor Potential Melastatin ion channel (SmTRPM_{PZQ}). To further investigate the genetic diversity of the SmTRPM_{PZQ}, an amplicon sequencing panel was designed to target the transmembrane region of the ion channel containing the praziquantel binding pocket.

Finally, in **Chapter 6** I summarise and contextualise the main findings from the research and discuss future research directions.

Aim and objectives

Aim:

This project aims to investigate the epidemiology and genetic basis of praziquantel treatment response of *Schistosoma mansoni* in preschool-aged children in Uganda.

Objectives:

1. Review the literature on the genetic determinants of praziquantel resistance in *Schistosoma mansoni* (Chapter 2).
2. Investigate the differences in efficacy between 40 mg/kg and 80 mg/kg praziquantel treatment arms in a cohort of preschool-aged children enrolled in the Praziquantel in Preschoolers clinical trial (Chapter 3).
3. Investigate the genetic diversity and population structure of Ugandan populations of *Schistosoma mansoni* (Chapter 4).
4. Investigate the genomic impact of a single round of praziquantel treatment on *Schistosoma mansoni* populations from Lake Albert (Chapter 5).
5. Discuss the main findings of the thesis and proposed directions for future studies (Chapter 6).

Chapter 2: A review of the genetic determinants of praziquantel resistance in *Schistosoma mansoni*: Is praziquantel and intestinal schistosomiasis a perfect match?

RESEARCH PAPER COVER SHEET

Please note that a cover sheet must be completed for each research paper included within a thesis.

SECTION A – Student Details

Student ID Number	Ish1901810	Title	Miss
First Name(s)	Shannan Star		
Surname/Family Name	Summers		
Thesis Title			
Primary Supervisor	Amaya Bustinduy		

If the Research Paper has previously been published please complete Section B, if not please move to Section C.

SECTION B – Paper already published

Where was the work published?	Frontiers in Tropical Diseases		
When was the work published?	22/08/2022		
If the work was published prior to registration for your research degree, give a brief rationale for its inclusion			
Have you retained the copyright for the work?*	Yes	Was the work subject to academic peer review?	Yes

*If yes, please attach evidence of retention. If no, or if the work is being included in its published format, please attach evidence of permission from the copyright holder (publisher or other author) to include this work.

SECTION C – Prepared for publication, but not yet published

Where is the work intended to be published?	
Please list the paper's authors in the intended authorship order:	
Stage of publication	Choose an item.

SECTION D – Multi-authored work

<p>For multi-authored work, give full details of your role in the research included in the paper and in the preparation of the paper. (Attach a further sheet if necessary)</p>	<p>I conceptualised and wrote the first draft of the manuscript. My supervisors and co-authors critically reviewed, edited and approved the final version of the manuscript.</p>
---	--

SECTION E

Student Signature		
Date	11/02/2024	

Supervisor Signature		
Date	13/02/2024	



OPEN ACCESS

EDITED BY
Stephen R. Doyle,
Wellcome Sanger Institute (WT),
United Kingdom

REVIEWED BY
John D. Chan,
University of Wisconsin–Oshkosh,
United Kingdom
Jose Ma. Moncada Angeles,
University of the Philippines Manila,
Philippines

*CORRESPONDENCE
Shannan Summers
Shannan.summers1@lshtm.ac.uk

SPECIALTY SECTION
This article was submitted to
Neglected Tropical Diseases,
a section of the journal
Frontiers in Tropical Diseases

RECEIVED 30 April 2022
ACCEPTED 01 July 2022
PUBLISHED 22 August 2022

CITATION
Summers S, Bhattacharyya T, Allan F,
Stothard JR, Edieliu A, Webster BL,
Miles MA and Bustinduy AL (2022) A
review of the genetic determinants of
praziquantel resistance in *Schistosoma
mansoni*: Is praziquantel and intestinal
schistosomiasis a perfect match?
Front. Trop. Dis. 3:933097.
doi: 10.3389/ftd.2022.933097

COPYRIGHT
© 2022 Summers, Bhattacharyya, Allan,
Stothard, Edieliu, Webster, Miles and
Bustinduy. This is an open-access article
distributed under the terms of the
[Creative Commons Attribution License
\(CC BY\)](https://creativecommons.org/licenses/by/4.0/). The use, distribution or
reproduction in other forums is
permitted, provided the original
author(s) and the copyright owner(s)
are credited and that the original
publication in this journal is cited, in
accordance with accepted academic
practice. No use, distribution or
reproduction is permitted which does
not comply with these terms.

A review of the genetic determinants of praziquantel resistance in *Schistosoma mansoni*: Is praziquantel and intestinal schistosomiasis a perfect match?

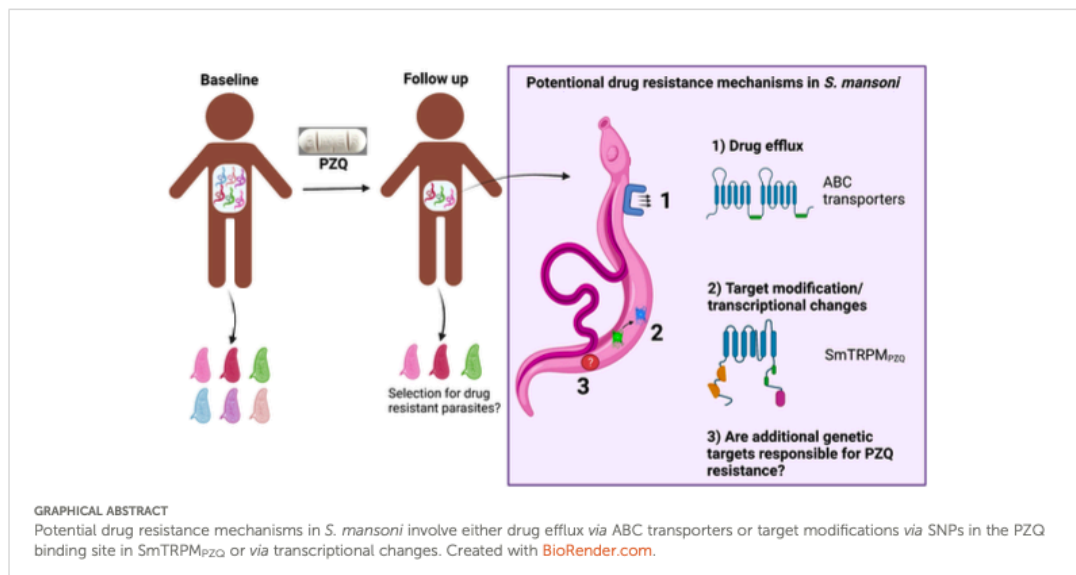
Shannan Summers^{1*}, Tapan Bhattacharyya², Fiona Allan^{3,4},
J Russell Stothard⁵, Andrew Edieliu^{1,6}, Bonnie L. Webster⁴,
Michael A. Miles² and Amaya L. Bustinduy¹

¹Department of Clinical Research, Faculty of Infectious and Tropical Diseases, London School of Hygiene and Tropical Medicine, London, United Kingdom, ²Department of Infection Biology, Faculty of Infectious and Tropical Diseases, London School of Hygiene and Tropical Medicine, London, United Kingdom, ³Scottish Oceans Institute, School of Biology, University of St Andrews, Scotland, United Kingdom, ⁴Wolfson Wellcome Biomedical Laboratories, Department of Life Sciences, Natural History Museum, London, United Kingdom, ⁵Department of Tropical Disease Biology, Liverpool School of Tropical Medicine, Liverpool, United Kingdom, ⁶Medical Research Council/ Uganda Virus Research Institute (MRC/UVRI) and London School of Hygiene and Tropical Medicine (LSHTM) Uganda Research Unit, Entebbe, Uganda

Schistosomiasis is a neglected tropical disease (NTD) caused by parasitic trematodes belonging to the *Schistosoma* genus. The mainstay of schistosomiasis control is the delivery of a single dose of praziquantel (PZQ) through mass drug administration (MDA) programs. These programs have been successful in reducing the prevalence and intensity of infections. Due to the success of MDA programs, the disease has recently been targeted for elimination as a public health problem in some endemic settings. The new World Health Organization (WHO) treatment guidelines aim to provide equitable access to PZQ for individuals above two years old in targeted areas. The scale up of MDA programs may heighten the drug selection pressures on *Schistosoma* parasites, which could lead to the emergence of PZQ resistant schistosomes. The reliance on a single drug to treat a disease of this magnitude is worrying should drug resistance develop. Therefore, there is a need to detect and track resistant schistosomes to counteract the threat of drug resistance to the WHO 2030 NTD roadmap targets. Until recently, drug resistance studies have been hindered by the lack of molecular markers associated with PZQ resistance. This review discusses recent significant advances in understanding the molecular basis of PZQ action in *S. mansoni* and proposes additional genetic determinants associated with PZQ resistance. PZQ resistance will also be analyzed in the context of alternative factors that may decrease efficacy within endemic field settings, and the most recent treatment guidelines recommended by the WHO.

KEYWORDS

preventive chemotherapy, praziquantel, drug resistance, drug tolerance, blood flukes, schistosomes, *Schistosoma mansoni*



1 Introduction

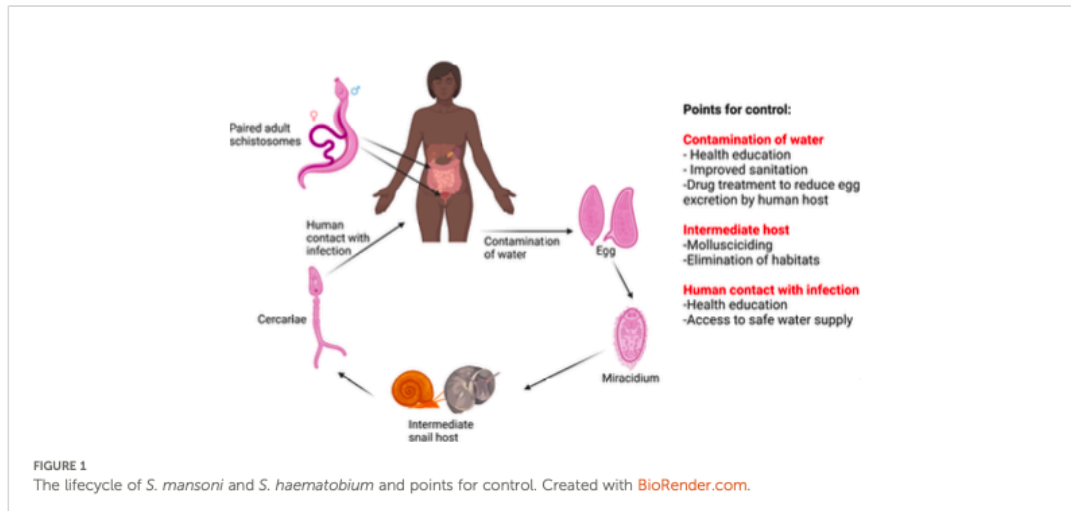
Schistosomiasis is a disabling NTD caused by an infection with dioecious *Schistosoma* flukes, affecting 240 million people; circa 95% of infections occur in sub-Saharan Africa; *S. mansoni* and *S. haematobium* are responsible for intestinal and urogenital schistosomiasis, respectively (1, 2). *Schistosoma* has a two-host life cycle: miracidia infect the intermediate freshwater snail host to produce infective cercariae, which penetrate the skin of the definitive mammalian host. Following infection of the mammalian host, mature female worms produce eggs that become trapped in host tissue and induce inflammation, granuloma and subsequent fibrosis due to the immunopathological host response resulting in debilitating downstream morbidities (3). Non-trapped eggs are passed in the faeces or urine (Figure 1).

Schistosomiasis has an age-dependent intensity of infection and focal epidemiology, influenced by human water-contact patterns (4). Infants (<1 year) and preschool aged children (PSAC) (<5 years) can commonly harbour a schistosomiasis infection (5, 6). The prevalence of infection peaks during adolescence (10 to 15 years of age) and declines during adulthood (7, 8), although high prevalence of infection can

remain in environmentally exposed subpopulations of adults (3, 4, 8).

The control and elimination of schistosomiasis requires interruption of a complex transmission pathway (4). There are several points of the lifecycle that can be targeted to reduce transmission; control measures to interrupt transmission include chemotherapy, snail control, health education, improved access to clean water, sanitation and hygiene (WASH) (4) (Figure 1).

The cornerstone of control programs is the administration of the drug PZQ, a broad-spectrum antihelminthic developed in the 1970s (9). The World Health Assembly (WHA) in 2001 endorsed preventive chemotherapy (PC) by PZQ as the main strategy of schistosomiasis control (10). PZQ is efficacious against all species of *Schistosoma* infecting humans and is given as a single oral dose (40 mg/kg recommended by the WHO) with minimal side effects, related to intensity of infection (11). MDA of PZQ began in sub-Saharan Africa from 2003; has been effective in reducing prevalence and intensity of infections (12, 13). The focus has now shifted to the elimination of schistosomiasis as a public health problem by 2030 (14). PZQ should be distributed for the first time to all age groups from two years of age. In recent years, the access to PZQ has been



improved primarily through the pledge from Merck-KGaA to donate 250 million PZQ tablets annually to school-age children (SAC) indefinitely (14) aiding in reducing morbidity through the reduction of heavy infections. Despite annual MDA, hotspots of unabated transmission and associated morbidity persist (15–19).

The scale-up of MDA heightens drug selection pressures on the *Schistosoma* populations and could lead to the selection of PZQ resistant phenotypes, as has emerged in other parasitic infections including malaria (20) and in veterinary helminths (21–23). Despite the lack of consensus as to the molecular and genetic basis of PZQ resistance in *S. mansoni*, several resistance markers have been proposed (24–27). Additionally, PZQ resistance has been shown to be able to be induced in laboratory strains of *S. mansoni*, maintained in laboratory rodents (28–30), and several field reports suggest reduced efficacy of PZQ in specific areas of endemicity (31–35) due to inadequate cure rates (CR), although there are many factors that may influence the PZQ efficacy in specific individuals i.e. inadequate dosing, high level of juvenile worms and high worm burdens. Suggestions of widespread PZQ resistance in the field remain controversial as these reports are likely explained by factors other than drug resistant schistosomes, for example rapid re-infection (36–39). In the absence of novel anti-schistosomal drugs in the development pipeline, there is a reliance on a single drug to treat a disease of this importance and magnitude, which is worrying should drug resistance develop (40). Thus, there is an unmet need to detect and track resistant *Schistosoma* parasites to elucidate the threat of drug resistance to control programs.

This review draws together the recent literature on the molecular basis of PZQ action in *S. mansoni* and highlights advances in understanding the molecular basis and the proposed genetic determinants associated with PZQ resistance. PZQ

resistance is also analyzed in the context of confounding factors within endemic field settings, and the most recent treatment guidelines recommended by the WHO.

2 Control of schistosomiasis: the new WHO guideline on control and elimination of human schistosomiasis

Schistosomiasis is a multifaceted disease with a complicated lifecycle, which requires a comprehensive control strategy. Over the past two decades, control efforts have led to a 58.3% decrease in the global burden of schistosomiasis (41). The new NTD roadmap (14) and guidelines on the control and elimination of schistosomiasis (42) set out to accelerate the progress made and are important milestones in the control of this disease. The new guidelines detail an integrated control strategy involving six evidence-based recommendations for endemic countries to facilitate the elimination of morbidity and interruption of transmission (42). The recommendations detail combining large scale PC programs, WASH, education, snail control and environmental modification to eliminate schistosomiasis as a public health problem (defined as <1% proportion of heavy intensity schistosomiasis infections) and to achieve interruption of transmission in selected countries (14, 42). Large-scale PC programs remain at the forefront of the control strategy. The main focus has been treatment of SAC, which neglected at risk populations, PSAC and adult populations including pregnant and lactating women. These programs will aim to provide equitable access to annual PZQ treatment to all age groups over the age of two years. The prevalence threshold for different

actin depolymerizing agent cytochalasin D (50). It has been demonstrated that although PZQ-mediated calcium influx in schistosomes is increased by cytochalasin D, they fail to display the expected sequence of events resulting in death (51). Additionally, juvenile schistosomes express the variant beta subunit of the VGCCs, but are not susceptible to PZQ. In the same report, the authors incubated adult and juvenile stages in medium containing radioactive Ca^{2+} and undertook *in vitro* PZQ exposure. Interestingly, the authors demonstrated that in the presence of the drug, PZQ-refractory juveniles experience a large influx of Ca^{2+} followed by muscular contraction and paralysis, but the worms are able to recover (51). PZQ induced Ca^{2+} influx was not correlated with worm death in two instances; in adult schistosomes incubated in cytochalasin D and in juvenile schistosomes. Whilst these *in vitro* findings are of interest, they only provide a partial insight into the mode of action of PZQ, a drug known to work in combination with the host's immune system in killing schistosomes *in vivo*. These findings do not rule out that PZQ could be acting on VGCCs as part of its mode of action.

3.2 *Schistosoma mansoni* transient receptor potential melastatin ion channel PZQ

More recent significant advances have been made in genomic methods and work by Park et al. (55) and Le Clec'h et al. (27) on the *S. mansoni* transient receptor potential melastatin PZQ channel (SmTRPM_{PZQ}) as being a key genomic target of PZQ response in *S. mansoni*. The discovery that the human transient receptor potential melastatin ion channel 8 (hTRPM8) is activated by (S)-PZQ, provided a structural blueprint to search for homologous targets in *S. mansoni* and led to the identification of SmTRPM_{PZQ} candidate (Smp_246790.5) (55, 56). TRP channels are a diverse superfamily of cation channels, which can be activated by an extensive range of stimuli (57). Park et al. (55) used a pharmacological approach to elucidate that SmTRPM_{PZQ} is the major target of PZQ and identified residues essential for the activation of PZQ (45, 55). Using Ca^{2+} imaging assays in human embryonic kidney 293 cells (HEK293) with heterologous expression of SmTRPM_{PZQ} demonstrated that SmTRPM_{PZQ} was stereoselectively activated by (R)-PZQ in the nanomolar range ($\text{EC}_{50} \sim 150$ nM), which led to a sustained cellular Ca^{2+} signal. The characteristics of PZQ action at SmTRPM_{PZQ} nanomolar potency of PZQ, stereoselectivity and Ca^{2+} entry, mirror the key events of PZQ action in *S. mansoni* (45, 57). Currently, it is believed that SmTRPM_{PZQ} provides the link between PZQ and Ca^{2+} (57). To further support these findings, it was found that the TRP channel antagonist La^{3+} blocked PZQ induced muscular paralysis in 5/15 experiments (58). Modelling and mutagenesis data from Park et al. (55) suggest that (R)-PZQ interacts with

SmTRPM_{PZQ} through a transmembrane binding pocket to induce channel activity and subsequent calcium influx and muscle contraction. Intriguingly, sequences of the SmTRPM_{PZQ} homologues from PZQ sensitive flukes *Clonorchis* and *Opisthorchis* display complete conservation of the PZQ binding site (45, 55). Further studies are required to elucidate the properties of SmTRPM_{PZQ} homologues in other PZQ sensitive flukes.

SmTRPM_{PZQ} is a large gene (120 kb), and seven alternatively spliced isoforms exist but are yet to be functionally characterized. This is of importance as different isoforms will likely display unique properties, including isoforms that act as dominant negatives (59, 60). Characterization of the different isoforms will be important for understanding how SmTRPM_{PZQ} activity is regulated throughout the different *Schistosoma* lifecycle stages.

3.3 Other PZQ drug targets

It has been suggested that the anti-schistosomal action of PZQ is mediated through binding to myosin light chain (61), glutathione transferase (62), inhibition of sphingomyelinase activity (43), inhibition of phosphoinositide turnover (63), inhibition of nucleoside uptake (63), reduction of schistosomal glutathione concentration (63), alteration of membrane fluidity (63) or antagonism with *S. mansoni* tegumental allergen like protein 1 (SmTAL1) (64). However, these suggested targets require rigorous investigation beyond the initial report, and it is not clear if these targets facilitate the dual pillars of PZQ action in schistosomes (paralysis and tegumental damage) (57, 63).

4 Proposed drug resistance targets

4.1 SmTRPM_{PZQ}

Mutations of the drug target can alter the ability for the drug to bind and can interfere with the activity of the target. Potential PZQ resistance may result from genetic mutations in SmTRPM_{PZQ} reducing PZQ activity in *S. mansoni*. Mutagenesis data (55) generated from *in vitro* functional assays in cells heterologously expressing SmTRPM_{PZQ} found that mutations within 20 out of 23 residues lining the PZQ binding pocket in SmTRPM_{PZQ} decreased sensitivity with many resulting in a complete loss of PZQ activity (55). Sequence analysis revealed a single amino acid difference in the predicted PZQ binding pocket of *Fasciola hepatica* FhTRPM_{PZQ} that reflects a single nucleotide polymorphism (SNP) (ACT *F. hepatica* and AAT *S. mansoni*). This SNP, encoding an amino acid change from asparagine to threonine, rendered cells expressing FhTRPM_{PZQ} resistant to PZQ and reciprocal point mutations confirmed this finding (55). These

findings demonstrate that SNPs in the PZQ binding site in SmTRPM_{PZQ} may underlie PZQ resistance. However, *in vivo* studies involving mutagenesis of SmTRPM_{PZQ} in adult schistosomes are required to determine if SNPs in the drug-binding site causes PZQ resistance in *S. mansoni*.

Recently, Le Clec'h et al. (27) investigated the genetic basis underpinning the variation in PZQ sensitivity in a PZQ-selected *S. mansoni* laboratory population where 35% of worms survive high-dose PZQ treatment. The authors noted an unusual dose-response relationship in the laboratory derived 'PZQ resistant' *S. mansoni* strain, where worms demonstrated significant heterogeneity in response to PZQ. Some adult worms displayed a PZQ sensitive phenotype whilst others could withstand high drug doses, demonstrating that the 'PZQ resistant' *S. mansoni* strain was a mixed population with significant genetic variation for PZQ susceptibility/resistance. Therefore, a lactate assay to measure adult worm recovery following *in vitro* PZQ exposure was used to create pools of adult worms at either extreme (resistant or susceptible).

Genome-wide association analysis was used to compare the pools of worms at the differing extremes of PZQ response and map loci underlying PZQ sensitivity, two major peaks in the quantitative trait locus (QTL) on chromosome 2 and 3 were identified (27). Interestingly three partial ABC transporters, a VGCC subunit and SmTRPM_{PZQ} were identified under the QTLs on these chromosomes, indicating the involvement of multiple loci in the PZQ resistance phenotype. The causative gene underlying the extreme PZQ resistance phenotype, SmTRPM_{PZQ}, showed recessive inheritance, meaning only homozygotes carrying two copies of the SmTRPM_{PZQ}-741987C allele survived PZQ treatment. Two additional key findings were: firstly, the SNP (at position 1,029,621 T>C) marking the highest association peak was found in the SOX13 transcription factor which may be a role in the regulation of splicing variants (65); secondly, two large (150 kb) deletions were found, 6.5 kb adjacent to SmTRPM_{PZQ} and 170 kb from the SOX13 transcription factor, respectively.

The authors then used marker-assisted selection of *S. mansoni* at a single SNP in SmTRPM_{PZQ} to select for two populations: PZQ-enriched resistant and sensitive parasites. Comparison between the two populations showed a >377-fold difference in PZQ treatment response, and the resistant population exhibited reduced expression by 2.25-fold of SmTRPM_{PZQ}. The 150 kb deletions were found to be close to fixation in the resistant population. Interestingly, the PZQ resistant *S. mansoni* population showed long-term stability with no reported fitness cost. Known activators and blockers of SmTRPM_{PZQ} were shown to increase or decrease PZQ sensitivity respectively. Sex and stage differences in expression levels of SmTRPM_{PZQ} were found between the selected *S. mansoni* populations (27). Both adult male and female worms from the selected resistant population showed a reduction in SmTRPM_{PZQ} expression compared to the sensitive population.

Of note, expression in female adult worms was >11 fold lower than in male worms, consistent with females being naturally PZQ tolerant (27). However, an unexpected finding was that both female and male juvenile schistosomes demonstrated higher levels of expression compared to adult worms (27). This indicates that downstream events are responsible for the inaction of PZQ against juvenile stages. Together, these findings led authors to conclude that PZQ response in *S. mansoni* may be due to expression patterns controlled by regulatory variants associated with the SOX13 transcription factor or the adjacent 150kb deletion. Furthermore, more evidence is required to determine whether altering the expression of different isoforms of SmTRPM_{PZQ} can alter schistosome sensitivity to PZQ.

Further screening, by Le Clec'h et al. (27) of 259 field-collected/originated (Niger, Tanzania, Senegal, Oman, and Brazil) *S. mansoni* samples (miracidia, cercariae and adult worms) did not identify PZQ resistance conferring SNPs in natural *S. mansoni* populations. A single stop codon in a heterozygous state was identified from a *S. mansoni* sample collected from a rodent in Oman, thus unlikely to result in PZQ resistance. The study was not targeted towards samples from foci where PZQ efficacy maybe an issue, such as "hotspots" and so these would be good targets for future investigations. Interestingly whole genome sequencing (WGS) of miracidia from a Ugandan hotspot did not find evidence of genomic selection acting on SmTRPM_{PZQ} (66). A possible reason for the lack of detection of PZQ resistant alleles in field derived *S. mansoni* populations is that PZQ resistance may be focal and PZQ resistant alleles maybe rare (67). Sample sizes from current studies (27, 66) are underpowered to detect PZQ resistance at a low allele frequency. Another important consideration is that SmTRPM_{PZQ} was found to underlie resistance in a single laboratory-generated resistant line where PZQ resistance was induced in larval stages at the intramolluscan stage not typically exposed to drug pressure in the wild (27, 67). The selected drug resistance mechanism at the intramolluscan stage may differ from that in mammalian hosts. Additionally, the *S. mansoni* strain used is of Brazilian origin, which does not represent the extensive diversity observed in East African *S. mansoni* populations. It remains unclear if the PZQ resistance mechanism involving SmTRPM_{PZQ} is conserved in African *S. mansoni* populations.

4.2 ABC transporters

ATP-binding cassette (ABC) transporters are proteins involved in the transmembrane flow of toxins and xenobiotics (68, 69). P-glycoprotein (P-gp) and multi-drug resistance (MDR)-associated proteins (MRPs) represent two classes of these transporters (68, 69). ABC transporters have been associated with drug resistance in parasites such *Plasmodium falciparum* (70, 71) and parasitic helminths (70–73). The *S.*

mansoni genome has 24 genes predicted to encode ABC transporters (74) where three ABC transporters have been characterized: SMDR1, SMDR2 and SmMRP1 (25, 69). Increased activity of P-gp has been demonstrated in laboratory generated resistant isolates (25, 75, 76). PZQ is hypothesized to interact with MDRs or MRPs either as an efflux-substrate or as a competitor of transport mediated by the ABC-transport proteins (77). Other authors have also shown an increased expression of *SmMDR2* RNA in PZQ resistant clinical isolates of *S. mansoni* (24, 25, 73, 78, 79). Intriguingly, a recent study involving WGS of miracidia collected from an area of endemicity in Uganda, found evidence of positive selection on several genes including *SmMDR1* (66).

It has been hypothesized that the factors underpinning the PZQ refractory nature of juvenile schistosomes are two-fold: higher basal levels of SmMRP1 and SmMDR2 mRNA compared to mature adult schistosomes, and the ability to mobilize an effective transcriptomic response to PZQ (80). The transcriptomic flexibility of juvenile *S. mansoni* worms was demonstrated by Hines-Kay et al. (80); juveniles exposed to PZQ had significantly elevated expression of SMDR1, SMDR3, SmMRP1 and SmMRP2 transcripts (80).

Drug efflux through ABC transporters has also been proposed as a mechanism of PZQ resistance in adult schistosomes. Work involving the use of fluorescent substrates of Pgp and MRP as probes for the presence of these transporters discovered that ABC transporters are localized in the *S. mansoni* excretory system (81, 82). Following PZQ exposure, the pattern of fluorescence was dramatically disrupted (83, 84), but this did not occur in an experimentally induced PZQ resistant *S. mansoni* strain (85). Furthermore, a significant induction of SmMRP1 RNA in adult mixed sex infection and in mature males following six-hour exposure to PZQ was demonstrated (73). Pinto-Almeida et al. (75) demonstrated the potential involvement of SMDR2 in PZQ drug resistance in *S. mansoni*. An increase in P-gp-like efflux pump activity in male worms from resistant strains was shown as well as an increase in *SmMDR2* expression following incubation in a sub-lethal concentration of PZQ. However, PZQ resistant adult female worms showed no significant change in *SmMDR2* expression following exposure to PZQ and expression was approximately 10 times lower than in PZQ-susceptible females. Interestingly, PZQ has been shown to be an inhibitor and substrate for SMDR2. SMDR2 and SmMRP1 mRNA levels increase in females and males from single sex infections following exposure to PZQ (25).

4.3 Voltage gated calcium channels

Kohn et al. (86) observed that cells expressing the structurally unusual beta subunit of VGCCs exhibit novel PZQ sensitivity. This led to the hypothesis that mutations in the gene encoding the beta subunit are responsible in PZQ resistance in

schistosomes. This hypothesis was further investigated; no mutations in the sequence nor changes in expression levels of the beta subunits between *S. mansoni* isolates varying in PZQ sensitivity were found (87). Moreover, studies have failed to find a significant difference in the expression of the beta subunit between sensitive adults and PZQ refractory juveniles (88, 89). These findings suggest changes in expression or mutations in the beta subunit in VGCCs are unlikely to underlie the PZQ resistance phenotype in *S. mansoni*.

5 Performance of PZQ in the field

Resistance to PZQ treatment is a complex issue given that until recently no molecular targets of PZQ in schistosomes were known (45, 90). There is a lack of robust methods for detection of true resistance in the field and clear universal criteria to classify a schistosome strain 'PZQ resistant' (43, 91, 92). Furthermore, drug resistance studies are restricted due to inaccessibility of adult schistosomes, thus larval stages (eggs and miracidia) can be collected and preserved for genetic analyses, although this is constrained by small quantities of DNA available from larval stages (93). A phenotypic assay to test for reduced PZQ efficacy in miracidia has been proposed (94) however; it is unclear if the miracidial phenotypic change upon PZQ exposure is underlined by a resistance genotype. Most published discussions on this topic conclude that there is insufficient evidence for the emergence of PZQ resistance in field schistosome populations of clinical relevance (36–38, 95, 96). Yet there are concerns surrounding changes in susceptibility status of schistosome populations in the field due to low CRs reported in endemic areas, treatment failures in infected travelers, and laboratory selection for resistant schistosomes (97–99).

5.1 Senegal

Following mass scale use of PZQ in Senegal, low CRs (18–39%) were reported in 1991 (31). Despite increasing the dose to 60 mg/kg, the CRs remained significantly low (35). Early studies have hypothesized and suggested that the low CRs are due to drug resistant *S. mansoni* populations. However, the lack of PZQ resistance markers and poor knowledge of the *S. mansoni* genome at the time did not allow authors to test this hypothesis genetically (37). Reported egg reduction rates (ERR) were satisfactory at 86%. It is likely that the low CRs observed are due to focal epidemiological factors; very intense transmission, high worm burdens, expanded *S. mansoni* distribution, the presence of PZQ tolerant juveniles at the time of treatment, differences in drug metabolism and rapid re-infection, and possibly not drug resistance (37).

Initial studies involving the use of an *S. mansoni* laboratory passaged strain obtained from Senegal demonstrated decreased

susceptibility to PZQ (100–102). This finding may be an artefact of early treatment as mice were treated with PZQ at day 35-day post infection. The isolate was established from infected snails thus it is unclear as to the clinical relevance of these findings. A further study involved PZQ treatment of infected mice 60 days post infection, which showed, improved efficacy of treatment (100). Schistosome strains can vary in maturation times and thus the time it takes to become susceptible to PZQ (100). In addition, laboratory passage can impose genetic bottlenecks, sampling error and selection biases, therefore the resulting parasite line may not be representative of the true extent of genetic diversity seen in the original field population (103). Another study involved the comparison of oxfamiquine (OXA) and PZQ treatment in this area revealed CRs of 79% and 36% for each drug respectively (104). But the ERRs were found to be within the normal range for both groups despite the low CRs observed. Furthermore, the two drugs differ in their mode of action where OXA does not appear to require a host immune response for parasite clearance whereas PZQ does (104). Currently, there is no convincing evidence of PZQ resistance in *S. mansoni* in Senegal, however further investigations of larger sample sizes are warranted.

5.2 Egypt

Another important foci for PZQ resistance in *S. mansoni* is Egypt where PZQ treatment for schistosomiasis was widely adopted and involved the use of 60 million PZQ tablets between 1997 and 1999 (105). A study involving the treatment of *S. mansoni* infected patients with three doses of PZQ, with the last dose increased to 60 mg/kg, found that 2.4% of patients were still egg positive post treatment. Following the first dose of 40 mg/kg PZQ, satisfactory CRs were observed (34). It should be emphasised that patients were fasted prior to receiving the second and third PZQ treatment. This can impact key PK parameters as the bioavailability of PZQ increases with food administration, thus can play a role in the failure of patients to successfully clear the *S. mansoni* infection (106). Laboratory lifecycles were set up using eggs collected from stool before treatment from cured or uncured patients, respectively. *S. mansoni* isolates cultured *in vivo* from uncured patients gave rise to *S. mansoni* worms demonstrating lower sensitivity to PZQ when compared with isolates from cured patients (34, 107). Interestingly, following multiple passages through laboratory rodents and snails, in the absence of PZQ drug pressure, approximately half the isolates retained reduced efficacy to PZQ (108). This demonstrates the heritability of this trait and does not require PZQ drug pressure for maintenance. However, the dose of PZQ required to reduce schistosome worm counts in mice by 50% (ED₅₀) differs between the isolates from uncured and cured patients were modest (2–3 fold) and is not at the level indicative of resistance to PZQ. Further studies carried out 10

years later, within the same area, were unable to show any establishment of PZQ resistance despite a decade of annual drug pressure (96).

5.3 Kenya

More recent reports of suspected PZQ resistance have come from Kenya (32). Using an *in vitro* drug susceptibility assay it was found that miracidia varied in their susceptibility to PZQ; of interest, miracidia from patients who were previously treated with PZQ displayed significantly lower susceptibility to the drug. Eggs excreted by a patient (KCW- whose infection was never completely cured despite receiving over 18 PZQ treatments) were used for *in vivo* and *in vitro* drug susceptibility assays. Reduced susceptibility of a sub-isolate from KCW remained through at least six lifecycle passages which demonstrates the trait's heritability, despite the absence of drug pressure. Of interest, an estimated odds ratio of 2.42 was obtained when comparing survival of miracidia in a previously treated and an untreated group. This is a modest difference in PZQ susceptibility and is unlikely to reflect full PZQ resistance. It is important to highlight that the study cohort of car washers in Lake Victoria are exposed to *S. mansoni* contaminated water everyday for extended periods of time. Thus it is likely that the inability to achieve cure was due the elevated exposure to re-infection.

5.4 Uganda

An alarming finding from the Schistosomiasis in Mothers and Infants (SIMI) longitudinal study was that despite two PZQ administrations within a six-month period, there was little impact on reducing the local prevalence of intestinal schistosomiasis (109). Initially, this was thought to be due to rapid re-infection (109) or under dosing of PSAC (110). However, Sousa-Figueiredo et al. (111) compared PZQ efficacy from a random sample of children from the SIMI cohort 'previously treated' and a random sample of children who had not been previously treated with PZQ 'treatment naïve'. Results revealed lower CRs in previously treated children (41.7% in those receiving any prior treatment and 29.2% in those receiving three treatments) compared to CRs of 78% in treatment naïve children (111). Age and intensity of infection were not found to explain these differences (111).

These early reports of suspected reduced PZQ efficacy of *S. mansoni* within endemic field settings do not provide sufficient evidence to show that PZQ resistant schistosomes are responsible for apparent treatment failures. In support of this conclusion a recent meta-analysis of 146 articles reporting PZQ efficacy as CR and ERR, has concluded that PZQ has retained its efficacy despite its extensive use for over four decades (39). The

meta-analysis indicated that ERR is a more consistent measurement of PZQ efficacy compared to CR (39). The use of CRs to assess PZQ efficacy may lead to an underestimation of drug efficacy. The results from the analysis indicated that there was no evidence of schistosomes developing resistance or tolerance against PZQ. This raises the important question of why PZQ resistance in schistosomes has not been found widespread in field isolates

6 Factors preventing the establishment of PZQ resistance in the field

An array of factors could prevent the emergence and establishment of PZQ resistance in the field, and are further considered in this section (Figure 3).

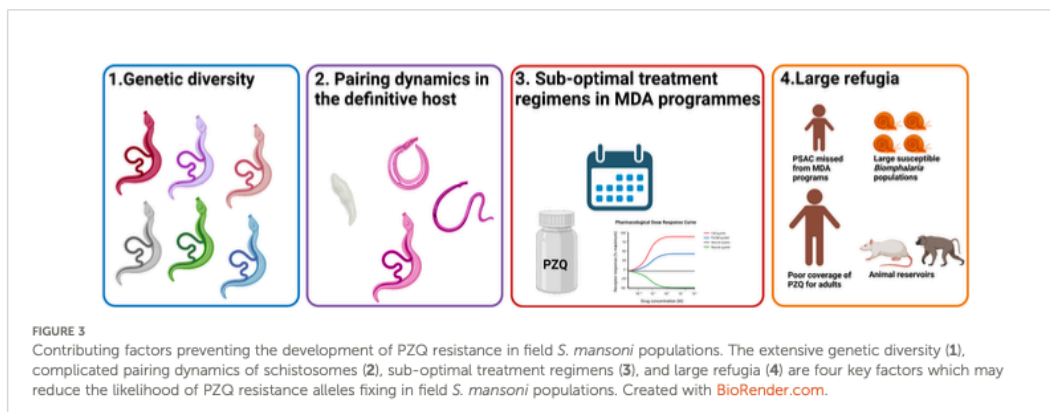
6.1 Genetic diversity of *S. mansoni* in response to PZQ treatment

Schistosoma mansoni exhibits high genetic diversity with a conspicuous amount of genetic diversity in East Africa (112) and displays a strong population structure at a country level (113–115). The high levels of genetic diversity seen in *S. mansoni* can reduce the likelihood of resistance alleles fixing within a population and help populations recover from bottlenecks following PZQ treatment (116).

Many factors can influence the genetic diversity of *S. mansoni* populations; the clonal nature of schistosomes within the intermediate snail host, and the fact that the snail host is typically infected with only few genotypes, may mitigate parasite genetic diversity (117, 123). In contrast, several factors can favor increase of the genetic diversity of schistosomes: mobility and long lifespan of the definitive host, genotype specific re-

infection, snail-parasite compatibility and the rapid turnover of infected snail hosts (117). Within this context, the definitive host acts as a 'genetic mixing bowl' for the parasite (124). Population genetic studies have reported panmictic populations (all individuals within the population are potential partners) with most genetic variation and diversity occurring within individual human hosts rather than between different hosts (66, 125, 126). Interestingly, *S. mansoni* does not appear to display a strong intra- or interpopulation structure between hosts (117). This may be due to hosts in the same village being exposed to different microenvironments, which can facilitate individuals being exposed to different parasite populations (127).

It is essential to monitor any changes in schistosome genetic diversity and population structure to understand the impact of PZQ MDA (97). A reduction in genetic diversity following PZQ treatment may indicate that the schistosome population will be less likely to adapt to drug pressure, whereas an increase in genetic diversity may indicate high gene flow between schistosome populations (97). Regular mass treatment with PZQ for the broad-scale elimination of schistosomiasis could exert a significant selective pressure on *Schistosoma* parasite infrapopulations (population within a human host), which may increase the risk for the development of drug resistance (38, 117). Population genetic studies have investigated how schistosome populations have changed following PZQ MDA (Supplementary Table 1). These studies have been restricted to a small number of molecular markers including *cytochrome oxidase subunit 1 (cox1)* and microsatellite markers. More recently, studies analyzing the whole genome or exome sequences have emerged for *S. mansoni* (66, 128, 129). Parameters such as population structure and genetic diversity can be used to deduce demographic changes and efficacy of schistosome control interventions (66). A study compared *S. mansoni* populations from two Tanzanian schools pre- and post-treatment, using microsatellite markers (97). A significant decrease in genetic diversity was found at six months following a



single round of PZQ treatment and the infrapopulations were significantly differentiated between the two time points. This is indicative of rapid re-infection. A reduction in genetic diversity was also observed in the control group of untreated PSAC, thus demonstrating the strong and long-term effect of PZQ on the population structure of *S. mansoni*. A follow up study (130) visited the same schools five years later and found a significant increase of genetic diversity in infrapopulations compared to the baseline estimates (97). A significant reduction in worm burdens within individual hosts was observed, indicating that PZQ had reduced infrapopulation sizes but not to the extent to result in a genetic bottleneck of the whole parasite population. These findings suggest that factors other than PZQ treatment may have caused the initial decline in genetic diversity (97) and the subsequent increase (130). This could reflect changes in temporal parasite transmission dynamics and high levels of re-infection as indicated by higher F_{ST} (the proportion of total genetic variance contained in a subpopulation) between years compared to between schools.

A long-term reduction in genetic diversity and the infrapopulation size following PZQ treatment could not be found by other studies. Studies had found either no change in genetic diversity or an increase in genetic diversity in *S. mansoni* populations following PZQ treatment (Supplementary Table 1). A study (116), which extensively sampled SAC from three primary schools at 11 time points, found a short-term reduction in allelic richness at 4 weeks after treatment, indicative of a PZQ induced genetic bottleneck, which rapidly recovered at six months post treatment. This indicates that high levels of gene flow ensure rapid recovery of the genetic diversity of *S. mansoni* populations, which may prevent the fixation of PZQ resistant/less tolerant genotypes (117–122). An interesting observation from Huysse et al. (131), was that despite six PZQ treatments within a two-year period, there was no difference in the genetic diversity of, and genetic differentiation between, *S. mansoni* infrapopulations before and after repeated PZQ treatment. This suggests that *S. mansoni* infrapopulations remained relatively stable over the course of treatment and is indicative of a surviving parasite population, which is tolerant to the administered PZQ dose (117).

Currently, it is difficult to apply comparative analyses to studies (Supplementary Table 1) due to the heterogeneity of methodologies used for example, differences in the molecular markers, follow up times, sampling design and genetic analysis used (117). Therefore, there is a need to adopt standardized procedures to investigate how *S. mansoni* populations respond to PZQ treatment. The lack of genetic markers for PZQ resistance has hindered the ability of these studies to understand schistosome genetic response to drug treatment. There is a need for the development of more powerful non-neutral molecular markers at the genome level to assess the extent of the genetic bottleneck post treatment and determine re-infection from persistent infections (13).

6.2 Schistosome pairing dynamics within the definitive host

Schistosomes are dioecious which enables the interaction between male and female parasites within the definitive mammalian host vasculature (130, 132). The male embraces the female schistosome within its gynaecophoric canal, forming a worm pair. Sexual development and egg production of female schistosomes is governed by this physical contact and expression of GLI1 (133). Interestingly, schistosomes do not form a worm pair 'for life' but are promiscuous and change partners (134).

The complex nature of schistosome pairing dynamics within the definitive host may pose a barrier to the establishment of the PZQ resistant trait in schistosome populations. For example, these interactions can lead to heterospecific worm pairings and subsequent hybridization, which may affect a range of phenotypic traits including PZQ sensitivity (135). Furthermore, studies have shown that PZQ sensitivity in schistosomes depends on several factors including the parasite stage, the state of adult pairing and the sex of schistosomes (43). Notably female schistosomes have demonstrated lower sensitivities to PZQ (136). Assuming PZQ randomly kills adult worms within the definitive host, a subset of the initial infrapopulation can remain (117). Studies have shown cessation of egg production following treatment despite infected individuals remaining antigen positive (137). This may be due to a single sex infection or disrupted sex ratio post-treatment. If female worms remain post-treatment, the lack of male worms lead females to revert to an immature stage and stop egg production (128). Notably, *in vivo* studies have found a decrease in the male: female ratio following PZQ treatment (136, 138).

Hosts in endemic areas are repeatedly exposed to contaminated water and become re-infected (139). Incoming schistosomes can pair with the remaining infrapopulation, which may coincide with the resumption of egg production. This can result in the PZQ resistance trait becoming rapidly outbred. Studies have demonstrated that PZQ resistance in schistosomes is recessively inherited, thus only homozygotes express this trait (27). There is a significant obstacle to the establishment of recessively inherited traits because they are present in heterozygotes at a low frequency and are consequently not exposed to selection (140). The bias against the establishment of recessives is referred to as 'Haldane's sieve' (141) and is of particular relevance in the evolution of drug resistance in diploid organisms as mutations in drug targets often result in a resistance phenotype when two copies are present (140). The rate that drug resistance alleles spread within a population in response to drug exposure is dependent on their initial frequency when the drug is introduced (142, 143). If no drug resistant alleles are present when a new drug is introduced, then there is a waiting time for them to arise and a low probability of fixation. However, it is predicted (140) that

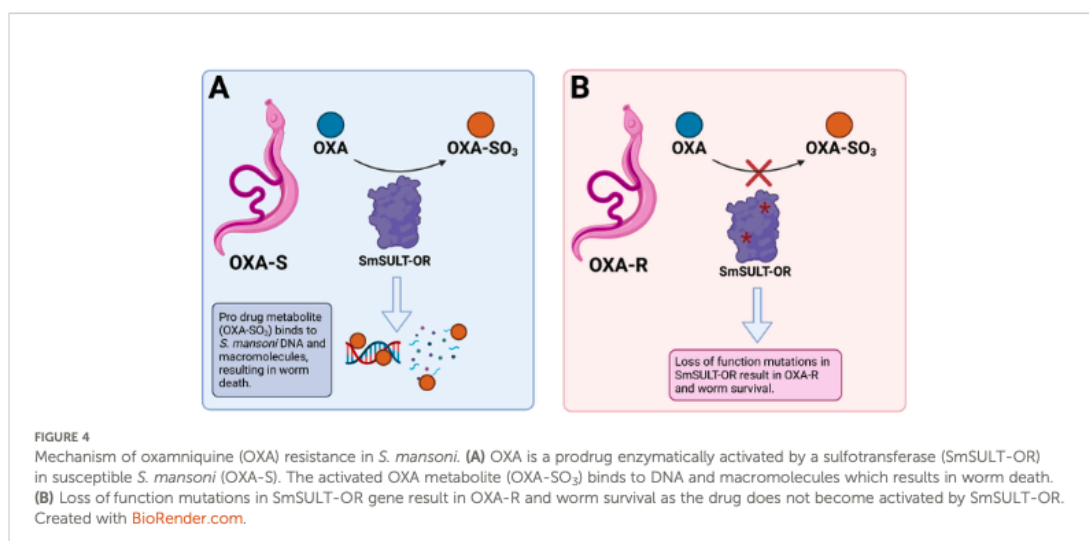
pre-standing variation for PZQ resistance is likely because this trait has been rapidly selected for by several groups (144, 145) in independent laboratory populations. Importantly, the laboratory populations used were isolated prior to the widespread availability of PZQ (144, 145), thus were not subject to PZQ selection, which strongly suggests PZQ resistant alleles were already present in these populations. This is concerning as this scenario was the case for OXA resistance (Figure 4), a trait which is also recessively inherited (146), but consequently rendered the drug futile (140).

6.3 Sub-optimal treatment regimens in MDA programs

Sub-optimal treatment regimens for schistosomiasis control may pose a significant barrier to the widespread development of PZQ resistance in schistosomiasis. PZQ is administered in PC programs to infected children at a dose (40 mg/kg) extrapolated from adult tolerance studies (147). Since 2006, PC programs have delivered PZQ as a single oral dose to SAC and/or at-risk adult populations, depending on prevalence, in endemic communities. The current treatment regime has been challenged by recent pharmacokinetic (PK; the dynamics of administered drug concentration) and pharmacodynamic (PD; the impact of drug concentrations on parasite density) data which support a higher dose (110). Bustinduy et al. (110) conducted the first PK/PD study in children to compare two doses of PZQ (40 mg/kg and 60 mg/kg) for schistosomiasis treatment (110). Vast inter-individual PK variability was seen. A higher proportion of children receiving 60 mg/kg PZQ dose achieved a better reduction in infection intensity, however no child achieved antigenic cure during the study, suggesting that

40 mg/kg is insufficient, with modelling suggesting up to 80 mg/kg to achieve WHO recommended CRs. Only 75% individuals receiving 80 mg/kg PZQ had an estimated CR of >85%. Efficacy of higher doses (80 mg/kg in a split dose) are currently being explored in a randomized placebo-controlled trial in preschool children in Uganda (148).

Interestingly, the study revealed differences in enantiomeric activity on worm burden and found that the probability of achieving cure was strongly associated with high levels of (S)-PZQ. It is typically assumed that (R)-PZQ is the anti-parasitic enantiomer, it is worth noting that the (S)-PZQ enantiomer is efficacious against *S. haematobium* (149). The high levels of (S)-PZQ may cause the hepatic shift of paralyzed adult schistosomes into the liver to be eliminated. Both enantiomers have been shown to have opposing effects on vascular tone [(R)-PZQ causes contraction (150) whereas S-PZQ causes relaxation (151)] and may play a role in optimizing blood flow through splanchnic beds where schistosomes reside, thus contributing to their displacement (57). Given the much reduced efficacy of (S)-PZQ for SmTRPM_{PZQ} (several logs), perhaps this enantiomer acts via a different schistosomal target that is still relevant for its mode of action. A recent PK study in *S. mansoni* or *S. haematobium* infected children also demonstrated higher area under the curves (AUC) for (S)-PZQ than (R)-PZQ (152). A relationship between (R)-PZQ AUC and C_{max} (peak plasma concentration) and the probability of cure was indicated using logistic regression (153). However, this interpretation was based on a small sample size and more studies are required to determine which enantiomer is the eutomer of PZQ. To achieve a greater treatment success of individuals with schistosomiasis, the treatment regimens should place more emphasis on the PK and PD characteristics of PZQ as well as schistosome biology rather than solely logistics.



When administered as a single oral dose, PZQ acts only on adult schistosomes because the drug is rapidly cleared from the body in (80% cleared within four days of which 90% occurs in 24 hours) (9). Consequently, PZQ tolerant juvenile schistosome stages are not affected by drug treatment and mature into adults, resulting in a treatment inefficiency. The intermittent drug exposure (typically annual) and insufficient dosing of PZQ means that schistosomes have not been subject to sufficient drug selective pressure to result in the development of PZQ resistance of clinical relevance. Ironically, the aim of control rather than elimination of schistosomiasis has decreased the likelihood of widespread PZQ resistance occurring.

6.4 Large refugia

Within the context of drug resistance in parasitic helminths, a *refugium* refers to the proportion of untreated hosts or environments, which allow for the maintenance of drug sensitive parasites (Figure 3) (154). To maintain drug efficacy and combat selection pressure in veterinary helminths, refugia are used and it appears that the limited MDA coverage in endemic communities may have exerted a similar effect (66, 154). Until recently, not all infected individuals within an endemic community have equitable access to PZQ treatment. Notably adult and PSAC groups did not receive PZQ treatment during control programs. These groups act as refugia of diverse parasites, which support the panmictic *S. mansoni* population structure (66). The high rates of gene flow and diversity of *S. mansoni* populations could prevent selection and fixation of PZQ resistance by providing pools of susceptible alleles to dilute those conferring PZQ resistance selected in treated populations

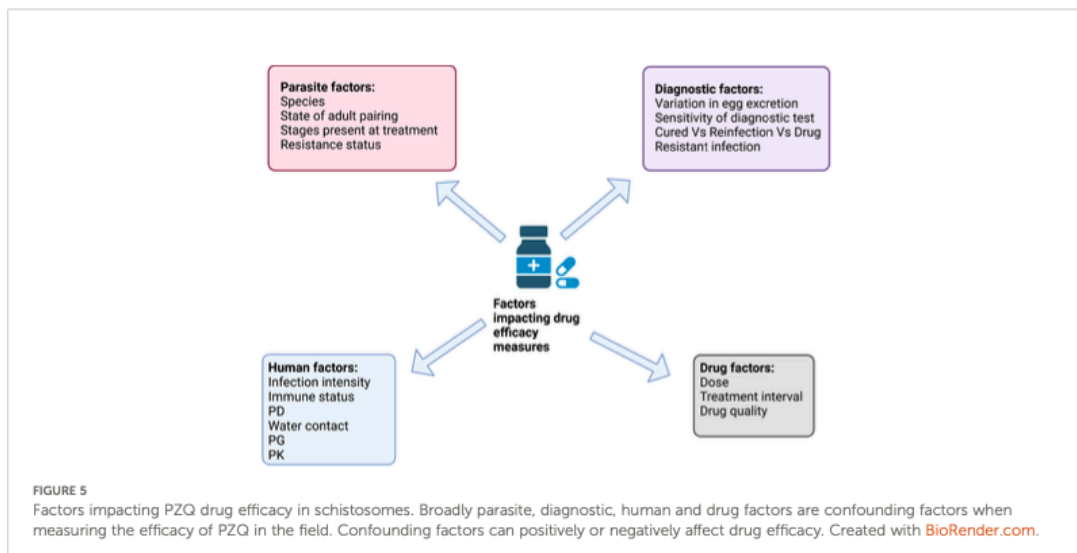
(SAC) (127). Despite multiple rounds of MDA, post-treatment schistosome populations are small in comparison to the size of refugia populations in snails, untreated humans and animal reservoirs of infection (primates (e.g., baboons and rodents) (127, 155). Mixing and high rates of gene flow between treated and untreated parasite populations allow for rapid recovery of parasite genetic diversity following treatment (66). Additionally, the long-life span of schistosomes is believed to increase the effectiveness of these reservoirs of parasite genetic diversity (66). Furthermore, the recent impact of the COVID-19 pandemic on PC delivery in endemic communities is expected to influence the refugia of schistosome populations. In 2020, 76.9 million people received PC compared to 105.5 million in 2019, due to pandemic control measures, which caused a suspension of PC programs in many endemic areas (156).

7 PZQ treatment failures within the context of confounding factors

Whilst drug resistant schistosomes have been suggested to play a role in the heterogeneity of CRs observed, it is important to investigate PZQ treatment failures in the context of confounding factors, which can affect drug efficacy. Quantifying PZQ treatment failures within the context of confounding factors are discussed in the following section (Figure 5).

7.1 Diagnostic factors

The WHO recommends quantifying changes in egg excretion before and after PZQ treatment, as ERR and CR, to



assess drug efficacy at an individual and community level (157). The tentative ERR threshold of 90% is an indicator of optimal efficacy for PZQ (11). By estimating the distribution of ERRs, changes in the efficacy of PZQ can be identified (158). Thus, the sensitivity of the diagnostic test used to assess PZQ efficacy is a key issue.

7.1.1 Parasitological diagnostics

Most drug efficacy studies use microscopy to quantify egg excretion, despite its lack of sensitivity to detect low intensity infections and treatment outcome. It has been demonstrated that individuals with low intensity infections are associated with decreased diagnostic accuracy before and after treatment (155, 159–161). This can lead to false negative results and the over estimation of drug efficacy. To improve diagnostic sensitivity, the number of parasitological samples should be increased (162). The use of at least six Kato-Katz (KK) tests (two smears per stool from three stools) has been suggested for more accurate prevalence assessment post-treatment (162). A recent meta-analysis (39) has demonstrated that an increase in the number of samples used had a significant impact for CR but not ERR, which demonstrates that ERR is less influenced by the diagnostic test sensitivity. Variation in egg excretion, can lead to incorrect diagnosis, underestimation of infection prevalence, and thus an inaccurate evaluation of drug efficacy (163, 164). Consequently, the ability to detect the emergence of drug resistant parasites is masked by the variable sensitivity of diagnostic methods based on egg detection following drug treatment. Diagnostic methods with superior sensitivity compared to microscopy are needed for the accurate mapping and identification of drug resistance hotspots.

7.1.2 Antigen detection

Antigen detection methods are a promising alternative to diagnostic microscopy. Specifically, the detection of schistosome gut-associated polysaccharides, circulating cathodic antigen (CCA) and circulating anodic antigen (CAA), have the potential to revolutionize field-based diagnostics (165). Urinary CCA-based diagnostic is used for detecting *S. mansoni* infections (166). CAA based diagnostic is able to detect all *Schistosoma* spp. infection and it is rapidly cleared from the bloodstream following PZQ treatment, thus its presence is indicative of an active infection (167). Hoekstra et al. (168) determined the efficacy of a single dose of PZQ (40 mg/kg) versus four repeated doses in SAC using either KK or point-of-care (POC)-CCA (168). The authors reported that POC-CCA gave considerably lower CRs compared to KK, which is suggestive of adult worms surviving treatment. Thus, depending on the diagnostic method used, the measures of drug efficacy (ERR and CR) can differ significantly. However, there are concerns surrounds false positive results from the POC-CCA (169, 170). Further explanations for a negative KK result and

positive POC-CCA result include the presence of single sex infections either acquired or the result of drug treatment could explain the disruption of egg production despite an active infection (171–174). Mature adult worms surviving drug treatment may cease or reduce egg production whilst still excreting CCA.

7.2 Parasite factors

Parasite factors are important to consider when quantifying drug efficacy, for example human hosts can harbor different *Schistosoma* lifecycle stages at the time of treatment, from recently acquired juvenile stages to adult schistosomes. Different lifecycle stages and parasite sex are differentially sensitive to PZQ. This can lead to a disruption in the female: male sex ratio within the host and cause cessation of egg production despite active infection. Furthermore, juvenile schistosomes are not susceptible to PZQ induced killing and survive treatment. Thus, post-treatment, juvenile schistosomes go on to mature into adult schistosomes and produce eggs. This can explain the resumption of egg production at follow up parasitological surveys, which can appear as treatment failure (175, 176). It is difficult to determine at follow up if the resumption of egg production in treated individuals is the result of reinfection, juvenile schistosomes present at treatment maturing into egg producing adults or drug resistant schistosomes. The inaccessibility of adult schistosomes from human hosts further complicates genetic analysis to determine the source of egg resumption at post-treatment (reinfection versus drug resistant schistosomes).

7.3 Drug factors

Variation in the concentration of PZQ in the systemic circulation may contribute towards treatment failure in field settings, as the drug concentration may not be present at a lethal concentration to kill schistosomes. Bioavailability is one of the most important factors, which is used to indicate the fraction of an orally administered dose that reaches the systemic circulation as intact drug and has an anti-schistosomal effect (177). Apparent drug failures may be the result of issues with the metabolism of PZQ rather than innate parasite resistance. The effect of drug metabolism on treatment outcome has been evaluated by PK and PD studies (178, 179).

Furthermore, it has been proposed that drug quality is an important confounding factor for affecting PZQ efficacy. A study using healthy mice to determine the PK profile of different PZQ brands revealed vast differences in bioavailability between different PZQ brands (180). Furthermore, the efficacy of different PZQ brands (% worm reduction) was compared in

mice infected with a PZQ susceptible or insusceptible *S. mansoni* strain. Diminished efficacy was reported in PZQ brands (Bilharzid, Epiquantel and T3A), which showed lower bioavailability (32-46% reduction), compared to pure PZQ, this difference was more prominent in the PZQ insusceptible *S. mansoni* (180). This study shows the importance of the quality of PZQ as an underlying factor for treatment failures in endemic areas.

Schistosomiasis is co-endemic with many other pathogens such as malaria, therefore, endemic populations are often subject to co-administration of different drugs that can give rise to drug-drug interactions (DDIs). CYPs are important enzymes in the first pass metabolism of many drugs. Proposed DDIs are discussed and reviewed in (181). Of interest, in humans it was found that the co-administration of PZQ and albendazole (ABZ) demonstrated a synergistic relationship where the AUC of (R)-PZQ increased by 76% (182). This is due to ABZ inhibiting CYP1A and CYP3A metabolic pathways involved in the metabolism of (R)-PZQ (182).

7.4 Human factors

It has been demonstrated that host factors, such as immune response and genetic variation in drug metabolizing enzymes, can influence the therapeutic response. PZQ is extensively metabolized by multiple Cytochrome P450 (CYP) enzymes, specifically CYP1A2, CYP2C19, CYP2C9, CYP2D6, CYP3A4 and CYP3A5 are involved (183). Host related factors can affect the metabolism and PK parameters of PZQ. Age-maturation of hepatic CYPs may affect the AUC of PZQ as the CYP pathways are not completely matured in children (110). For example, age-related metabolism has been shown where AUC values for PZQ were higher in PSAC compared to SAC (153). Higher concentrations of PZQ were found in PSAC whereas higher concentrations of (R)-4-OH-PZQ metabolite were found in SAC, suggesting that PSAC may metabolize PZQ more slowly. The comparatively higher exposure to PZQ may account for differences in CRs between the two age groups (153). Furthermore, liver morbidity has been shown to affect the metabolism of PZQ. Patients with liver cirrhosis were treated with PZQ and PK parameters were compared to healthy patients (147). Liver cirrhosis patients had a higher AUC and C_{max} , which increased with increasing severity of cirrhosis (147). However, the extent of the impact of *S. mansoni* related liver morbidity on PZQ PK parameters is largely unknown and warrants further attention.

A less studied area of PZQ efficacy is host pharmacogenetics (PG; how genes can affect an individual's response to a drug). Mutations in CYPs, primarily SNPs, have been associated with inter-individual variation of drug metabolism in efficacy and toxicity studies (152). It has been hypothesized that mutations in

CYPs results in different PK of PZQ (13). This can lead to a variable PK effect. Different populations vary significantly in the distribution of CYP alleles hence it is of importance to optimize drugs for the targeted population (181). Currently, there have been no PG studies carried out to determine the genetic influences on PK of PZQ and to identify clinically relevant CYP variants in the target population (181). Such studies are required alongside parasite population genetic studies.

8 Other schistosome species

The current landscape of literature for drug resistance in schistosomes is saturated with *S. mansoni* studies, due to several factors; *S. mansoni* laboratory strains are established and characterized, the high-quality *S. mansoni* genome, PZQ resistance can be rapidly selected for and reports of reduced susceptibility to PZQ in *S. mansoni*. There is no evidence of *S. haematobium* developing resistance to PZQ where reported CRs in endemic areas have remained favorable. Furthermore, drug resistance in *S. japonicum* has received more attention in comparison, where PZQ resistance has been selected for laboratory rodents (184). Despite the extensive use of PZQ in control programs in China, PZQ has retained its efficacy against *S. japonicum* (185–187). There is a need for future studies to focus on other *Schistosoma* spp. response to PZQ treatment in the field and to characterize the molecular basis for drug resistance.

9 Discussion

The mechanism of action of PZQ has been a significant enigma in the schistosomiasis field for decades. Great advances have been made recently with two independent research groups (27, 45) identifying SmTRPM_{PZQ} as a target of PZQ. Park et al. (55) used molecular modelling and targeted mutagenesis to identify the PZQ binding site. Le Clec'h et al. (27) used genome wide association followed by marker-assisted selection to identify SmTRPM_{PZQ} as being the key determinant of PZQ response. Collectively, we speculate that the mode of action of PZQ involves multiple protein targets including SmTRPM_{PZQ} and VGCCs, as part of a complex pathway resulting in disruption of *S. mansoni* calcium homeostasis and clearance. These recent advances provide a framework for future genetic surveillance for PZQ resistance. SmTRPM_{PZQ} genotyping of natural *S. mansoni* populations could provide valuable insights into the variation within this gene and how this may affect treatment efficacy. Furthermore, genome-wide approaches should be undertaken to identify additional genomic regions under selective pressure and candidate genes for monitoring PZQ resistance. Although candidate gene approaches to monitor

anthelmintic drug resistance have had mixed success to date, screening for non-synonymous mutations in the β -tubulin isotype 1, which confer resistance against the benzimidazole drug class used to treat the veterinary helminth *Haemonchus contortus* has been an useful example (188, 189).

These studies raised questions regarding the molecular basis for the natural tolerance of PZQ in juvenile schistosomes. It was shown that juveniles express higher levels of SmTRPM_{PZQ} compared to adult schistosomes (27). This should be considered with another line of evidence; juvenile *S. mansoni* worms experience a Ca²⁺ influx and muscle contraction, but they recover from PZQ exposure. Perhaps, the molecular target of PZQ is the same for juveniles and adults but the research focus should be on juvenile recovery from drug exposure. Juvenile schistosomes are younger compared to adult stages, thus may be more successful to adapt and recover from drug pressure. The recovery of juveniles from PZQ warrants further research attention and will provide insights into the downstream effects following drug exposure.

PZQ resistance is a complicated issue, which should be considered within the context of confounding factors. The review highlighted significant gaps in knowledge particularly the scarcity of studies focusing on the genetic basis underlying the variability in the metabolism of PZQ, which can impact the efficacy of treatment. Furthermore, this review found no strong evidence for the emergence of drug resistant *S. mansoni* populations within field settings. The review proposes four key factors, which may explain the lack of PZQ resistance observed in field *S. mansoni* populations; the extensive genetic diversity, complicated pairing dynamics of schistosomes, sub-optimal treatment regimens and large refugia. Studies focusing on the genetic diversity and population structure of *S. mansoni* populations in response to MDA, and have suggested that rapid re-infection occurs. High levels of gene flow and large refugia rapidly restore the genetic diversity and provide pools of PZQ susceptible alleles to dilute drug resistance alleles. Whilst these studies have provided insights into how *S. mansoni* populations respond to PZQ treatment, more extensive genome-wide analysis is required. Particularly to provide greater resolution in determining re-infection from an infection which has failed to clear. MDA alone is insufficient to eliminate schistosomiasis and the drug pressure exerted by current drug treatment regimens appears to be inadequate to select for PZQ resistance.

10 Conclusion

The newly introduced WHO NTD roadmap and guidelines set an ambitious control strategy to achieve the elimination of

schistosomiasis as a public health problem by 2030. PZQ remains at the forefront of schistosomiasis control and PC programs play a vital role in the integrated control strategy. However, the proposed scale up of PZQ use poses an increased risk to the development of PZQ resistance in schistosome populations. Thus, it is essential to monitor for changes in drug efficacy and for the emergence of PZQ resistant schistosomes to reduce the threat to the 2030 WHO control strategy. At present, there are no anti-schistosomal drugs undergoing clinical trials in humans, thus we must strive to retain the usefulness of PZQ in the schistosomiasis control toolbox.

Author contributions

SS conceptualized and wrote the first draft. TB, FA, JRS, AE, BLW, MAM, and ALB critically reviewed, edited, and approved the final version of the manuscript.

Funding

SS receives studentship funding from the UK Medical Research Council London Interdisciplinary Doctoral program (MR/N013638/1).

Conflict of interest

The authors declare that the research was conducted in the absence of any commercial or financial relationships that could be construed as a potential conflict of interest.

Publisher's note

All claims expressed in this article are solely those of the authors and do not necessarily represent those of their affiliated organizations, or those of the publisher, the editors and the reviewers. Any product that may be evaluated in this article, or claim that may be made by its manufacturer, is not guaranteed or endorsed by the publisher.

Supplementary material

The Supplementary Material for this article can be found online at: <https://www.frontiersin.org/articles/10.3389/fitt.2022.933097/full#supplementary-material>

References

- Schistosomiasis (2021). Available at: <https://www.who.int/news-room/fact-sheets/detail/schistosomiasis>.
- Standley CJ, Dobson A, Russell J. Out of animals and back again: Schistosomiasis as a zoonosis in Africa. In: *Schistosomiasis* (2012), 209–30. doi: 10.5772/25567
- Colley DG, Bustinduy AL, Secor WE, King CH. Human schistosomiasis. *Lancet* (2014) 382:2253–64. doi: 10.1016/S0140-6736(13)61949-2
- McManus DP, Dunne DW, Sacko M, Utzinger J, Vennervald BJ, Zhou XN. Schistosomiasis. *Nat Rev Dis Primers* (2018) 1:1–19. doi: 10.1038/s41572-018-0013-8
- Bosompem KM, Bentum IA, Otchere J, Anyan WK, Brown CA, Osada Y, et al. Infant schistosomiasis in Ghana: a survey in an irrigation community. *Trop Med Int Health* (2004) 8:917–22. doi: 10.1111/j.1365-3156.2004.01282.x
- Odogwu SE, Ramamurthy NK, Kabatereine NB, Kazibwe F, Tukahebwa E, Webster JP, et al. Schistosoma mansoni in infants (aged <3 years) along the Ugandan shoreline of lake Victoria. *Ann Trop Med Parasitol* (2006) 4:315–26. doi: 10.1179/136485906X105552
- Meurs L, Mbou M, Vereecken K, Menten J, Mboup S, Polman K. Epidemiology of mixed schistosoma mansoni and schistosoma haematobium infections in northern Senegal. *Int J Parasitol* (2012) 3:305–11. doi: 10.1016/j.ijpara.2012.02.002
- Squire B, Stothard JR. Schistosomiasis. In: N Beeching and G Gill, editors. *Tropical medicine lecture notes, 7th ed.* John Wiley & Sons, Ltd., The Atrium, Southern Gate, Chichester, West Sussex PO198SQ, UK (2014). p. 151–62.
- Andrews P, Thomas H, Pohlke R, Seubert. Praziquantel. *Medicinal Res Rev* (1983) 3:147–200. doi: 10.1002/med.2610030204
- World Health Organization. Prevention and control of schistosomiasis and soil-transmitted helminthiasis: Report of a WHO expert committee. *WHO Technical report series* (2002) 912:24–46.
- Crompton DWT/World Health Organization. Preventive chemotherapy in human helminthiasis – coordinated use of anthelmintic drugs in control interventions: A manual for health professionals and programme managers. World Health Organization (2006). Available at: <https://apps.who.int/iris/handle/10665/43545>
- World Health Organization. Schistosomiasis and soil-transmitted helminthiasis: numbers of people treated in 2019. *Wkly Epidemiol rec* (2020) 95:629–40.
- Mawa PA, Kincaid-Smith J, Tukahebwa EM, Webster JP, Wilson S. Schistosomiasis morbidity hotspots: Roles of the human host, the parasite and their interface in the development of severe morbidity. *Front Immunol* (2021) 0:751. doi: 10.3389/fimmu.2021.635869
- World Health Organization. Ending the neglect to attain the sustainable development goals – a road map for neglected tropical diseases 2021–2030. Geneva: World Health Organization (2021).
- Deol AK, Fleming FM, Calvo-Urbano B, Walker M, Bucumi V, Gnanidou I, et al. Schistosomiasis – assessing progress toward the 2020 and 2025 global goals. *N Engl J Med* (2019) 26:2519–28. doi: 10.1056/NEJMoal1812165
- Mutuku M, Laidemitt M, Beechler B, Mwangi I, Otiato F, Agola E, et al. A search for snail-related answers to explain differences in response of schistosoma mansoni to praziquantel treatment among responding and persistent hotspot villages along the Kenyan shore of lake Victoria. *Am J Trop Med Hyg* (2019) 1:65–77. doi: 10.4269/ajtmh.19-0089
- Assaré RK, NTamon RN, Bellai LG, Koffi JA, Mathieu TBI, Ouattara M, et al. Characteristics of persistent hotspots of schistosoma mansoni in western côte d'Ivoire. *Parasites Vectors* (2020) 13:1. doi: 10.1186/s13071-020-04188-x
- Kittur N, King C, Campbell C, Kinung'hi S, Mwinzi P, Karanja D, et al. Persistent hotspots in schistosomiasis consortium for operational research and evaluation studies for gaining and sustaining control of schistosomiasis after four years of mass drug administration of praziquantel. *Am J Trop Med Hyg* (2019) 3:617–27. doi: 10.4269/ajtmh.19-0193
- Wiegand RE, Mwinzi PNM, Montgomery SP, Chan YL, Andiego K, Omedo M, et al. A persistent hotspot of schistosoma mansoni infection in a five-year randomized trial of praziquantel preventative chemotherapy strategies. *J Infect Dis* (2017) 11:1425–33. doi: 10.1093/infdis/jix496
- Haldar K, Bhattacharjee S, Safeukui I. Drug resistance in plasmodium. *Nat Rev Microbiol* (2018) 3:156–70. doi: 10.1038/nrmicro.2017.161
- Kaplan R, Vidyashankar A. An inconvenient truth: global worming and anthelmintic resistance. *Vet Parasitol* (2012) 1–2:70–8. doi: 10.1016/j.vetpar.2011.11.048
- Rose H, Rinaldi L, Bosco A, Mavrot F, de Waal T, Skuce P, et al. Widespread anthelmintic resistance in European farmed ruminants: a systematic review. *Vet Rec* (2015) 21:546. doi: 10.1136/vr.102982
- Schwab AE, Boakye DA, Kyelem D, Prichard RK. Detection of benzimidazole resistance-associated mutations in the filarial nematode wuchereria bancrofti and evidence for selection by albendazole and ivermectin combination treatment. *Am J Trop Med Hygiene* (2005) 2:234–8. doi: 10.4269/ajtmh.2005.73.234
- Messerli SM, Kasinathan RS, Morgan W, Spranger S, Greenberg RM. Schistosoma mansoni p-glycoprotein levels increase in response to praziquantel exposure and correlate with reduced praziquantel susceptibility. *Mol Biochem Parasitol* (2009) 1:54–9. doi: 10.1016/j.molbiopara.2009.04.007
- Kasinathan RS, Morgan WM, Greenberg RM. Schistosoma mansoni express higher levels of multidrug resistance-associated protein 1 (SmMRP1) in juvenile worms and in response to praziquantel. *Mol Biochem Parasitol* (2010) 1:25–31. doi: 10.1016/j.molbiopara.2010.05.003
- Kohn AB, Roberts-Misterly JM, Anderson PAV, Khan N, Greenberg RM. Specific sites in the beta interaction domain of a schistosome Ca²⁺ channel β subunit are key to its role in sensitivity to the anti-schistosomal drug praziquantel. *Parasitology* (2003) 127:349–56. doi: 10.1017/S003118200300386X
- Le Clec'h W, Chevalier FD, Mattos ACA, Strickland A, Diaz R, McDew-White M, et al. Genetic analysis of praziquantel response in schistosome parasites implicates a transient receptor potential channel. *Sci Trans Med* (2021) 13(625):1–3. doi: 10.1126/scitransmed.abj9114
- Fallon PG, Doenhoff MJ. Drug-resistant schistosomiasis: Resistance to praziquantel and oxamniquine induced in schistosoma mansoni in mice is drug specific. *Am J Trop Med Hygiene* (1994) 51:83–8. doi: 10.4269/ajtmh.1994.51.83
- Couto FFB, Coelho PMZ, Araújo N, Kusel JR, Katz N, Jannotti-Passos LK, et al. Schistosoma mansoni: A method for inducing resistance to praziquantel using infected biomphalaria glabrata snails. *Memorias do Instituto Oswaldo Cruz* (2011) 106:153–7. doi: 10.1590/S0074-02762011000200006
- Mwangi I, Sanchez M, Mkoji G, Agola L, Runo S, Cupit P, et al. Praziquantel sensitivity of Kenyan schistosoma mansoni isolates and the generation of a laboratory strain with reduced susceptibility to the drug. *Int J Parasitol Drugs Drug Resist* (2014) 3:296–300. doi: 10.1016/j.ijpddr.2014.09.006
- Stelma FF, Talla I, Sow S, Kongs A, Niang M, Polman K, et al. Efficacy and side effects of praziquantel in an epidemic focus of schistosoma mansoni. *Am J Trop Med Hygiene* (1995) 2:167–70. doi: 10.4269/ajtmh.1995.53.167
- Melman SD, Steinauer ML, Cunningham C, Kubatko LS, Mwangi IN, Wynn NB, et al. Reduced susceptibility to praziquantel among naturally occurring Kenyan isolates of schistosoma mansoni. *PLoS Negl Trop Dis* (2009) 8:e504. doi: 10.1371/journal.pntd.0000504
- Crellen T, Walker M, Lamberton PHL, Kabatereine NB, Tukahebwa EM, Cotton JA, et al. Reduced efficacy of praziquantel against schistosoma mansoni is associated with multiple rounds of mass drug administration. *Clin Infect Dis* (2016) 63:1151–9. doi: 10.1093/cid/ciw506
- Ismail M, Metwally A, Farghaly A, Bruce J, Tao LF, Bennett JL. Characterization of isolates of schistosoma mansoni from Egyptian villagers that tolerate high doses of praziquantel. *Am J Trop Med Hygiene* (1996) 55:214–8. doi: 10.4269/ajtmh.1996.55.214
- Guisse F, Polman K, Stelma FF, Mbaye A, Talla I, Niang M, et al. Therapeutic evaluation of two different dose regimens of praziquantel in a recent schistosoma mansoni focus in northern Senegal. *Am J Trop Med Hygiene* (1997) 5:511–4. doi: 10.4269/ajtmh.1997.56.511
- King CH, Muchiri EM, Ouma JH. Evidence against rapid emergence of praziquantel resistance in schistosoma haematobium, Kenya. *Emerging Infect Dis* (2000) 6:585–94. doi: 10.3201/eid0606.000606
- Gryseels B, Mbaye A, De Vlas SJ, Stelma FF, Guissé F, Van Lieshout L, et al. Are poor responses to praziquantel for the treatment of schistosoma mansoni infections in Senegal due to resistance? an overview of the evidence. *Trop Med Int Health* (2001) 6:864–73. doi: 10.1046/j.1365-3156.2001.00811.x
- Fenwick A, Webster JP. Schistosomiasis: Challenges for control, treatment and drug resistance. vol. 19, current opinion in infectious diseases. *Curr Opin Infect Dis* (2006) 19:577–82. doi: 10.1097/01.qco.0000247591.13671.6a
- Fukushige M, Chase-Topping M, Woolhouse MEJ, Mutapi F. Efficacy of praziquantel has been maintained over four decades (From 1977 to 2018): A systematic review and meta-analysis of factors influence its efficacy. *PLoS Negl Trop Dis* (2021) 15:15(3). doi: 10.1371/journal.pntd.0009189
- Greenberg R. New approaches for understanding mechanisms of drug resistance in schistosomes. *Parasitology* (2013) 12:1534–46. doi: 10.1017/S0031182013000231
- Kokaliaris C, Garba A, Matuska M, Bronzan RN, Colley DG, Dorkenoo AM, et al. Effect of preventive chemotherapy with praziquantel on schistosomiasis among school-aged children in sub-Saharan Africa: a spatiotemporal modelling study. *Lancet Infect Dis* (2022) 1:136–49. doi: 10.1016/S1473-3099(21)00090-6

42. WHO guideline on control and elimination of human schistosomiasis. Geneva: World Health Organization (2022). Licence: CC BY-NC-SA 3.0 IGO.
43. Vale N, Gouveia MJ, Rinaldi G, Brindley PJ, Gärtner F, Da Costa JMC. Praziquantel for schistosomiasis: Single-drug metabolism revisited, mode of action, and resistance. *Antimicrobial Agents Chemother* (2017) 5:e02582-16. doi: 10.1128/AAC.02582-16
44. Olliaro P, Delgado-Romero P, Keiser J. The little we know about the pharmacokinetics and pharmacodynamics of praziquantel (racemate and r-enantiomer). *J Antimicrobial Chemother* (2014) 4:863-70. doi: 10.1093/jac/dkt491
45. Park SK, McCusker P, Dosa PI, Chan JD, Marchant JS. The anthelmintic drug praziquantel activates a schistosome transient receptor potential channel. *J Biol Chem* (2019) 294:18873-80. doi: 10.1074/jbc.AC119.011093
46. Cioli D, Pica-Mattoccia L, Basso A, Guidi A. Schistosomiasis control: Praziquantel forever? *Mol Biochem Parasitol Elsevier* (2014) 195:23-9. doi: 10.1016/j.molbiopara.2014.06.002
47. Harnett W, Kusel JR. Increased exposure of parasite antigens at the surface of adult male schistosoma mansoni exposed to praziquantel in vitro. *Parasitology* (1986) 2:401-5. doi: 10.1017/S0031182000051568
48. Pax R, Bennett JL, Fetterer R. A benzodiazepine derivative and praziquantel: Effects on musculature of schistosoma mansoni and schistosoma japonicum. *Naunyn-Schmiedeberg's Arch Pharmacol* (1978) 304:309-15. doi: 10.1007/BF00507974
49. Kohn AB, Anderson PAV, Roberts-Misterly JM, Greenberg RM. Schistosome calcium channel β subunits: Unusual modulatory effects and potential role in the action of the antischistosomal drug praziquantel. *J Biol Chem* (2001) 276:36873-6. doi: 10.1074/jbc.C100273200
50. Pica-Mattoccia L, Valle C, Basso A, Troiani AR, Vigorosi F, Liberti P, et al. Cytochalasin d abolishes the schistosomacidal activity of praziquantel. *Exp Parasitol* (2007) 115:344-351. doi: 10.1016/j.exppara.2006.09.017
51. Pica-Mattoccia L, Orsini T, Basso A, Festucci A, Liberti P, Guidi A, et al. Schistosoma mansoni: Lack of correlation between praziquantel-induced intraworm calcium influx and parasite death. *Exp Parasitol* (2008) 119:332-5. doi: 10.1016/j.exppara.2008.03.012
52. Nogi T, Zhang D, Chan JD, Marchant JS. A novel biological activity of praziquantel requiring voltage-operated Ca^{2+} channel β subunits: Subversion of flatworm regenerative polarity. *PLoS Negl Trop Dis* (2009) 3:e464. doi: 10.1371/journal.pntd.0000464
53. Chan JD, Agbedanu PN, Zamanian M, Gruba SM, Haynes CL, Day TA, et al. "Death and axes": Unexpected Ca^{2+} entry phenologs predict new antischistosomal agents. *PLoS Pathog* (2014) 10:e1003942. doi: 10.1371/journal.ppat.1003942
54. Jeziorski MC, Greenberg RM. Voltage-gated calcium channel subunits from platyhelminths: Potential role in praziquantel action. *Int J Parasitol* (2006) 36:625-32. doi: 10.1016/j.ijpara.2006.02.002
55. Park SK, Friedrich L, Yahya NA, Rohr CM, Chulkov EG, Maillard D, et al. Mechanism of praziquantel action at a parasitic flatworm ion channel. *Sci Transl Med* (2021) 13:625. doi: 10.1126/scitranslmed.abb5832
56. Babes RM, Selescu T, Domocos D, Babes A. The anthelmintic drug praziquantel is a selective agonist of the sensory transient receptor potential melastatin type 8 channel. *Toxicol Appl Pharmacol* (2017) 336:55-65. doi: 10.1016/j.taap.2017.10.012
57. Park SK, Marchant JS. The journey to discovering a flatworm target of praziquantel: A long TRP. *Trends Parasitol* (2020) 36:182-94. doi: 10.1016/j.pt.2019.11.002
58. Fetterer RH, Pax RA, Bennett JL. Praziquantel, potassium and 2,4-dinitrophenol: Analysis of their action on the musculature of schistosoma mansoni. *Eur J Pharmacol* (1980) 64(1):31-8. doi: 10.1016/0014-2999(80)90366-0
59. Zhang W, Chu X, Tong Q, Cheung JY, Conrad K, Masker K, et al. A novel TRPM2 isoform inhibits calcium influx and susceptibility to cell death. *J Biol Chem* (2003) 278:16222-9. doi: 10.1074/jbc.M300298200
60. Thomas H, Gönnert R. The efficacy of praziquantel against cestodes in animals. *Z für Parasitenkunde* (1977) 52:117-27. doi: 10.1007/BF00389898
61. Gnanasekar M, Salunkhe AM, Mallia AK, He YX, Kalyanasundaram R. Praziquantel affects the regulatory myosin light chain of schistosoma mansoni. *Antimicrobial Agents Chemother* (2009) 3:1054. doi: 10.1128/AAC.01222-08
62. McTigue MA, Williams DWR, Tainer JA. Crystal structures of a schistosomal drug and vaccine target: Glutathione s-transferase from schistosoma japonica and its complex with the leading antischistosomal drug praziquantel. *J Mol Biol* (1995) 246:21-7. doi: 10.1006/jmbi.1994.0061
63. Cupit P, Cunningham C. What is the mechanism of action of praziquantel and how might resistance strike? *Future Med Chem* (2015) 6:701-5. doi: 10.4155/fmc.15.11
64. Thomas CM, Fitzsimmons CM, Dunne DW, Timson DJ. Comparative biochemical analysis of three members of the schistosoma mansoni TAL family: Differences in ion and drug binding properties. *Biochimie* (2014) 108:40-7. doi: 10.1016/j.biochi.2014.10.015
65. Girardot M, Bayet E, Maurin J, Fort P, Roux P, Raynaud P. SOX9 has distinct regulatory roles in alternative splicing and transcription. *Nucleic Acids Res* (2018) 17:9106-18. doi: 10.1093/nar/gky553
66. Berger DJ, Crellen T, Lamberton PHL, Allan F, Tracey A, Noonan JD, et al. Whole-genome sequencing of schistosoma mansoni reveals extensive diversity with limited selection despite mass drug administration. *Nat Commun* (2021) 12:1-14. doi: 10.1038/s41467-021-24958-0
67. Cotton JA, Doyle SR. A genetic TRP down the channel to praziquantel resistance. *Trends Parasitol* (2022) 38:351-52. doi: 10.1016/j.pt.2022.02.006
68. Lespine A, Alvinerie M, Vercruyse J, Prichard RK, Geldhof P. ABC Transporter modulation: a strategy to enhance the activity of macrocyclic lactone anthelmintics. *Trends Parasitol* (2008) 24:293-8. doi: 10.1016/j.pt.2008.03.011
69. Bosch IB, Wang ZX, Tao LF, Shoemaker CB. Two schistosoma mansoni cDNAs encoding ATP-binding cassette (ABC) family proteins. *Mol Biochem Parasitol* (1994) 65:351-56. doi: 10.1016/0166-6851(94)90085-X
70. Lespine A, Ménez C, Bourguinat C, Prichard R. P-glycoproteins and other multidrug resistance transporters in the pharmacology of anthelmintics: Prospects for reversing transport-dependent anthelmintic resistance. *Int J Parasitol Drugs Drug Resist* (2011) 2:58-75. doi: 10.1016/j.ijpddr.2011.10.001
71. James C, Hudson A, Davey M. Drug resistance mechanisms in helminths: is it survival of the fittest? *Trends Parasitol* (2009) 7:328-35. doi: 10.1016/j.pt.2009.04.004
72. Kerboeuf D, Blackhall W, Kaminsky R, von Samson-Himmelstjerna G. P-glycoprotein in helminths: function and perspectives for anthelmintic treatment and reversal of resistance. *Int J Antimicrob Agents* (2003) 3:332-46. doi: 10.1016/S0924-8579(03)00221-8
73. Kasinathan RS, Greenberg RM. Pharmacology and potential physiological significance of schistosome multidrug resistance transporters. *Exp Parasitol* (2012) 1:2-6. doi: 10.1016/j.exppara.2011.03.004
74. Greenberg RM. ABC Multidrug transporters in schistosomes and other parasitic flatworms. *Parasitol Int* (2013) 6:647. doi: 10.1016/j.parint.2013.02.006
75. Pinto-Almeida A, Mendes T, Armada A, Belo S, Carrilho E, Viveiros M, et al. The role of efflux pumps in schistosoma mansoni praziquantel resistant phenotype. *PLoS One* (2015) 10:e0140147. doi: 10.1371/journal.pone.0140147
76. Kasinathan RS, Sharma LK, Cunningham C, Webb TR, Greenberg RM. Inhibition or knockdown of ABC transporters enhances susceptibility of adult and juvenile schistosomes to praziquantel. *PLoS Negl Trop Dis* (2014) 8:e3265. doi: 10.1371/journal.pntd.0003265
77. James CE, Hudson AL, Davey MW. An update on p-glycoprotein and drug resistance in schistosoma mansoni. *Trends Parasitol* (2009) 25:538-9. doi: 10.1016/j.pt.2009.09.007
78. Kasinathan RS, Goronga T, Messerli SM, Webb TR, Greenberg RM. Modulation of a schistosoma mansoni multidrug transporter by the antischistosomal drug praziquantel. *FASEB J* (2010) 24:128-35. doi: 10.1096/fj.09-137091
79. Liang YS, Wang W, Dai JR, Li HJ, Tao YH, Zhang JF, et al. Susceptibility to praziquantel of male and female cercariae of praziquantel-resistant and susceptible isolates of schistosoma mansoni. *J Helminthol* (2010) 84:202-7. doi: 10.1017/S0022149X0999054X
80. Hines-Kay J, Cupit PM, Sanchez MC, Rosenberg GH, Hanelt B, Cunningham C. Transcriptional analysis of schistosoma mansoni treated with praziquantel in vitro. *Mol Biochem Parasitol* (2012) 186:87-94. doi: 10.1016/j.molbiopara.2012.09.006
81. Sato H, Kusel J, Thornhill J. Excretion of fluorescent substrates of mammalian multidrug resistance-associated protein (MRP) in the schistosoma mansoni excretory system. *Parasitology* (2004) 128:43-52. doi: 10.1017/S0031182003004177
82. Sato H, Kusel JR, Thornhill J. Functional visualization of the excretory system of adult schistosoma mansoni by the fluorescent marker resorufin. *Parasitology* (2002) 6:527-35. doi: 10.1017/S0031182002002536
83. Kusel J, Oliveira F, Todd M, Ronchetti F, Lima S, Mattos A, et al. The effects of drugs, ions, and poly-l-lysine on the excretory system of schistosoma mansoni. *Memorias do Instituto Oswaldo Cruz* (2006) 101:293-8. doi: 10.1590/S0074-02762006000900046
84. Oliveira F, Kusel J, Ribeiro F, Coelho P. Responses of the surface membrane and excretory system of schistosoma mansoni to damage and to treatment with praziquantel and other biomolecules. *Parasitology* (2006) 132:321-30. doi: 10.1017/S0031182005009169
85. Couto F, Coelho P, Araújo N, Kusel J, Katz N, Mattos A. Use of fluorescent probes as a useful tool to identify resistant schistosoma mansoni isolates to praziquantel. *Parasitology* (2010) 12:1791-7. doi: 10.1017/S003118201000065X

86. Kohn AB, Anderson PAV, Roberts-Misterly JM, Greenberg RM. Schistosome calcium channel beta subunits. unusual modulatory effects and potential role in the action of the antischistosomal drug praziquantel. *J Biol Chem* (2001) 40:36873–6. doi: 10.1074/jbc.C100273200
87. Valle C, Troiani AR, Festucci A, Pica-Mattoccia L, Liberti P, Wolstenholme A, et al. Sequence and level of endogenous expression of calcium channel β subunits in schistosoma mansoni displaying different susceptibilities to praziquantel. *Mol Biochem Parasitol* (2003) 130:111–5. doi: 10.1016/S0166-6851(03)00171-3
88. Chen YH, Li MH, Zhang Y, He LL, Yamada Y, Fitzmaurice A, et al. Structural basis of the $\alpha 1$ - β subunit interaction of voltage-gated Ca²⁺ channels. *Nature* (2004) 6992:675–80. doi: 10.1038/nature02641
89. Salvador-Reccatalà V, Greenberg RM. Calcium channels of schistosomes: Unresolved questions and unexpected answers. *Wiley Interdiscip Rev. Membrane Transport Signalling* (2012) 1:85–93. doi: 10.1002/wmts.19
90. Harder A. Activation of transient receptor potential channel Sm (Schistosoma mansoni) TRPM PZQ by PZQ, enhanced Ca⁺⁺ influx, spastic paralysis, and tegumental disruption—the deadly cascade in parasitic schistosomes, other trematodes, and cestodes. *Parasitol Res* (2020) 119:2371–82. doi: 10.1007/s00436-020-06763-8
91. Fallon PG. Schistosome resistance to praziquantel. *Drug Resistance Updates* (1998) 1:236–41. doi: 10.1016/S1368-7646(98)80004-6
92. Van Wyk JA. Refugia - overlooked as perhaps the most potent factor concerning the development of anthelmintic resistance. *Onderstepoort J Veterinary Res* (2001) 68:55–67.
93. Le Clec'h W, Chevalier FD, McDew-White M, Allan F, Webster BL, Gouvras AN, et al. Whole genome amplification and exome sequencing of archived schistosome miracidia. *Parasitology* (2018) 13:1739. doi: 10.1017/S0031182018000811
94. Lamberton PHL, Hogan SC, Kabatereine NB, Fenwick A, Webster JP. In vitro praziquantel test capable of detecting reduced in vivo efficacy in schistosoma mansoni human infections. *Am J Trop Med Hygiene* (2010) 6:1340–7. doi: 10.4269/ajtmh.2010.10-0413
95. Hagan P, Appleton CC, Coles GC, Kusel JR, Tchuem-Tchuente LA. Schistosomiasis control: Keep taking the tablets. *Trends Parasitol Elsevier Ltd* (2004) 20:92–7. doi: 10.1016/j.pt.2003.11.010
96. Botros S, Sayed H, Amer N, El-Ghannam M, Bennett JL, Day TA. Current status of sensitivity to praziquantel in a focus of potential drug resistance in Egypt. *Int J Parasitol* (2005) 35:787–91. doi: 10.1016/j.ijpara.2005.02.005
97. Norton AJ, Gower CM, Lamberton PHL, Webster BL, Lwambo NJS, Blair L, et al. Genetic consequences of mass human chemotherapy for schistosoma mansoni: Population structure pre-and post-praziquantel treatment in Tanzania. *Am J Trop Med Hygiene* (2010) 4:951–7. doi: 10.4269/ajtmh.2010.10-0283
98. Doenhoff MJ, Pica-Mattoccia L. Praziquantel for the treatment of schistosomiasis: Its use for control in areas with endemic disease and prospects for drug resistance. *Expert Rev Anti-Infective Ther* (2006) 4:199–210. doi: 10.1586/14787210.4.2.199
99. Danso-Appiah A, De Vlas SJ. Interpreting low praziquantel cure rates of schistosoma mansoni infections in Senegal. *Trends Parasitol* (2002) 18:125–9. doi: 10.1016/S1471-4922(01)02209-7
100. Fallon PG, Mubarak JS, Fookes RE, Niang M, Butterworth AE, Sturrock RF, et al. Schistosoma mansoni: Maturation rate and drug susceptibility of different geographic isolates. *Exp Parasitol* (1997) 1:29–36. doi: 10.1006/expr.1997.4149
101. Fallon PG, Sturrock RF, Capron A, Niang M, Doenhoff MJ. Short report: Diminished susceptibility to praziquantel in a Senegal isolate of schistosoma mansoni. *Am J Trop Med Hygiene* (1995) 1:61–2. doi: 10.4269/ajtmh.1995.53.61
102. Liang YS, Coles GC, Doenhoff MJ, Southgate VR. In vitro responses of praziquantel-resistant and -susceptible schistosoma mansoni to praziquantel. *Int J Parasitol* (2001) 11:1227–35. doi: 10.1016/S0020-7519(01)00246-6
103. Gower C, Shrivastava J, Lamberton P, Rollinson D, Webster B, Emery A, et al. Development and application of an ethically and epidemiologically advantageous assay for the multi-locus microsatellite analysis of schistosoma mansoni. *Parasitology* (2007) 134:523–36. doi: 10.1017/S0031182006001685
104. Stelma FF, Sall S, Daff B, Sow S, Niang M, Gryseels B. Oxamniquine cures schistosoma mansoni infection in a focus in which cure rates with praziquantel are unusually low. *J Infect Dis* (1997) 1:304–7. doi: 10.1086/517273
105. Doenhoff M, Cioli D, Kimani G. Praziquantel and the control of schistosomiasis. *Parasitol Today* (2000) 16:364–6. doi: 10.1016/S0169-4758(00)01749-X
106. Castro N, Medina R, Sotelo J, Jung H. Bioavailability of praziquantel increases with concomitant administration of food. *Antimicrobial Agents Chemother* (2000) 10:2903–4. doi: 10.1128/AAC.44.10.2903-2904.2000
107. Ismail M, Botros S, Metwally A, William S, Farghally A, Tao LF, et al. Resistance to praziquantel: Direct evidence from schistosoma mansoni isolated from Egyptian villagers. *Am J Trop Med Hygiene* (1999) 6:932–5. doi: 10.4269/ajtmh.1999.60.932
108. Sabra ANA, Botros SS. Response of schistosoma mansoni isolates having different drug sensitivity to praziquantel over several life cycle passages with and without therapeutic pressure. *J Parasitol* (2008) 2:537–41. doi: 10.1645/GE-1297.1
109. Stothard JR, Sousa-Figueiredo JC, Betson M, Bustinduy A, Reinhard-Rupp J. Schistosomiasis in African infants and preschool children: let them now be treated! *Trends Parasitol* (2013) 4:197. doi: 10.1016/j.pt.2013.02.001
110. Bustinduy AL, Waterhouse D, de Sousa-Figueiredo JC, Roberts SA, Atuhaire A, van Dam GJ, et al. Population pharmacokinetics and pharmacodynamics of praziquantel in Ugandan children with intestinal schistosomiasis: Higher dosages are required for maximal efficacy. *mBio* (2016) 4:1–9. doi: 10.1128/mBio.00227-16
111. Sousa-Figueiredo JC, Betson M, Atuhaire A, Arinaitwe M, Navaratnam AMD, Kabatereine NB, et al. Performance and safety of praziquantel for treatment of intestinal schistosomiasis in infants and preschool children. *PLoS Negl Trop Dis* (2012) 10:e1864. doi: 10.1371/journal.pntd.0001864
112. Morgan JAT, Dejong RJ, Adeoye GO, Ansa EDO, Barbosa CÇS, Brémont P, et al. Origin and diversification of the human parasite schistosoma mansoni. *Mol Ecol* (2005) 14:3889–902. doi: 10.1111/j.1365-294X.2005.02709.x
113. Thiele EA, Sorensen RE, Gazzinelli A, Minchella DJ. Genetic diversity and population structuring of schistosoma mansoni in a Brazilian village. *Int J Parasitol* (2008) 3–4:389–99. doi: 10.1016/j.ijpara.2007.07.011
114. Stothard JR, Webster BL, Weber T, Nyakana S, Webster JP, Kazibwe F, et al. Molecular epidemiology of schistosoma mansoni in Uganda: DNA barcoding reveals substantial genetic diversity within lake Albert and lake Victoria populations. *Parasitology* (2009) 13:1813–24. doi: 10.1017/S00311820099031X
115. van den Broeck F, Maes GE, Larmuseau MHD, Rollinson D, Sy I, Faye D, et al. Reconstructing colonization dynamics of the human parasite schistosoma mansoni following anthropogenic environmental changes in Northwest Senegal. *PLoS Negl Trop Dis* (2015) 8:e0003998. doi: 10.1371/journal.pntd.0003998
116. Faust CL, Crotti M, Moses A, Oguttu D, Wamboko A, Adriko M, et al. Two-year longitudinal survey reveals high genetic diversity of schistosoma mansoni with adult worms surviving praziquantel treatment at the start of mass drug administration in Uganda. *Parasites Vectors* (2019) 1:1–12. doi: 10.1186/s13071-019-3860-6
117. Rey O, Webster BL, Huysse T, Rollinson D, Van den Broeck F, Kincaid-Smith J, et al. Population genetics of African schistosoma species. *Infect Genet Evol* (2021) 89:104727. doi: 10.1016/j.meegid.2021.104727
118. Lelo AE, Mburu DN, Magoma GN, Mungai BN, Kihara JH, Mwangi IN, et al. No apparent reduction in schistosoma burden or genetic diversity following four years of school-based mass drug administration in mwea, central Kenya, a heavy transmission area. *PLoS Negl Trop Dis* (2014) 10:e3221–1. doi: 10.1371/journal.pntd.0003221
119. Vianney TJ, Berger DJ, Doyle SR, Sankaranarayanan G, Serubanja J, Nakawungu PK, et al. Genome-wide analysis of schistosoma mansoni reveals population structure and praziquantel drug selection pressure within Ugandan hot-spot communities. *bioRxiv* (2022). doi: 10.1101/2022.01.25.477652
120. Trienekens SCM, Faust CL, Meginnis K, Pickering L, Ericssonid O, Nankasi A, et al. Impacts of host gender on schistosoma mansoni risk in rural Uganda—a mixed-methods approach. *PLoS Negl Trop Dis* (2020) 5:1–19. doi: 10.1371/journal.pntd.0008266
121. Barbosa LM, Reis EA, dos Santos CRA, Costa JM, Carmo TM, Aminu PT, et al. Repeated praziquantel treatments remodel the genetic and spatial landscape of schistosomiasis risk and transmission. *Int J Parasitol* (2016) 5–6:343–50. doi: 10.1016/j.ijpara.2016.01.007
122. Blanton RE, Blank WA, Costa JM, Carmo TM, Reis EA, Silva LK, et al. Schistosoma mansoni population structure and persistence after praziquantel treatment in two villages of bahia, Brazil. *Int J Parasitol* (2011) 10:1093. doi: 10.1016/j.ijpara.2011.06.002
123. Theron A, Sire C, Rognon A, Prugnolle F, Durand P. Molecular ecology of schistosoma mansoni transmission inferred from the genetic composition of larval and adult in populations within intermediate and definitive hosts. *Parasitology* (2004) 129:571–85. doi: 10.1017/S0031182004005943
124. Curtis J, Minchella DJ. Schistosome population genetic structure: When clumping worms is not just splitting hairs. *Parasitol Today* (2000) 2:68–71. doi: 10.1016/S0169-4758(99)01553-7
125. Gower CM, Gouvras AN, Lamberton PH, Deol A, Shrivastava J, Mutombo PN, et al. Population genetic structure of schistosoma mansoni and schistosoma haematobium from across six sub-Saharan African countries: Implications for epidemiology, evolution and control. *Acta Tropica* (2013) 2:261–74. doi: 10.1016/j.actatropica.2012.09.014
126. Webster B, Webster J, Gouvras A, Garba A, Lamine M, Diaw O, et al. DNA “barcoding” of schistosoma mansoni across sub-Saharan Africa supports

- substantial within locality diversity and geographical separation of genotypes. *Acta Trop* (2013) 2:250–60. doi: 10.1016/j.actatropica.2012.08.009
127. Betson M, Sousa-Figueiredo JC, Kabatereine NB, Stothard JR. New insights into the molecular epidemiology and population genetics of schistosoma mansoni in Ugandan pre-school children and mothers. *PLoS Negl Trop Dis* (2013) 12:e2561. doi: 10.1371/journal.pntd.0002561
128. Guzman MA, Rugel AR, Tarpley RS, Alwan SN, Chevalier FD, Kovalsky DP, et al. An iterative process produces oxamniquine derivatives that kill the major species of schistosomes infecting humans. *PLoS Negl Trop Dis* (2020) 8:e0008517. doi: 10.1371/journal.pntd.0008517
129. Crellen T, Allan F, David S, Durrant C, Huckvale T, Holroyd N, et al. Whole genome resequencing of the human parasite schistosoma mansoni reveals population history and effects of selection. *Sci Rep* (2016) 1:1–13. doi: 10.1038/srep20954
130. Gower CM, Gehrle F, Marques SR, Lambertson PHL, Lwambo NJ, Webster JP. Phenotypic and genotypic monitoring of schistosoma mansoni in Tanzanian schoolchildren five years into a preventative chemotherapy national control programme. *Parasites Vectors* (2017) 1:593. doi: 10.1186/s13071-017-2533-6
131. Huysse T, Van den Broeck F, Jombart T, Webster BL, Diaw O, Volckaert FAM, et al. Regular treatments of praziquantel do not impact on the genetic make-up of schistosoma mansoni in northern Senegal. *Infect Genet Evol* (2013) 18:100–5. doi: 10.1016/j.meegid.2013.05.007
132. Huysse T, Webster BL, Geldof S, Stothard JR, Diaw OT, Polman K, et al. Bidirectional introgressive hybridization between a cattle and human schistosome species. *PLoS Pathog* (2009) 9:e1000571. doi: 10.1371/journal.ppat.1000571
133. Chen R, Wang J, Gradinaru I, Deberardinis RJ, Ross EM, Collins JJ, et al. A male-derived nonribosomal peptide pheromone controls female schistosome development. *Cell* (2022) 185:1506–1520.e17. doi: 10.1016/j.cell.2022.03.017
134. Loker ES, Brant SV. Diversification, dioecy and dimorphism in schistosomes. *Trends Parasitol* (2006) 11:521–8. doi: 10.1016/j.pt.2006.09.001
135. Leger E, Webster JP. Hybridizations within the genus schistosoma: Implications for evolution, epidemiology and control. *Parasitology* (2017) 165:80. doi: 10.1017/S0033182016001190
136. Sanchez MC, Cupit PM, Bu L, Cunningham C. Transcriptomic analysis of reduced sensitivity to praziquantel in schistosoma mansoni. *Mol Biochem Parasitol* (2019) 228:6. doi: 10.1016/j.molbiopara.2018.12.005
137. Lu DB, Deng Y, Ding H, Liang YS, Webster JP. Single-sex schistosome infections of definitive hosts: Implications for epidemiology and disease control in a changing world. *PLoS Pathog* (2018) 3:e1006817. doi: 10.1371/journal.ppat.1006817
138. Lambertson PHL, Faust CL, Webster JP. Praziquantel decreases fecundity in schistosoma mansoni adult worms that survive treatment: evidence from a laboratory life-history trade-offs selection study. *Infect Dis Poverty* (2017) 6:1–11. doi: 10.1186/s40249-017-0324-0
139. Steinauer ML. The sex lives of parasites: investigating the mating system and mechanisms of sexual selection of the human pathogen schistosoma mansoni. *Int J Parasitol* (2009) 10:1157–63. doi: 10.1016/j.ijpara.2009.02.019
140. Chevalier F, le Clech W, McDew-White M, Menon V, Guzman M, Holloway S, et al. Oxamniquine resistance alleles are widespread in old world schistosoma mansoni and predate drug deployment. *PLoS Pathog* (2019) 10:1–25. doi: 10.1371/journal.ppat.1007881
141. Orr HA, Betancourt AJ. Haldane's sieve and adaptation from the standing genetic variation. *Genetics* (2001) 2:875–84. doi: 10.1093/genetics/157.2.875
142. Barrett RDH, Schluter D. Adaptation from standing genetic variation. *Trends Ecol Evol* (2008) 1:38–44. doi: 10.1016/j.tree.2007.09.008
143. Hermisson J, Pennings PS. Soft sweeps: molecular population genetics of adaptation from standing genetic variation. *Genetics* (2005) 4:2335–52. doi: 10.1534/genetics.104.036947
144. Coles GC, Mutahi WT, Kinoti GK, Bruce JI, Katz N. Tolerance of Kenyan schistosoma mansoni to oxamniquine. *Trans R Soc Trop Med Hyg* (1987) 5:782–5. doi: 10.1016/0035-9203(87)90032-0
145. Lewis FA, Stirewalt MA, Souza CP, Gazzinelli G. Large-Scale laboratory maintenance of schistosoma mansoni, with observations on three schistosome/snail host combinations. *J Parasitol* (1986) 6:813–29. doi: 10.2307/3281829
146. Cioli D, Pica-Mattocchia L, Moroni R. Schistosoma mansoni: hycanthone/oxamniquine resistance is controlled by a single autosomal recessive gene. *Exp Parasitol* (1992) 4:425–32. doi: 10.1016/0014-4894(92)90255-9
147. el Guiniady MA, el Touny MA, Abdel-Bary MA, Abdel-Fatah SA, Metwally A. Clinical and pharmacokinetic study of praziquantel in Egyptian schistosomiasis patients with and without liver cell failure. *Am J Trop Med Hygiene* (1994) 6:809–18. doi: 10.4269/ajtmh.1994.51.809
148. Webb E, Edielu A, Wu H, Kabatereine N, Tukaheba E, Mubangizi A, et al. The praziquantel in preschoolers (PIP) trial: study protocol for a phase II PK/PD-driven randomised controlled trial of praziquantel in children under 4 years of age. *Trials* (2021) 1:601. doi: 10.1186/s13063-021-05558-1
149. Kovač J, Vargas M, Keiser J. *In vitro* and *in vivo* activity of r- and s-praziquantel enantiomers and the main human metabolite trans-4-hydroxy-praziquantel against schistosoma haematobium. *Parasite Vectors* (2017) 10:365. doi: 10.1186/s13071-017-2293-3
150. Chan JD, Cupit PM, Gunaratne GS, McCorvy JD, Yang Y, Stoltz K, et al. The anthelmintic praziquantel is a human serotonergic G-protein-coupled receptor ligand. *Nat Commun* (2017) 8:1–7. doi: 10.1038/s41467-017-02084-0
151. Gunaratne GS, Yahya NA, Dosa PI, Marchant JS. Activation of host transient receptor potential (TRP) channels by praziquantel stereoisomers. *PLoS Negl Trop Dis* (2018) 12(4):1–18. doi: 10.1371/journal.pntd.0006420
152. Evans WE, Relling MV. Pharmacogenomics: Translating functional genomics into rational therapeutics. *Science* (1999) 5439:487–91. doi: 10.1126/science.286.5439.487
153. Kovač J, Meister I, Neodo A, Panic G, Coulibaly JT, Falcoz C, et al. Pharmacokinetics of praziquantel in schistosoma mansoni- and schistosoma haematobium-infected school- and preschool-aged children. *Antimicrob Agents Chemother* (2018) 8:1–11. doi: 10.1128/AAC.02253-17
154. Hodgkinson JE, Kaplan RM, Kenyon F, Morgan ER, Park AW, Paterson S, et al. Refugia and anthelmintic resistance: Concepts and challenges. *Int J Parasitol: Drugs Drug Resistance* (2019) 10:51–7. doi: 10.1016/j.ijpddr.2019.05.001
155. Enk MJ, Oliveira e Silva G, Rodrigues NB. Diagnostic accuracy and applicability of a PCR system for the detection of schistosoma mansoni DNA in human urine samples from an endemic area. *PLoS One* (2012) 6:38947. doi: 10.1371/journal.pone.0038947
156. WHO. Schistosomiasis and soil-transmitted helminthiasis: progress report. *Weekly epidemiological record* (2020) 48:1–12.
157. Cavalcanti MG, Peralta JM. Investment on new technologies for diagnosis of schistosomiasis is justified in the era of schistosoma elimination? *Contagion* (2018) 3:1.
158. Walker M, Mabud TS, Oliario PL, Coulibaly JT, King CH, Raso G, et al. New approaches to measuring anthelmintic drug efficacy: parasitological responses of childhood schistosome infections to treatment with praziquantel. *Parasites Vectors* (2016) 1:1–15. doi: 10.1186/s13071-016-1312-0
159. Ajibola O, Gulumbe B, Eze A, Obishakin E. Tools for detection of schistosomiasis in resource limited settings. *Med Sci* (2018) 6(2):39. doi: 10.3390/medsci6020039
160. Cavalcanti MG, Silva LF, Peralta RHS, Barreto MGM, Peralta JM. Schistosomiasis in areas of low endemicity: A new era in diagnosis. *Trends Parasitol* (2013) 29:75–82. doi: 10.1016/j.pt.2012.11.003
161. Ibrionke OA, Phillips AE, Garba A, Lamine SM, Shiff C. Diagnosis of schistosoma haematobium by detection of specific DNA fragments from filtered urine samples. *Am J Trop Med Hygiene* (2011) 84(6):998–1001. doi: 10.4269/ajtmh.2011.10-0691
162. Lambertson PHL, Kabatereine NB, Ogutu DW, Fenwick A, Webster JP. Sensitivity and specificity of multiple kato-Katz thick smears and a circulating cathodic antigen test for schistosoma mansoni diagnosis pre- and post-repeated-praziquantel treatment. *PLoS Negl Trop Dis* (2014) 8(9):1–15. doi: 10.1371/journal.pntd.0003139
163. Kongs A, Marks G, Verle P, van der Stuyf P. The unreliability of the kato-Katz technique limits its usefulness for evaluating s. mansoni infections. *Trop Med Int Health* (2001) 6(3):163–9. doi: 10.1046/j.1365-3156.2001.00687.x
164. Vinkles Melchers NVS, van Dam GJ, Shaproski D, Kahama AI, Brienen EAT, Vennervald BJ, et al. Diagnostic performance of schistosoma real-time PCR in urine samples from Kenyan children infected with schistosoma haematobium: Day-to-day variation and follow-up after praziquantel treatment. *PLoS Negl Trop Dis* (2014) 8(4):1–9. doi: 10.1371/journal.pntd.0002807
165. Cavalcanti MG, Cunha AFA, Peralta JM. The advances in molecular and new point-of-care (POC) diagnosis of schistosomiasis pre- and post-praziquantel use: In the pursuit of more reliable approaches for low endemic and non-endemic areas. *Front Immunol* (2019) 1:858. doi: 10.3389/fimmu.2019.00858
166. Kittur N, Castleman JD, Campbell CH Jr., King CH, Colley DG. Comparison of schistosoma mansoni prevalence and intensity of infection, as determined by the circulating cathodic antigen urine assay or by the kato-Katz fecal assay: A systematic review. *Am J Trop Med Hygiene* (2016) 94(3):605. doi: 10.4269/ajtmh.15-0725
167. Corstjens PLAM, de Dood CJ, Knopp S, Clements MN, Ortu G, Umulisa I, et al. Circulating anodic antigen (CAA): A highly sensitive diagnostic biomarker to detect active schistosoma infections—improvement and use during SCORE. *Am J Trop Med Hygiene* (2020) 103:50. doi: 10.4269/ajtmh.19-0819
168. Hoekstra Id PT, Casacuberta-Partal M, Van Lieshout L, Corstjens PLAM, Tsonaka R, Assaré RK, et al. Efficacy of single versus four repeated doses of praziquantel against schistosoma mansoni infection in school-aged children from côte d'Ivoire based on kato-Katz and POC-CCA: An open-label, randomised controlled trial (RePST). *PLoS Neglected Tropical Diseases* (2020) 14:e0008189. doi: 10.1371/journal.pntd.0008189

169. Casacuberta-Partal M, Beenakker M, de Dood CJ, Hoekstra PT, Kroon L, Kornelis D, et al. Specificity of the point-of-Care urine strip test for schistosoma circulating cathodic antigen (POC-CCA) tested in non-endemic pregnant women and young children. *Am J Trop Med Hygiene* (2021) 104(4):1412–7. doi: 10.4269/ajtmh.20-1168
170. RMD. Technical brochure—rapid test for qualitative detection of: Bilharzia (Schistosomiasis). (2018).
171. Utzinger J, Booth M, N'Goran EK, Müller I, Tanner M, Lengler C. Relative contribution of day-to-day and intra-specimen variation in faecal egg counts of schistosoma mansoni before and after treatment with praziquantel. *Parasitology* (2001) 122(5):537–44. doi: 10.1017/S0031182001007752
172. Engels D, Sinzinkayo E, Gryseels B. Day-to-day egg count fluctuation in schistosoma mansoni infection and its operational implications. *Am J Trop Med Hygiene* (1996) 54(4):319–24. doi: 10.4269/ajtmh.1996.54.319
173. Colley DG, Andros TS, Campbell CH. Schistosomiasis is more prevalent than previously thought: What does it mean for public health goals, policies, strategies, guidelines and intervention programs? *Infect Dis Poverty* (2017) 6:1–8. doi: 10.1186/s40249-017-0275-5
174. Haggag AA, Rabiee A, Abd Elaziz KM, Campbell CH, Colley DG, Ramzy RMR. Thirty-day daily comparisons of kato-Katz and CCA assays of 45 Egyptian children in areas with very low prevalence of schistosoma mansoni. *Am J Trop Med Hygiene* (2019) 100(3):578–83. doi: 10.4269/ajtmh.18-0829
175. Xiao SH, Catto BA, Webster LT. Effects of praziquantel on different developmental stages of schistosoma mansoni *in vitro* and *in vivo*. *J Infect Dis* (1985) 151:1130–1137. doi: 10.1093/infdis/151.6.1130
176. Pica-Mattoccia L, Cioli D. Sex- and stage-related sensitivity of schistosoma mansoni to *in vivo* and *in vitro* praziquantel treatment. *Int J Parasitol* (2004) 34:527–33. doi: 10.1016/j.ijpara.2003.12.003
177. Rang H, Dale M JMR, Rang R JFDale's Pharmacology. (2007), 106 p.
178. Nsanabana C, Djalle D, Guérin P, Ménard D, González I. Tools for surveillance of anti-malarial drug resistance: an assessment of the current landscape. *Malar* (2018) 1:1–16. doi: 10.1186/s12936-018-2185-9
179. White NJ. Assessment of the pharmacodynamic properties of antimalarial drugs *in vivo*. *Antimicrobial Agents Chemother* (1997) 7:1413. doi: 10.1128/AAC.41.7.1413
180. Botros S, El-Lakkany N, Seif el-Din SH, Sabra AN, Ibrahim M. Comparative efficacy and bioavailability of different praziquantel brands. *Exp Parasitol* (2011) 2:515–21. doi: 10.1016/j.exppara.2010.10.019
181. Zdesenko G, Mutapi F. Drug metabolism and pharmacokinetics of praziquantel: A review of variable drug exposure during schistosomiasis treatment in human hosts and experimental models. *PLoS Negl Trop Dis* (2020) 9:1–26. doi: 10.1371/journal.pntd.0008649
182. Lima RM, Ferreira MAD, de Jesus Ponte Carvalho TM, Dumêt Fernandes BJ, Takayanagi OM, Garcia HH, et al. Albendazole-praziquantel interaction in healthy volunteers: kinetic disposition, metabolism and enantioselectivity. *Br J Clin Pharmacol* (2011) 4:528. doi: 10.1111/j.1365-2125.2010.03874.x
183. Wang H, Fang ZZ, Zheng Y, Zhou K, Hu C, Krausz KW, et al. Metabolic profiling of praziquantel enantiomers. *Biochem Pharmacol* (2014) 2:166–78. doi: 10.1016/j.bcp.2014.05.001
184. Li HJ, Liang YS, Dai JR, Wang W, Qu GL, Li YZ, et al. Studies on resistance of schistosoma to praziquantel XIV experimental comparison of susceptibility to praziquantel between PZQ-resistant isolates and PZQ-susceptible isolates of schistosoma japonicum in stages of adult worms, miracidia and cercariae. *Chin J Schistosomiasis Control* (2011) 23:611–9. doi: 10.16250/j.32.1374.2017101
185. Seto EYW, Wong BK, Lu D, Zhong B. Human schistosomiasis resistance to praziquantel in China: Should we be worried? *Am J Trop Med Hygiene* (2011) 1:74–82. doi: 10.4269/ajtmh.2011.10-0542
186. Wang W, Dai JR, Li HJ, Shen XH, Liang YS. Is there reduced susceptibility to praziquantel in schistosoma japonicum? evidence from China. *Parasitology* (2010) 137:1906–12. doi: 10.1017/S0031182010001204
187. Wang W, Dai JR, Li HJ, Shen XH, Liang YS. Short report: The sensitivity of schistosoma japonicum to praziquantel: A field evaluation in areas with low endemicity of China. *Am J Trop Med Hygiene* (2012) 5:834–6. doi: 10.4269/ajtmh.2012.11-0701
188. Kwa MSG, Veenstra JG, Roos MH. Benzimidazole resistance in haemonchus contortus is correlated with a conserved mutation at amino acid 200 in β -tubulin isotype 1. *Mol Biochem Parasitol* (1994) 63:299–303. doi: 10.1016/0166-6851(94)90066-3
189. Doyle SR, Cotton JA. Genome-wide approaches to investigate anthelmintic resistance. *Trends Parasitol* (2019) 35:289–301. doi: 10.1016/j.pt.2019.01.004

Supplementary Material

Table 1: Studies on the genetic diversity of *S. mansoni* field populations in response to PZQ treatment.

Country	Year	PZQ dose	Study design and major findings
Tanzania	2005 (1)	40 mg/kg	Used seven microsatellite markers to compare the genetic diversity of <i>S. mansoni</i> populations in SAC at baseline and 12-month post treatment. A small significant difference was found in allelic richness and genetic diversity estimated per infrapopulation at the two time points.
	2010 (2)	40 mg/kg	Revisited the schools and replicated methodologies from (1) with the addition of a phenotypic test for PZQ sensitivity. SAC had received two or four rounds of treatment depending on the school. A significant increase in infrapopulation allelic richness and genetic diversity in 2010 was found. The dataset was re-analyzed by (3) and confirmed the finding that a single round of PZQ significantly reduced <i>S. mansoni</i> genetic diversity.
Senegal	2007 (4)	Double treatment (2 x 40 mg/kg PZQ at each time point)	Used nine microsatellite markers to compare the genetic diversity of <i>S. mansoni</i> and <i>S. haematobium</i> populations from SAC at baseline, six months and two years post treatment. No significant change in genetic diversity and structure of <i>S. mansoni</i> populations despite repeated PZQ treatment.
Kenya	2008 (5)	40 mg/kg	Used 12 microsatellite markers in 15 SAC to compare the genetic diversity of <i>S. mansoni</i> populations at four time points (annual samples prior to MDA). It was determined that PZQ had no impact on the genetic diversity of <i>S. mansoni</i> .
Uganda	2004 (6)	40 mg/kg	Used seven microsatellite markers to compare the genetic diversity of <i>S. mansoni</i> from SAC sampled at 11 time points over a two-year period. A reduction in allelic richness was observed at four weeks post treatment but recovered at six months post treatment.
	2009 (7)	40 mg/kg	Used mitochondrial <i>cox1</i> to compare the genetic diversity of <i>S. mansoni</i> populations from PSAC and mothers at baseline and six-month post

			treatment. No decline in nucleotide or haplotype diversity was detected. Nucleotide diversity at non-synonymous sites was significantly higher in Lake Victoria than Lake Albert.
	2012 (8)	40 mg/kg	Involved whole genome sequencing of <i>S. mansoni</i> from eight study villages: four villages receiving annual PZQ treatment and four receiving four annual doses of PZQ. A small significant difference in genetic diversity was reported between pre and post treatment samples. Lower genetic diversity was reported in villages receiving 'intensive treatment'.
	2014 (9)	40 mg/kg	Involved whole genome sequencing of <i>S. mansoni</i> from SAC from two districts varying in PZQ treatment history. Genomic diversity was compared between baseline and 25-27 days post treatment. Negative genome-wide Tajima's D values was observed at the district level. Comparison of pre and post-treatment populations revealed that one PZQ treatment did not reduce genomic diversity at the infrapopulation level.
	2017 (10)	40 mg/kg	Used seven microsatellite markers to compare genetic diversity of <i>S. mansoni</i> from eight boys and eight girls at baseline and five months post treatment. Genetic diversity of <i>S. mansoni</i> was not found to differ significantly between male and female hosts. Genetic diversity remained high at baseline and at follow up.
Brazil	2009 (11)	50 mg/kg	Used 11 microsatellite markers to compare the genetic diversity of <i>S. mansoni</i> from the whole community (>1 year old) in two remote villages between 2009 and 2013. A decline in genetic diversity and effective population size was detected following PZQ treatment.
	2009 (12)	50 mg/kg	Used 15 microsatellite markers to compare the genetic diversity of <i>S. mansoni</i> from the whole community in two villages. No change in genetic diversity and little genetic differentiation between <i>S. mansoni</i> parasites at baseline and follow up was found.

References

1. Norton AJ, Gower CM, Lamberton PHL, Webster BL, Lwambo NJS, Blair L, et al. Genetic consequences of mass human chemotherapy for *Schistosoma mansoni*: Population structure pre-and post-praziquantel treatment in Tanzania. *American Journal of Tropical Medicine and Hygiene* (2010) 4:951–7.

2. Gower CM, Gehre F, Marques SR, Lamberton PHL, Lwambo NJ, Webster JP. Phenotypic and genotypic monitoring of *Schistosoma mansoni* in Tanzanian schoolchildren five years into a preventative chemotherapy national control programme. *Parasites and Vectors* (2017) 1:593.
3. French MD, Churcher TS, Basáñez MG, Norton AJ, Lwambo NJS, Webster JP. Reductions in genetic diversity of *Schistosoma mansoni* populations under chemotherapeutic pressure: The effect of sampling approach and parasite population definition. *Acta Tropica* (2013) 2:196–205.
4. Huyse T, Van den Broeck F, Jombart T, Webster BL, Diaw O, Volckaert FAM, et al. Regular treatments of praziquantel do not impact on the genetic make-up of *Schistosoma mansoni* in Northern Senegal. *Infect Genet Evol* (2013) 18:100–5.
5. Lelo AE, Mburu DN, Magoma GN, Mungai BN, Kihara JH, Mwangi IN, et al. No apparent reduction in schistosome burden or genetic diversity following four years of school-based mass drug administration in mwea, central kenya, a heavy transmission area. *Plos Neglected Tropical Diseases* (2014) 10:e3221–e3221.
6. Faust CL, Crotti M, Moses A, Oguttu D, Wamboko A, Adriko M, et al. Two-year longitudinal survey reveals high genetic diversity of *Schistosoma mansoni* with adult worms surviving praziquantel treatment at the start of mass drug administration in Uganda. *Parasites and Vectors* (2019) 1:1–12.
7. Betson M, Sousa-Figueiredo JC, Kabatereine NB, Stothard JR. New Insights into the Molecular Epidemiology and Population Genetics of *Schistosoma mansoni* in Ugandan Pre-school Children and Mothers. *PLOS Neglected Tropical Diseases* (2013) 12:e2561.
8. Vianney TJ, Berger DJ, Doyle SR, Sankaranarayanan G, Serubanja J, Nakawungu PK, et al. Genome-wide analysis of *Schistosoma mansoni* reveals population structure and praziquantel drug selection pressure within Ugandan hot-spot communities. *bioRxiv* (2022).
9. Berger DJ, Crellen T, Lamberton PHL, Allan F, Tracey A, Noonan JD, et al. Whole-genome sequencing of *Schistosoma mansoni* reveals extensive diversity with limited selection despite mass drug administration. *Nature Communications* (2021) 1:1–14.
10. Trienekens SCM, Faust CL, Meginnis K, Pickering L, Ericssonid O, Nankasi A, et al. Impacts of host gender on *Schistosoma mansoni* risk in rural Uganda-A mixed-methods approach. *PLoS Negl Trop Dis* (2020) 5:1–19.
11. Barbosa LM, Reis EA, dos Santos CRA, Costa JM, Carmo TM, Aminu PT, et al. Repeated praziquantel treatments remodel the genetic and spatial landscape of schistosomiasis risk and transmission. *Int J Parasitol* (2016) 5–6:343–50.
12. Blanton RE, Blank WA, Costa JM, Carmo TM, Reis EA, Silva LK, et al. *Schistosoma mansoni* population structure and persistence after praziquantel treatment in two villages of Bahia, Brazil. *Int J Parasitol* (2011) 10:1093.

Chapter 3: Analysis of praziquantel treatment response in preschool-aged children

3.1 Introduction

Schistosomiasis affects over 200 million people worldwide, with over 90% of the disease burden found in sub-Saharan Africa, of which 123 million are children (89,90). Despite children representing a significant proportion of the disease burden, preschool-aged children (PSAC), defined as those aged five years or younger, were until recently overlooked by mapping and mass drug administration (MDA) programmes. This was due to the assumption that PSAC had minimal exposure to *Schistosoma* cercariae-infested water and, thus, were considered low-risk for infection (91). However, it is estimated that at least 50 million PSAC in Africa have schistosomiasis (92). The treatment gap experienced by PSAC may be partially attributed to the fact that praziquantel (PZQ) has regulatory approval only for children aged four years or above (95) and, until recently the lack of a paediatric formulation (96).

The new WHO NTD roadmap for the control and elimination of schistosomiasis and treatment guidelines now recommend treating PSAC \geq two years old with PZQ delivered by MDA programmes, aiming to provide equitable access to annual PZQ treatment to all age groups over two years old (99,100). However, PSAC $<$ 2 years old may be considered for PZQ treatment on an individual clinical basis from health facilities to control schistosomiasis morbidity. Currently, PZQ is administered to PSAC as crushed tablets under direct supervision with bread or juice to enhance the bioavailability of the drug (101,102). The WHO recommends that PSAC are treated with the standard PZQ dose of 40 mg/kg, which is a dose extrapolated from relatively few pharmacokinetic/pharmacodynamic (PK/PD) studies from healthy European adults and adults with differing degrees of liver failure (103,104). Despite the known limitations of this approach, including evidence from quantitative pharmacological studies showing that extrapolation does not accurately determine paediatric dosing, it continues to be used to determine dosing in children. The most recent PK/PD study compared two doses of PZQ (40 mg/kg and 60 mg/kg PZQ) in children aged 3-8 years with intestinal schistosomiasis in Uganda and found both doses to be insufficient where no child achieved antigenic cure (80). Modelling suggested up to 80 mg/kg is required to achieve the WHO-recommended cure rates (CRs) of 85%.

Commercial preparations of PZQ consist of a racemic mixture of two isomers in a 1:1 ratio: R-PZQ and S-PZQ (105). The R-PZQ isomer is responsible for the *in vitro* and *in vivo* antischistosomal action, whereas the S-PZQ isomer is significantly less effective (106). Praziquantel directly binds to the *Schistosoma mansoni* transient receptor melastatin channel ($\text{SmTRPM}_{\text{PZQ}}$) present on the tegument of the adult worm; upon activation, there is

an influx of calcium ions into the adult worm. This rapid influx of calcium ions leads to spastic paralysis and breakdown of the parasite's tegument, facilitating subsequent immunological attack and clearance of the parasite (106). However, juvenile stages (schistosomulum) are insensitive to PZQ (107). Due to the intravascular location of adult worms, adult worm death cannot be measured directly; the efficacy of PZQ is estimated using faecal egg clearance 3 to 4 weeks post-treatment (108). Worm clearance inferred by worm antigen detection using circulating cathodic antigen (CCA) and circulating anodic antigen (CAA) may provide a promising measure of worm clearance compared to traditional parasitological methods, such as egg microscopy following Kato-Katz (KK) or urine filtration (109–111).

The term PK describes the movement of a drug within the body, which encompasses the absorption, distribution, metabolism and elimination of a drug (112). Praziquantel is a pyrazinoisoquinoline drug which is rapidly absorbed and metabolised, with peak plasma concentration occurring within 1-2 hours following oral administration. The bioavailability of PZQ significantly increases with concomitant food administration and the area under the curve (AUC, represents the total exposure of a drug over time) was found to be four-fold higher with a high-carbohydrate meal (113) undergoes extensive first-pass metabolism in the liver by cytochrome P450 (CYP450) enzymes (CYP1A2, CYP2B1, CYP3A4, CYP3A4 and CYP2C19) (105) where the drug is primarily excreted in the urine (80% is cleared within four days where 90% occurs in 24 hours) (114). Several factors can impact the PK of PZQ such as age and liver health.

Globally, the performance of PZQ is generally considered satisfactory. However, there are persistent hotspots for *S. mansoni* infections throughout Africa, and despite several years of MDA with PZQ, the prevalence has remained high. The shoreside villages within the Hoima and Buliisa districts of Lake Albert in Uganda are considered hotspots for *S. mansoni* infection (115). A study found that the prevalence of *S. mansoni* was 57% among children aged three to five years in villages in the Buliisa district (116). Several studies have reported poor worm clearance in PSAC when administered the standard 40 mg/kg PZQ dose (102–104,117). The first randomised control trial (Praziquantel in Preschoolers, PIP) of PZQ in PSAC to examine the impact of 40 mg/kg vs 80 mg/kg PZQ on cure rate (CR) and egg reduction rate (ERR) has recently concluded in the Hoima district in Lake Albert, Uganda (118). The results from the cohort of 354 children showed a CR of 67% in the 40 mg/kg PZQ arm and 90% in the 80 mg/kg PZQ arm at four weeks. The difference between the ERRs from the two arms was 2% (95% CI: 1%, 3%; $P < 0.001$) and 22% (95% CI: 5%, 59%; $P < 0.001$) based on geometric and arithmetic means, respectively (Bustinduy *et al.* Under Review).

This chapter analyses the secondary data from a subset of participants from the PIP trial to investigate *S. mansoni* clearance using KK, urine CCA and CAA to determine the CR and ERR for each treatment dose (40 mg/kg vs 80 mg/kg PZQ). The impact of demographic and PK factors on the cure was then explored.

3.2 Methods

3.2.1 Ethics statement

Ethical approval was given by the Uganda National Council for Science and Technology (HS 2650), Uganda Virus Research Institute (GC/127/19/07/708), National Drug Authority (CTC 0133/2020) and the London School of Hygiene and Tropical Medicine (26571). Parental informed consent was obtained as detailed (118).

3.2.2 Study design

This is a secondary data analysis obtained from a subset of children from the PIP randomised phase II clinical trial, which is described in detail elsewhere (118). The participants were selected based on those children who were sampled for *Schistosoma mansoni* miracidia for genetic analysis in subsequent chapters. The children were primarily selected based on convenience sampling; this was the last group of children to go through baseline treatment during the November 2021 sampling visit. A total of 96 children were included in the genetic analysis, determined by the availability of miracidia samples and logistical feasibility of processing them.

The PIP trial was conducted in communities endemic for *S. mansoni* located on the shores of Lake Albert in Buliisa district, Uganda (Figure 3.1). The age of participants ranged between 12-47 months. All participants were randomised in a 1:1:1:1 ratio to one of the four treatment arms: (i) 40 mg/kg PZQ at baseline, (ii) 80 mg/kg PZQ (administered as two doses of 40 mg/kg three hours apart) at baseline, (iii) 40 mg/kg PZQ with a repeat dose at 6 months, or (iv) 80 mg/kg PZQ at baseline with a repeat dose at 6 months. Half the cohort of participants received an additional PZQ dose (the same dose given at baseline) at 6 months and the remaining half received placebo (Figure 3.1A). Due to the large PZQ tablet size, tablets were crushed, mixed with juice and administered following a meal.

Participants were randomly divided into two groups: one group underwent additional blood sampling for PK analysis and the other group underwent additional blood sampling for the assessment of immune responses to *S. mansoni* infection (data unavailable for analysis).

3.2.3 Pharmacokinetic sampling and analysis

Blood was collected at 0, 1.5, 3, 4 and 6 hours post PZQ treatments by the field team for PK analysis, using an indwelling cannula. Blood samples were centrifuged, and separated plasma was stored at -80°C.

The PK data from a subset of children who participated in the original study was kindly shared by Boniface Obura (PhD student). Briefly, PZQ plasma concentrations were quantified using liquid chromatography coupled to a mass spectrometer (LC-MS/MS) assay. Noncompartmental analysis was used to calculate R-PZQ and S-PZQ PK parameters; the maximum plasma concentration (C_{max}), time to reach C_{max} (T_{max}) and the area under the concentration-time curve (AUC) from 0 h to the last observed measurable concentration (AUC_{last} ; mg*h/L). AUC_{last} was calculated using the linear trapezoidal rule (Obura, personal communication). Total drug AUC was of particular interest due to its association with parasitological cure (80).

3.2.4 Parasitological detection and clearance

Field workers collected stool samples on at least two consecutive days for the detection of *S. mansoni* and soil-transmitted helminths using the KK technique (119), where the mean egg counts per gram of stool (epg) were calculated by the trial statistician (Emily Webb). Infection intensities were stratified into three categories: light (1-100 epg), moderate (101-400 epg), and heavy (>400 epg) (120). To assess PZQ efficacy in accordance with the WHO guidelines, the egg reduction rate (ERR), defined as the percentage decrease in egg burden from baseline to four weeks post-treatment, and CR, defined as the proportion of participants who are KK negative on all stool samples at four weeks post-treatment (an acceptable CR >85% is set by WHO (121)), were calculated.

Urine samples were also collected by the trial team for CCA and CAA antigen testing. The trial team undertook the detection of CCA antigen in urine using the point-of-care CCA (POC-CCA) rapid diagnostic test (Rapid Medical Diagnostics, South Africa). Upon visual inspection, the test strips were given a G score (a previously validated intensity visual reading score) ranging from 1 to 10 (G1-G10) for a more standardised interpretation and quantification of the outcome (122). Frozen urine samples were also sent to the Medical Research Council Uganda Research Unit in Entebbe to quantify CAA levels using the up-converting phosphor labels lateral flow (UCP-LF)-based CAA assay (123) conducted by Gloria Kakoba. The cutoff for positive of the UCP-LF assay was 2 pg/ml. The CR, the proportion of participants who were CCA or CAA antigen negative at four weeks

post-treatment, were calculated. The CCA 'trace' results were considered negative for the analyses.

3.2.5 Data analysis

Data were analysed using R Statistical Software (version 4.3.1; R Core Team 2023), table one package (version 0.13.2) (124,125) and STATA/SE (version 18.0). The first outcomes of interest were parasitological and antigen clearance rates post PZQ treatment, and then exposure covariates to achieving cure were investigated.

Respective CRs by antigen and egg clearance at four weeks were shown with the associated 95% confidence interval (95% CI). An initial comparison between treatment arms groups (40 mg/kg and 80 mg/kg PZQ) was made using a chi-squared test. The ERR at four weeks was shown as the percent decrease in egg burden at follow-up; bootstrap resampling with 10,000 replications was employed to estimate the CI. The random seed was set to 1234 for reproducibility. The ERR at four weeks between different treatment arms was compared using the Wilcoxon rank-sum test. Univariable and multivariable logistic regression models were used to understand the association between potential risk factors (weight, age, sex, baseline intensity of infection, anaemia, village, treatment regimen and pharmacokinetic parameters) and the outcome of cure (defined as egg-negative at week 4 by KK). Initially, models were constructed by adding one variable at a time in a univariate analysis with the outcome of cure, giving crude odds ratios (ORs) for each variable. Finally, a multivariable logistic regression model was built using all available risk factors (weight, age, sex, baseline intensity of infection, anaemia, village and treatment regimen), giving adjusted ORs.

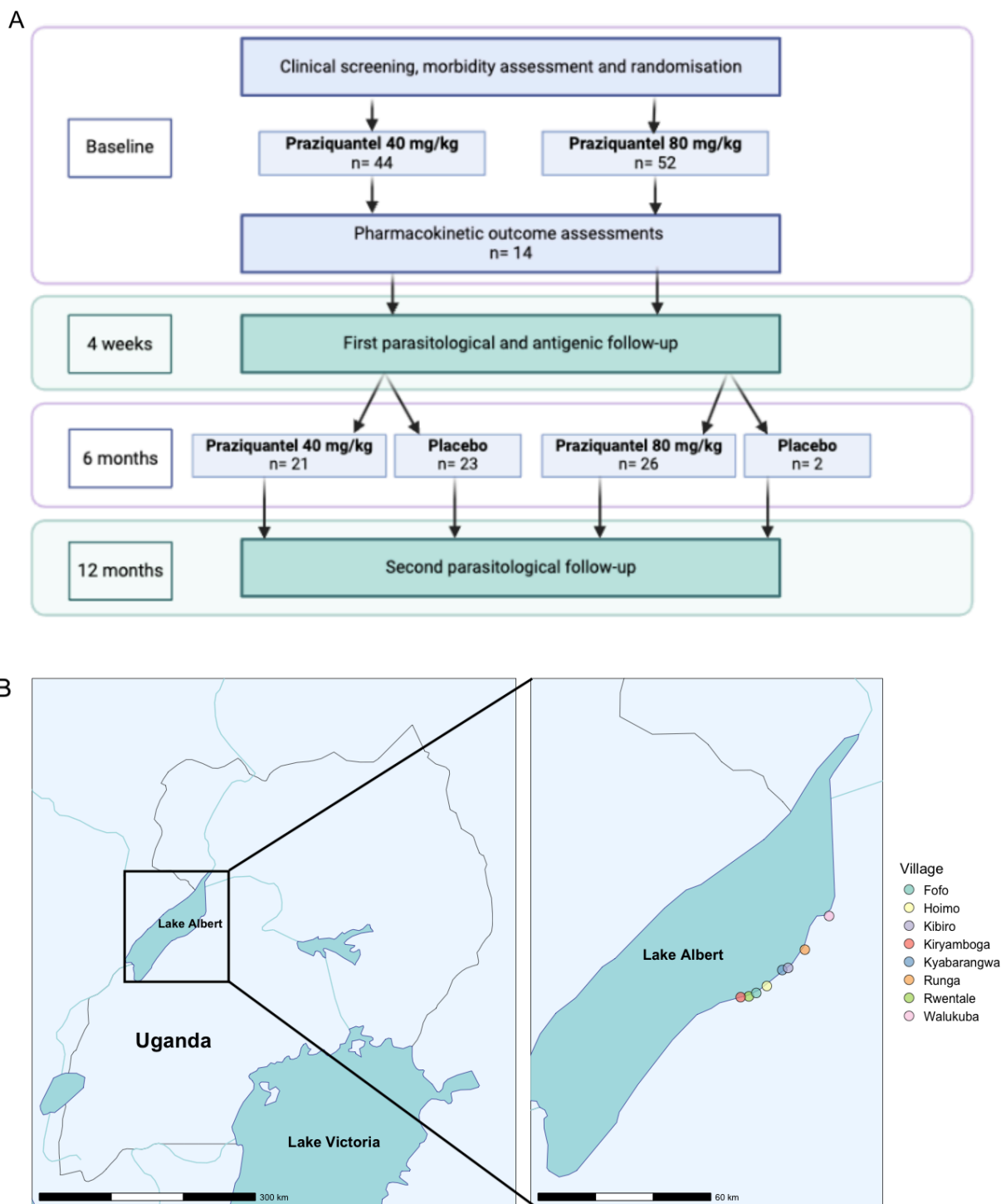


Figure 3.1: Study design and data availability. A) Schematic of the sub-study design for this work. The subset of 96 children followed in this study are from the PIP overall pool of children ($n = 354$). Figure made using Biorender.com. B) The distribution of study sites on Lake Albert, Uganda: Fofu, Hoimo, Kibiro, Kiryamboga, Kyabarangwa, Runga, Rwentale and Walukuba.

3.3 Results

3.3.1 Baseline characteristics of the sub-study cohort

Out of 354 children enrolled in the PIP clinical trial, a subset of data from 96 participants was analysed as part of a secondary data analysis within this chapter. A study flow chart of data completeness is detailed in Figure 3.2. The mean age of participants was 36 months (range 12-47 months), and 48 (50%) were male. Participants resided in eight villages bordering Lake Albert (Figure 3.1B), with the majority (55.2%) from Fofu and Kyabarangwa. A large proportion (85.4%) reported daily water contact within Lake Albert, whilst only 7.3% indicated no water contact. The participants' primary drinking water source was lake water, accounting for 99% (Table 3.1). Amongst the participants, 17.7% tested positive for malaria by rapid diagnostic test (RDT).

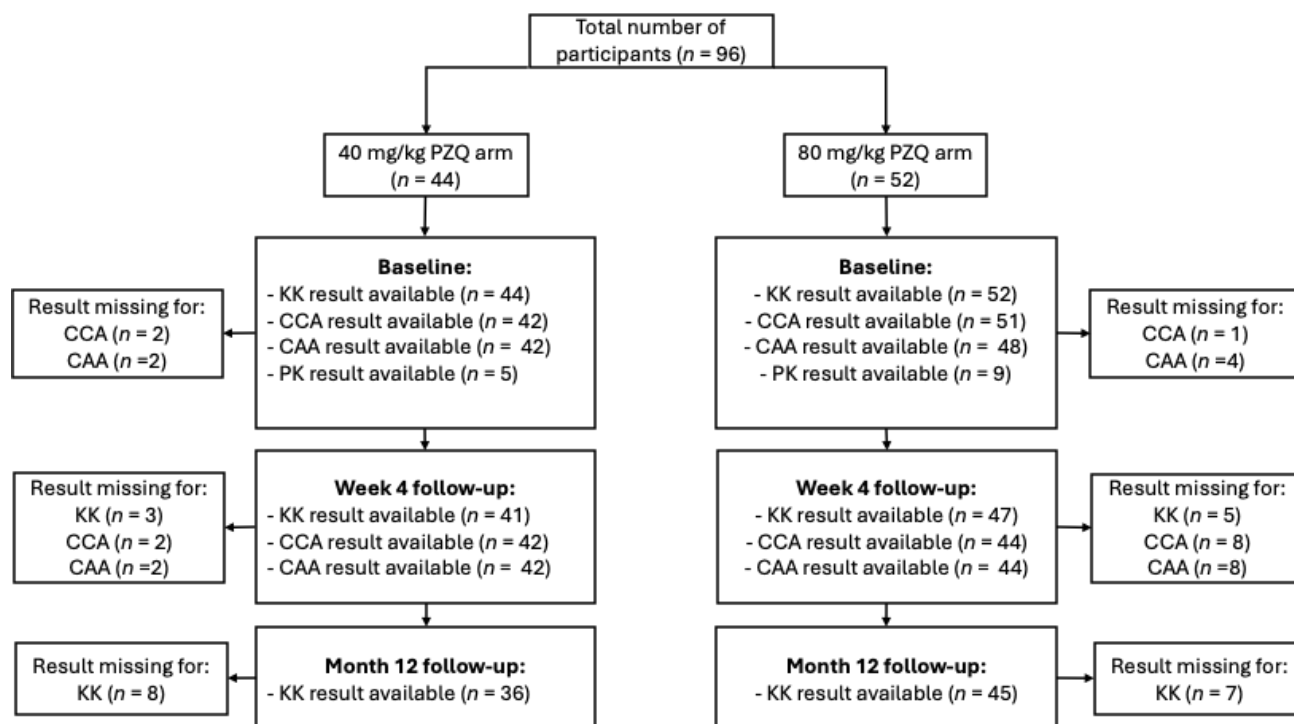


Figure 3.2: Study flow chart showing the data completeness at baseline, week four and month 12 follow-up.

Before enrolment, potential participants were screened for *S. mansoni* infection using the urine CCA, where children with a positive result were considered positive for *Schistosoma* infection. To be eligible for enrolment in the PIP trial, participants must then have tested positive for *S. mansoni* infection of any intensity as determined by KK at baseline. Therefore a KK result was available for 96/96 (100%) participants at baseline, where 55/96 (57.3%)

had moderate-to-heavy infection intensities (Table 3.1). The proportion of participants with moderate-to-heavy infections before treatment was similar between the two treatment arms ($p > 0.05$).

Table 3.1: Descriptive characteristics of study participants.

Characteristic	n= (%)			P value ^b
	Total number of children (N = 96)	40 mg/kg PZQ (N = 44)	80 mg/kg (N = 52)	
Village				0.860
Kyabarangwa	24 (25.0)	10 (22.7)	14 (26.9)	
Kibiro	5 (5.2)	3 (6.8)	2 (3.8)	
Hoimo	13 (13.5)	5 (11.4)	8 (15.4)	
Rwentale	14 (14.6)	8 (18.2)	6 (11.5)	
Runga	5 (5.2)	2 (4.5)	3 (5.8)	
Walukuba	2 (2.1)	1 (2.3)	1 (1.9)	
Kiryamboga	4 (4.2)	3 (6.8)	1 (1.9)	
Fofo	29 (30.2)	12 (27.3)	17 (32.7)	
Sex				
Male (%)	48 (50.0)	21 (47.7)	27 (51.9)	0.838
Age, months [mean (range)]	36 (12-47)	37 (12-47)	35 (16-46)	0.261
Lake contact frequency				0.281
Never	7 (7.3)	5 (11.4)	2 (3.8)	
Daily	82 (85.4)	35 (79.5)	47 (90.4)	
Weekly	7 (7.3)	4 (9.1)	3 (5.8)	
Source of drinking water				
Lake (%)	95 (99.0)	44 (100.0)	51 (98.1)	1.000
Borehole (%)	9 (9.4)	4 (9.1)	5 (9.6)	1.000
Piped (%)	5 (5.2)	3 (6.8)	2 (3.8)	0.848
Parasitic infection				
<i>S. mansoni</i> epg stool [arithmetic mean (SD)]	433.8 (788.5)	427.4 (836.5)	439.2 (753.7)	0.942
Infection intensity				0.872
Light (1-100 epg)	41 (42.7)	20 (45.5)	21 (40.3)	
Moderate (101-400 epg)	34 (36.5)	15 (34.1)	20 (38.5)	
Heavy (>400 epg)	21 (20.8)	9 (20.4)	11 (21.2)	
CCA urine				0.718
Negative	2 (2.2)	1 (2.4)	1 (2.0)	
Trace	7 (7.5)	2 (4.8)	5 (9.8)	
+	5 (5.4)	3 (7.1)	2 (3.9)	
++	1 (1.1)	0 (0.0)	1 (2.0)	
+++	78 (83.9)	36 (85.7)	42 (82.4)	
CAA conc in urine, pg/ml [mean (SD)]	526.8 (865.6)	591.8 (1001.1)	468.4 (728.3)	0.500
Malaria RDT				
Positive	17 (17.7)	9 (20.5)	8 (15.4)	0.704

^aSD, standard deviation; epg, eggs per gram; CCA, circulating cathodic antigen; CAA, circulating anodic antigen; RDT, rapid diagnostic test.

^b P value is derived from the difference between groups by Fisher exact test or Student's *t*-test.

3.3.2 Population parasitological clearance

To investigate the clearance of *S. mansoni* in the PSAC, CRs and ERRs for each treatment regimen (standard and intensive) were calculated using KK data collected at baseline and four weeks post-treatment (Appendix Table 3.1 & 3.2 and Figure 3.3). In the standard treatment arm (40 mg/kg PZQ), 30 out of 41 children were KK negative at week four (Figure 3.4A), resulting in a CR of 73% (Figure 3.3A). In contrast, the intensive treatment arm (80 mg/kg PZQ) showed a higher proportion of KK-negative children post-treatment, with 39 out of 47 achieving negative status (Figure 3.4B), yielding a CR of 83% (Figure 3.3A). However, the difference between the arms was not statistically significant ($p = 0.265$) (Appendix Table 3.1). Figure 3.3B compares ERRs between the two arms, revealing the highest ERR of 99.4% (95% CI: 98.7-99.8) in the intensive treatment group, where mean intensity decreased from 427.4 epg to 7.3 epg. Conversely, the standard group achieved an ERR of 98.3% (95% CI: 95.7-99.4), reducing mean intensity from 439.2 epg to 2.3 epg. The difference in ERRs between standard and intensive treatments was not significant ($p > 0.05$) (Appendix Table 3.2).

At six months post-treatment, children received either the same dose at baseline or placebo (Figure 3.1A) and faecal egg microscopy was done a further six months after this second treatment round (12 months post-baseline treatment). The treatment arms receiving an additional dose showed the highest proportion of egg-negative children, with 30.0% in the 80 mg/kg PZQ group, followed by 16.6% in the 40 mg/kg PZQ group. Furthermore, the proportion of moderate-heavy infections was highest in those receiving a placebo at the 6-month follow-up, with 61% in the 40 mg/kg PZQ group and 48% in the 80 mg/kg PZQ group. There was almost a 50% reduction in moderate-heavy infections in those who received the additional 40 mg/kg PZQ dose (61% vs 33%).

Antigen-based CRs were much lower than CRs based on the faecal egg microscopy in both treatment groups (Appendix Table 3.1). When CR was measured by urine POC-CCA, the CR was double in children in the intensive arm (66%) compared to those in the standard arm (33%); the difference was of statistical significance ($p=0.003$) (Figure 3.3C and Appendix Table 3.1). Additionally, the intensive treatment group demonstrated a more substantial decrease in median POC-CCA G-score than the standard treatment group, leading to a reduction from G10 before treatment to G5 and G2 in the standard and intensive groups, respectively (Figure 3.5). However, when CR was measured by urine CAA, the CRs were considerably lower, 24% and 32% in the standard and intensive arms, respectively (Figure 3.3C). Despite these lower CRs, there was a significant reduction in the mean urine CAA

concentration following PZQ treatment, with decreases of 73.3% in the standard arm and 84.5% in the intensive arm. Across all three diagnostic tests (KK, POC-CCA and CAA), there was a greater reduction in the intensity of infection and an increased CR in the intensive compared to the standard treatment arm. Despite the reductions in infection intensity reported, the CRs fall below the WHO-recommended CR of 85% for *S. mansoni*.

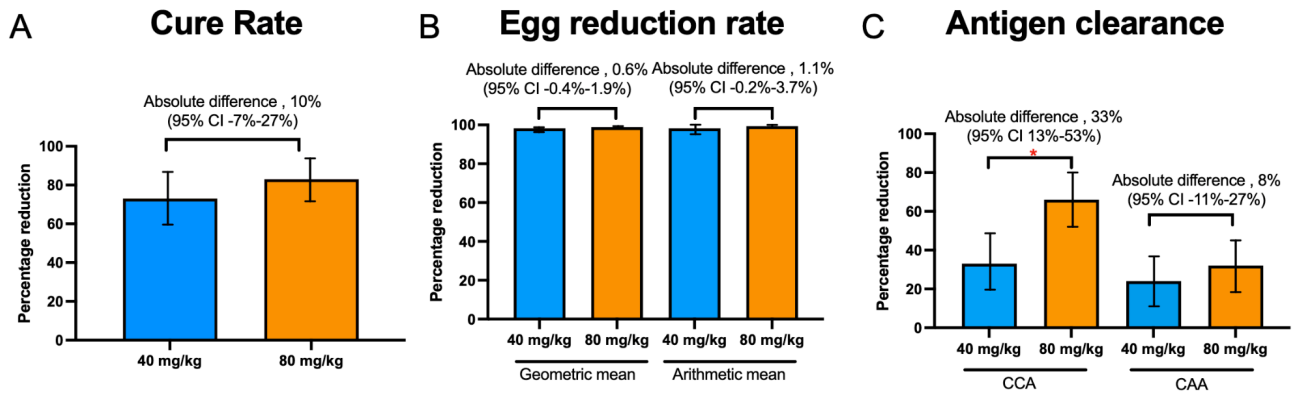


Figure 3.3: *Schistosoma mansoni* clearance outcomes comparing baseline 40 mg/kg PZQ vs 80 mg/kg PZQ at four weeks post-treatment in this sub-study. A) Parasitological cure rates; B) Egg reduction rates; C) Antigenic cure rates (CAA and CCA). The significant difference between the treatment arms is assessed using a chi-squared test and a statistically significant difference is indicated by *.

3.2.3 Individual parasite clearance by Kato-Katz

To investigate parasite clearance at an individual level, individual KK values are reported at each time point (Figure 3.4). There was a sustained drop in egg counts estimated by KK at 4 weeks post-treatment. KK negativity was achieved in 69/88 (78.4%) children (30 in the standard arm and 39 in the intensive arm) (Figure 3.4). The maximum recorded intensity decreased from 3684 epg to 0 epq in the standard arm (Figure 3.4A) and from 3222 epq to 0 epq in the intensive arm (Figure 3.4B). Additionally, both treatment arms saw substantial reductions in moderate to heavy-intensity infections, with only one child showing moderate intensity at week four post-treatment in the standard treatment arm (Figure 3.4A). This child's *S. mansoni* infection reduced from a heavy to moderate infection, where an 86.2% reduction in egg output post-treatment was observed (780 epq to 108 epq). No child had a higher egg output at 4 weeks post-treatment than pre-treatment (Figure 3.4).

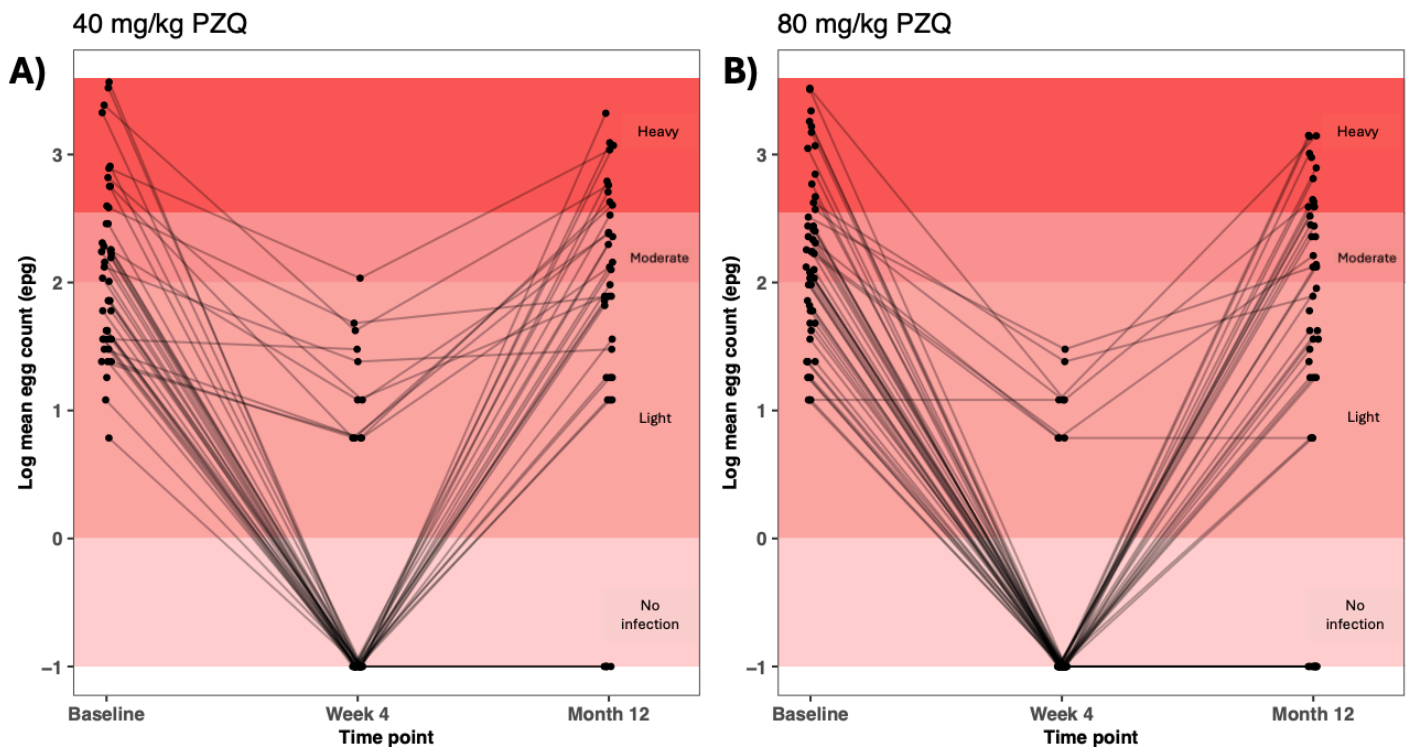


Figure 3.4: Distribution of log egg counts at three time points: baseline, week four and month 12 follow-up stratified by treatment regimen. A) 40 mg/kg PZQ arm and B) 80 mg/kg PZQ arm. Treatment arms reflect the PZQ doses administered at baseline.

3.2.3 Individual antigen clearance

To investigate antigen clearance at an individual level, individual CAA and POC-CCA values are reported at each time point (Figure 3.5). In both treatment regimens, there was a significant reduction in the mean urine CAA concentration following PZQ treatment, with a larger reduction seen in the intensive arm (Figure 3.5A and 3.5B). Despite this reduction, only 24/86 (27.9%) participants achieved CAA antigenic cure (10 in the standard arm and 14 in the intensive arm). However, CAA levels increased in 7/86 participants (2 in the standard arm and 5 in the intensive arm) (Figure 3.5A and 3B). Furthermore, more children achieved antigenic cure by POC-CCA compared to CAA, where 43/86 (50%) achieved cure (14 in the standard arm and 29 in the intensive treatment arm) (Figure 3.5B and 3.5C). After treatment, there was a considerable reduction in the prevalence of strong (++) POC-CCA results within the intensive arm (baseline= 84.3% follow-up= 25.0%) compared to the standard arm (baseline= 85.7% follow-up= 47.6%) (Figures 3B and 3C). Despite the considerable reduction in CCA intensity, 30/86 children (23.3%) had strong POC-CCA results at both

pre-treatment and post-treatment (20 in the standard arm and 10 in the intensive arm) (Figures 3B and 3C).

The agreement between KK, POC-CCA and CAA diagnostics at 4 weeks post-treatment was investigated. In total, 71 (80.7%) individuals were positive by at least one of the three diagnostic tests (36 in the standard arm and 35 in the intensive arm). Both antigen-based diagnostic tests detected the majority of the KK stool microscopy positives. However, KK stool microscopy did not detect over half of the CAA-positive cases (46/88, 52.3%). In contrast, the POC-CCA-positive cases showed more overlap with the CAA-positive cases, in which there was only disagreement in 27/88 (30.7%) of CAA positives. Only 11/71 (15.5%) participants were positive across all diagnostics at week 4 post-treatment (8 in the standard and 3 in the intensive arm).

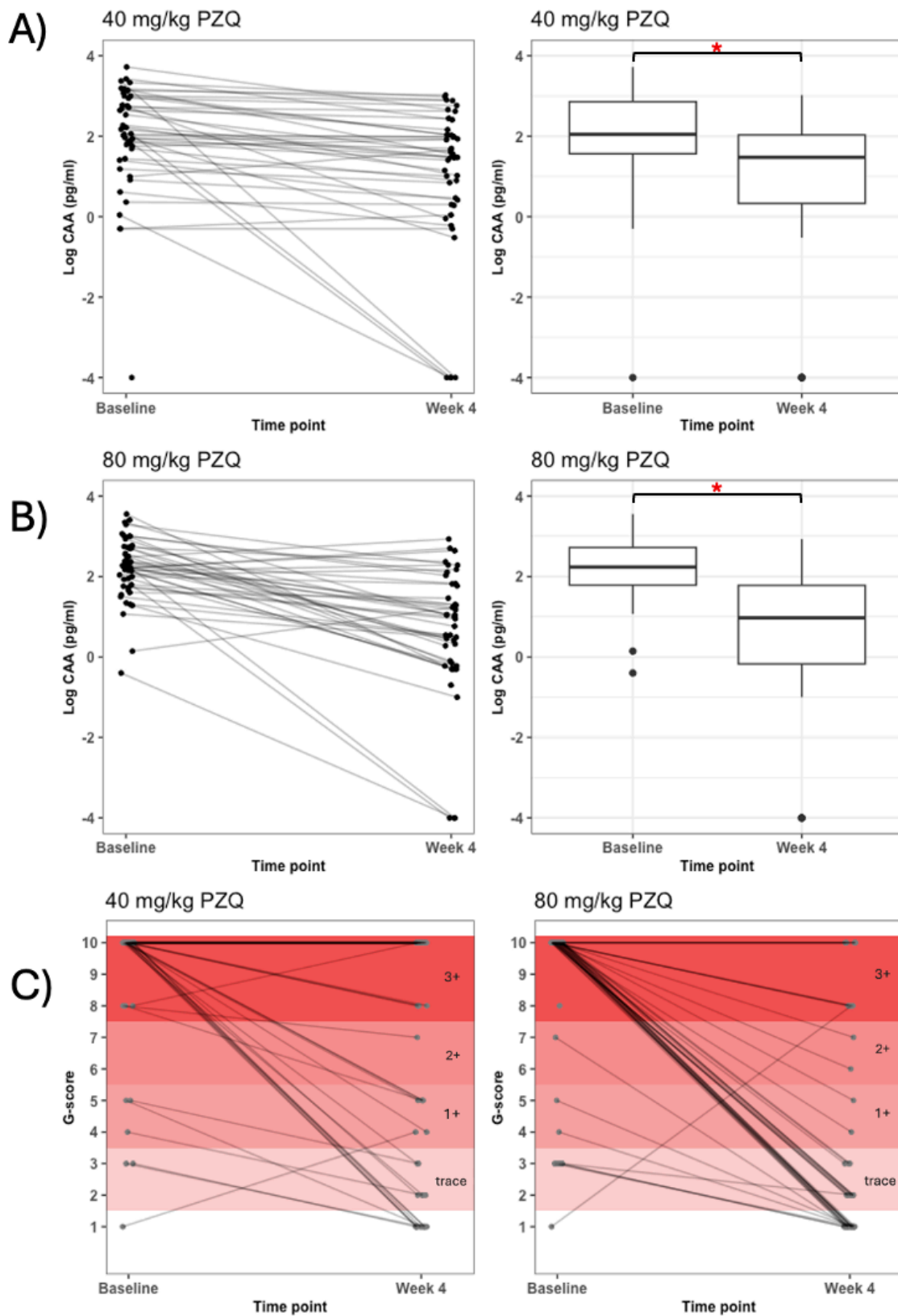


Figure 3.5: A & B) distribution of CAA antigen concentration measured in urine (pg/mL) at baseline and week 4 follow-up, stratified by treatment regimen. C) G-score distribution from the urine-based POC-CAA, stratified by treatment regimen. The significant difference

between the time points is assessed using the Wilcoxon signed-rank test and a statistically significant difference is indicated with *.

3.2.4 Impact of demographic and pharmacokinetic factors on cure rate

Univariate and multivariable logistic regression models were built to explore the relationship between CR and demographic and drug exposure parameters. The odds ratios from the logistic regression models of CR are shown in Table 3.2. Univariate logistic regression analysis investigating the impact of individual demographic factors (age, weight, gender and village) on CR did not show a significant association with cure within the models. The OR for the higher PZQ dose (80 mg/kg PZQ) was 1.788 (95% CI: 0.640-4.995) however, this did not show a significant association ($p = 0.268$). There was some evidence for an association of CR with the initial parasite load, which approached statistical significance in the multivariable logistic model (Table 3.2).

Table 3.2: Effect of infection intensity, sex, weight, age, treatment regimen, anaemia and village on cure by Kato-Katz. Testing for association was undertaken using the Wald test.

Variable	Crude OR (95% CI)*	p-value	Adjusted OR (95% CI)**	p-value
Baseline infection intensity	0.571 (0.296 -1.099)	0.094	0.472 (0.222-1.002)	0.050
Age (months)	0.968 (0.904-1.037)	0.358	0.976 (0.906-1.052)	0.531
Sex	0.667 (0.239-1.860)	0.439	0.609 (0.191-1.945)	0.402
Weight (per kg)	0.955 (0.772-1.181)	0.670	1.032 (0.801-1.329)	0.808
Anaemia	1.003 (0.359-2.806)	0.995	1.051 (0.316-3.501)	0.935
Village	1.273 (0.966-1.678)	0.066	1.293 (0.978-1.710)	0.072
Treatment regimen	1.788 (0.640- 4.995)	0.268	1.555 (0.509-4.747)	0.438

*Crude OR generated from univariate analysis of a single risk factor with the outcome of cure.

**Adjusted OR is adjusted for all variables listed within the table.

To investigate the difference in drug exposure parameters between treatment regimens, available pharmacokinetic data was used which was available from 14 individuals (five from the standard arm and nine from the intensive arm). Plasma PZQ enantiomer concentration-time profiles for individuals are shown in Figure 3.6. There was considerable inter-individual PK variability in the plasma levels of both enantiomers, with S-PZQ (Figure 3.6A) showing higher levels and slower clearance in both treatment arms than R-PZQ (Figure 3.6B). Notably, the plasma levels of both enantiomers are considerably elevated in the intensive arm compared to the standard treatment arm, though this was not statistically significant ($p > 0.05$) (Appendix Table 3.3). In the intensive arm, a double peak in the plasma concentrations of PZQ was observed approximately six hours after the initial dose, corresponding to the administration of the second PZQ dose 3 hours after the initial dose. As a result, the T_{max} was significantly different ($p = 0.0005$) between the standard (mean $T_{max} = 2.767$, SD = 0.931) and the intensive treatment arm (mean $T_{max} = 5.296$, SD = 0.974). Meanwhile, the plasma concentrations in the standard arm display the expected decrease of PZQ consistent with the drug's PK profile.

The available PK data were analysed using univariate logistic models to investigate whether an association exists between CR and drug exposure parameters. Univariate logistic regression analysis did not show a significant association between PK variables (AUC, T_{max} , and C_{max}) and cure within the models. Despite observing higher AUC values for total PZQ and AUC for both enantiomers in the cured group compared to the non-cured group, the difference was not statistically significant ($p > 0.05$). Additionally, the time to reach maximum concentration (T_{max}) was similar between the cured and non-cured groups, indicating no significant difference in the rate of absorption of PZQ between these groups. Interestingly, the maximum concentration (C_{max}) of both PZQ enantiomers was higher in the cured individuals than those not cured, although this difference also did not reach statistical significance. There was insufficient data (with only 3 “non-cured” events) to allow exploration of multivariable models.

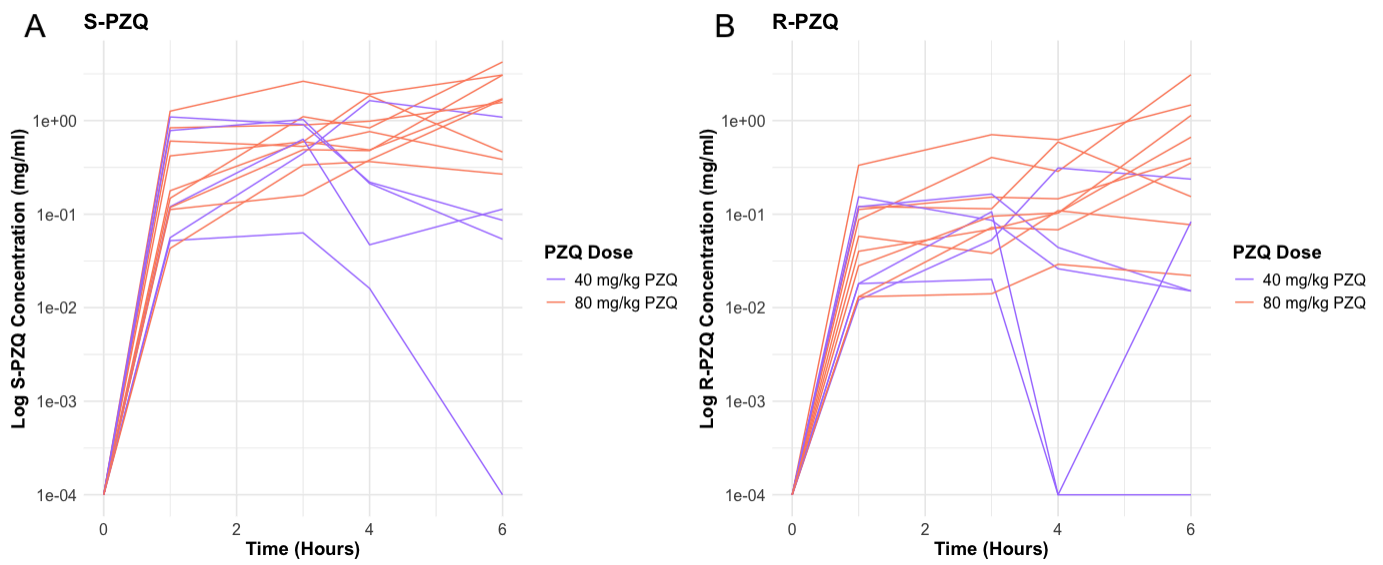


Figure 3.6: Individual PZQ plasma levels from 14 children, stratified by baseline treatment received and PZQ enantiomer. A) S-PZQ and B) R-PZQ.

3.4 Discussion

Intestinal schistosomiasis in shoreline villages of Lake Albert in our study sites represents a chronic public health problem where there is an urgent need for PZQ treatment of PSAC. At baseline, a high proportion of participants were found to have moderate-to-heavy intensity infections based on KK (55/96 57.3%), which highlights the need for PZQ treatment within this age group. The new WHO treatment guidelines for schistosomiasis recommend treating PSAC with a paediatric formulation of PZQ (99). This paediatric formulation is not yet widely available, and crushed PZQ administered with food is also recommended. However, it is likely that both the paediatric formulation and crushed PZQ tablets will co-exist in endemic settings because the paediatric formulation, while recommended by the new WHO guidelines, is not yet widely available. In many endemic settings, crushed PZQ tablets administered with food is a more accessible option for treating PSAC. Until the paediatric formulation becomes more broadly distributed and integrated into local health systems, the use of crushed tablets will likely continue as a practical and effective alternative.

This chapter investigated *S. mansoni* clearance in PSAC by determining the CR and ERR for two treatment regimens: 40 mg/kg PZQ and 80 mg/kg PZQ. In the cohort of participants followed, treatment with 80 mg/kg PZQ resulted in higher CRs compared to 40 mg/kg PZQ, although the ERR was less affected. Specifically, the CRs determined by KK were 73% for the 40 mg/kg group and 83% for the 80 mg/kg group, with an absolute CR difference of 10% (95% CI: -7% to 27%). Although this difference was not statistically significant ($p=0.265$), the observed 10% difference is notable and suggests that this study may have been underpowered to detect a significant effect. The relatively small sample size limits the ability to assess subgroup effects and potential confounders such as infection intensity, PK variability, and host factors with confidence. However, the larger PIP trial, which included a sufficiently powered cohort of 336 participants, found a strongly significant difference between treatment regimens favouring the higher dose of 80 mg/kg (Bustinduy *et al.*, unpublished). The CRs reported from the PIP cohort were 67% for the 40 mg/kg group and 90% for the 80 mg/kg group, with an absolute CR difference of 23% (95% CI: 14% to 31%). These findings indicate that the higher clearance observed in the 80 mg/kg group in this subset of participants followed in this chapter is consistent with the PIP trial results, demonstrating that the 80 mg/kg regimen is more effective and that our findings may not be due to chance.

The CRs estimated by KK are sub-optimal and below the WHO-recommended CR of 85% for *S. mansoni* (121). Several factors could contribute to the sub-optimal CRs observed in

this study. First, the high prevalence of moderate-to-heavy intensity infections at baseline (57.3%) may have led to a higher burden of infection that is more difficult to clear, even with increased PZQ dosage. Additionally, the potential for reinfection, given the high levels of water contact reported by the majority of participants, could have influenced the CRs measured at follow-up. The lakeside environment and frequent water exposure present ongoing risks for reinfection, which could partially account for the lower-than-expected CRs post-treatment. The extent of re-infection is particularly apparent in the 12-month post-baseline treatment follow-up, where the infection intensities by KK appear to have almost recovered to baseline levels. Similar findings have been reported from the Schistosomiasis in Mothers and Infants (SIMI) project in Uganda where the overall parasitological CR in PSAC was 56.4%, with significantly lower CRs reported in those children with a history of several PZQ treatments (102). Furthermore, PZQ sensitivity is dependent on the maturity of the *Schistosoma* parasite and it has been suggested that a larger proportion of cases in PSAC are from newly contracted infections consisting of PZQ-refractory juveniles (102,126). No second-round treatment was administered between baseline and four weeks post-treatment follow-up, meaning that parasite maturity may be a contributing factor to reduced PZQ efficacy (127). If juvenile stages of the parasite were present at the time of treatment, a situation most likely to occur within this region in Uganda of intense transmission, they mature and develop into adult schistosomes, leading to treatment failure (127).

Another factor to consider is the diagnostic limitations. Whilst the KK technique is commonly used for assessing CRs, its sensitivity decreases with lower infection intensities, potentially leading to an underestimation of the true burden of infection post-treatment (128). To improve the diagnostic sensitivity of KK taken post-treatment, it is recommended to use at least six KK tests (two smears per stool from three stools) (128). However, the KK data analysed in this study was generated from two stool samples taken on consecutive days, with two KK smears taken per stool sample, which may be insufficient to assess PZQ efficacy. This issue is further highlighted by the discrepancies observed between KK and antigen-based diagnostic tests, such as POC-CCA and CAA, which often detected cases that KK missed. The lower CRs determined by CAA and POC-CCA indicate that some residual infection persisted, which KK failed to detect, thus questioning the reliability of CRs based solely on stool microscopy (80).

It is not possible to directly measure the burden of *S. mansoni* adult worms due to their location in the mesenteries. Instead, eggs counted from KK are used to estimate infection intensity. Antigen-based diagnostics for adult worm CCA or CAA antigens detect active

infections and are potentially more sensitive than KK in low-transmission areas (128). The CRs were significantly lower when using urine-antigen-based diagnostics compared to using KK. Although very poor CRs were obtained when POC-CCA was used to measure cure, a significantly higher proportion of children achieved antigenic negativity when given an 80 mg/kg PZQ dose (Figure 3.3C). The poor POC-CCA CRs found in this study are consistent with findings reported elsewhere (102). The disparity between KK and POC-CCA CRs may be due to the lower specificity of the POC-CCA, particularly in PSAC, a population where high rates of false positives have been reported in children with no previous exposure to *S. mansoni* (129). The presence of false positives in non-endemic populations suggests that POC-CCA might have a reduced specificity, potentially leading to overestimating active infections when used alone. Other issues have been reported surrounding the interpretation of the POC-CCA test, particularly with trace signals (130–133) and batch variation (134–136). This raises concerns about the reliability of POC-CCA as a diagnostic tool in endemic areas, particularly when assessing CRs post-treatment and particularly in PSAC and pregnant women.

The CRs estimated by the CAA diagnostic assay were the lowest of the three diagnostic tests used. The upconverting phosphor lateral flow (UCP-LF) assay to detect CAA has been found to be highly sensitive and specific for the detection of all human-infecting *Schistosoma* species (111,137–142) and is particularly useful in quantifying low-worm burdens. Urine CAA levels experienced a significant drop at follow-up, with a greater effect seen in the 80 mg/kg PZQ arm, therefore confirming the specificity of the CAA test. It is important to highlight that the diagnostics used in this study detect different lifecycle stages; KK detects eggs examined under a microscope, and antigen-based diagnostics detect antigens released by adult worms (143). Individuals found positive by an antigen test after treatment, whilst no eggs are detected with KK, indicate that the infection has not fully cleared. Mature adult worms may have been affected by PZQ but not killed, resulting in a temporary cessation of egg production (embryostasis) (128), whilst still excreting CAA and CCA antigens. Drug-induced embryostasis has been reported in other parasitic helminths, such as *Ascaris suum* and *Onchocerca volvulus* (144,145). Further explanations for a negative KK result and a positive CAA or CCA result include the presence of single-sex infections, either acquired or the result of drug treatment, which could explain the disruption of egg production despite active infection (146–149).

Furthermore, insufficient dosing and PK factors pose another potential explanation for the poor CRs observed. This study found that the standard 40 mg/kg PZQ dose was insufficient to achieve the WHO-recommended CR of 85%, which has been found elsewhere (80). The

PK data, although limited, suggest that there is considerable interindividual variability in drug absorption and metabolism, which could influence PZQ treatment efficacy. Despite higher plasma concentrations of PZQ enantiomers in the intensive arm, this did not translate into significantly higher CRs. There was insufficient data (with only 3 “non-cured” events) to allow exploration of the potential impact PK factors have on cure and it is difficult to see differences in this study, which is likely underpowered.

Another potential factor contributing to the low CRs observed in this study is the emergence of drug-resistant *S. mansoni* parasites to PZQ. Although drug resistance is not yet widely documented in endemic areas, the possibility of resistance developing should be considered, particularly in Uganda, where repeated MDA has been ongoing since 2003. This topic is explored in more detail in Chapter 5, where genetic data from individual *S. mansoni* miracidia was generated to investigate the genetic impacts of PZQ treatment in these populations.

This study highlights the challenges of achieving WHO-recommended CRs in PSAC and the need for improved treatment regimens in young children. The findings indicate that an 80 mg/kg PZQ dose results in higher clearance than the standard 40 mg/kg regimen, though factors such as baseline infection intensity, reinfection risk, and diagnostic limitations complicate the interpretation of treatment efficacy. The small sample size reduces the statistical power to detect certain effects, particularly in relation to PK variability and host factors. Larger studies and genomic analyses of *S. mansoni* populations are needed to further investigate treatment outcomes and the potential for emerging drug resistant *S. mansoni*.

Chapter 4: Population genomic
characterisation of Ugandan
Schistosoma mansoni

4.1 Introduction

There has been a significant interest in understanding the genetic dynamics of parasite populations, particularly *Schistosoma* species that infect humans (150–154) and livestock (155,156). Understanding the genetic structure of natural *Schistosoma* populations provides insights into transmission and epidemiology (154,157,158). The population structure of *Schistosoma mansoni* parasites spans various spatial scales, and it is the most studied species across these geographical levels. At a global scale, populations are sampled within different endemic countries or continents. Regionally, populations are sampled within the same district across multiple infection foci. Locally, populations originate from the same village or infection foci, such as a specific lake shoreline or river. At the intrapopulation level, samples consist solely of schistosomes or their offspring from the same individual snail or human host. Understanding the relatedness of *S. mansoni* populations at different spatial scales will allow the study of the diversity and distribution of populations. This will provide insights into host mobility, immunity and the impact of control interventions such as mass drug administration (MDA) of praziquantel (PZQ).

Schistosoma mansoni exhibits high genetic diversity at both mitochondrial and nuclear loci, with clear geographical structuring on a global scale and a notable genetic separation between East and West African populations (150,152,154,159,160). Most studies have used mitochondrial markers such as the *cytochrome oxidase subunit 1 (cox1)* and nuclear microsatellites (154,160–165) to explore the population structure and diversity of African *S. mansoni* populations. These studies have shown that African *S. mansoni* populations display substantial diversity, with East African populations exhibiting the highest genetic diversity (154,160). Mitochondrial analysis of *S. mansoni* samples from East Africa (Uganda, Coastal Kenya, Kenya, Tanzania and Zambia), West Africa (Senegal, Niger, Mali, Nigeria and Cameroon), the Middle East (Oman, Egypt and Saudi Arabia) and South America (Brazil) showed geographical separation into five discrete lineages, where East African samples formed three of the lineages (160). Lower genetic diversity is observed in South American *S. mansoni* populations, and several studies, including genomic data have hypothesised that *S. mansoni* was recently transported to South America through the trans-Atlantic slave trade from West Africa (150,160,166,167).

Several studies have attempted to explore the population structure of *S. mansoni* at a regional scale, particularly in Uganda. Stothard *et al.* (165) sampled miracidia from children attending schools in Lake Albert and Lake Victoria, two major intestinal schistosomiasis

hotspots (approximately 175 km apart). Using a 396 bp region of the *cox1* gene, they identified clear genetic differentiation between *S. mansoni* populations from the two lakes. However, the samples analysed within this earlier study were adult worms from field isolates that had been passaged through laboratory snails and rodents. This isolation and passaging has a selection effect, meaning that these samples may not fully represent the diversity within natural settings (19). Despite this, later findings from Betson *et al.* (161) using the same region of *cox1* to explore the population structure in *S. mansoni* miracidia collected from preschool-aged children (PSAC) and their mothers from both lakes, again identified clear population separation between the two lakes. Recently, whole genome sequencing data confirmed this separation and showed that Ugandan *S. mansoni* populations displayed regional structuring (152). However, the study was constrained by the small sample size of Lake Albert samples ($n = 2$), with a bias towards those collected from Lake Victoria ($n = 222$) (152), limiting a full evaluation of genetic differentiation. This study found that any distinct population structure tends to fade at the local village level where *S. mansoni* appears to form diverse panmictic populations. This has also been found in other African countries, which report diverse panmictic populations with a lack of population structure at relatively smaller scales, particularly at the village level and between sites up to 60 km apart (168–171), suggesting high rates of gene flow and few barriers to transmission (168–171). At a local scale, several factors are expected to promote the homogenisation of *S. mansoni* between populations, including sexual reproduction of adult schistosomes and long-lived and mobile human hosts (172).

Generating high-resolution genomic data from *Schistosoma* populations under drug pressure could provide valuable insights into evolutionary changes in parasite populations due to drug treatment, especially in light of the shift from morbidity control to elimination (173). Exploring the geographical structuring of *S. mansoni* at a regional scale is essential for discerning how potential PZQ resistance may spread. Clear geographical structuring could limit the spread of any resistance, keeping it localised, whereas a lack of structuring suggests extensive gene flow, potentially leading to the rapid spread of PZQ-resistant *S. mansoni* populations. The availability of high-quality genomic resources for *S. mansoni* (174,175), particularly its highly contiguous reference chromosome-level genome assembly, provides an important prerequisite for informative genomic investigations of *S. mansoni*. However, the size and complexity of the *S. mansoni* genome presents a financial and analytical obstacle in sequencing whole genomes despite the falling sequencing costs (176). An additional challenge in conducting population genetic studies from living mammalian hosts is the inaccessibility of the adult stages within human hosts, as only eggs or miracidia are directly available. However, these progeny may not necessarily go into transmission, so there is

some uncertainty in using them to infer transmission dynamics. Furthermore, the very low quantities of DNA that can be obtained from individual *Schistosoma* larval stages have, until recently, restricted population genetic studies to a small number of genetic loci, which limits the genetic information that could be obtained from each sample (177). To overcome the low DNA quantities, whole genome amplification (WGA) of genomic DNA (gDNA) from individual larval stages has been applied to increase DNA levels and this has enabled exome (176,178) and whole genome sequencing (WGS) (151,152,177) of individual *Schistosoma* miracidia. Recently, WGA was applied to individual *S. mansoni* larval stages collected from endemic regions in Uganda to allow the generation of short-read whole genome sequence data (152). This study represents an important milestone in schistosome genomics and provides a foundation for genomic surveillance of *Schistosoma* and other helminths. However, WGA can have several drawbacks, including increased cost, incomplete genome coverage, allelic dropout and amplification bias, which have been reported in single-cell genome sequencing (179). To avoid potential issues with WGA of extracted DNA prior to sequencing, a low-input library preparation method has been developed to generate whole genome libraries for short-read sequencing (Illumina) from small cell populations (180). This methodology has been successfully applied to generate whole genome libraries and genomic data from individual *S. mansoni* larval stages (153,177).

Most genome-level investigations of *S. mansoni* populations sampled in Uganda are from shoreline villages around and islands within Lake Victoria (151–153), whilst investigations of Lake Albert *S. mansoni* have been scarce. This current study aims to address this gap by generating whole genome sequence data using low-input library preparation methodology for 96 individual *S. mansoni* miracidia collected from shoreline villages in Lake Albert. Published WGS data from shoreline villages and islands in Lake Victoria and an inland district were included in the analysis. Using these datasets, this chapter aimed to explore the genetic diversity and the regional structuring of *S. mansoni* populations within Uganda. Furthermore, by comparing miracidial populations from shoreline villages of Lake Albert (Hoima district) and Lake Victoria (Mayuge and Koome Islands) and inland (Tororo), the gene flow and population dynamics between the two major water bodies were investigated.

4.2 Methods

In this chapter, whole genome sequence data were generated from 96 *Schistosoma mansoni* miracidia, which I then compared to published *S. mansoni* genomic data from six countries (Appendix Table 4.1). The methodology below focuses on the collection and generation of sequence data for the samples sequenced in this study only.

4.2.1 Ethics statement

The Uganda National Council for Science and Technology (HS 2650), Uganda Virus Research Institute (GC/127/19/07/708), National Drug Authority (CTC 0133/2020), and the London School of Hygiene and Tropical Medicine (26571) gave ethical approval for the collection of samples. Parental informed consent was obtained as detailed (118). A material Transfer Agreement was obtained to transfer samples from Uganda to LSHTM (Appendix Figure 4.10).

4.2.2 Sample collection

Samples were obtained from the Praziquantel in Preschoolers (PIP) trial carried out in *S. mansoni* endemic villages located on the shores of Lake Albert in the Buliisa district in Western Uganda (118). The trial focused on comparing parasitological cure rates (CRs) of participants aged 12-47 months receiving either 40 mg/kg or 80 mg/kg PZQ. The prevalence of *S. mansoni* infection in children aged 3-5 years in these villages has recently been found to be 57% by Kato-Katz (116). These samples were obtained from three villages in the Hoima district (Fofu, Kyabarangwa and Rwentale), which is adjacent to Lake Albert, an area endemic for *S. mansoni* (115) (Figure 4.1). The detailed protocol for miracidial hatching is detailed in Appendix Figure 4.1. In brief, at baseline and six months post-treatment, schistosome eggs were isolated from the stool of participants with *S. mansoni* infection. To isolate eggs, stool samples were homogenised through a 425 µm steel sieve, then diluted in bottled water (Rwenzori, Uganda) and further filtered using an adaptation of the Pitchford-Visser funnel method (181). For each sample, the concentrated stool solution containing the *S. mansoni* eggs was transferred to a Petri dish in clean bottled water and exposed to torchlight for several hours to induce miracidial hatching. Single miracidia were visualised under a dissecting microscope, picked in 2 µl and washed twice in Petri dishes containing clean bottled water to dilute stool-derived bacterial contamination before being placed on an FTA indicator card (Qiagen) (182). My reflections from fieldwork in Uganda are detailed in Appendix Figure 4.2.

4.2.3 DNA extraction

For gDNA extraction from each *S. mansoni* miracidium, a 2.0 mm disc containing the sample spot was removed from the FTA card using a Harris-Micro-Punch (Fisher Scientific, UK) and placed into a 0.2 ml microcentrifuge tube. 30 µl of lysis buffer was prepared (1.25 µg/mL protease (Qiagen 19155), 30 mM Tris-HCl pH 8.0, 0.5% IGEPAL/NP40 (Merck) plus 0.5% Tween 20 (Sigma Aldrich) (177,183) and added to each punch containing the *S. mansoni* miracidia DNA. Samples were incubated at 50°C for 60 min, followed by heating to 70°C for 30 min to allow protease inactivation. Following incubation, samples were spun down to recover maximum volume, and the lysate was transferred to a clean 0.2 mL microcentrifuge tube before being stored at -80°C until further use.

The *S. mansoni*-specific TRP1 PCR (described in detail in Chapter 5) was used to check for the presence of *S. mansoni* DNA in each lysate. Briefly, the TRP1 PCRs had a total reaction volume of 25 µL, which included 3 µL of the lysate, 12.5 µL Phusion high-fidelity PCR master mix with HF buffer (New England Biolabs, UK) and 10 pmol of each primer. Thermal cycling conditions were: 30 sec denaturing at 98°C, 40 cycles of 98°C for 10 sec, 65°C for 30 sec and 72°C for 45 sec, followed by 10 min at 72°C. Four microlitres of each reaction were visualised by 1% agarose gel electrophoresis with GelRed staining. Samples which successfully amplified TRP1 proceeded to sequencing library preparation. Specifically, DNA extractions were selected for WGS from miracidial samples collected from 24 children with four miracidia per child.

4.2.4 Optimisation of sequencing library preparation

The low-input enzymatic fragmentation-based library preparation method (180,184) was optimised on TRP1 positive DNA extractions from single miracidia to meet the sequencing requirements for Novogene's lane sequencing service, specifically for the NovaSeq 6000 PE150. The sequencing requirements included a library size of 320-520 bp with adapters and an overall library concentration of 0.5 ng/µl. Fragmentation times (12-20 mins), the number of PCR cycles (12-14 cycles), polymerases (PCRBioSystems VeriFi polymerase vs NEB Ultra II Q5), magnetic bead ratios, and bead brands (KAPA Pure Beads vs NEB sample purification beads) were optimised. The optimised conditions and reagents used are described in the methods below.

4.2.5 Library preparation

Library preparation was performed in batches of eight samples. For each sample, 22 μL of lysate was mixed with 63 μL (0.9x beads: sample ratio) of KAPA Pure Beads (Roche Diagnostics) and 48 μL of TE buffer followed by a 5 min binding reaction at room temperature. Magnetic bead separation was then undertaken to purify gDNA, followed by two 80% ethanol washes. The beads were then resuspended in 26 μL TE buffer, facilitating the release of DNA from the beads. The solution containing the DNA elution plus the magnetic beads was integrated into the library preparation workflow to avoid the loss of high molecular weight gDNA, which has been reported in previous studies (180). For DNA fragmentation and A-tailing, each sample was mixed with 7 μL NEBNext Ultra II FS buffer and 2 μL NEBNext Ultra II FS enzyme (New England Biolabs). The reactions were incubated in a thermal cycler at 37°C for 12 min followed by 65°C for 30 min with the heated lid set to 75°C. To generate adaptor-ligated libraries, 30 μL NEBNext Ultra II ligation master mix, 1 μL NEBNext ligation enhancer and 2.5 μL diluted 1:25 NEBNext Adaptor for Illumina was added to the reaction, followed by incubation at 20°C for 20 min with the thermal cycler heated lid off. 3 μL of USER enzyme was added to the ligation mixture and incubated at 37°C for 15 min with the heated lid set to 50°C. Adaptor-ligated DNA was cleaned by adding 72 μL KAPA Pure Beads (0.6x beads: sample ratio) and 50 μL TE buffer. Libraries were amplified by adding 25 μL NEBNext Ultra II Q5 Master Mix, 10 μL Index/Universal Primer to 15 μL of ligated DNA fragments. Each sample was then thermo-cycled under the following conditions: 98°C for 30 sec, 14 cycles of 98°C for 10 sec, 65°C for 75 sec and a final extension of 65°C for 5 min. To purify the amplified libraries, KAPA Pure Beads were added in a 0.8:1 volumetric ratio of beads to the library and eluted in 25 μL 0.1x TE.

Each library was quantified using the Qubit high-sensitivity kit (Invitrogen), and DNA fragment size distributions were confirmed in a random subset of samples using a D1000 ScreenTape on TapeStation (Agilent). Library concentrations were adjusted to 0.5 ng/ μL , and all 96 libraries were combined in a single pool. The pooled library was quantified using a Qubit high-sensitivity kit, and DNA size distributions were confirmed using a D1000 ScreenTape on TapeStation. To achieve the required fragment size range (320-520 bp), a size selection bead clean-up using KAPA Pure Beads was undertaken on the pooled library, which involved two cuts; the first 0.6x cut excludes DNA >450 bp from the library-containing supernatant and the second 0.2x volumes of KAPA Pure Beads results in the binding of all DNA fragments > 250 bp but < 450 bp to the beads. Finally, the pooled library was eluted from the magnetic beads in 65 μL 0.1x TE. The size and density distribution of the DNA fragments in the final pooled library met the sequencing requirements, as shown in Appendix

Figure 4.5. Whole genome sequencing of the pooled library was undertaken externally on an Illumina Novaseq 6000 S4 lane (Novogene, UK).

4.2.6 Sequence quality control and mapping

Raw sequencing data generated has been uploaded to the European Nucleotide Archive (ENA) repository. Novogene UK removed adapters from the raw sequencing reads. Read mapping was performed using a Nextflow pipeline developed at the Wellcome Sanger Institute (185). Raw sequencing reads were aligned to the *S. mansoni* (version 10) (174,186,187) reference genome using minimap2 (version 2.16), and PCR duplicates were removed using Sambamba markdup (version 1.0) (188). Sequencing coverage across the genome was calculated in 25 kb non-overlapping sliding windows and per chromosome, using bamtools (version 2.5.1) (189), bedtools makewindows (version 2.31) (190) and samtools bedcov (version 1.17) (191). To explore the variation in mapping rates and coverage, raw reads were screened with Kraken2 (version 2.1.2) against a database containing Human, Mouse, Bacteria, Virus and Plasmid datasets (192), and Kraken2 reports were visualised using MultiQC (version 1.17) (193).

4.2.7 Published datasets

Raw sequencing reads were downloaded (Appendix Table 4.1) from the European Nucleotide Archive (ENA, <https://www.ebi.ac.uk/ena>) for 150 *S. mansoni* WGS accessions from previously published studies (150–152). Forty-seven published WGS datasets were from samples collected from the Koome, Damba, and Lugumba Islands (Uganda), collectively referred to as the Koome Islands (151), and 96 were from samples collected from Southern Uganda from two districts, Tororo and Mayuge (152). The remaining published WGS datasets were from samples collected from outside of Uganda, including Guadeloupe ($n=3$), Cameroon ($n=1$), Puerto Rico ($n=1$), Coastal Kenya ($n=1$) and Senegal ($n=1$) (150). The geographical distribution of samples is detailed in Figure 4.1. Raw reads were mapped to the *S. mansoni* genome (Version 10) using the same Nextflow pipeline described above.

4.2.8 Sample geographical distribution

The geographical location from which each sample was collected for both the published and newly generated datasets was plotted using the longitude and latitude for sample origins. The map detailing the geographic distribution of each sample incorporated in the analyses (Figure 4.1) was prepared using R packages ggplot2 (version 3.5.1), rnaturalearth (version 1.0.1), sf (version 1.0.16), patchwork (version 1.2.0), ggspatial (version 1.1.9), dplyr (version

1.1.4) and grid (version 4.3.1). Administrative boundaries were sourced from Natural Earth <https://www.naturalearthdata.com/>, excluding Antarctica.

4.2.9 Sex determination

To determine the potential sex bias that might influence drug resistance analysis, the sex of each *S. mansoni* miracidia was inferred by analysing specific regions of the sex chromosomes with females being heterogametic (ZW) and males homogametic (ZZ). In the genome assembly, the Z chromosome is flanked by two regions termed pseudoautosomal regions (PAR) 1 and 2, which are common to both sex chromosomes. A sequence termed the Z-specific region (ZSR) displays a lower coverage in heterogametic females.

To identify the sex of the *S. mansoni* miracidia analysed, the median coverage in 2 kb windows across PAR1 (coordinates 1-10,680,111 bp), PAR2 (coordinates 43,743,322-86,692,428 bp) and the Z-specific region on the Z chromosome (ZSR) (coordinates 10,680,112- 43,743,322 bp) was calculated. From these, the ZSR: PAR ratio was calculated; miracidia with >0.7 ZSR/PAR ratio and a PAR/ZSR <1.5 were inferred males, and miracidia with <0.7 ZSR/PAR ratio and a PAR/ZSR >1.5 were inferred females (152,174).

4.2.10 Variant calling and filtering

Variant calling for each sample was performed using GATK Haplotype Caller (version 4.1.4.1) by generating individual per sample genomic VCFs (GVCFs) (`--minimum-mapping-quality 30 --min-base-quality 20 --standard-min-confidence-threshold-for-calling 30`). Sample GVCFs were merged using GATK CombineGVCFs before joint genotyping using GATK GenotypeGVCFs. Using GATK SelectVariants, the output was split into mitochondrial and nuclear variants, then again into single nucleotide polymorphisms (SNPs) and indels, to be filtered separately by GATK VariantFiltration. Variant distributions were plotted, and variants were hard filtered based on removing the relevant tails from the distributions (usually the upper and/or lower 1%) on the following quality metrics: Quality (QUAL), QualByDepth (QD), FisherStrand (FS), StrandOddsRatio (SOR), RMSMappingQuality (MQ), MappingQualityRankSumTest (MQRanksum), ReadPosRankSumTest (ReadsPosRankSum), Depth (DP) (Appendix Figures 4.3 and 4.4). Using VCFtools (version 0.1.16), variants were further filtered using the following criteria: minimum and maximum alleles = 2, minor allele frequency < 1%, per sample missingness > 0.55, site missingness > 0.125, and low inbreeding coefficient > -0.5.

4.2.11 Sample relatedness

Pairwise sample relatedness between pairs was calculated using VCFtools (`--relatedness2`) based on the KING inference (21). Pairwise kinship coefficient values > 0.45 , $0.20-0.45$, $0.10-0.20$ and $0.05-0.10$ were used to classify monozygotic twins, full-siblings or parent-child (first-degree), cousins (second-degree), and great-grandchildren from shared grandparents (third-degree) relationships, respectively. A network graph was constructed using tidyverse (194) and igraph (195) packages in R to visualise the relationships among samples, with nodes representing individuals and the thickness of edges indicating kinship coefficients.

4.2.12 Population structuring

Within this chapter, a population is defined as miracidia from one district: Hoima, Tororo, Koome Islands and Mayuge. To investigate the broad-scale genetic relatedness between populations, variants found in strong linkage disequilibrium (LD) were removed using PLINK (version 1.9). Genome scans were conducted using 50 variant sliding windows in steps of 10 variants, and an r^2 threshold of >0.15 was used to remove highly linked variants in windows. Variants from the Z and W chromosomes were excluded due to the presence of both male and female *S. mansoni* miracidia in this dataset.

Autosomal SNPs were converted into Phylip format (<https://github.com/edgardomortiz/vcf2phylip/vcf2phylip.py>), and invariant sites were removed (<https://github.com/btmartin721/raxml/ascbias/ascbias.py>). A maximum-likelihood phylogenetic tree was created using IQ-TREE software (version 2.2.6) (196). IQTREE was run using ModelFinder, the best-fit substitution model (GTR+F+ASC+R10) and 1000 ultrafast bootstraps were used. The phylogenetic tree was visualised in iTOL (197) (version 6.9.1) with midpoint rooting.

Principal component analyses (PCA) were conducted using PLINK (version 1.9) on four variant datasets. The first was unlinked autosomal SNPs from all samples from all locations, followed by analysis of only Ugandan samples; unlinked autosomal, mitochondrial, and mitochondrial *cox1*.

4.2.13 Within population diversity

A VCF file containing all sites (including variant and invariant sites) was derived from the per-sample GVCFs generated by GATK (as described above). Pixy (198) (version 1.2.8.beta) calculates nucleotide diversity (π) whilst accounting for invariant sites, which is

essential for calculating π . VCFtools (version 0.1.16) was used to filter the VCF; indels and any sites with $\geq 20\%$ missing data were removed. This was used as an input for pixy to calculate genome-wide π in 5 kb non-overlapping sliding windows along each autosome and Z chromosome for each population from Ugandan districts. The mean π within each population was calculated individually, and the symmetric 99% bootstrap confidence intervals of the mean were estimated using R. The Wilcoxon Rank sum test was used to assess the statistical significance of π comparisons.

4.2.14 Between population diversity

The all-sites VCF was used to calculate genome-wide relative (F_{st}) and absolute (D_{xy}) divergence between pairs of populations using pixy (version 1.2.8.beta) in 5 kb sliding windows along each autosome and the Z chromosome. Prior to the calculation of genome-wide mean F_{st} values, negative F_{st} values were adjusted to 0. The mean F_{st} and D_{xy} between each population comparison was calculated individually, and the 95% confidence intervals of the mean were estimated using R.

To investigate the ancestral composition of Ugandan *S. mansoni* populations by district, ancestral analysis was performed using unlinked autosomal variants and running ADMIXTURE (version 1.3.0) (199) with K values (the number of ancestral populations) ranging from 2-10, 10-fold cross-validation, standard error estimation with 250 bootstraps. A random seed of 64 was used. The most likely number of ancestral populations (K) was predicted by ADMIXTURE using cross-validation error (Appendix Figure 4.8).

4.3 Results

4.3.1 Whole genome sequencing of miracidia

In this chapter, 96 *S. mansoni* miracidia from PSAC enrolled in the PIP clinical trial (see Chapter 3 for more details) (1) were selected for whole-genome sequencing, a sample size constrained by funding limitations. I analysed this data in addition to 150 published *S. mansoni* genomic data from six countries, making a final dataset of 246 samples (Figure 4.1).

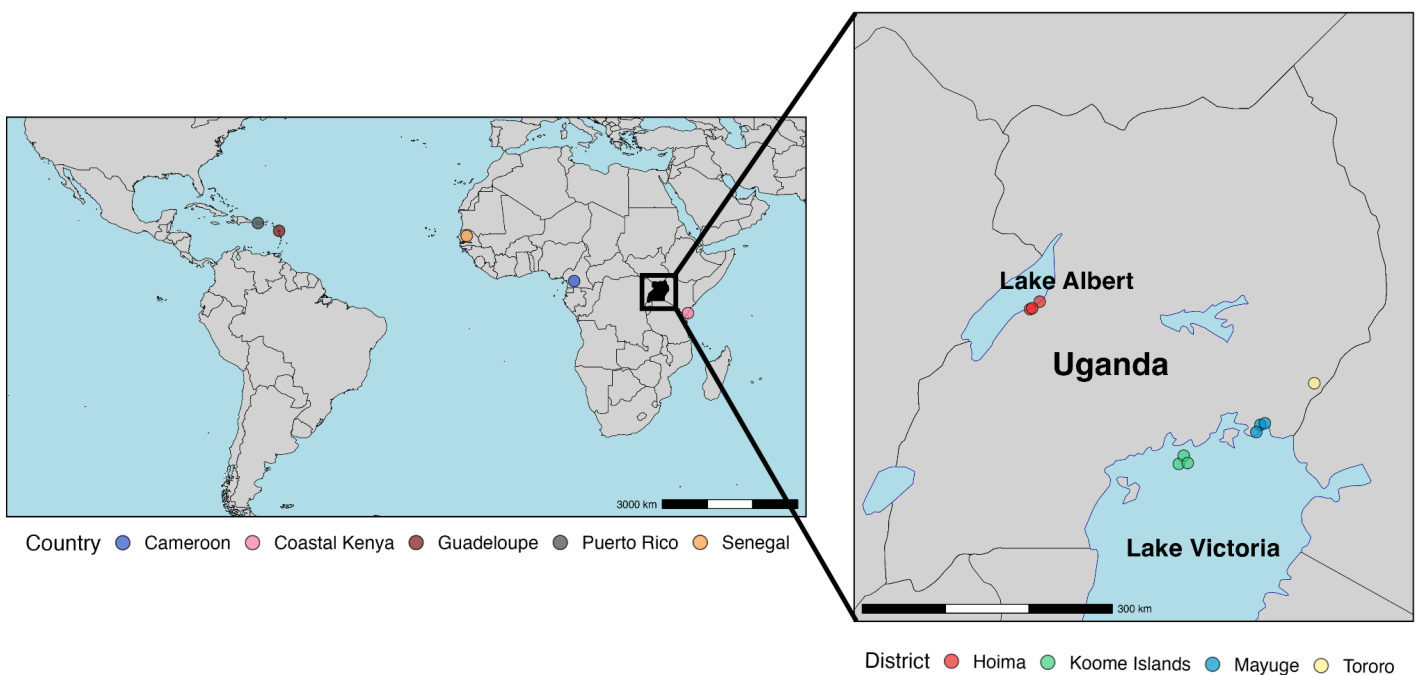


Figure 4.1: Map displaying the geographical location from which the samples originated. Cameroon ($n=1$), Coastal Kenya ($n=1$), Guadeloupe ($n=3$), Puerto Rico ($n=1$) and Senegal ($n=1$). Ugandan samples are coloured by district: Hoima ($n=96$), Koome Islands ($n=47$), Mayuge ($n=79$) and Tororo ($n=17$).

In total, 6,414,551,966 sequencing reads were generated from the 96 samples, with a mean of 66,818,250 reads (range = 14,359,800-145,882,240 reads) per miracidium. Following the removal of duplicate reads and alignment to the *S. mansoni* reference genome, 2,736,182,462 reads were successfully mapped with a mean of 28,501,901 reads (range = 182,403-73,280,785 reads) per miracidium.

Nuclear mapping rates per sample were highly variable, ranging from 0.2-69.2%. The resulting mean coverage of the nuclear and mitochondrial genomes was 6.6x (range = 0-16.5x) and 472.2x (range = 1.4-1320.4x), respectively (Appendix Table 4.2). To investigate

the variable per sample mapping rates, Kraken was run to estimate the extent of contamination in raw sequencing reads. The Kraken analysis showed that each sample had a small degree of contamination, which contributed to mapping rate variation between samples. The percentage of unclassified reads for each sample was used as a proxy for *S. mansoni* reads as it is not in the Kraken database (Appendix Table 4.2). The mean percentage of unclassified reads was 74% (range = 11%-91%). There were three clear outlier samples (BU196_B2, BU200_F2 and BU189_F1), which showed the lowest percentage of unassigned reads (<30%). These samples also had the lowest mean coverage. However, this did not explain the overall mapping variation in these samples.

Due to the presence of both male (ZZ) and female (ZW) miracidia, there was lower coverage over the Z-specific region within the Z chromosome. The sex of *S. mansoni* miracidia was determined for all 246 samples by analysing the differential coverage between the pseudoautosomal (PAR1 and PAR2) and Z-specific regions on the Z chromosome. 120 males and 126 females were identified (Appendix Table 4.3), showing no significant sex biases that needed to be considered within the further analyses.

From the 246 samples, 25,005,974 nuclear variants were identified. These comprised 21,506,087 SNPs and 3,499,887 indels. Additionally, 3,950 mitochondrial variants, consisting of 3,678 SNPs and 272 indels, were discovered (see Appendix Table 4.3). The standard pre-set hard filters for GATK were designed and optimised specifically for the analysis of human genetic data; thus, using the same pipeline for a non-model organism such as *S. mansoni* can lead to some inaccuracy. Therefore, a systematic approach was undertaken involving querying the SNP and indel QC profiles to determine the thresholds for variant filtering. Variant distributions for nuclear and mitochondrial SNPs and indels were plotted separately based on the following quality metrics: DP, QUAL, QD, FS, MQ, MQRankSum, SOR, and ReadPosRankSum (Appendix Figures 4.3 and 4.4). Variant filters were set by removing the relevant tails from the distributions (usually the upper and/or lower 1%) on the quality metrics. Following filtering, 5,930,196 nuclear (5,565,589 SNPs, 364,607 indels) and 1,075 mitochondrial (1,047 SNPs, 28 indels) variants were identified. Of the 246 individuals, 233 passed the nuclear variant filtering, and 244 passed the mitochondrial variant filtering (Table 4.1).

Table 4.1: The total number of variants, SNPs, indels and individuals detailed for each dataset before and after filtering.

Dataset	Total	SNPs	Indels	Individuals
Original nuclear variants	25,005,974	21,506,087	3,499,887	246
Filtered nuclear variants	5,930,196	5,565,589	364,607	233
Original mitochondrial variants	3,950	3,678	272	246
Filtered mitochondrial variants	1,075	1,047	28	244

4.3.2 Broad-scale genetic diversity of Ugandan *Schistosoma mansoni*

The relatedness between samples was investigated by calculating pair-wise kinship coefficients from autosomal variant data. One first-degree, one second-degree, and one third-degree relationship (Appendix Figure 4.2) was identified within the samples. The first-degree relationship was between samples originating from within the Koome Islands group, including Damba Island (Kakeeka) and Koome Island (Busi), collected from different individuals and time points. This was expected as the original study found evidence of first-degree relatives between miracidia collected from Kakeeka and Busi villages (151). The second and third-degree relationships were found within the three samples originating from Guadeloupe, with one sample (ERR539843) showing relationships with the other two samples. As a result, two samples were removed (ERR539843 and ERR6798495) to avoid the enrichment of rare alleles.

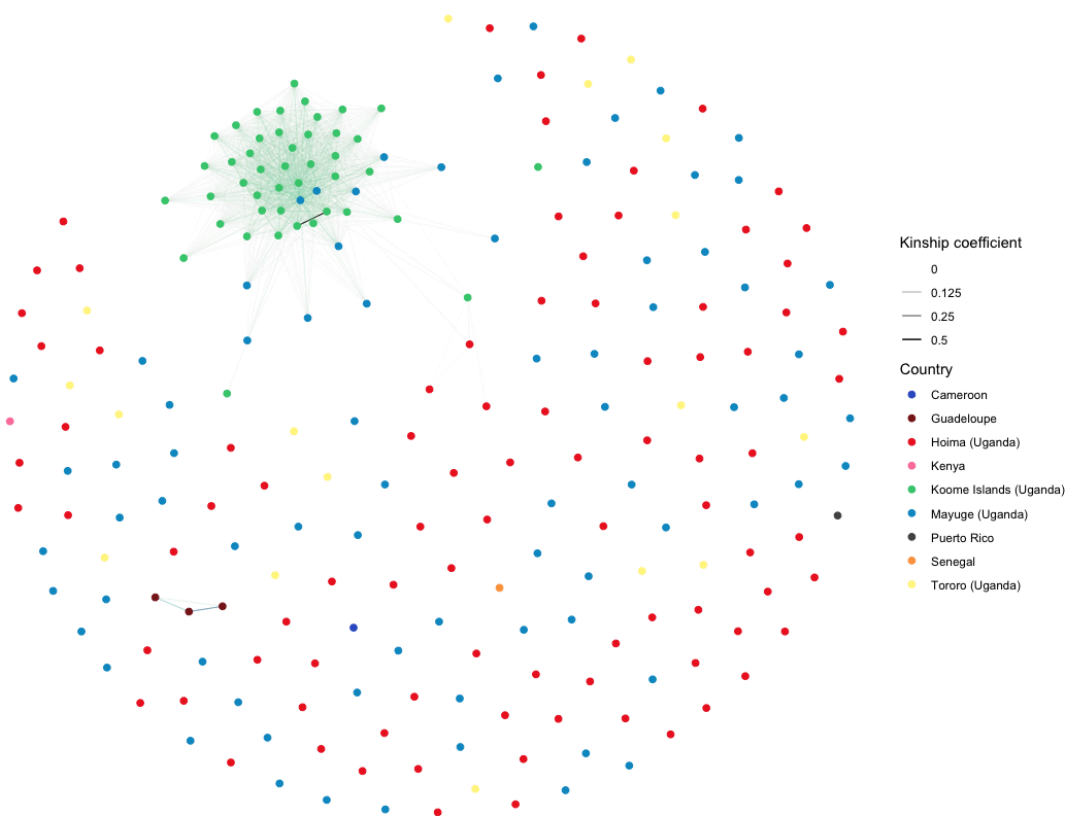


Figure 4.2: Kinship network of 246 miracidial samples. Nodes represent individual samples and the thickness of lines between nodes is proportional to the size of the kinship coefficient. Points in all plots are coloured by country of origin. Pairwise kinship coefficient values of: > 0.45 , $0.20-0.45$, $0.10-0.20$ and $0.05-0.10$ were used to classify monozygotic twins, full-sib (first-degree), second degree and third-degree relationships, respectively.

To investigate the genetic diversity of the *S. mansoni* samples on a broad scale, I analysed a subset of 1,281,806 autosomal variants, following the filtering of variants in strong LD. Autosomal variants were used because the dataset comprised a mix of male and female parasites. Removing linked variants was necessary because principal component analysis (PCA) assumes that the individual data points, i.e., SNPs, are independent; thus, allele frequencies should not be correlated due to physical linkage and LD. Using the unlinked autosomal variants, a maximum-likelihood (ML) phylogenomic tree was constructed, and PCA was performed to characterise the population structure of *S. mansoni*. The SNP-based ML tree and PCA revealed the expected country-level separation of the *S. mansoni* samples with distinct population clustering outside of Uganda (Figures 4.3A and 4.3B), as seen in another study (152). Notably, PC1 vs PC2 accounted for 31% of the variance, with the first principal component reflecting country separation and the second principal component reflecting Ugandan district separation (Figure 4.3B).

Within the Ugandan samples ($n=223$), PCA analysis based on 1,171,938 SNPs revealed district-level separation (Figure 4.3B). The first principal component separated Western (Hoima) and Eastern Ugandan (Mayuge and Koome Islands) samples, with the Tororo district joining the two districts. The second principal component separated Eastern Ugandan districts, where Tororo, Mayuge, and Koome Islands formed clusters (Figure 4.3C). However, there was an exception of a single Koome Islands sample (ERR6798464) clustering with samples from the Hoima district, which was also supported by the ML tree (Figures 4.3A and 4.3C).

The genetic diversity of the *S. mansoni* samples was also assessed using mitochondrial data (whole mitochondrial genomic variants and variants in the *cox1* gene). The mitochondrial PCA based on 950 SNPs formed five clusters: (i) a cluster comprising a mix of *S. mansoni* from all districts, (ii) a cluster primarily consisting of *S. mansoni* from Tororo, with the exception of two samples from Mayuge and Koome Islands, (iii) a cluster primarily consisting of *S. mansoni* from Hoima with the exception of two samples from Koome Island, (iv) a cluster primarily consisting of parasites from Mayuge with one parasite from Koome Island and (v) a cluster exclusively comprising parasites from Koome Island (Figure 4.3D). The *cox1* PCA plot based on 91 SNPs revealed a similar pattern of less distinct clustering of populations (Figure 4.3E). Parasites did not display any apparent population structuring at the village level in any of the datasets (nuclear, mitochondrial or *cox1* variants) (Appendix Figure 4.6), but outliers from mitochondrial and *cox1* variant clusters appear to be due to per-sample missingness (Appendix Figure 4.7A and 9B) rather than true biological genetic differences. Clustering in the nuclear SNP-based PCA plots, however, did not cluster by per-sample missingness (Appendix Figure 4.7C and 9D).

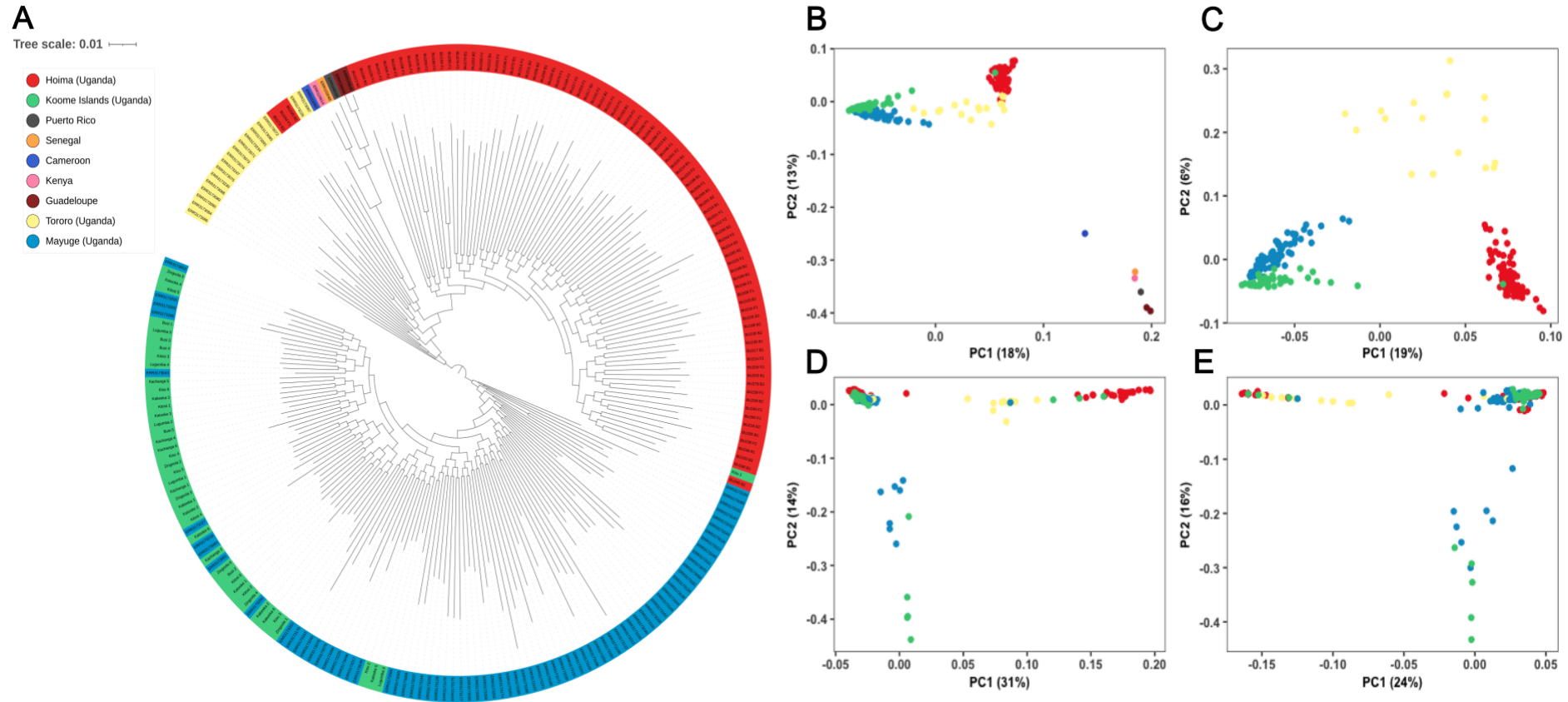


Figure 4.3: Population structure of the *Schistosoma mansoni* samples. A) Maximum-likelihood (ML) tree using 1,281,806 unlinked autosomal SNPs from 229 individuals. The ML tree was visualised in iTOL with midpoint rooting. The outer circle is coloured by country and district (Ugandan samples only). B) Principal component analysis (PCA) of 1,281,806 unlinked autosomal SNPs from all samples ($n=229$). The remaining PCA plots are from Uganda samples ($n=223$), focused on (C) unlinked autosomal SNPs ($n=1,171,938$); (D) all mitochondrial SNPs ($n=950$); and (E) mitochondrial *cox1* SNPs ($n=91$). Samples were coloured by country, and Ugandan samples were coloured by district.

4.3.3 Within-population genetic diversity

To explore within-population variation, π was calculated in 5 kb non-overlapped sliding windows across the genome. There was nucleotide variation throughout the genome within each population, with discrete peaks of high π values identified (Figure 4.4B). Across all genome-wide π plots, there was a decrease in π specifically within the ZSR of the Z chromosome compared to the autosomes. This is expected as the ZSR exhibits a lower copy number in the genome, reflecting a ratio of 3 copies of the ZSR for every 4 copies of autosomal regions in the population under equal sex ratios, leading to lower π (200). Genome-wide π tended to increase at the end of chromosomes (Figure 4.4B), possibly due to high rates of recombination and higher mutation rates typically observed in sub-telomeric and telomeric regions (201).

π was significantly different between populations ($p < 0.001$, Wilcoxon rank sum test), where it was highest in samples from Koome Islands (mean $\pi = 0.00369$, 99% CI: 0.00369-0.00374), followed by Tororo (mean $\pi = 0.00344$, 99% CI: 0.00342-0.00347), then Mayuge (mean $\pi = 0.00339$, 99% CI: 0.00336-0.00341) with Hoima populations showing the lowest (mean $\pi = 0.00328$, 99% CI: 0.00326-0.00330) (Figure 4.4A and Appendix Table 4.4). Similar findings were found in another study, which found that *S. mansoni* populations sampled from villages within the Lake Victoria region were more diverse than Lake Albert populations (161).

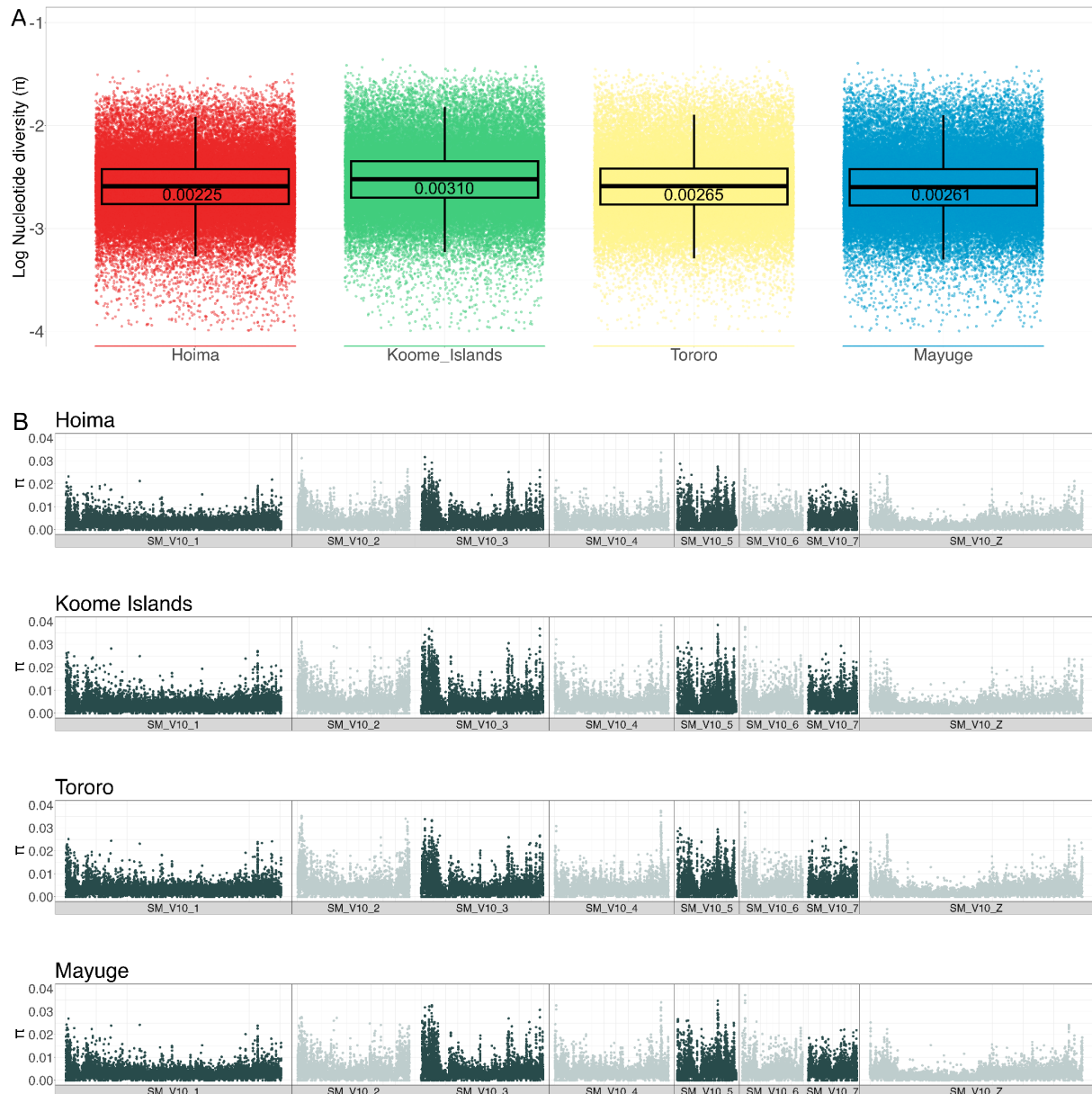


Figure 4.4: Autosomal nucleotide diversity (π) of Ugandan *Schistosoma mansoni* populations. A) Box plots show the log π distributions for each Ugandan district. Median π are shown in each box plot. B) Genome-wide plots of π for each Ugandan district: Hoima ($n=89$), Koome Islands ($n=43$), Tororo = 17, and Mayuge ($n=84$).

4.3.4 Between population genetic diversity

To further investigate the clustering of the Ugandan *S. mansoni* populations by district, genome-wide estimates of relative (F_{st}) and absolute (D_{xy}) differentiation between districts were calculated. This revealed low levels of differentiation between *S. mansoni* populations at the district level (Figures 4.6A and 4.6B). However, F_{st} and D_{xy} values do increase with

greater geographical distance. For example, the Mayuge district and Koome Islands show the lowest F_{st} value (mean $F_{st} = 0.00556$) and are the closest distance apart. Comparing the district on the shoreline of Lake Albert (Hoima) with districts on the shoreline of Lake Victoria region (Mayuge) and in Lake Victoria (Koome Islands) revealed the highest F_{st} values (Hoima vs Mayuge, $F_{st} = 0.0417$; Hoima vs Koome Islands, $F_{st} = 0.0413$) (Figure 4.6A) and are the greatest distance apart.

The *S. mansoni* populations appear almost panmictic, with low mean values of relative (F_{st}) and absolute (D_{xy}) divergence (Figures 4.6A and 4.6B). However, the clustering by district on the PCA plot (Figure 4.3C) suggests that these populations are isolated to some degree and that genetic differences exist between them. Genome-wide comparisons of F_{st} between different Ugandan districts were plotted to identify regions of differentiation (Figure 4.5). The genome-wide plots show regions of the genome with high genetic differentiation between most district comparisons. However, the Koome Islands vs. Mayuge F_{st} genome-wide plot displayed low levels of genetic differentiation, indicating parasites between these two districts form a diverse panmictic population, which is expected given their close geographical proximity.

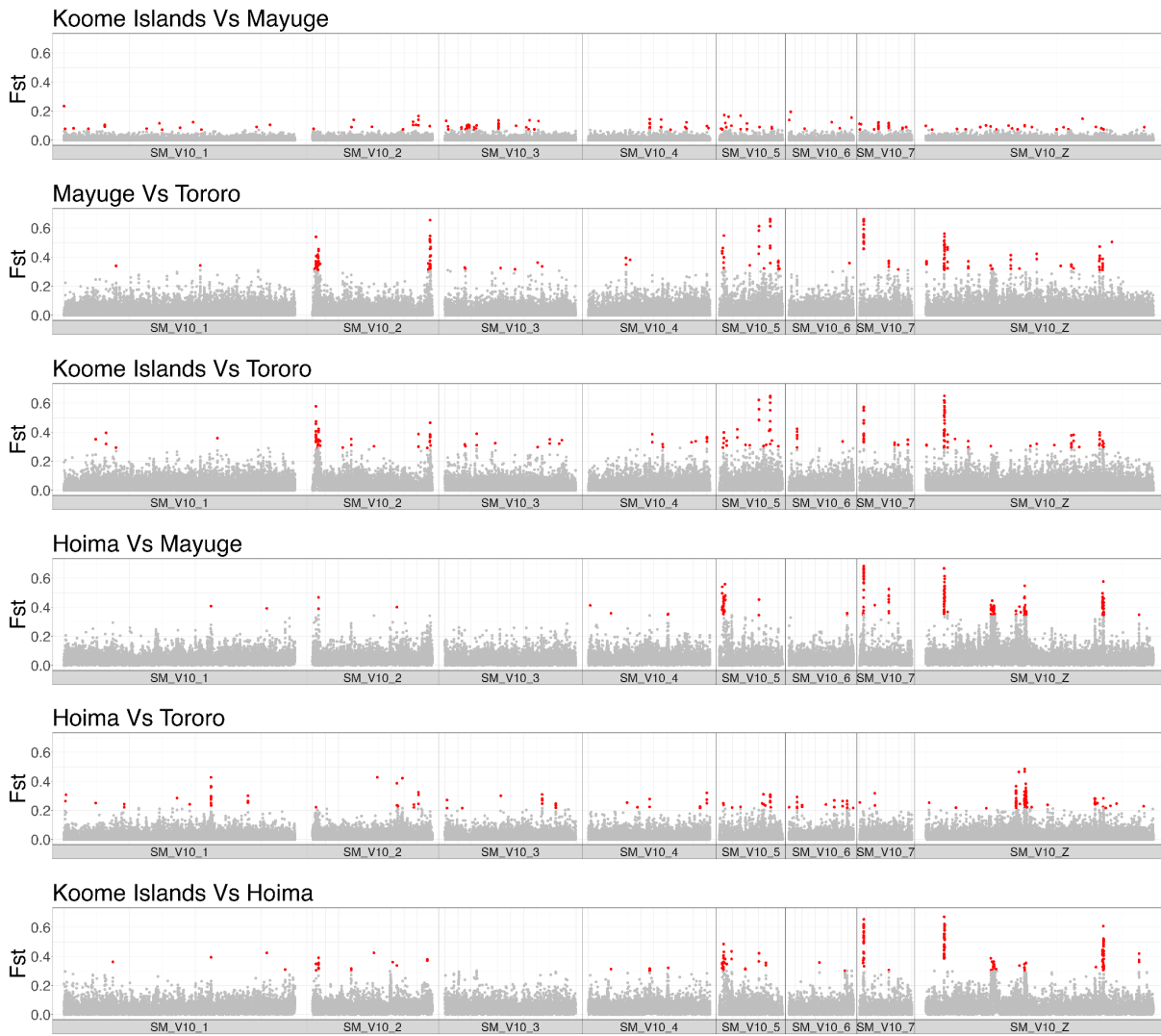


Figure 4.5: Genome-wide genetic differentiation (F_{st}) between different Ugandan districts. Each point represents median F_{st} values between genomic sliding windows of 5 kb. Genomic windows with the highest 0.25% of F_{st} values are coloured red and values below are coloured grey.

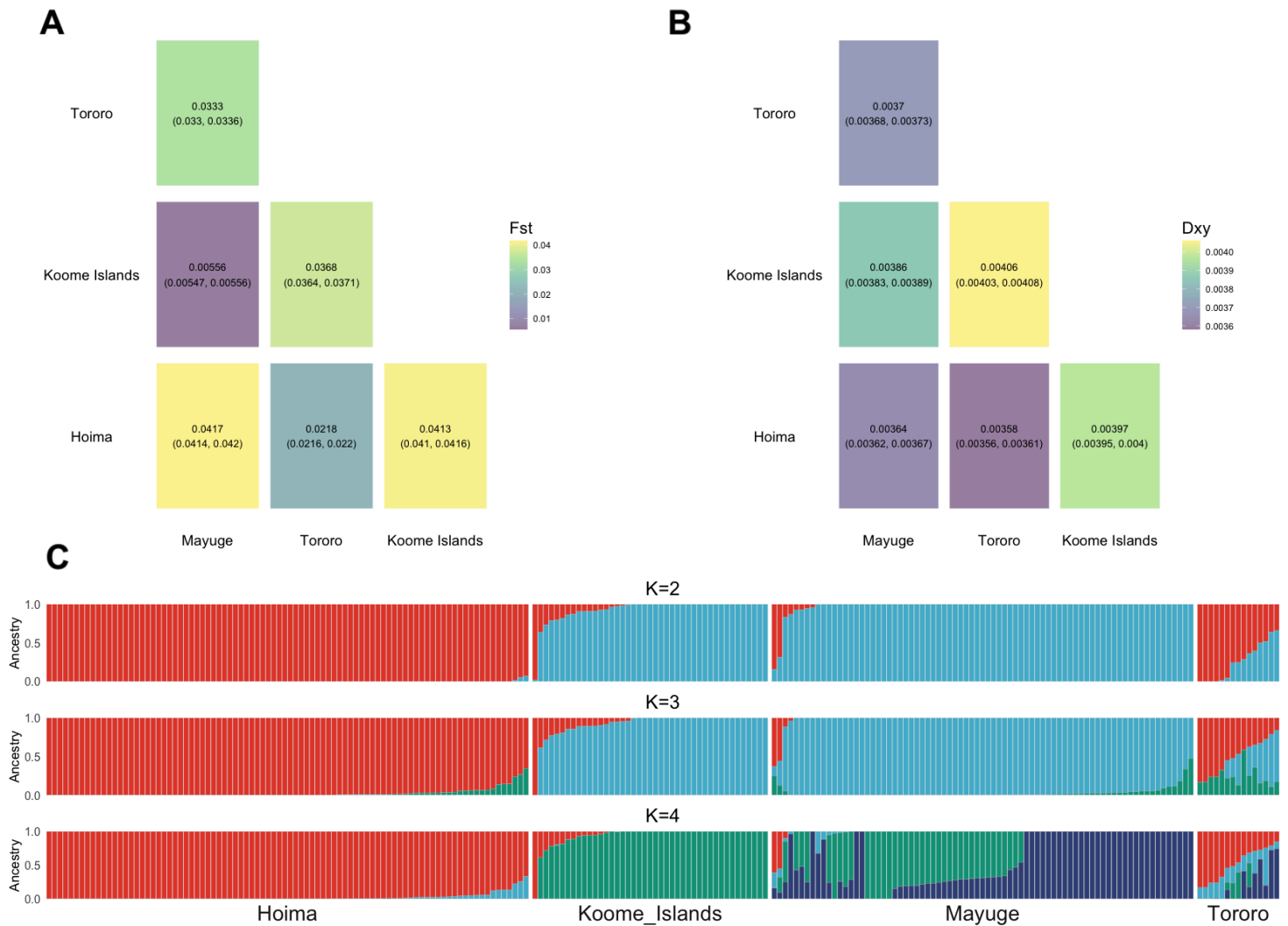


Figure 4.6: Between-population diversity. Heatmap of the average pairwise comparisons between populations measured by the mean relative (F_{st}) (A) and absolute (D_{xy}) divergence (B). The 99% confidence intervals are detailed in parentheses. C) Admixture plots depicting ancestry proportions generated using ADMIXTURE, with theoretical K values ($K=2-4$). Each colour indicates a different population, and K values represent the number of ancestral populations.

The nuclear PCA plot (Figure 4.3C), ML tree (Figure 4.3A), and measures of differentiation (F_{st} and D_{xy}) suggest district-level separation of *S. mansoni* populations with minor outliers. To explore this further, admixture proportions across a range of K (ancestral populations) values ($K=2-10$), where $K=2-4$ is displayed in Figure 4.6C, and $K=5-10$ is displayed in Appendix Figure 4.8, were determined. Using a cross-validation error approach, three ancestral populations were inferred ($K = 3$) (Appendix Figure 4.9). This is broadly consistent with the population structure in the Ugandan nuclear PCA (Figure 4.3C); however, $K=4$ reflects the more subtle population structuring observed in the PCA plot (Figure 4.3C). For example, $K=3$ explains the three clusters found in the PCA plot but does not explain that

even though samples from Koome Islands and Mayuge cluster together, they separate from each other within the cluster. Whereas, $K=4$ explains this through Mayuge sharing Koome Islands ancestry, while Koome Islands does not contain Mayuge ancestry (Figure 4.6C).

The Tororo district displayed the most diverse ancestry profile and showed mixed ancestry with all districts with no obvious dominant ancestral population (Figure 4.6C). Unlike the other sampling districts, Tororo is inland and does not border Lake Victoria. PC1 did not resolve Tororo populations from parasites sampled from the shores of Lake Albert and Lake Victoria (Figure 4.3C). Tororo populations appear mixed between parasite populations from both lakes, most strikingly with Lake Albert (Hoima), with low F_{st} and D_{xy} values reflecting this (Figure 4.3C, 4.6A, and 4.6B).

The admixture analysis differentiated *S. mansoni* from the Hoima district from Mayuge, Tororo and Koome Islands (Figure 4.6C), where Hoima had one dominant ancestral population. All districts shared partial ancestry with the Hoima district, which is most noticeable in the Tororo district. However, the admixture plot identified a single Koome Island sample, that showed complete Hoima ancestry, consistent with the single Koome Island sample outlier identified in the Ugandan nuclear PCA and ML tree (Figure 4.3A). This Koome Island sample maintains the same admixture profile throughout all values of K .

4.4 Discussion

To provide insights into both local and broader-scale *Schistosoma mansoni* population dynamics in Uganda, this study integrated novel genomic data from individual *S. mansoni* miracidia from shoreline villages of Lake Albert with published WGS data from *S. mansoni* miracidia collected around and inland of Lake Victoria (150–152). The main findings highlight the distinct genetic structure between *S. mansoni* populations in different regions of Uganda and their relationship to populations from South America and other African countries.

In this study, reads unclassified by Kraken were used as a proxy for *S. mansoni* reads based on the assumption that they likely originate from *S. mansoni* but remain unclassified due to its absence in the reference database. However, this approach has limitations, some unclassified reads may originate from other eukaryotic and bacterial species sequenced in the sample but are also absent from the standard Kraken database. To improve classification accuracy, a custom Kraken database incorporating *S. mansoni* should be constructed and implemented to better estimate the proportion of *S. mansoni* reads sequenced.

The geographical structuring of *S. mansoni* populations is evident at both global and district levels in Uganda, as shown by nuclear variants, a pattern reported by previous studies (152–154,160). However, at a local level, *S. mansoni* formed highly diverse panmictic populations, and no population structure was found at the village level. A distinct genetic separation exists between *S. mansoni* populations from Lake Albert and Lake Victoria, approximately 400 km apart, indicating limited gene flow between these regions, consistent with findings from other studies (161,165). A prior study involving a cohort of mothers and infants with intestinal schistosomiasis from Lakes Albert and Victoria reported little movement between the two lakes, possibly contributing to this genetic differentiation within those populations (161). This genetic differentiation has also been linked to differences in the composition of *Biomphalaria* snail species, with Lake Victoria hosting *B. sudanica*, *B. choanomphala* and *B. pfeifferi*, and Lake Albert has reports of *B. stanleyi*, *B. sudanica* and *B. pfeifferi* (202,203). Variation in *S. mansoni* infection susceptibility has been shown between and within different *Biomphalaria* species; some individuals within a species are less susceptible, and some are more successfully infected. This is likely due to the “matching” hypothesis, which proposes that the success or failure of infection is determined by the level of compatibility between the snail host and individual schistosome phenotype. Sites with more genetically diverse snail and *Schistosoma* populations likely have a higher probability of the schistosome encountering a compatible snail host. Of the *Biomphalaria* species found in these lakes, *B. choanomphala* has been reported as consistently having a

low infection prevalence (202,204), whereas *B. stanleyi* has been reported as having a higher prevalence of *S. mansoni* infection (202,204,205). This likely explains the higher reported prevalence of *S. mansoni* infection in Lake Albert compared to Lake Victoria. Furthermore, the transmission dynamics are considerably different between Lake Albert and Lake Victoria, where the lake shoreline of Lake Albert is linear and uniform compared to the intricate and expansive shoreline of Lake Victoria, with many islands and islets found providing microenvironments for transmission. There is considerable human movement around the lake shore of Lake Albert. This could partially explain why Lake Albert *S. mansoni* populations were found to be considerably less genetically diverse compared to those in Lake Victoria. Microenvironments created along the shoreline of Lake Victoria could lead to individuals residing within the same village coming into contact with different *S. mansoni* populations. Similar findings were found in another study, which found that *S. mansoni* populations sampled from villages within the Lake Victoria region were more diverse than Lake Albert populations (161).

Many studies have used mitochondrial markers, particularly small regions of the *cox1* gene, to explore the genetic diversity and structuring of African *S. mansoni* populations (160,161,165). In this dataset, variants from both the whole mitochondrial genome and *cox1* gene revealed similar patterns of population structuring, but a loss of resolution in population clustering was found for both compared to nuclear data. Principal component analysis of nuclear variants, based on 1,171,938 SNPs, revealed a clear distinction between Western and Eastern Ugandan samples, with further separation by district in the East. The observed differences in population structuring between mitochondrial (whole and *cox1*) and nuclear variants may be due to several factors, such as the vastly different number of SNPs and mtDNA evolving more rapidly compared to nuclear DNA, leading to different patterns of genetic diversity and structure. Additionally, mtDNA is maternally inherited and has a smaller effective population size which may result in greater genetic drift, which can obscure fine-scale population structuring. The discrepancy between the variants underscores the robustness of nuclear data in capturing detailed population structuring of *S. mansoni* in Uganda compared to mitochondrial data, which might reflect broader, less resolved patterns of genetic diversity.

Despite *S. mansoni* displaying district-level population structure in Uganda, evidence of gene flow between inland (Tororo) and shoreline districts (Hoima and Mayuge) was found. Ancestral analysis revealed mixed ancestry within the inland Tororo district, which showed ancestral contributions from all districts, particularly Hoima and Mayuge. This is unexpected as previous studies that generated the published datasets from these districts found inland

S. mansoni populations to be highly divergent from shoreline (Mayuge) and island (Koome Islands) populations. However, the findings from Berger *et al.* (152) are limited due to the small number of samples included from Lake Albert ($n=2$) compared to this study. Despite the small sample size, the samples from Lake Albert clustered with those from the Tororo district. Thus supporting the findings in this study of gene flow between shoreline villages of Lakes Albert and villages inland of Lake Victoria. It is important to highlight that MDA in Tororo commenced in 2013 with a reported coverage of 21%, whereas MDA has been ongoing since 2003 in Mayuge and Hoima (206). The samples were collected in Tororo in 2014 when there had only been one round of MDA; the diversity seen in Tororo may reflect the diversity of *S. mansoni* populations before the effects of long-term MDA. Furthermore, human movement from areas of higher endemicity, such as that from Lake Albert and Lake Victoria, may result in the mixing of *S. mansoni* populations, changing the local transmission dynamics. Local fishermen in shoreline communities are known to travel inland to recruit young men for fishing activities in the Lakes, which may in part explain the genetic admixture observed here.

Further evidence of parasite movement was found between Damba Island (Koome Islands) and Hoima (Lake Albert). Phylogenetic analysis showed that a single sample from Kisu village from Damba Island formed a clade with Lake Albert samples, and PCA analysis further supported this clustering. Ancestral analysis shows small ancestral contributions from Lake Albert in Koome Island samples, indicating gene flow between these populations. In the original study (151), 39% of the participants from Kisu village were fishermen, and 20% of participants were Alur, meaning local to Lake Albert (Webb, personal communication). Thus, the gene flow can likely be attributed to the significant movement of fishermen between the two lakes. Recent findings from Berger *et al.* (153) also found evidence of a recently imported *S. mansoni* lineage from Lake Albert, which has dispersed across Damba Island. The movement of parasites between districts highlights the role human movement plays in facilitating gene flow between geographically distinct populations. Adult schistosomes can live for up to 40 years, and each human host accumulates a diverse population of worms from a variety of snails in different locations and over years (207,208). Mixing of parasite populations may introduce genetic diversity, potentially impacting the efficacy of PZQ treatment. It emphasises the need for targeted interventions in high-risk, mobile populations such as fishing communities and highlights the interconnectedness of these lake systems in shaping parasite population dynamics. Similar patterns of parasite movement driven by human movement have been observed in other endemic settings. For example, Catalano *et al.* (209) found a lack of geographic population structure and gene flow in *S. mansoni* populations across the Senegal River Basin which authors hypothesised may

be due to changes in land use associated with the Diama Dam construction and the extensive human movement within Senegal and other countries within West Africa. Interestingly, the study highlighted the role of multi-host transmission, with *S. mansoni* being maintained in humans and rodents, further facilitating dispersal of parasite populations across transmission foci. Furthermore, in Kenya it has been found that boundaries of watersheds and water bodies can restrict gene flow, with strong population structuring observed across different watersheds in east, west and southwest regions of the country (210). Within Lake Victoria watershed, genetic subdivision was observed among streams, marshes and the lake itself, though no population structure was detected within the Kenyan portion of the lake, suggesting in the absence of physical barriers, gene flow can occur across these large geographic distances (169).

Schistosoma mansoni populations from Lake Albert showed the lowest genetic diversity amongst the other regions, whilst the Island populations (Koome Islands) were the most diverse, which aligns with previous findings (151). Sampling heterogeneity, such as the year of sampling and the age of individuals from which the parasites were collected from, is a likely contributing factor. Samples from Lake Albert were collected more recently (2021–2022) and exclusively from PSAC, whereas Koome Islands samples were collected in 2017 from a broader age range. Mayuge and Tororo samples, collected in 2014 from school-aged children, likely reflect the cumulative exposure over a longer period, contributing to their higher genetic diversity. At the infrapopulation level, infections in PSAC are expected to show lower genetic diversity compared to school-aged children and adults. This is due to the trickle infection model (211,212), where the *S. mansoni* populations in young children would show a lower genetic diversity due to a shorter window of cumulative exposure. However, at the broader population level, genetic diversity is influenced by additional factors such as the long-term effects of MDA. Annual MDA with PZQ has been ongoing in endemic areas like Mayuge and Hoima since 2003. By the time of sampling, Mayuge had undergone between five and nine rounds of MDA, while Hoima had completed around 15 rounds. This prolonged drug pressure may have induced selection, reducing genetic diversity in these populations.

There is a need to incorporate population genetic studies into routine monitoring and evaluation of large-scale MDA programmes to gain a more comprehensive understanding of the genetic diversity and gene flow of *S. mansoni* populations over space and time (154). Currently, available genetic data from Uganda (150–153,161,165) have been focused on sampling sites close to Lakes Victoria and Albert, likely due to their historically high and consistent prevalence and proximity to established research centres. Both lakes are

physically connected via the Victoria Nile, which originates in Jinja and flows northward, expanding into Lakes Kyoga and Kwanja and eventually feeding into the northern part of Lake Albert before continuing as the Albert Nile (165). Given the physical connection between these lakes through the Victoria Nile, there is a need to sample along this route and along the Albert Nile, particularly in Lakes Kyoga and Kwanja, which are located between Lakes Victoria and Albert. Intestinal schistosomiasis has been reported in Lake Kyoga, where it is co-endemic with *Schistosoma haematobium*, the cause of urogenital schistosomiasis (213). These intermediate areas remain unrepresented in genetic studies and may provide insights into potential gene flow and parasite movement across different regions of Uganda. It is important to highlight that parasite populations are not static. Little is known about the natural genetic variation of *S. mansoni* over spatial and temporal scales, as well as its implications for transmission dynamics and evolutionary responses to drug-induced selection.

This study provides insights into the population structuring and movement of *S. mansoni* populations in Uganda, highlighting regional genetic differentiation between Lake Albert and Lake Victoria, and evidence of gene flow between inland and shoreline populations. Nuclear variants demonstrated strong population structuring, whereas mitochondrial markers showed reduced resolution, emphasising the need for nuclear data for fine-scale population genetic analysis. The findings suggest that genetic diversity is influenced by factors such as human movement, local transmission dynamics, and long-term PZQ treatment. Expanding genomic studies to unsampled regions, such as Lakes Kwanja and Kyoga, would provide further insights into parasite movement and transmission across Uganda, informing schistosomiasis control programmes.

Chapter 5: Investigating the genetic impact of praziquantel treatment on *Schistosoma mansoni* populations in Lake Albert

5.1 Introduction

The emergence of drug resistance poses a significant threat to controlling parasitic diseases of both veterinary and medical importance. Resistance has been reported in several parasitic diseases, most notably in malaria where drug resistance against all known antimalarials has been observed (214). Furthermore, anthelmintic resistance is already a serious problem in veterinary nematodes infecting livestock which threatens the feasibility of agricultural farming (215). There have been cases of farms harbouring parasitic gastrointestinal helminths resistant to every major drug class reported (216). The same drugs are used globally in extensive mass drug administration (MDA) programmes for soil-transmitted helminths and filarial worms infecting humans. Although drug resistance is less established in human-infecting helminths, there is a global state of emergency around antimicrobial resistance which will have serious socioeconomic impacts on those infected and could derail the significant progress made (217,218).

For over two decades, MDA of praziquantel (PZQ) has been the cornerstone of schistosomiasis control. MDA was introduced in sub-Saharan Africa in 2003, with Uganda being one of the first countries to implement MDA of school-aged children (SAC), supported by the Schistosomiasis Control Initiative (SCI) (219,220). The new WHO NTD roadmap sets an ambitious target to eliminate schistosomiasis as a public health problem (defined as <1% proportion of heavy-intensity infections) by 2030, alongside achieving transmission interruption in selected countries (173). To achieve these targets, the WHO proposes extending access to PZQ; historically, MDA programmes have focused on treating SAC, neglecting other at-risk populations such as preschool-aged children (PSAC) and adults. These programmes now aim to provide equitable access to annual PZQ treatment to all age groups above the age of two years. However, the scale-up and reliance on a single drug make the emergence and spread of PZQ resistance a concerning problem. Consequently, genetic surveillance of *Schistosoma* populations is crucial for understanding the impact of PZQ treatment on schistosome population genetics for changes in population structure and genetic diversity as well as the implications of PZQ resistance on future control efforts (173,221).

In the absence of genetic markers to detect and monitor PZQ resistance, it has remained an enigma in schistosomiasis research since the 1990s. There have been reports of suspected resistance of *Schistosoma* populations in endemic foci (171,206,222–224) and also of *Schistosoma* species infecting travellers. Laboratory studies have also shown that PZQ resistance can be selected for (225–227). Despite the initial effects caused by PZQ on the

schistosome being well described, for example, calcium influx into the schistosome, muscle contraction and surface modifications (127), the molecular target of PZQ has been unclear. However, a recent breakthrough by Park *et al.* (228) has shown that PZQ binds to and activates a parasite ion channel belonging to the transient receptor potential melastatin family, named SmTRPM_{PZQ}. Molecular modelling and targeted mutagenesis were used to demonstrate how PZQ binds to SmTRPM_{PZQ} by mapping the PZQ binding pocket within the ion channel (228). The properties displayed by the SmTRPM_{PZQ} in response to PZQ mirror the characteristics of PZQ action on schistosomes and support the long-held Ca²⁺ hypothesis for PZQ action in *Schistosoma mansoni*. Furthermore, a recent genome-wide association study (GWAS) aimed to determine the genetic basis for PZQ resistance by comparing the genome-wide allele frequencies in *S. mansoni* adult worms that either failed to recover or recovered from PZQ treatment (227,229). A single quantitative trait locus (QTL) associated with drug response was found on chromosome 3 where the gene encoding SmTRPM_{PZQ} was found to be the cause of variation in PZQ response. The *S. mansoni* resistant and sensitive populations were fixed for alternative alleles at a SNP (2723187C, p.11020I) within SmTRPM_{PZQ} as well as two large deletions (around 150 kb), one close to the channel itself and one near a transcription factor. Additionally, lower expression of SmTRPM_{PZQ} gene was found in resistant worms, suggesting that expression levels may underpin the PZQ response phenotype.

Despite the recent advances in understanding PZQ action in a laboratory *S. mansoni* population, there is a need to explore the genetic basis of PZQ resistance in natural *Schistosoma* populations from endemic regions. Genome-wide data has emerged for Ugandan *S. mansoni* populations under drug pressure, particularly from shoreline and island communities of Lake Victoria (151–153), which is one of the most persistent hotspots of schistosomiasis in Africa (230). The most recent study by Berger and colleagues (153) reported extensive, low-frequency variation within SmTRPM_{PZQ} from 570 *S. mansoni* samples. Four mutations were identified that led to either a loss or reduced channel responsiveness to PZQ using targeted mutagenesis and functional *in vitro* genetic assays. The variation observed indicates the presence of standing variation for PZQ resistance in *S. mansoni* populations across Lake Victoria (153). However, the genome-wide studies did not find any evidence of selection acting on the SmTRPM_{PZQ} linked to drug selection (151–153). This may be due to several reasons: selection may be acting on another gene which impacts the expression of SmTRPM_{PZQ}, it is hard to identify genetic variants that impact expression and PZQ resistance may be focal with resistance alleles being rare and the sample sizes from current studies are likely underpowered to detect it (231). Furthermore, it is important to emphasise that the evidence implicating SmTRPM_{PZQ} in PZQ resistance was generated

using a single *S. mansoni* laboratory strain where resistance was selected for at the intra-molluscan stage which is not typically exposed to PZQ in the wild. Therefore, the resistance mechanism may vary from that seen in endemic settings. Finally, the laboratory strain was an inbred isolate of Brazilian origin which does not reflect the extensive genetic diversity seen in East African *S. mansoni* populations; it remains unclear if the resistance mechanism is conserved in African populations.

To elucidate the genomic impact of PZQ treatment on *S. mansoni* populations, miracidia were collected from a cohort of PSAC enrolled in a clinical trial in shoreline villages in Lake Albert, a significant hotspot of intestinal schistosomiasis (118). School-based annual MDA has occurred in these villages since 2003 and from 2005 as community-based MDA. Due to the COVID-19 pandemic, there was no delivery of PZQ through MDA in 2020. Community-based MDA in these regions have not included the treatment of PSAC, primarily due to concerns over the administration of large, bitter-tasting tablets, which present a potential choking hazard and due to little formal documentation confirming its use in young children (95). Crushed PZQ tablets have been used in off-label settings, and its safety and efficacy have been demonstrated in PSAC (97). This mode of drug administration was used in the Praziquantel in Preschoolers (PIP) clinical trial (118). Low cure rates (CRs) were reported in this cohort of PSAC (detailed in Chapter 3) and potential confounding factors including demographic and pharmacokinetic factors did not explain these. Participants received either 40 mg/kg or 80 mg/kg PZQ at baseline, and the same participants were subsequently followed up at six months post-treatment (Table 5.1). In this chapter, I aimed to explore the genetic basis of low CRs using whole genome sequencing of individual *S. mansoni* miracidia sampled from participants from the two treatment regimens at pre- and post-treatment. This is the first whole genome analysis to explore the genetic effect of PZQ treatment in *S. mansoni* from shoreline villages of Lake Albert and more specifically, the genetic diversity of the candidate gene underpinning PZQ resistance, SmTRPM_{PZQ}. The genetic diversity of the PZQ binding pocket located within the transmembrane region of SmTRPM_{PZQ} was further investigated using a custom amplicon sequencing panel.

5.2 Methods

5.2.1 Ethics statement

Ethical approval was given by the Uganda National Council for Science and Technology (HS 2650), Uganda Virus Research Institute (GC/127/19/07/708), National Drug Authority (CTC 0133/2020) and the London School of Hygiene and Tropical Medicine (26571). Parental informed consent was obtained as detailed (118).

5.2.2 Genomic methods

5.2.2.1 Whole genome sequence analyses of *Schistosoma mansoni* miracidia collected from study participants from Lake Albert, pre- and post-treatment

Whole genome sequence data generated from the 96 *S. mansoni* miracidia analysed from PSAC residing in villages in the Hoima district bordering Lake Albert, Uganda collected as part of the PIP clinical trial (118) (Figure 5.1) (see Chapter 4 for detailed methods of data generation) were further analysed.

Data were available from *S. mansoni* miracidia collected from the same infected individuals at baseline (November 2021) and also 6 months post PZQ treatment (May 2022). Data were analysed from miracidia from selected study participants that were *S. mansoni* egg positive, by Kato Katz (KK) at baseline and also at four weeks post-treatment. Equal numbers of miracidia were analysed from participants within the two PZQ treatment arms (40 mg/kg and 80 mg/kg PZQ) and also pre- and post-treatment from the same individual participants at each time point (Table 5.1).

Table 5.1: Number of *Schistosoma mansoni* miracidia with whole genome sequence data generated per village, sampling time point, and treatment arm (40mg/kg and 80 mg/kg PZQ). The number of children from which the miracidia were sequenced are detailed in (parentheses).

Village	Number of children	Standard 40 mg/kg PZQ		Intensive 80 mg/kg PZQ	
		Pre-treatment	Post-treatment	Pre-treatment	Post-treatment
Kyabarangwa	17	20 (10)	20 (10)	14 (7)	14 (7)
Rwentale	3	4 (2)	4 (2)	2 (1)	2 (1)
Fofu	4	0	0	8 (4)	8 (4)
Total	24	24	24	24	24

5.2.2.2 Preparation of whole genome sequencing data and variant calling

Quality control, mapping, variant calling and filtering on the genomic data were conducted as documented in Chapter 4. Subsequently, genomic variants specific to the miracidia collected from Lake Albert were subsetted from the VCF file (Chapter 4), a minor allele frequency (MAF) of 0.01 was applied, and invariant sites (which were polymorphic in the larger dataset analysed in Chapter 4 but not the Lake Albert population) were removed using VCFtools (version 0.1.16). Following variant calling and filtering conducted in Chapter 4, the VCF file was subsetted to include only Lake Albert (Hoima) samples. A total of 88/96 samples passed QC filtering and were used in the analysis (Table 5.2). Analysis of differential coverage in pseudoautosomal regions (PAR)1 and PAR2 regions to Z-specific region (ZSR) inferred that there were 48 male and 48 female miracidia in this dataset (see Chapter 4 for more details).

Table 5.2: Number of *Schistosoma mansoni* miracidia that passed quality control and were used in the analysis. The village, sampling time point, and treatment arm (40mg/kg and 80 mg/kg PZQ) are detailed. The number of children from which the miracidia were sequenced are detailed in (parentheses).

Village	Number of children	Standard 40 mg/kg PZQ		Intensive 80 mg/kg PZQ	
		Pre-treatment	Post-treatment	Pre-treatment	Post-treatment
Kyabarangwa	17	18 (10)	19 (10)	12 (7)	12 (7)
Rwentale	3	4 (2)	3 (2)	2 (1)	2 (1)
Fofu	4	0	0	8 (4)	8 (4)
Total	24	22	22	22	22

5.2.2.3 Population structuring

To investigate the impact of PZQ treatment on the population structure of *S. mansoni* in Lake Albert, variants found in strong linkage disequilibrium were removed using PLINK (version 1.9). Genome scans were conducted using 50 variant sliding windows in steps of 10 variants, and an r^2 threshold of >0.15 was used to remove highly linked variants in windows. Variants from the Z and W chromosomes and mitochondrial genome were excluded. Principal component analysis (PCA) was conducted on 955,853 autosomal SNPs using PLINK (version 1.9).

5.2.2.4 Sample relatedness

Pairwise sample relatedness between pairs was calculated using VCFtools (—relatedness2) based on the KING inference (232). Pairwise kinship coefficient values of > 0.45, 0.20-0.45, 0.10-0.20 and 0.05-0.10 were used to classify monozygotic twin, full-sibling (first-degree), cousins (second-degree), and great-grandchildren from shared grandparents (third-degree) relationships, respectively. A network graph was constructed using tidyverse (194) and igraph (195) packages in R to visualise the relationships among samples, with nodes representing individuals and the thickness of edges indicating kinship coefficients.

5.2.2.5 Genomic diversity

A subset of all sites VCF, generated in Chapter 4, was used to include only Lake Albert samples. For the analysis in this chapter, a population is defined by the treatment regimen and time point: standard treatment pre-treatment, standard treatment post-treatment, intensive treatment pre-treatment and intensive post-treatment are considered separate populations (Table 1).

Genome-wide nucleotide diversity (π) within populations was calculated using PIXY (version 1.2.8.beta) in 5 kb sliding windows along each autosome and Z chromosome for baseline, follow-up and each treatment regimen. The mean π within each treatment and time point group was calculated individually, and the symmetric 99% bootstrap confidence intervals of the mean were estimated using R. The Wilcoxon Rank sum test was used to assess the statistical significance of π comparisons. To detect any subtle differences in π between pre- and post-treatment populations, the ratio of π values in 5 kb windows between treatment groups was calculated. Windows with a greater than 1 pre π / post π ratio indicate a decrease in π in post-treatment populations compared to pre-treatment populations and may indicate the effect of PZQ treatment.

5.2.2.6 Between population differentiation and selection

Statistical phasing of variant data was performed using Beagle (version 5.3) with the effective population size set to 65,000 based on Crellen *et al.* (150). The genomes were scanned for signatures of selection using the REHH package (version 3.2.2) in R. Cross-population extended haplotype homozygosity (XP-EHH) was calculated to determine signals of selection between two populations (standard pre- vs post-treatment, intensive pre- vs post-treatment, and standard post-treatment vs intensive post-treatment). XP-EHH compares the extended haplotype homozygosity (EHH) between two populations at a given SNP; if one population shows significantly longer homozygosity around the SNP compared

to the other, it indicates a recent selective sweep unique to that population. Negative values represent extended haplotype homozygosity in post-treatment populations, consistent with selection.

The fixation index (Fst) between pairs of populations was calculated using PIXY (version 1.2.8.beta) in 5 kb sliding windows along each autosome and Z chromosome for baseline, follow-up and each treatment regimen. Prior to the calculation of genome-wide mean Fst values, negative Fst values were adjusted to 0.

The highest 0.25% XP-EHH and Fst windows were identified as potential candidate regions under selection. A region was considered a candidate region of selection if windows were within 250 kb of each other with at least 5 windows with elevated values across any statistic.

5.2.2.7 Analysis of the SmTRPM_{PZQ} genomic region

Functional annotation of SNPs and indels from the exons of SmTRPM_{PZQ} (*Smp_24790*) was undertaken using SnpEff (version 5.1d) with annotations from the *S. mansoni* reference genome (version 10) downloaded from WormBase ParaSite V19 (187). This resulted in the generation of an annotated VCF containing predictions of the annotations and effects of exonic genetic variants on SmTRPM_{PZQ}. Non-synonymous mutations found were searched against a database of mutagenesis data detailing the functional impact on the SmTRPM_{PZQ} and its sensitivity to PZQ (<https://www.trptracker.live/all-mutagenesis-data>). Specifically, the focus was on isoform 1 (*Smp_24790.1*), which was implicated as a candidate gene for PZQ resistance (227,229). The distribution and frequency of exonic variants were plotted along the protein structure of the SmTRPM_{PZQ}.

Large structural variants were identified using LUMPY (Version 0.3.0) and genotyped using SVTyped (0.7.1) as part of the Smoove (Version 0.2.8) structural variant calling pipeline. Variants were annotated using the reference GFF file.

5.2.3 Amplicon sequencing of the transmembrane region of SmTRPM_{PZQ}

5.2.3.1 Sample Information

To investigate the genetic diversity of the PZQ binding pocket within the transmembrane region of SmTRPM_{PZQ} amplicon sequencing of 462 miracidia collected from participants from the PIP trial was undertaken. Three miracidia were randomly selected from 77 participants at

baseline and six-month follow-up, respectively, where possible. The participants were from a subset of seven out of the ten villages which were included in the PIP trial, detailed in Figure 5.1.

5.2.3.2 Primer design

Sequence data (introns and exons) of the SmTRPM_{PZQ} gene (Smp_246790.1) were downloaded in FASTA format from WormBase ParaSite V19 (187). This 7,534 bp gene consists of 36 exons. The proposed PZQ binding pocket (228) is present across four exons, which are separated by large introns (>1,500 bp). Four sets of primer pairs were designed to target each exon encoding the PZQ binding pocket (228) (Appendix Figure 5.1 and Appendix Table 5.1) using Primer BLAST (NCBI www.ncbi.nlm.nih.gov/tools/primer-blast) and were required to be approximately 500 bp in length.

Five primer sets were tested per TRP target, using DNA extracted from individual FTA preserved miracidia from the standard *S. mansoni* NMRI life-cycle maintained within the Schistosome and Snail Resource (SSR) (Grant number: 221368/Z/20/Z) using the CGP methodology described in Chapter 4. The different primer sets were tested using standard PCR. Each 25 µl reaction contained 3 µl of DNA, 12.5 µl Phusion high-fidelity (HF) PCR master mix with HF buffer (New England Biolabs, UK) and 10 pmol of each primer to test. Gradient PCR reactions were undertaken to determine the optimal melting temperature for each primer pair. Four microlitres of each reaction were visualised using 1.5% agarose gels with GelRed staining to determine the presence and size of PCR products. A single primer pair per target was selected based on successful amplification, the production of a single band using standard PCR and an amplicon size of approximately 500 bp. Each primer set was named TRP1, TRP2, TRP3 and TRP4.

To enable multiplex amplicon NGS sequencing, a 5' tag inline barcode (8 bp long) was added to each forward and reverse primer sequence (TRP1-4) (Appendix Table 5.2). A total of 20 unique forward and 20 reverse barcodes were used. A total of 20 unique combinations were used for each target as each barcode was used once per target in each sequencing pool. The custom primer sequences containing the barcodes were ordered and synthesised by Integrated DNA Technologies (IDT, Belgium). For multiplex sequencing, each miracidium was assigned a unique barcode combination before PCR amplification, leading to the incorporation of the specific barcode into the PCR product (233).

5.2.3.3 PCR reactions and generation of the barcoded TRP amplicons from each miracidia

Genomic DNA was extracted from the individual miracidia using the methods described in Chapter 4. The first PCR step involved amplifying the TRP target with the specific barcode incorporated. The barcode combination is detailed in Appendix Table 5.2. For each *S. mansoni* miracidium, the four TRP targets (Appendix Figure 5.1) were amplified in separate 25 µl PCR reactions. Each reaction contained 3 µl of DNA, 12.5 µl Phusion high-fidelity (HF) PCR master mix with HF buffer (New England Biolabs, UK) and 10 pmol of each unique barcoded primer set. From 462 miracidial DNA extractions, 456 successfully amplified all four TRP amplicon targets (Table 5.3).

The final thermal cycling conditions were: 30 sec denaturing at 98°C, 40 cycles of 98°C for 10 sec, 63-65°C for 30 sec and 72°C for 45 sec, followed by 10 min at 72°C. Four microlitres of each reaction were visualised using 1.5% agarose gels with GelRed staining to determine the presence and size of PCR products.

Table 5.3: Sample information for miracidia that successfully amplified all four amplicons for amplicon sequencing. The number of *Schistosoma mansoni* miracidia sequenced are detailed and the number of children are shown in (parentheses). The villages, sampling time point and treatment arm (standard 40 mg/kg PZQ; intensive 80 mg/kg PZQ) are detailed.

Village	Number of children	Standard 40 mg/kg PZQ		Intensive 80 mg/kg PZQ	
		Pre-treatment	Post-treatment	Pre-treatment	Post-treatment
Fofu	17	38 (11)	35 (12)	45 (15)	41 (15)
Hoimo	12	14 (5)	6 (2)	21 (7)	11 (5)
Kibiro	5	11 (3)	11 (3)	8 (2)	8 (2)
Kiryamboga	4	9 (3)	5 (2)	4 (1)	3 (1)
Runga	3	6 (2)	2 (1)	6 (2)	5 (2)
Rwentale	13	23 (8)	7 (3)	15 (5)	11 (5)
Kyabarangwa	23	23 (8)	29 (10)	37 (13)	22 (8)
Total	77	124	95	136	101

5.2.3.4 Pooling of amplicons and multiplex amplicon sequencing

Five µl of each target amplicon, TRP1, 2, 3 or 4, each tagged with a unique 5' / 3' barcode combination from each individual miracidium, were pooled into a single tube for each of the four TRP targets, respectively (Appendix Figure 5.2). DNA from each pool was purified using

KAPA pure beads (Roche Diagnostics, USA) according to the manufacturer's protocol, at a volumetric ratio of 0.9:1 (beads:DNA). The DNA concentration of the purified amplicon pool for each target was quantified using a Qubit high-sensitivity reagent (Invitrogen, UK) and normalised to a final concentration of 20 ng/μl. Then, 6.25 μl of each TRP target pool was combined into a single tube, resulting in a final volume of 25 μl for the final pool containing all four amplicon targets. This pooling process was repeated for 24 pools of amplicons which were sent externally to the Illumina-based Amplicon-EZ service (GENEWIZ, Germany) for sequencing on the Illumina MiSeq platform (2 x 250 bp) where a minimum of 50,000 reads were obtained per pool. A maximum of 80 amplicons were pooled in each sequencing pool to achieve high sequencing coverage.

5.2.3.5 Bioinformatic analysis of amplicon data

Raw sequences were de-multiplexed to separate sequence data from each TRP target from the individual miracidia based on the unique barcodes assigned to each miracidium sample using an in-house analysis pipeline (<https://github.com/LSHTMPathogenSeqLab/amplicon-seq>). Raw sequences were trimmed using Trimmomatic (234) and aligned to the *S. mansoni* (version 10) (200) reference genome using BWA-MEM (version 0.7.17-r1188) to produce a BAM file for each miracidium. Variants were called using GATK HaplotypeCaller (version 4.1.4.1) by generating individual per sample GVCFs (--minimum-mapping-quality 30 --min-base-quality 20 --standard-min-confidence-threshold-for-calling 30). Sample GVCFs were merged using GATK CombineGVCFs before joint genotyping using GATK GenotypeGVCFs. Variants were filtered using BCFtools (version 1.16) for a minimum read depth of 7 (SNPs) and 12 (INDELS), minimum allele depth of 10 and phred score of >30 per base. Variants were annotated using SnpEff (version 5.1d). Genotyping of variants was undertaken based on the percentage of the alternative allele to total depth coverage (233): homozygous reference (<25% alternative allele reads); heterozygous alternate (25-75% alternate allele reads); and homozygous alternate (>75% alternate allele reads). Only variants which were present in more than one miracidia and present in at least two independent sequencing pools were retained to minimise the inclusion of sequencing errors or artefacts. Allele frequencies were calculated using VCFtools using the -freq tag and plotted using R. The distribution and frequency of variants were plotted within the transmembrane protein structure SmTRPM_{PZQ} with the functional impact detailed from the SnpEff output.

5.3 Results

5.3.1 Population structure of *Schistosoma mansoni* populations in Lake Albert pre and post-treatment

To determine the impact PZQ treatment had on the population structuring of *S. mansoni* populations in Lake Albert, PCA was performed on 955,853 autosomal variants, which were filtered to remove variants in strong linkage disequilibrium. Principal component (PC) 1 vs PC2 explained 12% of the total variance, and PC3 vs PC4 explained 12% of the total variance. However, together PC1-4 accounted for 24% of the total variance and revealed no clear population structure with samples forming a single cluster (Figures 5.2A and 5.2B). There was no population stratification between pre and post-treatment samples or by treatment arm (standard vs intensive arms). Four samples appeared distinct from the central cluster on PC1 and PC2, which could not be explained by individual missingness or village location (Appendix Figure 5.3). However, these samples had more homozygous sites than expected; homozygosity is the likely reason for this outlying cluster. The lack of population structuring could suggest insufficient sampling to fully characterise the genetic diversity or that there is no genetic difference and that these populations are closely related.

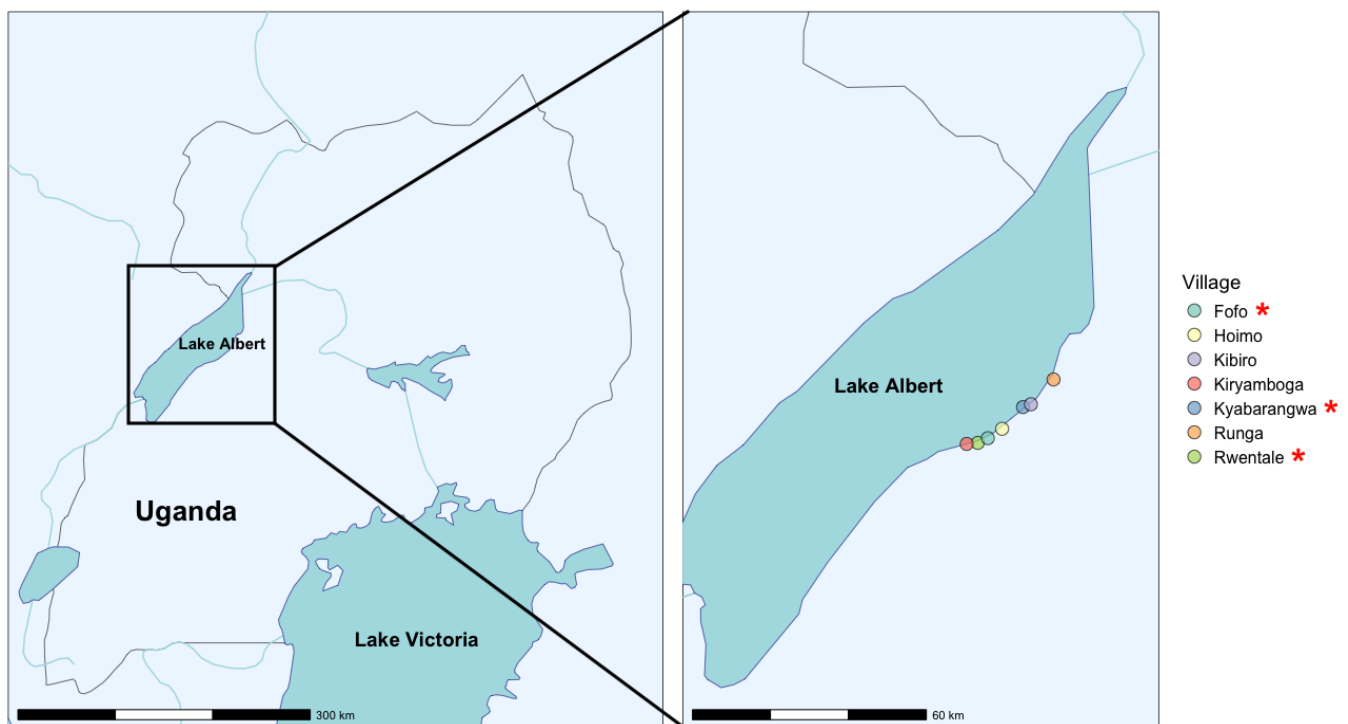


Figure 5.1: Map displaying the geographical distribution of villages bordering Lake Albert, Uganda, where *S. mansoni* miracidia were selected for whole genome sequencing (indicated with *) and amplicon sequencing.

To investigate the relatedness between individual samples, pairwise kinship coefficients between samples were calculated from autosomal variants. Related miracidia between time points could indicate adult worms surviving PZQ treatment. No related miracidia were found (up to third-degree) (Figure 5.2C), which is expected given the limited size of infrapopulations (number of miracidia sampled per host) analysed in this study (up to four miracidia per infrapopulation). Similar findings have been reported in a study which found no evidence of related miracidia between pre-and post-treatment despite sampling up to 10 miracidia per infrapopulation and having a short follow-up time frame (4 weeks) to identify treatment failures and not eggs associated with pre-patent infections (152). However, Vianney *et al.* (151) sampled up to five miracidia per host infrapopulation from the Koome Islands and found that 24% of pairs of miracidial samples from one individual were related, and 10% of other comparisons appeared related. Despite this, the authors found no significant enrichment of related miracidia by treatment regimen or treatment time points.

Earlier studies have used microsatellite markers to characterise the relatedness of *Schistosoma* miracidial populations. The majority of these studies have used sibship reconstruction to identify the number of unique parental genotypes or the number of full-sibling families. For example, Faust *et al* (235) genotyped 3576 *S. mansoni* miracidia from 203 children from the Lake Victoria region of Uganda, at seven microsatellite loci. Full siblings were identified at pre and four weeks post-treatment suggesting adult worms surviving PZQ treatment. Similar microsatellite-based approaches have been applied in other settings (236,237) and have also reported family structure and the presence of full siblings in *S. mansoni* miracidial infrapopulations sampled (238,239). However, these approaches have not related the relatedness patterns to the number of fecund female worms. A statistical method has been developed to estimate the number of fecund adult worms from the number of unique parental genotypes (240). When applied to *S. mansoni* miracidia genotyped from school children in Tanzania, this approach demonstrated that the accuracy and reliability of worm burden estimated are highly dependent on the number of miracidia sampled.

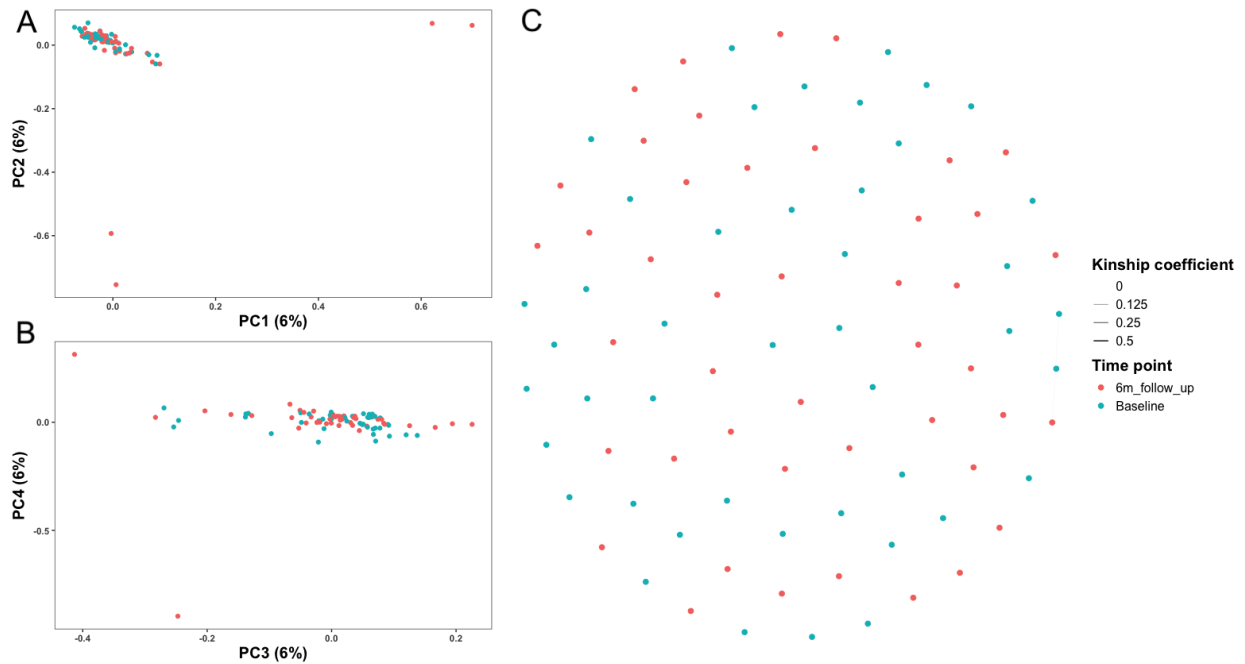


Figure 5.2: Population structure of Lake Albert *Schistosoma mansoni* miracidia. Principal component analysis of genetic differentiation between 88 *S. mansoni* miracidia. (A) Principal component (PC) 1 vs PC2 and (B) PC3 vs PC4. (C) Kinship network where nodes represent individual samples, and the thickness of lines between nodes is proportional to the size of the kinship coefficient, no lines between nodes indicate unrelated miracidia. Pairwise kinship coefficient values of > 0.45, 0.20-0.45, 0.10-0.20 and 0.05-0.10 were used to classify monozygotic twin, full-sib (first-degree), second-degree, and third-degree relationships, respectively. Points in all plots are coloured by sampling time point: baseline (pre-treatment) and six-month post-treatment.

5.3.2 The effect of praziquantel treatment on pre- and post-treatment populations

To understand the effect of PZQ treatment on genetic diversity within each treatment group, nucleotide diversity (π) was calculated. Genome-wide estimates of π within populations were consistent across treatment time points and treatment regimens (Figure 5.3). The mean π was highest in pre-treatment populations (Standard pre-treatment mean π =0.00312, 99% CI: 0.00310-0.00314; Intensive pre-treatment mean π =0.00315, 99% CI: 0.00313-0.00317), where there was no statistical difference between standard and intensive π at pre-treatment, indicated by overlapping 99% CIs (p =0.0719, Wilcoxon rank sum test) (Appendix Table 5.3). Any observable changes in π post-treatment can be attributed to PZQ treatment rather than pre-existing differences between groups.

Post-treatment samples showed small but significant reductions ($p < 0.05$, Wilcoxon rank sum test) in the mean π in both the standard and intensive post-treatment populations compared to the pre-treatment populations (Appendix Table 5.3) but there was no significant difference between populations collected after standard or intensive treatment. This demonstrates the small effect of a single round of PZQ treatment on the genetic diversity of *S. mansoni* populations. Interestingly, both treatment regimens appear to have similar reductions in π , where it appears that the intensive treatment arm did not impose a larger reduction in π compared to the standard treatment arm.

To detect any subtle differences in π between pre-and post-treatment groups, the ratio of π between pre-treatment and post-treatment groups was compared (Figures 5.3B and 5.3C). A total of 208 and 138 outlier windows were identified as three SD (π ratio > 0.527) and five SD (π ratio > 0.859) above the genome-wide mean, respectively, most of which were present in chromosome 3 ($n = 58$ or $n = 35$, respectively). Of those 208 instances, at least five consecutive 5 kb windows were recorded in four cases (three of which were present on chromosome 3), whereas only one instance of at least five consecutive 5 kb windows was recorded above the mean π ratio in chromosome 3. The candidate regions of low π in post-treatment samples on chromosome 3 did not encode for any genes; however, the region on chromosome 1 contained two genes (Smp_140840 and Smp_034550, encoding for a kinase and putative alpha-actinin, respectively). These results suggest genomic regions, particularly on chromosomes 1 and 3, may be involved in the response to PZQ treatment.

In the intensive treatment arm, a total of 222 and 129 outlier windows were identified as three SD (π ratio > 0.511) and five SD (π ratio > 0.835) above the genome-wide mean, respectively, most of which were present in chromosome Z ($n = 86$ or $n = 39$, respectively) followed by chromosome 3 ($n = 32$ or $n = 25$, respectively). No such candidate regions of low π were found in the autosomes in post-treatment samples from the intensive treatment arm. However, the π ratio comparison revealed a decrease in π (mean π value ratio $+ 3$ or 5 SDs) within the ZSR (coordinates 10,680,112- 43,743,322 bp) in the Z chromosome in the intensive post-treatment group between positions 34,225,001- 36,340,000 bp (Figure 5.3C). This is expected as the ZSR has fewer copies in the genome (0.75 compared to 1.0 for autosomes), leading to lower π (200). Furthermore, there was also a female bias at post-treatment (14 females compared to 8 males), which likely led to a further decrease in π in the ZSR because female parasites are heterogametic (ZW) compared to homogametic males (ZZ).

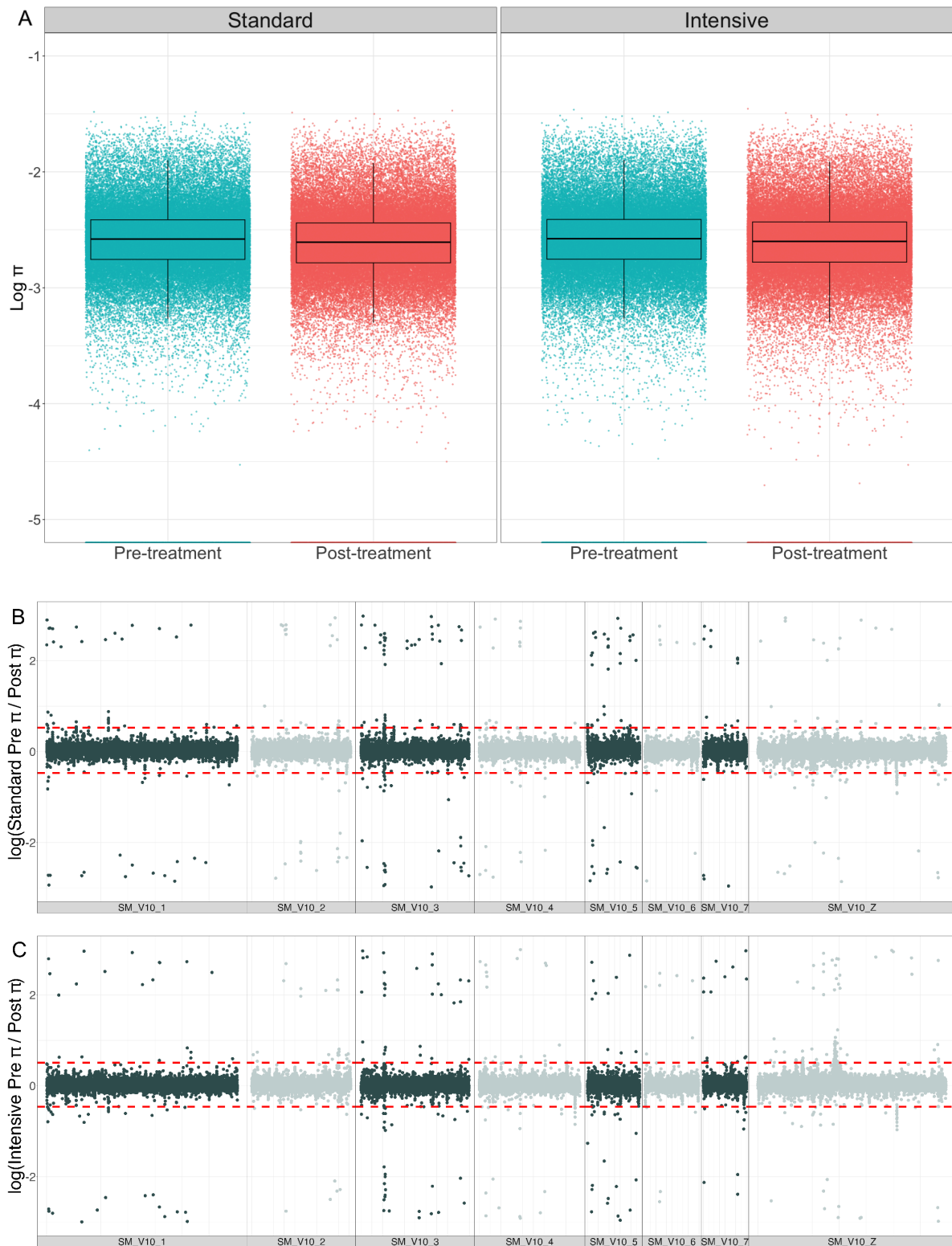


Figure 5.3: Nucleotide diversity comparisons for each time point (pre- and post-treatment) and between treatment regimens. (A) Box plots show the log nucleotide diversity (π) distributions for each population. Nucleotide diversity was calculated as a mean across each chromosome for each treatment group and time point. The ratio between the standard (B) and intensive (C) pre- and post-treatment π calculated in 5 kb windows is shown. Dashed red lines represent mean \pm 3 SDs.

5.3.3 Genetic differentiation between pre-treatment and post-treatment stratified by treatment arms

To identify PZQ treatment-induced genetic changes, pairwise genetic differences (F_{st}) between pre- and post-treatment populations from each treatment regimen were estimated in 5 kb windows throughout the genome. Pairwise F_{st} analysis revealed low levels of genetic differentiation between pre- and post-treatment populations from both treatment regimens (Standard arm mean = 0.00564, 95% CI: 0.00554-0.00574; Intensive arm mean = 0.00538, 95% CI: 0.00529-0.00548) (Appendix Table 5.4). Despite the reported low levels of average genetic differentiation between pre- and post-treatment populations, variation and discrete peaks in F_{st} values were observed across the genome (Figure 5.4). Genome-wide differentiation between pre-treatment samples from the standard and intensive treatment arms was expected to show that the populations were genetically indistinguishable and act as a control (Figure 5.4A). However, several discrete regions of high F_{st} values were found, suggesting that a proportion of these signals represent noise associated with sampling variation and is likely unrelated to selection (Figure 5.4A).

To identify candidate regions of genetic differentiation, a region was classified as a candidate for selection if it contained at least 5 windows within the top 0.25% of elevated F_{st} values within 250 kb distance of each other. A total of 184 outlier 5 kb windows were identified in the top 0.25% of elevated F_{st} values in both pre- vs post-treatment comparisons from each treatment group (Figures 5.4B and 5.4C). Most of which were present on chromosome Z ($n = 38$ or $n = 76$), followed by chromosomes 1 ($n = 39$) and 2 ($n = 34$) for standard and intensive arms, respectively (Figures 5.4B and 5.4C). Of those 184 outlier windows, instances of at least 5 consecutive 5 kb windows were recorded in 9 cases, most of which were present on chromosome 1 ($n = 4$). Six of the outlier regions were from the standard treatment arm and three were from the intensive treatment arm (Appendix Table 5.5). The six candidate regions identified in the standard arm contained 11 genes, and the 3 candidate regions identified in the intensive arm contained 13 genes (Appendix Table 5.5). No overlapping peaks of differentiation were found between treatment regimen comparisons (Figures 5.4B and 5.4C). Two regions were of particular interest in the intensive arm (peak 2 on chromosome 1 and peak 3 on chromosome 2), which contained genes that may be candidates for PZQ-linked selection. Peak 2 on chromosome 1 contained a calcium ion channel (*Smp_160820*). Praziquantel mediates calcium influx into the schistosome and it has been suggested that calcium ion channels facilitate this (241–244) and are hypothesised to be involved in resistance (245,246). Peak 3 on chromosome 2 contained a G-protein

coupled receptor (GPCR) (Smp_161210). R-Praziquantel has been shown to act as a GPCR ligand in the host, but a parasite GPCR target has yet to be identified (247).

To assess the impact of differential treatment intensities on *S. mansoni* populations, a comparison of post-treatment populations from the standard and intensive treatment arms was undertaken (Figure 5.4D). A total of 184 outlier 5 kb windows were identified in the top 0.25% of elevated F_{st} values, most of which were present in chromosome Z ($n = 70$) followed by chromosome 3 ($n = 33$). Of those 184 outlier windows, instances of at least 5 consecutive 5 kb windows were recorded in 6 cases, most of which were present on chromosome 3 ($n = 3$) (Appendix Table 5.5). Of the 11 genes within the six identified regions, no clear candidates for PZQ selection were identified.

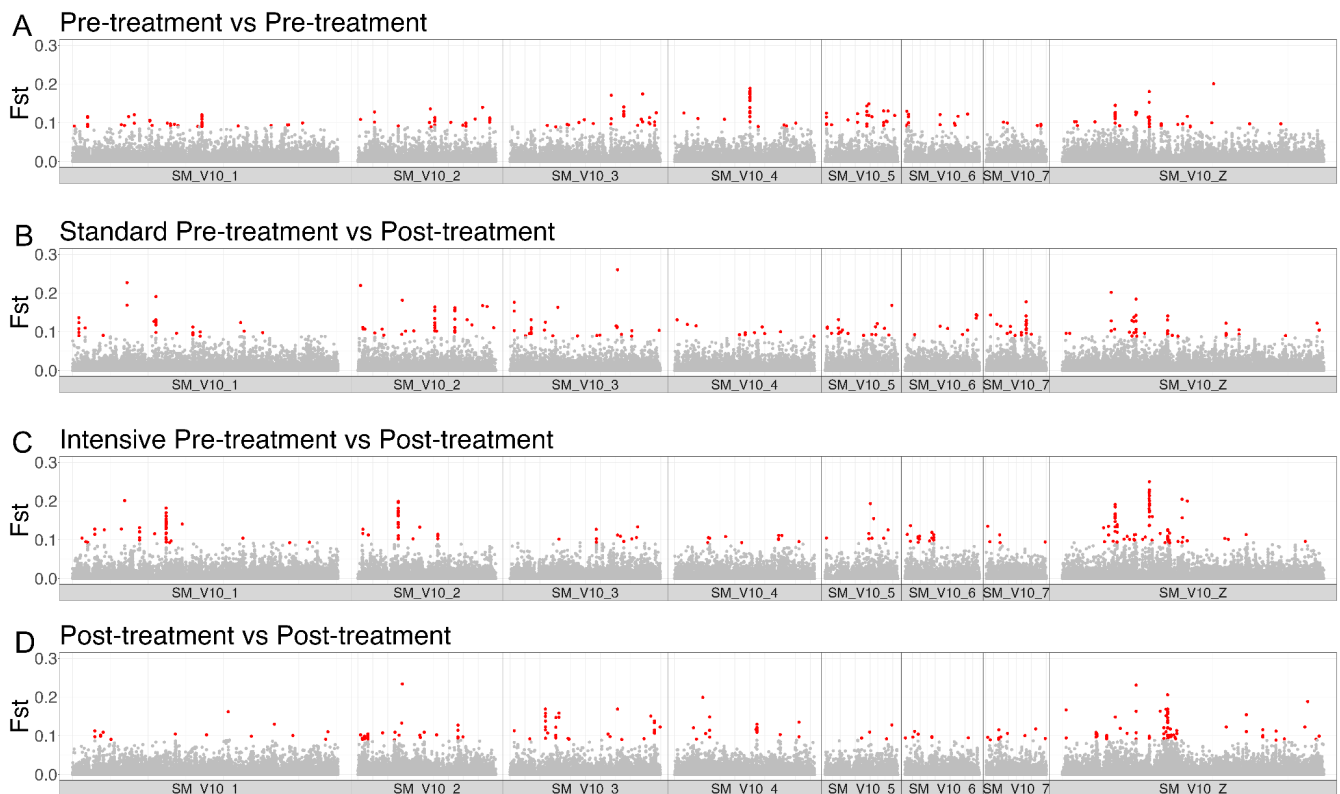


Figure 5.4: Genome-wide genetic differentiation (F_{st}) between standard and intensive treatment populations. (A) pre- vs pre-treatment samples; (B) standard pre- vs post-treatment samples; (C) intensive pre- vs post-treatment samples; (D) standard post- vs intensive post-treatment samples. Each point represents median F_{st} values between genomic sliding windows of 5 kb. Genomic windows with the highest 0.25% of F_{st} values are coloured red, and the values below are coloured grey.

5.3.4 Selection between pre-and post-treatment populations

Genome-wide scans to detect population-specific positive selection were conducted using the cross-population extended haplotype homozygosity (XP-EHH) statistic for pre- and post-treatment populations for each treatment regimen (Figure 5.5). A total of 180 outlier 5 kb windows were identified in the bottom 0.25% of XP-EHH values, most of which were present in chromosome Z ($n = 44$ or $n = 60$) followed by chromosomes 1 ($n = 38$) and 4 ($n = 29$) for standard and intensive arms, respectively (Figures 5.5A and 5.5B). Of those 180 outlier windows, instances of at least 5 consecutive 5 kb windows were recorded in 8 cases, most of which were present on chromosome 1 ($n = 4$). Four of the outlier regions were from the standard treatment arm, and four from the intensive treatment arm. However, the outlier regions from each post-treatment population did not overlap (Appendix Table 5.6). The enrichment of the windows of extreme XP-EHH values in the Z chromosome likely reflects a technical artefact due to difficulty mapping the highly repetitive Z chromosome (200). However, the enrichment is particularly present within the ZSR region (coordinates 10,680,112- 43,743,322), which is present within the population at a lower copy number as it is present as a single copy in females. Thus this finding may represent a population genetic effect rather than a technical error.

Of the eight candidate regions of selection identified in post-treatment populations using XP-EHH statistic, two regions overlap with Fst candidate regions identified on chromosomes 1 (Standard pre vs post) and 2 (Intensive pre- vs post-treatment) (Appendix Tables 5.5 and 5.6). The first overlapping candidate region in chromosome 1 (total length = 35 kb) contained 3 genes (Smp_176850, Smp_1766840, Smp_099690) (Appendix Tables 5.5 and 5.6). However, no clear candidates for PZQ selection were identified. The second candidate region of interest was found on chromosome 1 where there was Fst and XP-EHH overlap from comparing pre- and post-treatment populations from the intensive PZQ treatment arm. This region implicated six genes (total length = 105 kb), one of which was a calcium ion channel (Smp_160820). No protein encoding variants were found within this gene.

To determine if there was a differential impact of standard (40 mg/kg PZQ) vs intensive (80 mg/kg PZQ) treatment, a comparison of post-treatment populations from the standard and intensive treatment arms was undertaken (Figure 5.5C). Negative XP-EHH values indicate windows under stronger selection in the intensive post-treatment population. A total of 180 outlier 5 kb windows were identified in the bottom 0.25% of XP-EHH values, most of which were present in chromosome Z ($n = 119$) followed by chromosome 1 ($n = 24$). Two candidate regions of selection were identified on chromosomes 1 (total length = 220 kb) and 5 (total

length 160 kb), containing 7 and 2 genes, respectively (Appendix Table 5.6). However, these regions did not overlap with Fst candidate regions identified in the post-treatment population comparison (Figure 5.4D), and no clear candidates for PZQ selection were identified.

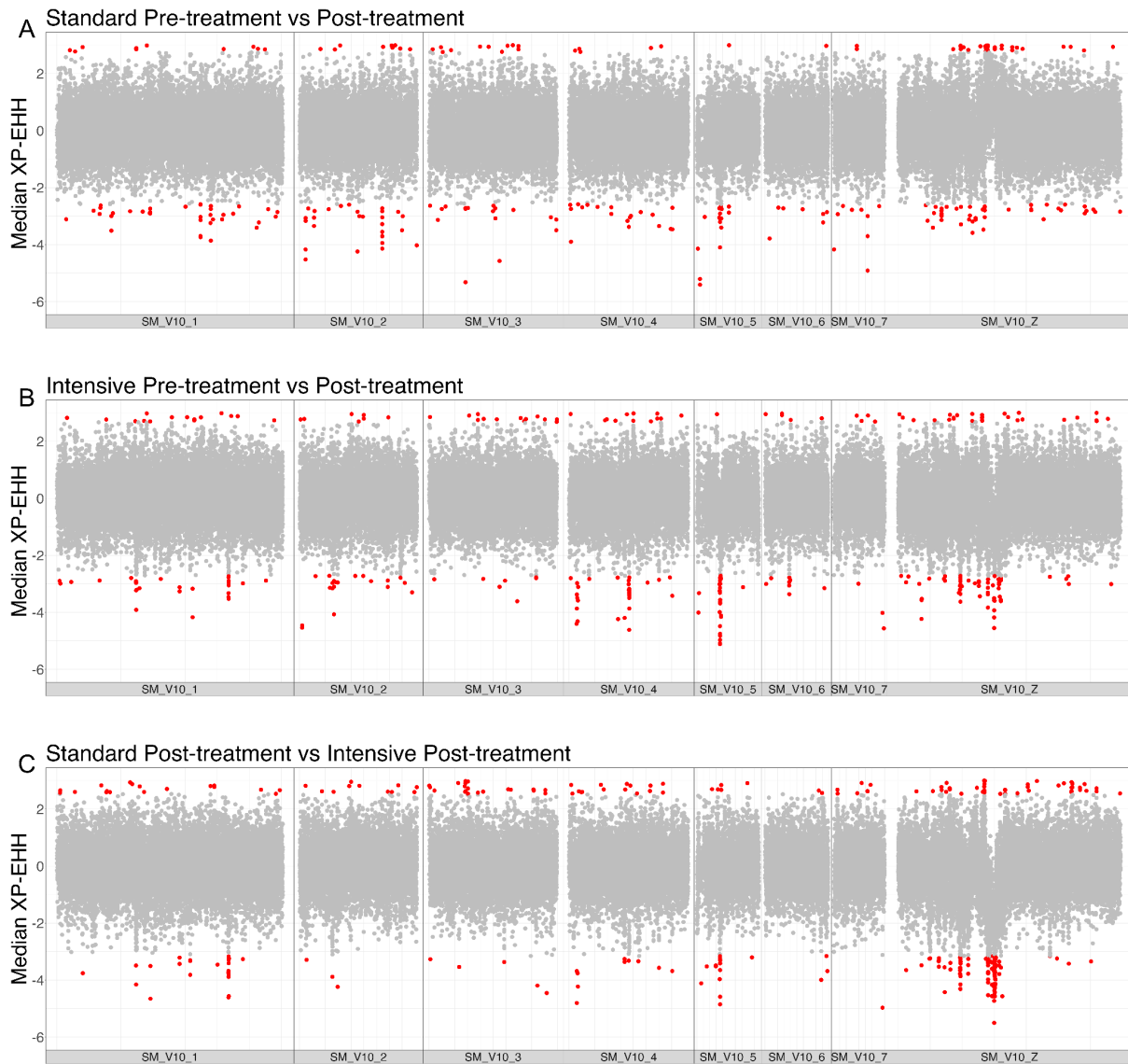


Figure 5.5: Genome-wide XP-EHH comparisons between pre and post-treatment groups, stratified by treatment regimen. Comparison of XP-EHH values across the genome for (A) standard and (B) intensive; standard and (C) intensive post-treatment samples. Each point represents median XP-EHH values for 5 kb sliding windows. Genomic windows with the highest 0.25% of XP-EHH values are coloured red, and values below are coloured grey. Negative values represent windows under stronger selection in post-treatment populations (A-B) and in intensive post-treatment populations (C).

5.3.5 Genetic diversity of SmTRPM_{PZQ}

To investigate the genetic diversity of the SmTRPM_{PZQ} ion channel, the exons encoding SmTRPM_{PZQ} were scanned for genetic variants. In line with findings from other genomic surveys (151,152), no evidence of recent selection acting on SmTRPM_{PZQ} (Smp_246790) using XP-EHH was found. However, analysis of the genetic variation within the exons encoding the SmTRPM_{PZQ} revealed the presence of 60 exonic mutations (24 protein-altering variants) (Figure 5.6). A high prevalence mutation within the five prime UTR region (A2627629G) was identified, resulting in a premature start codon which was present as a homozygous form in 18 samples (20.5% of samples). However, A2627629G was not enriched in any of the post-treatment samples (Figure 5.5C).

The dataset was examined to detect the presence of known mutations that lead to a loss or reduced sensitivity of SmTRPM_{PZQ} to PZQ (153). One of these mutations (p.R1843Q) present in the COOH-terminal coiled-coil region of SmTRPM_{PZQ} was found in 42% of the miracidia analysed (28.4% in a heterozygous form and 13.6% in a homozygous form) (Figure 5.6). The homozygous mutation was present at a higher frequency at post-treatment (7/42 post-treatment miracidia from 6 children) compared to pre-treatment (5/44 pre-treatment miracidia from 3 children). This mutation was found to result in lower sensitivity to PZQ due to in silico predicted tetramer misfolding and lower channel expression (153). Furthermore, another variant resulting in reduced PZQ sensitivity was found (p.M1068I) (<https://www.trptracker.live/>) in pre-treatment samples. This mutation was found in 36.3% of miracidia (26.1% in heterozygous form and 10.2% in homozygous form). However, there was no enrichment for this variant in post-treatment populations.

To explore the genetic basis of PZQ sensitivity, regions most likely to impact drug response were prioritised. Focus was placed on the transmembrane region of SmTRPM_{PZQ} protein because mutagenesis data within this region (228) revealed that mutation of 20/23 amino acid residues resulted in a reduction or complete loss of PZQ sensitivity. Notably no mutations were found within the transmembrane region of SmTRPM_{PZQ} or the PZQ binding pocket in the genomic dataset (Figure 5.6A).

To further investigate this, an amplicon panel comprising four primer pairs were designed to target the exons encoding the protein domains in the PZQ binding pocket in SmTRPM_{PZQ} (Figure 5.6B). Amplicon sequencing on 462 miracidia from pre- and post-treatment time points from seven villages was undertaken, after which 445 miracidia passed QC. The amplicon data identified a total of 37 high-quality SNPs and three indels (Figure 5.6B and

Appendix Table 5.7). The average coverage per amplicon was high but variable (range: 47.26 to 669.29) (Appendix Table 5.7). Most of the SNPs and indels identified were intronic, not leading to any changes in the protein sequence (Appendix Tables 5.8 and 5.9). Only two SNPs (R1375H and I1464V) were found to result in a non-synonymous mutation and were in the heterozygous form (Figure 5.6B). The first non-synonymous mutation (R1375) is present in the S1 transmembrane helix, which increased in allele frequency by two (1.26% to 2.47%) and three-fold (0.85% to 2.86%) in post-treatment populations in the standard and intensive treatment arms respectively (Appendix Table 5.10 and Figure 5.6C). The second non-synonymous mutation (I1464V) is present in the S3 transmembrane helices, which increased in allele frequency in both treatment arms (standard 0% to 0.56%; intensive 0.42% to 1.06%) (Figure 5.6C). However, since PZQ resistance is a recessive trait, heterozygous mutations are unlikely to result in PZQ resistance (227).

Furthermore, this dataset was searched to identify the three markers implicated in PZQ resistance (227). The first was a homozygous SNP present in *SmTRPM_{PZQ}* (2723187C, p.I1020I), which is predicted to cause a synonymous mutation. The first marker (2723187C, p.I1020I) was present in 13.6% of miracidia (12 miracidia from 11 children) and was more common in pre-treatment populations ($n = 8$ miracidia from 8 children). 26.1% of miracidia (23 miracidia from 18 children) were heterozygous for the marker. The second and third markers are two large (~1,500 kb) deletions present close to *SmTRPM_{PZQ}* and *SOX13* genes (positions 2,775,001-2,900,000 bp and 3,175,001-3,300,000 bp, respectively). To identify structural variants in my data, including the two large deletion markers associated with PZQ resistance described above, structural variant calling was undertaken. The first large deletion marker close to *SmTRPM_{PZQ}* was not found nor any deletions close to *SmTRPM_{PZQ}* were identified. Three smaller deletions were found adjacent to *SOX13*; an 869 bp deletion (position 3,178,004-3,178,873 bp) found in 3.4% miracidia ($n = 3$ miracidia from 3 children), a 5,054 bp deletion (position 3,202,891-3,207,945 bp) found in 4.5% miracidia ($n = 4$ miracidia from 4 children), and a large 13,915 bp deletion (position 3,289,401-3,303,316 bp) found in 2.3% miracidia ($n = 2$ miracidia from 2 children). These deletions were all present in a low frequency and in a heterozygous state.

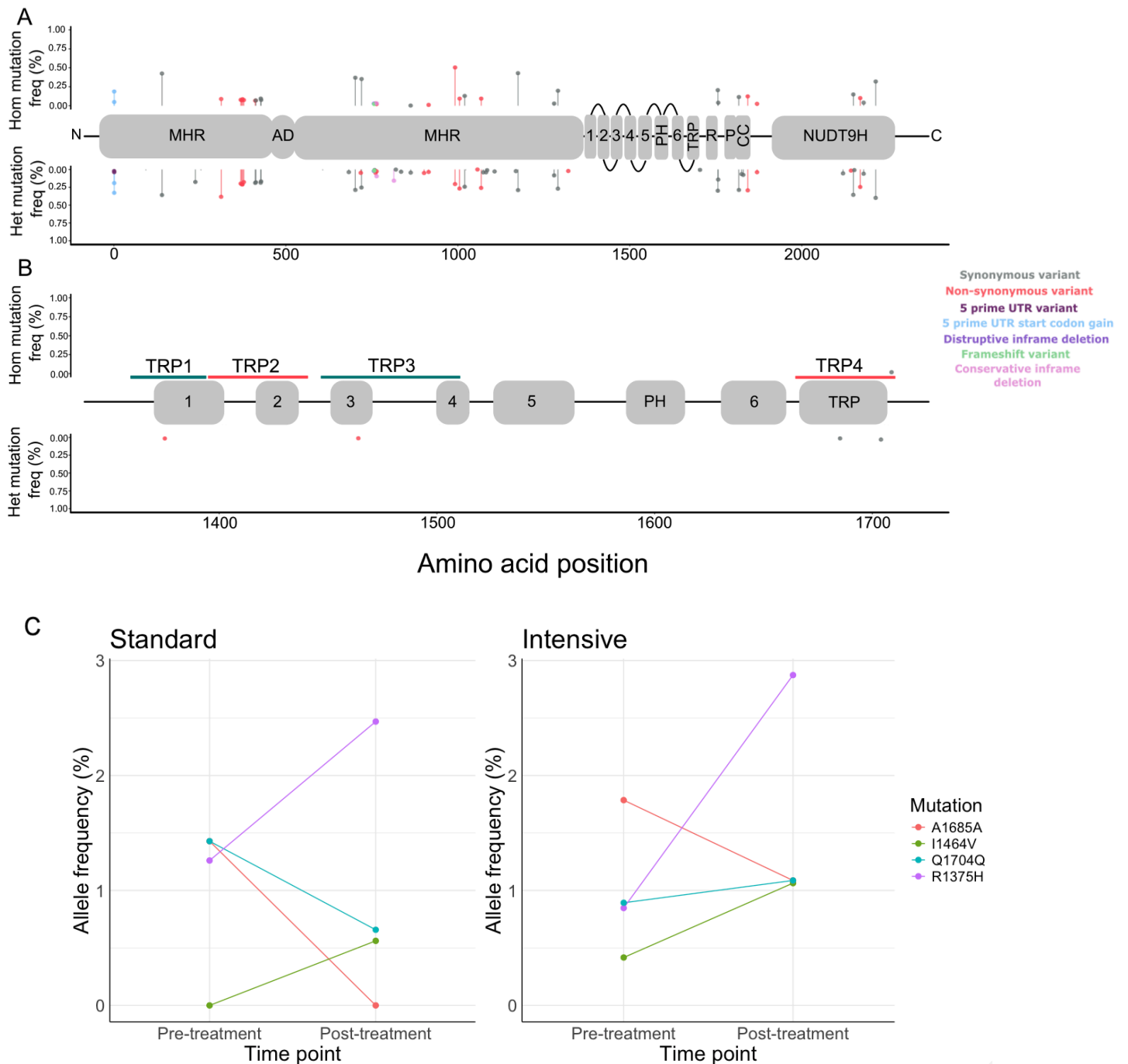


Figure 5.6: Distribution and frequency of genetic variation in SmTRPM_{PZQ}. A) Frequency of exonic variants across the protein structure of SmTRPM_{PZQ} (Smp_246790.1) reported across 88 *S. mansoni* miracidia. B) Frequency of variants within the transmembrane region of SmTRPM_{PZQ} containing the proposed PZQ binding site using amplicon sequencing. TRP1-4 indicates the name and the protein domain/s the primers target. The bars and terminal points are coloured by the impact of each variant predicted using SnpEff. C) Allele frequencies for synonymous and non-synonymous SNPs detected in the PZQ binding pocket, stratified by treatment regimen: standard (40 mg/kg PZQ) and intensive (80 mg/kg PZQ).

5.4 Discussion

With the proposed expansion of mass treatment of PZQ to achieve the new WHO NTD roadmap goal for the elimination of schistosomiasis as a public health problem in endemic areas by 2030, there is a need to monitor the impact of PZQ intervention on schistosome populations. Therefore, whole genome sequencing of individual *S. mansoni* miracidia sampled from Lake Albert, a persistent schistosomiasis hotspot in Uganda, despite over two decades of annual PZQ treatment, was undertaken. Miracidia were sampled from two treatment regimens (40 mg/kg vs 80 mg/kg PZQ) to determine if there is differential impact on the genetic response of *S. mansoni*.

Generating genomic data from *S. mansoni* populations under PZQ selection pressure in endemic areas may lead to new insights into the mechanism by which drug resistance may act. There was no genetic structure observed in the overall Lake Albert *S. mansoni* population, however, there is evidence that PZQ treatment had an effect on the genetic diversity of *S. mansoni* populations. Small but significant reductions in genome-wide genetic diversity were observed in post-treatment *S. mansoni* populations. Comparable reductions in genetic diversity were observed between the standard and intensive treatment arms. The intensive treatment did not appear to have a larger effect on the reduction of genetic diversity; it would be expected that the intensive treatment would be more effective in reducing the parasite population, as evidenced by the higher CRs observed in Chapter 3, compared to the standard treatment arm. High rates of gene flow between *S. mansoni* populations likely allowed for the rapid recovery of genetic diversity post-PZQ treatment, and the long follow-up of six months is too long to detect a genetic bottleneck caused by treatment. The large follow-up time between pre- and post-treatment sample collection likely facilitated reinfection and the development of pre-patent infections. Several studies have demonstrated that PZQ treatment has either no impact on genetic diversity (161,171,237,248,249) or a temporary reduction in genetic diversity that recovers within months post-treatment (221,235,250). No studies to date have demonstrated long-term reductions in population genetic diversity in areas of high prevalence. This demonstrates the resilience of *S. mansoni* populations to repeated PZQ treatment (235).

Minimal population differentiation between pre- and post-treatment *S. mansoni* populations from both treatment arms was found, indicating that post-treatment populations do not represent a distinct subpopulation. Despite the low levels of population differentiation, a candidate region of genetic differentiation was found which was of interest. The candidate

region on chromosome 1 contained a calcium ion channel (Smp_160820) and was also found to be under positive selection in the intensive post-treatment *S. mansoni* population. Praziquantel mediates calcium influx into the schistosome, and it has been suggested that calcium ion channels facilitate this (38–41) and are hypothesised to be involved in resistance (42,43). However, no protein-encoding variants were found in this gene.

Consistent with previous studies (151–153), no evidence of selection acting on SmTRPM_{PZQ} was found in post-treatment *S. mansoni* populations. However, extensive low-frequency variation was identified throughout this gene which is in line with a recent study exploring the genetic diversity of this gene (153). Of particular interest was the identification of three mutations: p.R1843Q, p.M1068I and p.I1020I, the first two mutations have been functionally profiled and cause reduced channel responsiveness to PZQ (153,251). The latter mutation is a marker associated with PZQ resistance in a laboratory *S. mansoni* line resistant to PZQ (227). There was no significant enrichment of these mutations in post-treatment *S. mansoni* populations. This suggests that a single round of PZQ treatment did not exert a strong selective pressure on *S. mansoni* populations. It is likely that extensive refugia in snails, untreated humans and animal reservoirs, and high rates of gene flow provide pools of susceptible alleles to dilute those conferring PZQ resistance in treated populations. Mixing of untreated and treated parasite populations allows for rapid recovery of genetic diversity following treatment. Though there is strong genetic and biochemical evidence that PZQ activates SmTRPM_{PZQ} and the channel is involved in differential PZQ response, the causal variant has yet to be identified. This makes genotyping *S. mansoni* collected in endemic settings under drug pressure for PZQ resistance difficult. Genome-wide data, including this study have failed to link variation in this gene to drug selection (151–153). Furthermore, the mechanism of PZQ resistance mediated by SmTRPM_{PZQ} in a laboratory-resistant *S. mansoni* strain involved significantly reduced expression of the gene compared to the susceptible strain (227). Future work should focus on determining if changes in expression or genetic variation within this gene are associated with reduced PZQ efficacy in field populations of *S. mansoni* (231).

The most striking finding in this chapter was the lack of genetic diversity observed within the transmembrane region of the SmTRPM_{PZQ} in the genomic data. Further exploration of the PZQ binding pocket in the transmembrane region of the protein using targeted amplicon sequencing supported this finding, despite sequencing more miracidia and achieving a higher sequencing depth. However, two non-synonymous mutations were identified (R1375H and I1464V) which increased in frequency in post-treatment populations, notably the greatest effect was seen in the intensive arm where R1375H increased three-fold in

post-treatment populations. Neither of these non-synonymous mutations have been functionally profiled and represent candidates to determine their impact on PZQ sensitivity on SmTRPM_{PZQ}. Furthermore, Berger *et al.*, (153) identified variation within this region using a larger sample size but found no high-frequency functionally impactful variants. The transmembrane region is likely highly conserved as it is essential for the binding of its endogenous ligand and for its function within *S. mansoni*. Different parasitic flatworms differ in their sensitivity to PZQ and it has been suggested that the differences in amino acids lining the transmembrane region underpin this variability (252,253). Functional analysis of TRPM_{PZQ} revealed the basis of PZQ insensitivity in *Fasciola hepatica*, a single SNP which causes an amino acid change within the PZQ binding pocket from an asparagine to threonine residue. This emphasises that even minimal and conservative amino acid change can cause a loss of PZQ sensitivity (228,252). Further work is required to understand the endogenous role of this ion channel throughout the schistosome life cycle.

The sample size of *S. mansoni* miracidia whole genome sequenced may have limited the power to detect genetic changes associated with PZQ treatment. Whilst amplicon sequencing had a larger sample size and provided deeper coverage of the PZQ binding site in TRPM_{PZQ}, additional genetic markers to capture the broader population structure could have provided deeper insights into the genetic impact of PZQ treatment. Furthermore, the six-month follow up period between pre- and post-treatment sampling was likely too long to capture potential genetic bottlenecks caused by PZQ treatment. Rapid re-infection and the development of pre-patent infections during this follow up time likely facilitated the recovery of genetic diversity following PZQ treatment. Although this study identified candidate variants for potential PZQ resistance however, these variants require functional validation. To better investigate the genetic response of *S. mansoni* to PZQ treatment in endemic settings such as Lake Albert, future studies should focus on shorter follow up periods, longitudinal sampling and undertake the functional validation of candidate variants.

To conclude, the findings in this chapter demonstrate the complexity of genetically monitoring *S. mansoni* populations under PZQ treatment pressure in endemic settings. In summary, a small but significant reduction in genome-wide diversity as a result of PZQ treatment was found. It is likely that high levels of gene flow and reinfection contributed to the rapid recovery of genetic diversity, which may obscure any short-term bottlenecks caused by PZQ treatment. Analysis of the variation of PZQ resistance loci (SmTRPM_{PZQ}) led to the identification of mutations which may be linked to PZQ resistance. Though these mutations were present at low frequencies, they represent standing variation for PZQ resistance in natural *S. mansoni* populations.

Chapter 6: Discussion and Conclusion

6.1 Recapitulation and directions for future work

Praziquantel (PZQ) is the only drug used to treat schistosomiasis and is thus considered the cornerstone of schistosomiasis control programmes. Large scale-up of mass drug administration (MDA) programmes delivering PZQ to endemic areas plays a pivotal role in achieving the ambitious goals outlined by the WHO NTD roadmap. However, using a single drug to treat a disease of this magnitude is worrying should resistance develop and spread. Praziquantel resistance has been a significant enigma in schistosomiasis research for decades. Recent progress has been made in the identification of a molecular target of PZQ, SmTRPM_{PZQ}, which has also been implicated in PZQ resistance in *Schistosoma mansoni* (227–229). However, our knowledge of PZQ resistance in field settings is limited in light of recent advances. This project sets out to investigate 1) the efficacy of PZQ treatment in a cohort of preschool-aged children (PSAC) from a clinical trial in Uganda, 2) the population diversity and structuring of Ugandan *S. mansoni* populations, 3) the genomic impact of PZQ treatment on the structure and diversity of *S. mansoni* populations.

Table 6.1: Summary of major findings in each chapter of the thesis.

Thesis chapter	Major findings
Analysis of praziquantel treatment response in preschool-aged children	<ul style="list-style-type: none"> ● Both the 40 mg/kg PZQ and 80 mg/kg PZQ treatment groups demonstrated sub-optimal clearance of <i>Schistosoma mansoni</i>, with parasitological cure rates falling below the WHO-recommended threshold of 85%. ● Antigen-based cure rates were significantly lower than the parasitological cure rates. ● Logistic regression models indicated no significant association between cure rates and demographic or drug exposure factors. ● Significant inter-individual pharmacokinetic variability in plasma levels of both praziquantel enantiomers was found.
Population genomic characterisation of Ugandan <i>Schistosoma mansoni</i>	<ul style="list-style-type: none"> ● Clear geographical structuring of <i>Schistosoma mansoni</i> populations was observed at both the global and regional levels in Uganda. ● Distinct genetic separation was found between <i>Schistosoma mansoni</i> populations from Lake Albert and Lake Victoria. ● Mitochondrial variants indicated a loss of resolution in population clustering compared to nuclear variants where samples did not show the expected district-level

	<p>population structure.</p> <ul style="list-style-type: none"> • Evidence of gene flow was identified between districts in Uganda, particularly between inland (Tororo) and shoreline districts (Hoima and Mayuge) and between Damba Island (Koome Islands) and Hoima.
<p>Investigating the genetic impact of praziquantel treatment on <i>Schistosoma mansoni</i> populations in Lake Albert</p>	<ul style="list-style-type: none"> • A small but significant reduction in genetic diversity in post-treatment populations compared to pre-treatment. • The intensive treatment arm did not result in a greater reduction in the genetic diversity of <i>Schistosoma mansoni</i> populations compared to the standard treatment arm. • A candidate region on chromosome 1 was identified containing a calcium ion channel under selection in the intensive post-treatment population. • No evidence of selection was acting on the SmTRPM_{PZQ} in post-treatment <i>S. mansoni</i> populations but extensive low frequency variation was found. • Three mutations in the SmTRPM_{PZQ} were found (p.R1843Q, p.M1068I and p.I1020I), the first two mutations have been functionally profiled and cause reduced channel responsiveness to PZQ. • A lack of genetic diversity was found in the transmembrane region of the SmTRPM_{PZQ}. • Amplicon sequencing of the transmembrane region of SmTRPM_{PZQ} identified two non-synonymous mutations (R1375H and I1464V), which increased in frequency in post-treatment populations, particularly in the intensive treatment arm.

6.1.1 Future directions

The poor CRs and the extent of re-infection reported in **Chapter 3** highlight a crucial need for increased funding in drug discovery and drug development in schistosomiasis. Though PZQ remains the cornerstone of schistosomiasis control and the only drug available for treatment, it has limitations that should not be overlooked, particularly with efforts to eliminate schistosomiasis as a public health problem by 2030. The primary drawbacks of PZQ include its ineffectiveness against juvenile stages and its rapid elimination, with 80% of the drug cleared from the body within four days. Given the extensive water contact in endemic settings, infected individuals are likely to harbour juvenile parasites at the time of treatment, leading to incomplete clearance and, thus, treatment failure. Additionally, this combination of high water exposure and the rapid elimination of PZQ creates a perfect storm for re-infection. Relying solely on PZQ chemotherapy is insufficient to interrupt transmission and effectively control schistosomiasis. A new antischistosomal drug with specific properties would be desirable: a single-dose curative agent with a long shelf life, minimal side effects, low production cost, and efficacy against both juvenile and adult worms, including those of medical and veterinary importance. Advances in high-throughput compound screening, medicinal chemistry and parasite biology as well as collaborations with the pharmaceutical industry offer promising research avenues for schistosomiasis drug discovery. A recent study has identified several compounds with single-dose efficacy against both juvenile and adult worms *in vivo* which are predicted to cure schistosomiasis infection in humans at a single dose less than 5 mg/kg (10 fold less than PZQ) (254) However, progressing these candidate compounds from preclinical development to Phase I clinical trials remains a major bottleneck in the drug development process. Helminth drug development has historically been underfunded, and progressing beyond early-stage trials requires substantial funding. Beyond drug development, consideration is needed regarding how the drug will be funded and distributed, particularly to endemic communities. Deciding whether the new drug will be donated or made available at an affordable cost will be important for determining its impact on control and elimination efforts. Furthermore, comprehensive PK and pharmacogenetic (PG) studies across all age groups, from PSAC to adults, are essential to establish an optimised dosing regimen that achieves optimal CRs.

Chapter 4 revealed evidence of gene flow between *S. mansoni* populations across different districts in Uganda. This is somewhat expected with known human movement between Lake

Albert and Lake Victoria, particularly among mobile populations such as fishing communities, and highlights the interconnectedness of these lake systems in shaping parasite population dynamics. The extent of human movement is concerning from a schistosomiasis control perspective, especially if individuals miss MDA of PZQ while travelling between lakes, which can sustain transmission across regions. Understanding the population structure of *S. mansoni* and the extent of gene flow between geographical areas is crucial for predicting the spread of traits, such as PZQ resistance. If resistance were to emerge, gene flow could facilitate and reduce the time for resistance mutations to emerge and reach high frequencies between regions, undermining control efforts; conversely, limited gene flow might confine resistance to specific areas, enabling targeted interventions.

Whole genome sequencing has been successfully applied to several *Schistosoma* species, including those of veterinary importance (151,153,155). These studies and the findings in this thesis have increased our understanding of the genomic landscapes of *Schistosoma* species. To build upon the population genomic analyses presented within this thesis, more *Schistosoma* samples should be sampled from a broader geographical range. The data generated and analysed within the thesis is from *S. mansoni* populations from two major hotspot regions in Uganda. There is a need for more comprehensive sampling across Uganda and from West African countries to improve the resolution of population genomic analyses and to determine if the patterns of population structure observed in Ugandan *S. mansoni* are unique to this region or are seen in other populations. Much of what we know about the population structuring of *S. mansoni* is from using a limited number of genetic markers, including the commonly used mitochondrial *cox1* gene. Findings in **Chapter 4** demonstrated a loss of resolution when using a single gene to characterise the population structuring of *S. mansoni* populations. We should be pushing for the application of genomics to not only *S. mansoni* but other *Schistosoma* species to unravel the complexities of natural *Schistosoma* populations. The current literature for the population genetics of schistosomes is saturated with those focusing on *S. mansoni* and evidence from other *Schistosoma* species is severely lacking; with the extensive genetic diversity observed within the *Schistosoma* genus, it is evident that there is more to learn.

To investigate drug resistance, whole genome sequencing of individuals has been increasingly employed in tropical diseases such as malaria and insecticide resistance in vectors (255,256). The generation of genomic data at single-nucleotide resolution allows for the correlation between genotype and phenotype. However, conducting association studies for anthelmintic resistance in schistosomiasis presents challenges, particularly due to the difficulty in sampling adult worms from human hosts, which are the target for investigating

PZQ resistance. Miracidia provide a biased sample of the total genetic diversity in the adult *S. mansoni* population as they represent only a proportion of the genetic diversity found in the adult population. Phenotypes such as cure rates and egg reduction rates are assessed at the host level, whilst genotypes are derived from offspring, usually miracidia sampled from human stool rather than adult worms. This disconnect between the phenotype (measured at the host level) and genotype (inferred from offspring) which complicates the establishment of a direct link between treatment outcomes and genotype. To address this, longitudinal studies could be employed to monitor phenotypic changes (such as cure rate and egg reduction rate) in human hosts over time and correlate genetic changes in miracidia.

Much of what we know about anthelmintic resistance is based on candidate gene approaches. Using candidate gene approaches alone prevents the discovery of other genomic loci and mechanisms which may be involved. Furthermore, a key issue is that very few studies consider the broader genomic landscape beyond the candidate genes being studied. Focusing solely on single candidate genes without understanding the surrounding genomic context can lead to misleading conclusions, making it challenging to distinguish between true selection and confounding bias. More WGS studies are needed to provide further insights into the impact of selection on the broader genomic architecture which is required to fully understand the complex genetics of anthelmintic drug resistance.

Accessibility to WGS in field settings is largely limited due to the relatively high costs, particularly when sequencing large genomes and the requirement for high DNA concentrations, which is often not possible from *Schistosoma* larval stages that are available for sampling. Furthermore, the requirement for high-performance computing clusters and relevant bioinformatic skills to analyse genomic data represent potential barriers to the application of genomics in field settings.

Overall, this thesis demonstrates the utility of next generation sequencing in generating WGS data to capture the broader genomic landscape and amplicon data to identify potential target site resistance candidates. Before the work conducted for this thesis, there were fewer than five samples with WGS data available for *S. mansoni* from Lake Albert and there was no available data detailing the diversity of the SmTRPM_{PZQ} in these populations. This thesis represents a significant expansion of the available genomic data from this hotspot region.

There is a need for multi-locus, high-throughput molecular screening of *S. mansoni* for PZQ resistance which has been highlighted several times, and **Chapter 5** represents the beginning of the development of such panels. The amplicon panel designed in **Chapter 5**

was used to detect potential target site resistance mutations within the drug-binding site of the SmTRPM_{PZQ}. However, the findings in this chapter demonstrated that this approach could be difficult to develop due to the limited functional validation of mutations in SmTRPM_{PZQ}. Further development of this amplicon panel to ideally target any functionally validated mutations in SmTRPM_{PZQ}, genetic markers tagging selective sweeps in *S. mansoni* in response to drug treatment and other candidate genomic loci of interest. However, the lack of annotational information of specific genes, particularly detailing their function in those which were found in candidate regions of selection, limited the conclusions.

The application of the amplicon sequencing panel developed in **Chapter 5** may be limited within a field setting due to several factors, including the potentially limited access to Illumina sequencing platforms and a lack of bioinformatic expertise. To overcome this, the amplicon sequencing panel could be adapted for use on a portable sequencer such as the Oxford Nanopore long-read MinION. The MinION has a user-friendly graphical web interface (such as MinKNOW) for real time base calling and basic quality control. This has already been successfully implemented in other infectious diseases (257). However, more extensive downstream bioinformatic analysis such as variant calling requires additional bioinformatic tools.

6.2 Conclusion

In conclusion, the findings presented in this thesis underscore the urgent need to address the challenges posed by PZQ in the control of schistosomiasis. The findings provide insights into the genetic population structuring of *S. mansoni* in Uganda, highlighting both district-level clustering and gene flow between Lake Albert and Lake Victoria. This has potential implications for schistosomiasis control, particularly within the context of the WHO 2030 roadmap, which aim to reduce morbidity, interrupt transmission and achieve elimination of schistosomiasis as a public health problem. The gene flow observed suggests that local transmission dynamics may complicate control efforts, reinforcing the need for sustained MDA alongside surveillance to monitor for the emergence of potential drug resistance. District-level clustering suggests for the need for geographically targeted interventions.

Furthermore, the sub-optimal CRs observed in PSAC from both treatment regimens highlight significant gaps in the efficacy of PZQ, which may present a barrier to the ambitious control strategy set out by the WHO NTD roadmap. As we look to the future, it is imperative to prioritise funding for new drug discovery and development efforts aimed at identifying a more

effective treatment option for schistosomiasis. The genomic approaches optimised and developed provide a foundational step towards future genetic surveillance of field populations of *Schistosoma* across endemic regions, particularly for tracking potential drug resistance and spread. This would provide valuable insights into how current control strategies impact the genetics of *Schistosoma* populations and have the power to provide early warning of the emergence of PZQ resistance. Given the limitations of MDA alone, these findings reinforce the need for integrated control strategies, including snail control and WASH interventions, to achieve sustainable reductions in schistosomiasis transmission by 2030.

Appendix

Appendix Table 3.1: Effect of 80 mg/kg versus 40 mg/kg praziquantel on cure rates based on three diagnostic tests: KK, CCA and CAA. The cure rate is defined by the proportion of participants who no longer test positive for schistosomiasis at week 4. The significant difference between the treatment arms is assessed using a chi-squared test.

Outcome	Baseline 40 mg/kg PZQ	Baseline 80 mg/kg PZQ	Difference (95% CI)	p-value
Cure rate at 4 weeks, n/N(%) based on KK	30/41 (73%)	39/47 (83%)	10% (-7%, 27%)	0.265
Cure rate at 4 weeks, n/N(%) based on CCA	14/42 (33%)	29/44 (66%)	33% (13%, 53%)	0.003
Cure rate at 4 weeks, n/N(%) based on CAA	10/42 (24%)	14/44 (32%)	8% (-11%, 27%)	0.408

Appendix Table 3.2: Effects of 80 mg/kg versus 40 mg/kg PZQ on egg reduction rate (ERR). The egg reduction rate is calculated by taking the reduction in mean egg count per trial arm and dividing by the mean egg count pre-treatment, then multiplying by 100. The significance between the treatment arms is assessed using the Willcoxon rank-sum test.

Outcome	Baseline 40 mg/kg PZQ	Baseline 80 mg/kg PZQ	Difference (CI)	p-value
Egg reduction rate at week 4 (geometric mean, 95% CI)	98.3% (97.1, 99.0)	98.9% (98.3, 99.3)	0.6 (-0.4, 1.9)	0.301
Egg reduction rate at week 4 (arithmetic mean, 95% CI)	98.3% (95.7, 99.4)	99.4% (98.7, 99.8)	1.1 (-0.2, 3.7)	0.262

Appendix Table 3.3: Comparison of mean pharmacokinetic parameters between two treatment regimens (40 mg/kg PZQ vs 80 mg/kg PZQ). The significant difference between the treatment arms is assessed using an independent t-test.

Pharmacokinetic parameter	40 mg/kg PZQ (std)	80 mg/kg PZQ (std)	p-value
Total PZQ AUC	2.833 (2.184)	6.214 (4.055)	0.113
AUC (R-PZQ)	0.413 (0.334)	1.484 (1.377)	0.118
AUC (S-PZQ)	2.421 (1.861)	4.730 (2.795)	0.127
Cmax (R-PZQ)	0.151 (0.106)	0.873 (0.955)	0.124
Cmax (S-PZQ)	0.891 (0.585)	2.037 (1.220)	0.0746
Tmax (R-PZQ)	2.767 (0.931)	5.296 (0.974)	0.0005
Tmax (S-PZQ)	2.767 (0.931)	5.296 (0.974)	0.0005

Appendix Table 4.1: Sample information, including the accession number, country, and district of the published whole genome sequencing data used.

Accession	Country	District	Source
ERR3173134	Uganda	Mayuge	Berger <i>et al.</i> , 2021
ERR3173113	Uganda	Mayuge	Berger <i>et al.</i> , 2021
ERR3173101	Uganda	Mayuge	Berger <i>et al.</i> , 2021
ERR3173102	Uganda	Mayuge	Berger <i>et al.</i> , 2021
ERR3173069	Uganda	Mayuge	Berger <i>et al.</i> , 2021
ERR3173070	Uganda	Mayuge	Berger <i>et al.</i> , 2021
ERR3173139	Uganda	Mayuge	Berger <i>et al.</i> , 2021
ERR3173103	Uganda	Mayuge	Berger <i>et al.</i> , 2021
ERR3173109	Uganda	Mayuge	Berger <i>et al.</i> , 2021
ERR3173111	Uganda	Mayuge	Berger <i>et al.</i> , 2021
ERR3173104	Uganda	Mayuge	Berger <i>et al.</i> , 2021
ERR3173128	Uganda	Mayuge	Berger <i>et al.</i> , 2021
ERR3173147	Uganda	Mayuge	Berger <i>et al.</i> , 2021
ERR3173259	Uganda	Mayuge	Berger <i>et al.</i> , 2021
ERR3173192	Uganda	Mayuge	Berger <i>et al.</i> , 2021
ERR3173196	Uganda	Mayuge	Berger <i>et al.</i> , 2021
ERR3173227	Uganda	Mayuge	Berger <i>et al.</i> , 2021
ERR3173248	Uganda	Mayuge	Berger <i>et al.</i> , 2021
ERR3173144	Uganda	Mayuge	Berger <i>et al.</i> , 2021
ERR3173130	Uganda	Mayuge	Berger <i>et al.</i> , 2021
ERR3173205	Uganda	Mayuge	Berger <i>et al.</i> , 2021
ERR3173230	Uganda	Mayuge	Berger <i>et al.</i> , 2021
ERR3173209	Uganda	Mayuge	Berger <i>et al.</i> , 2021
ERR3173221	Uganda	Mayuge	Berger <i>et al.</i> , 2021
ERR3173216	Uganda	Mayuge	Berger <i>et al.</i> , 2021
ERR3173078	Uganda	Mayuge	Berger <i>et al.</i> , 2021
ERR3173079	Uganda	Mayuge	Berger <i>et al.</i> , 2021
ERR3173080	Uganda	Mayuge	Berger <i>et al.</i> , 2021
ERR3173260	Uganda	Mayuge	Berger <i>et al.</i> , 2021
ERR3173256	Uganda	Mayuge	Berger <i>et al.</i> , 2021
ERR3173200	Uganda	Mayuge	Berger <i>et al.</i> , 2021

ERR3173261	Uganda	Mayuge	Berger <i>et al.</i> , 2021
ERR3173153	Uganda	Mayuge	Berger <i>et al.</i> , 2021
ERR3173232	Uganda	Mayuge	Berger <i>et al.</i> , 2021
ERR3173242	Uganda	Mayuge	Berger <i>et al.</i> , 2021
ERR3173262	Uganda	Mayuge	Berger <i>et al.</i> , 2021
ERR3173152	Uganda	Mayuge	Berger <i>et al.</i> , 2021
ERR3173246	Uganda	Mayuge	Berger <i>et al.</i> , 2021
ERR3173203	Uganda	Mayuge	Berger <i>et al.</i> , 2021
ERR3173118	Uganda	Mayuge	Berger <i>et al.</i> , 2021
ERR3173180	Uganda	Mayuge	Berger <i>et al.</i> , 2021
ERR3173225	Uganda	Mayuge	Berger <i>et al.</i> , 2021
ERR3173208	Uganda	Mayuge	Berger <i>et al.</i> , 2021
ERR3173151	Uganda	Mayuge	Berger <i>et al.</i> , 2021
ERR3173243	Uganda	Mayuge	Berger <i>et al.</i> , 2021
ERR3173043	Uganda	Mayuge	Berger <i>et al.</i> , 2021
ERR3173185	Uganda	Mayuge	Berger <i>et al.</i> , 2021
ERR3173166	Uganda	Mayuge	Berger <i>et al.</i> , 2021
ERR3173084	Uganda	Tororo	Berger <i>et al.</i> , 2021
ERR3173085	Uganda	Tororo	Berger <i>et al.</i> , 2021
ERR3173086	Uganda	Tororo	Berger <i>et al.</i> , 2021
ERR3173087	Uganda	Tororo	Berger <i>et al.</i> , 2021
ERR3173088	Uganda	Tororo	Berger <i>et al.</i> , 2021
ERR3173089	Uganda	Tororo	Berger <i>et al.</i> , 2021
ERR3173090	Uganda	Tororo	Berger <i>et al.</i> , 2021
ERR3173091	Uganda	Tororo	Berger <i>et al.</i> , 2021
ERR3173234	Uganda	Tororo	Berger <i>et al.</i> , 2021
ERR3173226	Uganda	Tororo	Berger <i>et al.</i> , 2021
ERR3173071	Uganda	Tororo	Berger <i>et al.</i> , 2021
ERR3173072	Uganda	Tororo	Berger <i>et al.</i> , 2021
ERR3173073	Uganda	Tororo	Berger <i>et al.</i> , 2021
ERR3173074	Uganda	Tororo	Berger <i>et al.</i> , 2021
ERR3173075	Uganda	Tororo	Berger <i>et al.</i> , 2021
ERR3173247	Uganda	Tororo	Berger <i>et al.</i> , 2021
ERR3173239	Uganda	Tororo	Berger <i>et al.</i> , 2021
ERR3173060	Uganda	Mayuge	Berger <i>et al.</i> , 2021

ERR3173061	Uganda	Mayuge	Berger <i>et al.</i> , 2021
ERR3173174	Uganda	Mayuge	Berger <i>et al.</i> , 2021
ERR3173126	Uganda	Mayuge	Berger <i>et al.</i> , 2021
ERR3173105	Uganda	Mayuge	Berger <i>et al.</i> , 2021
ERR3173179	Uganda	Mayuge	Berger <i>et al.</i> , 2021
ERR3173106	Uganda	Mayuge	Berger <i>et al.</i> , 2021
ERR3173201	Uganda	Mayuge	Berger <i>et al.</i> , 2021
ERR3173132	Uganda	Mayuge	Berger <i>et al.</i> , 2021
ERR3173186	Uganda	Mayuge	Berger <i>et al.</i> , 2021
ERR3173181	Uganda	Mayuge	Berger <i>et al.</i> , 2021
ERR3173095	Uganda	Mayuge	Berger <i>et al.</i> , 2021
ERR3173245	Uganda	Mayuge	Berger <i>et al.</i> , 2021
ERR3173206	Uganda	Mayuge	Berger <i>et al.</i> , 2021
ERR3173177	Uganda	Mayuge	Berger <i>et al.</i> , 2021
ERR3173175	Uganda	Mayuge	Berger <i>et al.</i> , 2021
ERR3173120	Uganda	Mayuge	Berger <i>et al.</i> , 2021
ERR3173170	Uganda	Mayuge	Berger <i>et al.</i> , 2021
ERR3173237	Uganda	Mayuge	Berger <i>et al.</i> , 2021
ERR3173165	Uganda	Mayuge	Berger <i>et al.</i> , 2021
ERR3173171	Uganda	Mayuge	Berger <i>et al.</i> , 2021
ERR3173213	Uganda	Mayuge	Berger <i>et al.</i> , 2021
ERR3173217	Uganda	Mayuge	Berger <i>et al.</i> , 2021
ERR3173250	Uganda	Mayuge	Berger <i>et al.</i> , 2021
ERR3173136	Uganda	Mayuge	Berger <i>et al.</i> , 2021
ERR3173048	Uganda	Mayuge	Berger <i>et al.</i> , 2021
ERR3173049	Uganda	Mayuge	Berger <i>et al.</i> , 2021
ERR3173052	Uganda	Mayuge	Berger <i>et al.</i> , 2021
ERR3173053	Uganda	Mayuge	Berger <i>et al.</i> , 2021
ERR3173055	Uganda	Mayuge	Berger <i>et al.</i> , 2021
ERR3173056	Uganda	Mayuge	Berger <i>et al.</i> , 2021
ERR6798399	Uganda	Koome	Vianney <i>et al.</i> , 2022
ERR6798506	Uganda	Koome	Vianney <i>et al.</i> , 2022
ERR6798511	Uganda	Koome	Vianney <i>et al.</i> , 2022
ERR6798382	Uganda	Koome	Vianney <i>et al.</i> , 2022
ERR6798532	Uganda	Koome	Vianney <i>et al.</i> , 2022

ERR6798463	Uganda	Koome	Vianney <i>et al.</i> , 2022
ERR6798445	Uganda	Damba	Vianney <i>et al.</i> , 2022
ERR6798503	Uganda	Damba	Vianney <i>et al.</i> , 2022
ERR6798540	Uganda	Damba	Vianney <i>et al.</i> , 2022
ERR6798491	Uganda	Damba	Vianney <i>et al.</i> , 2022
ERR6798457	Uganda	Damba	Vianney <i>et al.</i> , 2022
ERR6798509	Uganda	Damba	Vianney <i>et al.</i> , 2022
ERR6798476	Uganda	Damba	Vianney <i>et al.</i> , 2022
ERR6798425	Uganda	Damba	Vianney <i>et al.</i> , 2022
ERR6798544	Uganda	Damba	Vianney <i>et al.</i> , 2022
ERR6798434	Uganda	Damba	Vianney <i>et al.</i> , 2022
ERR6798495	Uganda	Damba	Vianney <i>et al.</i> , 2022
ERR6798395	Uganda	Damba	Vianney <i>et al.</i> , 2022
ERR6798546	Uganda	Damba	Vianney <i>et al.</i> , 2022
ERR6798492	Uganda	Damba	Vianney <i>et al.</i> , 2022
ERR6798529	Uganda	Damba	Vianney <i>et al.</i> , 2022
ERR6798433	Uganda	Damba	Vianney <i>et al.</i> , 2022
ERR6798502	Uganda	Damba	Vianney <i>et al.</i> , 2022
ERR6798379	Uganda	Damba	Vianney <i>et al.</i> , 2022
ERR6798464	Uganda	Damba	Vianney <i>et al.</i> , 2022
ERR6798504	Uganda	Damba	Vianney <i>et al.</i> , 2022
ERR6798436	Uganda	Damba	Vianney <i>et al.</i> , 2022
ERR6798520	Uganda	Damba	Vianney <i>et al.</i> , 2022
ERR6798456	Uganda	Damba	Vianney <i>et al.</i> , 2022
ERR6798524	Uganda	Damba	Vianney <i>et al.</i> , 2022
ERR6798450	Uganda	Koome	Vianney <i>et al.</i> , 2022
ERR6798545	Uganda	Koome	Vianney <i>et al.</i> , 2022
ERR6798470	Uganda	Koome	Vianney <i>et al.</i> , 2022
ERR6798514	Uganda	Koome	Vianney <i>et al.</i> , 2022
ERR6798543	Uganda	Koome	Vianney <i>et al.</i> , 2022
ERR6798533	Uganda	Koome	Vianney <i>et al.</i> , 2022
ERR6798442	Uganda	Lugumba	Vianney <i>et al.</i> , 2022
ERR6798471	Uganda	Lugumba	Vianney <i>et al.</i> , 2022
ERR6798422	Uganda	Lugumba	Vianney <i>et al.</i> , 2022
ERR6798513	Uganda	Lugumba	Vianney <i>et al.</i> , 2022

ERR6798461	Uganda	Lugumba	Vianney <i>et al.</i> , 2022
ERR6798377	Uganda	Koome	Vianney <i>et al.</i> , 2022
ERR6798467	Uganda	Koome	Vianney <i>et al.</i> , 2022
ERR6798469	Uganda	Koome	Vianney <i>et al.</i> , 2022
ERR6798430	Uganda	Koome	Vianney <i>et al.</i> , 2022
ERR6798386	Uganda	Koome	Vianney <i>et al.</i> , 2022
ERR6798510	Uganda	Koome	Vianney <i>et al.</i> , 2022
ERR119614	Kenya	NA	Crellen <i>et al.</i> , 2016
ERR103050	Cameroon	NA	Crellen <i>et al.</i> , 2016
ERR103049	Senegal	NA	Crellen <i>et al.</i> , 2016
ERR046038	Puerto Rico	NA	Crellen <i>et al.</i> , 2016
ERR539843	Guadeloupe	NA	Crellen <i>et al.</i> , 2016
ERR539848	Guadeloupe	NA	Crellen <i>et al.</i> , 2016
ERR539845	Guadeloupe	NA	Crellen <i>et al.</i> , 2016

Appendix Figure 4.1: Protocol for collection of miracidia on Whatman FTA cards.

Stool samples:

- Collect stool samples from *S. mansoni*-positive children (regardless of infection intensity, avoid selection bias). Each stool sample must be labelled with an individual I.D. number that relates back to the individual child (to link epidemiological data).
- Place a good amount of stool (about the size of a walnut) on a 212 µm steel sieve in a plastic pot. Using a toothbrush/applicator, break up and push the stool sample through the steel sieve, washing with approximately 1 litre of distilled/bottled water. The water will collect in the pot around the steel sieve. Carefully rinse the sieve with bottled water, taking care to lift and rinse the bottom of the sieve that has been sitting in the water. This will remove any eggs that may be attached to the underside of the sieve.
- Take the Pitchford funnel (Figure 1), ensuring that the inner funnel and the outer funnels are clean and correctly assembled. The tap at the bottom of the 38-40 micron outer funnel MUST BE CLOSED (the tap should be horizontal when closed). Lift the plastic pot with filtered stool water and carefully pour the water through both the inner and outer parts of the Pitchford funnel.

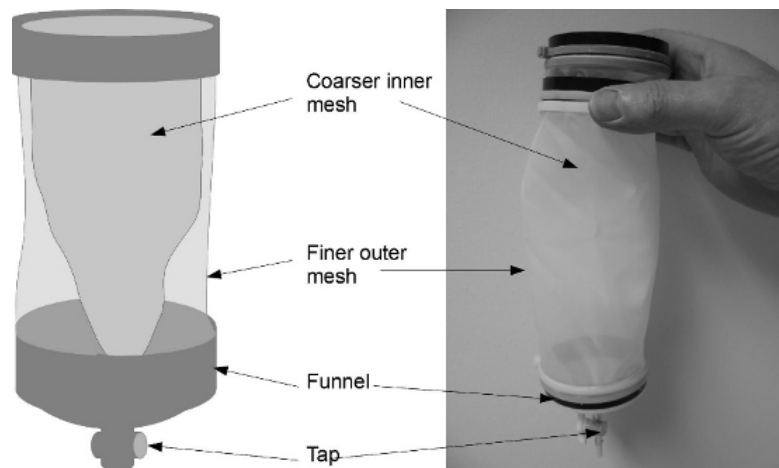


Figure 1: Pitchford funnel.

- While supporting the base, shake/twirl the Pitchford funnel around gently in order to drain the water. Add more distilled/bottled water, lift the inner funnel carefully and rinse the end of it so that any eggs stuck to the outside of the inner funnel will be rinsed into the outer funnel. Remove the inner funnel and add more water. Rinse and wash the eggs thoroughly with about 1 litre of water – until the water is clear. Shake the outer funnel until there is only a small amount of water left (it has to fit in a Petri dish).
- Take the Petri dish (labelled with the child's/sample's ID number). Hold the outer funnel over the Petri dish and GENTLY open the tap to allow the eggs and water to

flow into it. If the water doesn't come out, GENTLY tap the funnel on the bottom of the dish. Very carefully pour a small amount of water (a few millilitres) through the open funnel into the Petri dish to ensure you have all the eggs.

- Make sure there is enough water within the Petri dish to induce hatching (if not, add a little more). Place the Petri dish in indirect sunlight/shade for up to 6 h. Check the Petri dish after 20-30 min for miracidia (under the microscope at around x10 – x20 magnification) and keep checking every half hour for the next 5 to 6 h. Eggs will hatch at different times depending on light, temperature and potentially genetic characteristics. You will find different samples will hatch at very different rates, so keep checking them. Additionally, you may find only a few miracidia in a Petri dish within the first hour, and then when you check 2 h later, there may be lots more hatched out. It is a game of practice and patience! If it is possible, you can also leave unhatched petri dishes overnight and check them the next day.
- Debris in the plate can be moved towards the centre of the dish by using a gentle swirling rotation, allowing a clear area around the edge for collecting the miracidia. Once the miracidia start hatching, pick up individual miracidia using a Gilson P20 pipette set at 3-5 μl (3 μl is best) and transfer directly onto an FTA card. Make sure the miracidia spots do not touch each other. Allow the FTA card to dry for one hour. This stores the genetic material of the miracidia without damage. CHANGE PIPETTE TIPS BETWEEN EACH SAMPLE/PETRI DISH to avoid cross-sample contamination.

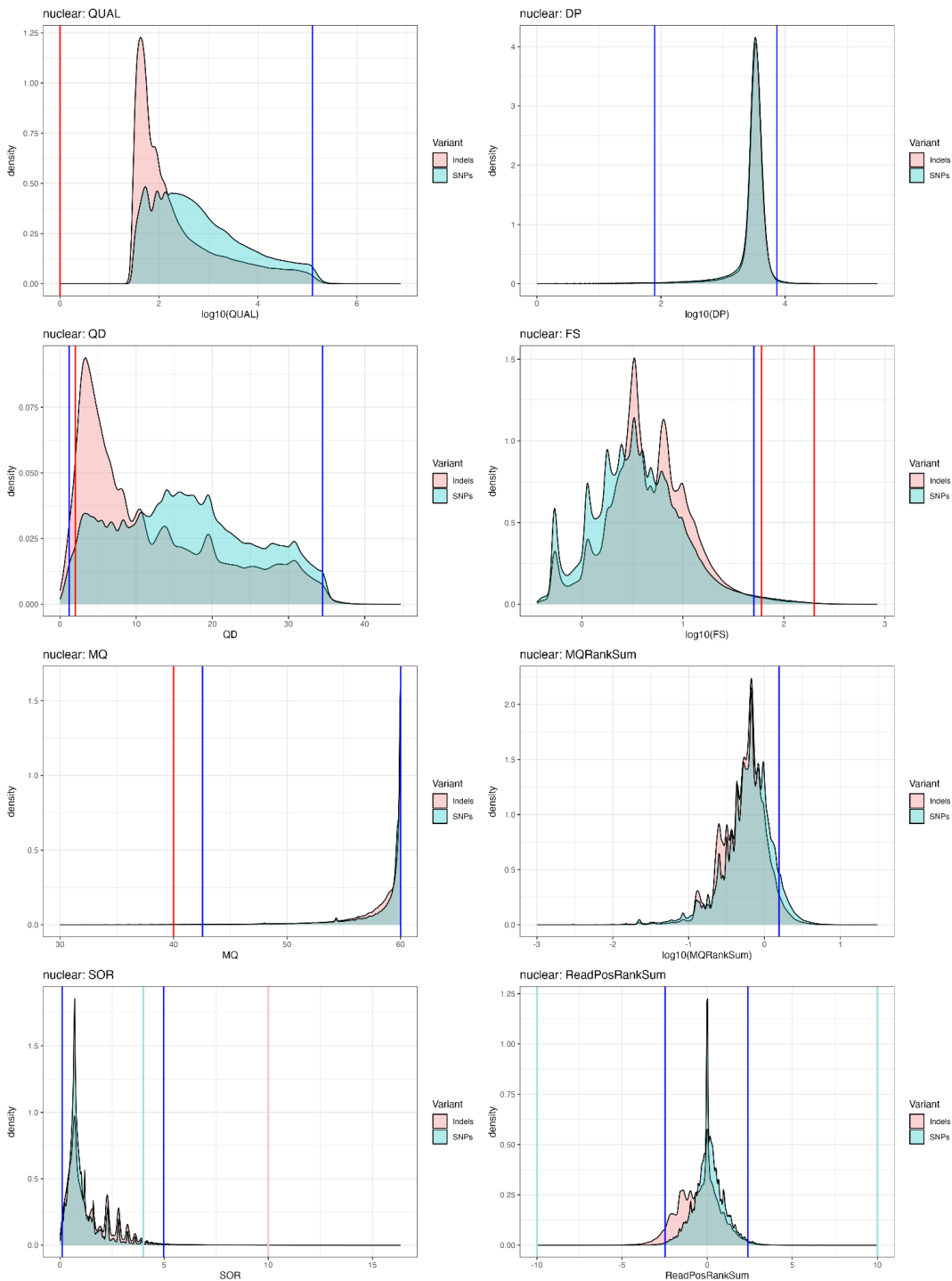
Water control samples for miracidia FTA cards:

- Pipette a few (4-8) drops of the distilled/bottled water used to wash and hatch the eggs. This is a control we use to ensure that no genetic material is contaminating our results in the water used.

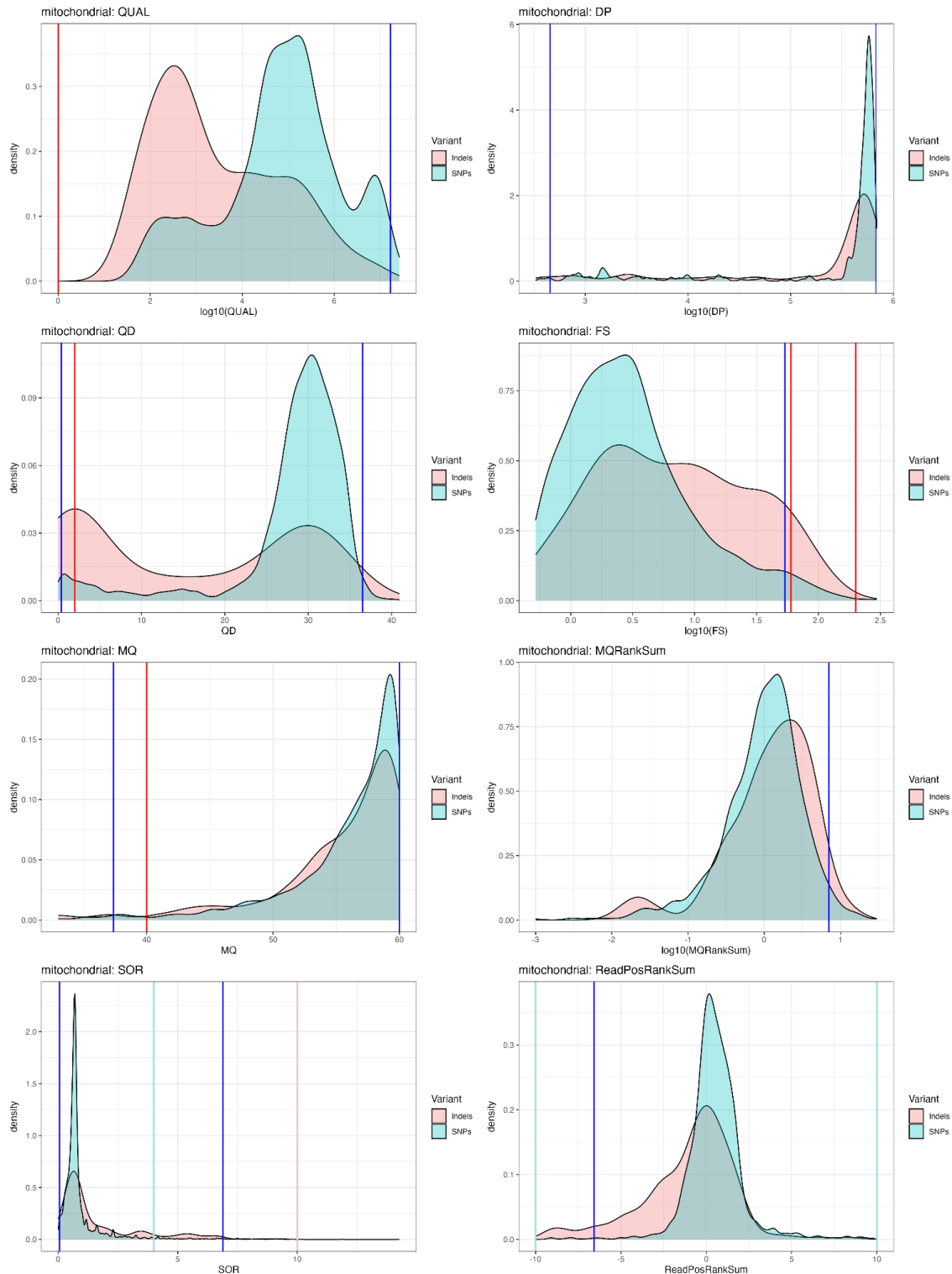


Appendix Figure 4.2: A selection of images from fieldwork in Uganda in November 2021. Top left: miracidia catching and cleaning using a dissection microscope. Top right: an example of the roads used by the field team to collect study participants. Bottom left: processing stool samples to separate *S. mansoni* eggs from stool samples and subsequently storing them in water to induce hatching. Bottom right: miracidia placed into FTA cards for storage.

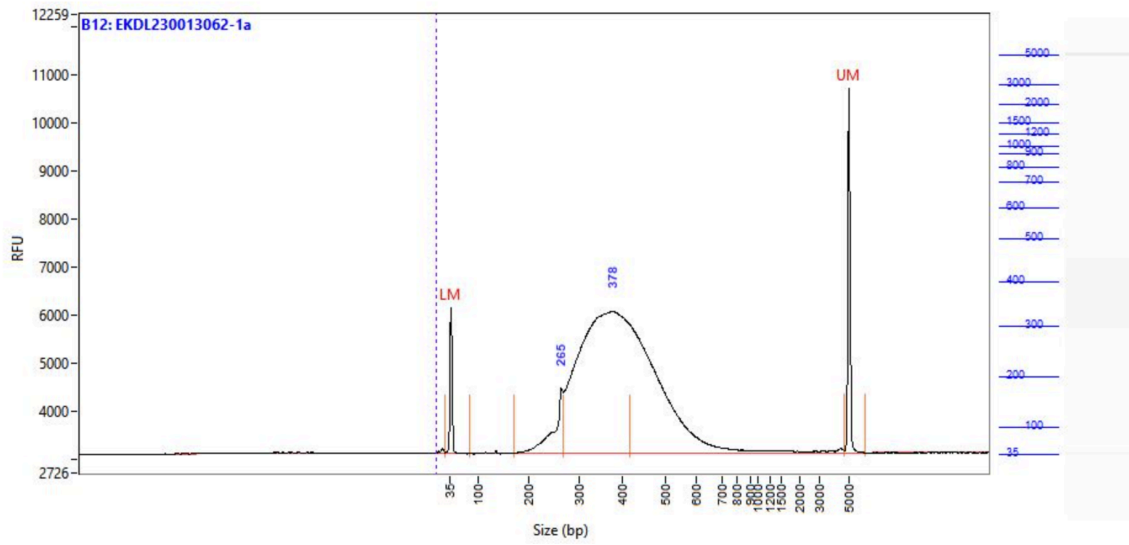
To allow for the collection of samples, I travelled to Uganda twice to join the field team in Bugoigo to collect baseline and six-month post-treatment follow-up miracidia samples from stool samples from PIP trial participants. I aimed to collect miracidia from 100 participants, and from each participant, I aimed to collect at least 30 miracidia. I started at 7:30 am to expose the previous night's samples to light to aid miracidial hatching. After breakfast I would begin collecting miracidia from stool samples and placing them onto FTA cards. I would finish this around 6:30 pm. After dinner, we would process the next lot of participant stool (methods detailed in Appendix 1) until 10 pm and leave overnight for hatching. My reflections from the field experience are that fieldwork to collect samples can be logistically challenging. For example, the road infrastructure from the camp to the more remote villages was very poor and challenging. An important aspect of the fieldwork was understanding the social context of schistosomiasis and seeing first-hand the clinical pathology of the disease. This has been an invaluable experience for my PhD work as it has highlighted the difficulties surrounding logistics, and sample collection and emphasised how valuable the participant's samples are once they have been collected. I have grown from this experience.



Appendix Figure 4.3: Distribution and density of nuclear variant quality metrics (QUAL, DP, MQ, SOR, FS, QD, MQRankSum, and ReadPosRankSum). The distributions are colour-coded by variant type: SNP (pink) and indel (light blue). The red lines indicate the default GATK hard filters, while the blue lines represent the 1st and 99th percentiles. The peach-coloured lines show variant-specific thresholds for SNPs and indels, and the turquoise lines are specific to the SOR and RankPosRankSum plots, representing additional hard filter thresholds that are specific to each variant type.



Appendix Figure 4.4: Distribution and density of mitochondrial variant quality metrics (QUAL, DP, MQ, SOR, FS, QD, MQRankSum, and ReadPosRankSum). The distributions are colour-coded by variant type: SNP (pink) and indel (light blue). The red lines indicate the default GATK hard filters, while the blue lines represent the 1st and 99th percentiles. The peach-coloured lines show variant-specific thresholds for SNPs and indels, and the turquoise lines are specific to the SOR and RankPosRankSum plots, representing additional hard filter thresholds that are specific to each variant type.



Appendix Figure 4.5: Bioanalyzer results generated from Novogene for the pooled library. The trace details the density and fragment size of the pooled library.

Appendix Table 4.2: Quality control measures for 96 miracidia whole genome sequenced.

Sample ID	Mean library concentration (ng/ul)	Total number of reads	Duplicate reads (%)	Mapped reads (million)	Mapped reads (%)	Mean nuclear coverage	Standard deviation	Mean mitochondrial coverage	GC (%)	Kraken unassigned (%)	Homo sapiens (%)	Top 5 Species (%)
BU189_B1	4.84	89860390	35.4	48.6	54.1	11	3.53	857.4	38	74	5.2	8.4
BU189_B2	5.86	138642796	44.4	73.3	52.9	16.5	4.94	1173.1	37	84	7.1	8.5
BU193_B1	1.66	100335544	53.5	39.6	39.5	9	2.96	1210.3	37	87	6.2	7.3
BU193_B2	3.05	56138212	33.6	37.4	66.6	9	2.77	361.7	36	88	4	5.3
BU196_B1	5.7	106027222	34.3	42.6	40.1	10.6	3.58	661.9	41	58	2.7	4
BU196_B2	2.41	80431038	41.3	0.2	0.2	0	0.97	1.8	49	11	2.6	6.4
BU198_B1	4.39	69334280	36.1	36.5	52.7	8.1	2.8	481.3	39	74	6.8	8.6
BU198_B2	4.69	50187028	31.7	28.6	57	6.6	2.39	512.9	39	78	3.4	5.4
BU200_B1	2.63	20511690	28.1	14.1	68.6	3.5	1.24	252.2	37	84	5.7	7.2
BU200_B2	4.4	67991752	37.2	36.7	54	9.3	3.48	500.4	38	86	5.1	6.6
BU201_B1	5.6	73447788	36.1	45.9	62.5	10.8	3.75	603.7	37	83	6.4	7.8
BU201_B2	3.19	145882240	49.2	36.4	24.9	8.2	2.5	539.1	40	56	21.7	24.2
BU203_B1	6.38	73422920	39.8	33.8	46	7.8	2.4	367.9	40	76	6.1	7.8
BU203_B2	2.68	59492894	43.2	27.3	45.9	5.7	2.33	355.6	41	75	5.5	7.5
BU206_B1	6.86	70215114	36.3	29.3	41.7	7	2.17	386.7	40	68	2.8	5
BU206_B2	3.1	62392712	54.6	22.8	36.5	4.8	1.51	216.6	38	80	4	5.3
BU209_B1	2.65	100904432	62.1	25	24.8	4.9	1.48	172.9	41	72	9.8	11.6
BU209_B2	8.89	48679144	33	31	63.7	7.9	2.82	503.2	38	86	3.8	4.8
BU211_B1	0.66	18993438	59.1	4.4	23.3	0.8	0.5	61.8	44	61	14.3	17.4
BU211_B2	2.31	44487382	51.9	18.7	42.1	3.7	1.38	303.4	39	81	6.5	7.6
BU212_B1	3.41	53171304	48.3	24.2	45.5	5.2	1.95	207.9	38	85	3.9	4.8

BU212_B2	3.49	64441454	47.9	26.4	40.9	5.8	2.22	635.8	40	82	4.8	5.6
BU213_B1	3.42	68236784	44.8	26.9	39.4	6.5	2.02	535	40	77	6.8	7.6
BU213_B2	1.26	79964050	67.8	15.9	19.9	2.7	0.88	247.1	41	66	6.2	7.8
BU214_B1	3.01	70694566	52.1	27.9	39.5	6.5	2.03	282.9	37	87	6	7
BU214_B2	3.18	53592590	42.9	29.6	55.2	6.3	2.22	530.1	37	86	6.2	7.6
BU216_B1	4.43	79474754	45.7	38.5	48.5	8.3	2.94	559.1	38	80	3.7	6.1
BU216_B2	4.62	71531518	42.7	38.2	53.4	9.2	2.79	696.1	36	87	4.4	5.7
BU217_B1	8.54	87252868	41.3	48.9	56	11.7	4.26	605.2	37	89	4.2	5.1
BU217_B2	4.3	63937324	45.5	34.2	53.5	7.2	2.55	387.3	38	86	4.9	6.5
BU225_B1	3.15	60490546	42.8	27	44.7	6.3	1.93	560.8	39	77	6	7.7
BU225_B2	8.94	105392200	36.2	23.1	21.9	5.7	1.81	352.1	45	47	1.9	5.7
BU226_B1	3.48	75528542	46.6	28.2	37.4	6	2.12	429.3	40	75	4.1	6
BU226_B2	5.38	93854568	38.7	35.8	38.2	8.6	2.65	617.7	40	71	4.8	7.4
BU239_B1	7.16	87557028	39	40.3	46	9.3	2.77	609	39	76	3.6	5.5
BU239_B2	9.57	134628226	40	37.1	27.5	8.7	3.11	510.5	47	69	2.6	3.3
BU244_B1	2.71	28906380	33.2	15.4	53.3	3.8	1.18	176.5	38	78	6.8	9.7
BU244_B2	5.43	79523364	35.3	49.7	62.5	12.2	3.71	748.7	37	85	3.9	6.2
BU245_B1	5.85	107947006	44.2	42.9	39.8	10.5	3.13	640	38	80	3.7	5
BU245_B2	1.55	24309180	38.6	5.9	24.4	1.1	1.15	37.3	45	57	15.7	18.1
BU246_B1	4.05	102344088	45.9	54.5	53.3	12.2	3.75	696.1	37	87	4.8	6.1
BU246_B2	17.87	72101966	34.5	46	63.8	11.7	4.16	525.6	37	87	4	4.8
BU272_B1	3.94	49654838	47.1	21.2	42.7	4.6	1.65	537.2	39	81	4.7	5.4
BU272_B2	1.55	24793198	41.8	7.3	29.5	1.5	0.98	63.4	45	60	6.9	8.3
BU279_B1	2.65	49314016	44.2	25.3	51.3	5.2	1.67	389.3	38	76	4.2	9.9

BU279_B2	6.73	62980260	38.7	37	58.8	9.1	2.9	517.7	38	87	2.6	7.2
BU285_B1	8.8	59110686	38.6	35.8	60.6	8.6	3.03	1047	37	91	4.2	4.7
BU285_B2	6.42	80189954	41	42.7	53.2	10	3.58	741.6	39	85	4.5	6
BU189_F1	1.37	44563674	51.5	1.1	2.4	0.1	1.17	1.9	48	30	21.7	29.6
BU189_F2	4.57	64611014	36.3	24.5	37.9	5.8	2.19	536.5	42	64	9.3	64.4
BU193_F1	2.94	67851234	42.4	24.9	36.7	5.7	1.81	335.6	41	73	6.8	72.8
BU193_F2	4.96	81362728	33.7	18.4	22.6	4.4	1.41	184.7	43	62	9	62.4
BU196_F1	5.73	90489826	40.6	16.6	18.3	3.7	1.41	296.2	45	51	9.5	51.2
BU196_F2	1.96	81466948	56.1	11.1	13.6	2.3	0.72	204.4	43	51	9.1	51.4
BU198_F1	3.22	82501688	51.8	20.3	24.6	4.3	1.35	303.4	42	61	8.6	74.3
BU198_F2	5.12	67710078	44.8	21.2	31.2	4.9	1.53	457.5	41	64	5.4	78
BU200_F1	8.24	62286444	38.4	26.2	42	6.3	2.35	563.9	40	71	10.9	71.2
BU200_F2	1.63	76964456	54.9	4.1	5.3	0.7	0.36	29	48	27	30.8	26.7
BU201_F1	3.72	71066922	41.1	34.3	48.2	7.4	2.57	298.1	39	77	5.8	77.2
BU201_F2	6.66	64378296	35.2	32.5	50.5	8.2	2.55	402.6	39	80	4.7	80.2
BU203_F1	5.91	103451682	37.7	20.6	19.9	4.9	1.56	415.6	43	57	4.5	9.4
BU203_F2	2.47	61459678	40.9	0.5	0.7	0	0.57	1.4	46	43	2.5	10.1
BU206_F1	7.09	45484044	34.4	27.4	60.2	6.7	2.05	415.8	37	85	3.9	5
BU206_F2	0.95	14359800	26.7	9.6	67.2	2.5	0.79	219.6	37	85	6.2	7.5
BU209_F1	7.65	65769300	39.5	30.6	46.5	7.2	2.77	383.5	39	77	5.9	7.2
BU209_F2	0.5	26840716	27.3	13.8	51.4	3.5	1.15	213	40	73	3.2	5.6
BU211_F1	4.16	66540406	38	34.7	52.1	7.9	2.44	470.5	38	77	4.2	6.4
BU211_F2	3.73	50395470	43.7	12.1	23.9	2.5	0.94	158.6	41	63	2.7	8
BU212_F1	7.84	57927636	35	33.1	57.1	8.7	2.66	484.7	37	84	3.4	4.1

BU212_F2	4.95	56251516	36.3	30.3	53.9	7.1	2.15	384.2	38	75	7.6	9.7
BU213_F1	5.01	58637206	41.6	24.4	41.7	5.6	2.19	563.2	39	75	4.9	6.8
BU213_F2	4.21	44490308	36	26.4	59.4	5.9	2.07	391.6	38	79	4.9	6.4
BU214_F1	2.9	53623520	43	29.7	55.4	6.1	2.27	526.8	38	80	4.6	7
BU214_F2	5.17	61265128	42.4	34.2	55.8	7.9	2.8	522	37	87	3.6	5.2
BU216_F1	5.81	55374904	40.3	30.4	54.8	7.2	2.19	507.6	37	87	3.5	4.8
BU216_F2	2.33	65152186	55.2	26.4	40.5	5	1.73	508	38	82	6.2	7.4
BU217_F1	8.38	132351456	48.2	67.6	51.1	15.4	5.25	1208.9	36	90	3.7	4.5
BU217_F2	5.09	45128792	36.1	25.1	55.7	6.4	1.97	420.3	38	84	3.8	5.7
BU225_F1	12.53	56678128	32.9	39.2	69.2	9.8	3.53	450.4	37	87	3.8	5
BU225_F2	9.38	53253034	33.5	36	67.6	8.6	3.1	874.8	38	83	3.7	4.8
BU226_F1	13.5	54792772	30.6	20	36.6	5	1.81	426.3	44	64	3.3	7
BU226_F2	13.5	65149992	30.8	22.5	34.6	5.2	1.83	506.3	44	61	3.6	7.9
BU239_F1	8.93	78088862	37.4	47.3	60.6	11.3	3.9	454.1	37	84	6.9	8.2
BU239_F2	6.13	52720270	40	27.3	51.8	7	2.2	381.1	36	87	6.3	7.1
BU244_F1	8.04	16260146	29.1	6.2	38.3	1.5	0.57	107.5	39	65	5.7	8.5
BU244_F2	2.39	57175272	36.2	23.4	41	5	1.97	727.6	40	64	7.8	11.2
BU245_F1	9.04	69287170	37	43.3	62.5	10.4	3.73	734.2	37	89	3.6	4.7
BU245_F2	2.33	44639032	41.5	23.2	52	5.4	1.66	963.6	37	83	4.8	6.3
BU246_F1	4.83	83292092	35.8	37.7	45.3	9.2	2.93	949.2	38	69	11.7	13.4
BU246_F2	4.14	60919434	36.5	24.9	40.8	6.1	1.99	1320.4	39	70	8.3	10.3
BU268_F1	8.02	73072570	32.9	42.8	58.6	10.7	3.27	492	37	82	3.4	5.4
BU268_F2	4.87	61222948	33.7	26.3	42.9	6.4	2.26	476.7	39	71	5.5	8.8
BU279_F1	4.25	50012788	36.5	16.8	33.6	3.4	1.19	149.2	45	51	4.2	9.9

BU279_F2	11.57	52151190	29.6	20.9	40.2	5.2	1.65	393.9	43	63	2.6	7.2
BU285_F1	3.81	45529916	37	19.7	43.3	4.2	1.52	610.4	40	71	6.6	9.5
BU285_F2	6.78	52248020	33.3	28.5	54.6	6.7	2.38	491.9	38	78	4.1	7.3

Appendix Table 4.3: Miracidia sex determination for *S. mansoni* miracidia.

Sample ID	ZSR	PAR	ZSR/PAR	PAR/ZSR	Sex
BU189_B1	12.1387	11.609	1.04563	0.956363	Male
BU189_B2	17.2684	18.2444	0.946504	1.05652	Male
BU189_F1	0.02296	0.04868	0.471652	2.12021	Female
BU189_F2	2.96528	6.65616	0.445494	2.2447	Female
BU193_B1	10.0385	9.65676	1.03953	0.961972	Male
BU193_B2	9.74984	9.8954	0.98529	1.01493	Male
BU193_F1	5.14136	6.34776	0.809949	1.23465	Male
BU193_F2	4.66688	4.91648	0.949232	1.05348	Male
BU196_B1	10.867	11.9374	0.910332	1.0985	Male
BU196_B2	0.012	0.01832	0.655022	1.52667	Female
BU196_F1	2.02604	4.22768	0.479232	2.08667	Female
BU196_F2	2.34428	2.46352	0.951598	1.05086	Male
BU198_B1	4.4486	9.20976	0.483031	2.07026	Female
BU198_B2	3.5736	7.54476	0.473653	2.11125	Female
BU198_F1	4.3822	4.7728	0.918161	1.08913	Male
BU198_F2	5.059	5.42488	0.932555	1.07232	Male
BU200_B1	1.8428	4.04872	0.455156	2.19705	Female
BU200_B2	5.13828	10.6872	0.480788	2.07992	Female
BU200_F1	3.32796	7.17156	0.46405	2.15494	Female
BU200_F2	0.34352	0.85812	0.400317	2.49802	Female
BU201_B1	5.79136	12.6953	0.456181	2.19211	Female
BU201_B2	8.4086	8.90744	0.943997	1.05932	Male
BU201_F1	3.93004	8.40368	0.467657	2.13832	Female
BU201_F2	8.27284	9.4048	0.87964	1.13683	Male
BU203_B1	7.95636	8.62216	0.92278	1.08368	Male
BU203_B2	2.96128	6.48588	0.456573	2.19023	Female
BU203_F1	4.84364	5.46436	0.886406	1.12815	Male
BU203_F2	0.012	0.024	0.5	2	Female
BU206_B1	7.29156	7.80748	0.93392	1.07076	Male
BU206_B2	4.80284	5.26916	0.9115	1.09709	Male
BU206_F1	7.13672	7.42712	0.9609	1.04069	Male
BU206_F2	2.45248	2.82764	0.867324	1.15297	Male
BU209_B1	5.06376	5.27644	0.959693	1.042	Male

BU209_B2	4.1336	9.30308	0.444326	2.2506	Female
BU209_F1	3.58664	8.54476	0.419747	2.38239	Female
BU209_F2	3.52876	4.03288	0.874998	1.14286	Male
BU211_B1	0.40572	0.8532	0.475527	2.10293	Female
BU211_B2	1.90212	4.31228	0.441094	2.26709	Female
BU211_F1	8.69368	8.488	1.02423	0.976341	Male
BU211_F2	1.37752	2.76264	0.498625	2.00552	Female
BU212_B1	2.67528	6.03176	0.443532	2.25463	Female
BU212_B2	3.02124	6.67316	0.452745	2.20875	Female
BU212_F1	9.33512	9.64364	0.968008	1.03305	Male
BU212_F2	7.4042	7.8546	0.942658	1.06083	Male
BU213_B1	6.68316	7.14512	0.935346	1.06912	Male
BU213_B2	2.8744	2.86252	1.00415	0.995867	Male
BU213_F1	3.179	6.25732	0.508045	1.96833	Female
BU213_F2	6.2664	6.47968	0.967085	1.03404	Male
BU214_B1	7.2064	6.85868	1.0507	0.951748	Male
BU214_B2	3.35504	7.16232	0.468429	2.13479	Female
BU214_F1	3.49504	6.92308	0.504839	1.98083	Female
BU214_F2	4.20276	9.18828	0.457404	2.18625	Female
BU216_B1	4.62408	9.29296	0.49759	2.00969	Female
BU216_B2	10.1105	9.87712	1.02363	0.976917	Male
BU216_F1	7.43596	8.00364	0.929072	1.07634	Male
BU216_F2	2.6704	5.75488	0.464024	2.15506	Female
BU217_B1	6.22444	13.7254	0.453498	2.20508	Female
BU217_B2	3.9354	8.26712	0.47603	2.10071	Female
BU217_F1	8.55136	17.6508	0.484474	2.06409	Female
BU217_F2	6.57588	7.09756	0.926499	1.07933	Male
BU225_B1	6.83648	6.89816	0.991058	1.00902	Male
BU225_B2	6.07368	6.231	0.974752	1.0259	Male
BU225_F1	5.29856	11.4073	0.464489	2.15291	Female
BU225_F2	4.65312	9.81564	0.474052	2.10947	Female
BU226_B1	3.21024	6.96424	0.460961	2.16938	Female
BU226_B2	9.05644	9.37692	0.965822	1.03539	Male
BU226_F1	2.62152	5.778	0.453707	2.20406	Female
BU226_F2	2.85496	5.96724	0.478439	2.09013	Female
BU239_B1	9.93892	10.4042	0.95528	1.04681	Male
BU239_B2	4.50284	10.1995	0.441477	2.26513	Female

BU239_F1	6.37508	12.6973	0.502082	1.99171	Female
BU239_F2	7.75728	7.59332	1.02159	0.978864	Male
BU244_B1	3.85324	4.21388	0.914416	1.09359	Male
BU244_B2	12.8759	13.6944	0.940231	1.06357	Male
BU244_F1	0.87508	1.67836	0.52139	1.91795	Female
BU244_F2	2.79472	5.58072	0.500781	1.99688	Female
BU245_B1	11.3682	11.3657	1.00022	0.99978	Male
BU245_B2	0.61152	1.27012	0.481466	2.07699	Female
BU245_F1	5.6604	11.9835	0.472349	2.11708	Female
BU245_F2	5.79192	5.85724	0.988848	1.01128	Male
BU246_B1	12.805	13.4198	0.954187	1.04801	Male
BU246_B2	6.09032	14.1706	0.429786	2.32674	Female
BU246_F1	10.5785	9.60088	1.10183	0.907584	Male
BU246_F2	6.99456	6.23784	1.12131	0.891813	Male
BU268_F1	11.326	11.8011	0.959741	1.04195	Male
BU268_F2	6.798	6.90128	0.985035	1.01519	Male
BU272_B1	2.4314	5.20284	0.467322	2.13985	Female
BU272_B2	1.5532	1.63552	0.949667	1.053	Male
BU279_B1	5.59816	5.50488	1.01694	0.983337	Male
BU279_B2	8.989	10.4523	0.860002	1.16279	Male
BU279_F1	2.3172	3.92252	0.590743	1.69278	Female
BU279_F2	5.51992	5.80508	0.950878	1.05166	Male
BU285_B1	4.62432	9.91732	0.466287	2.1446	Female
BU285_B2	5.13584	11.9537	0.429644	2.32751	Female
BU285_F1	2.31912	4.7466	0.488586	2.04672	Female
BU285_F2	3.71032	7.70992	0.48124	2.07797	Female
ERR046038	21.905	40.706	0.53812706	1.85829719	Female
ERR103049	52.1209	53.3466	0.97702384	1.02351648	Male
ERR103050	38.9052	39.3024	0.98989375	1.01020943	Male
ERR119614	53.5071	54.4969	0.9818375	1.01849848	Male
ERR3173043	12.3179	12.8764	0.95662608	1.04534052	Male
ERR3173048	11.8831	12.263	0.96902063	1.03196977	Male
ERR3173049	9.33136	9.81634	0.95059462	1.05197313	Male
ERR3173052	13.2412	13.8733	0.95443766	1.04773737	Male
ERR3173053	6.34772	14.8893	0.42632763	2.34561386	Female
ERR3173055	8.00192	8.36976	0.95605131	1.04596897	Male
ERR3173056	12.3478	12.3779	0.99756825	1.00243768	Male

ERR3173060	11.8623	12.3557	0.96006701	1.04159396	Male
ERR3173061	6.92864	13.8101	0.50170817	1.99319058	Female
ERR3173069	8.07376	8.3434	0.96768224	1.03339708	Male
ERR3173070	3.30732	6.25318	0.52890209	1.89070909	Female
ERR3173071	9.30612	9.09836	1.02283488	0.97767491	Male
ERR3173072	13.3309	13.9742	0.95396516	1.04825631	Male
ERR3173073	24.828	24.0409	1.03274004	0.96829789	Male
ERR3173074	24.5919	22.5986	1.08820458	0.91894486	Male
ERR3173075	10.6835	23.0035	0.46442933	2.15318014	Female
ERR3173078	18.7661	40.2677	0.46603357	2.14576817	Female
ERR3173079	5.41384	11.2421	0.48156839	2.07654825	Female
ERR3173080	6.88576	14.2948	0.48169684	2.07599452	Female
ERR3173084	12.3585	26.0284	0.47480829	2.1061132	Female
ERR3173085	20.882	23.2854	0.89678511	1.11509434	Male
ERR3173086	9.10372	20.9769	0.43398786	2.3042119	Female
ERR3173087	1.8784	2.26244	0.83025406	1.2044506	Male
ERR3173088	3.99096	11.4247	0.34932733	2.86264458	Female
ERR3173089	4.71728	12.9878	0.36320855	2.75323915	Female
ERR3173090	4.30496	11.1393	0.38646594	2.58755017	Female
ERR3173091	4.81128	9.48106	0.50746225	1.97058995	Female
ERR3173095	0.73872	0.80322	0.91969821	1.08731319	Male
ERR3173101	3.88656	8.4355	0.46073855	2.17042835	Female
ERR3173102	2.35904	5.10894	0.46174745	2.16568604	Female
ERR3173103	2.33808	4.73874	0.49339698	2.02676555	Female
ERR3173104	2.51536	6.28026	0.40051845	2.49676388	Female
ERR3173105	3.99672	8.57304	0.46619636	2.14501892	Female
ERR3173106	3.06452	6.73976	0.45469275	2.19928733	Female
ERR3173109	5.10544	12.7704	0.39978701	2.50133191	Female
ERR3173111	2.08452	4.20756	0.49542253	2.01847907	Female
ERR3173113	1.06116	2.23004	0.47584797	2.10151155	Female
ERR3173118	1.61724	4.06364	0.39797817	2.51270065	Female
ERR3173120	2.84024	8.23862	0.34474706	2.90067741	Female
ERR3173126	3.11904	3.25988	0.95679596	1.04515492	Male
ERR3173128	2.88064	6.32988	0.45508604	2.19738669	Female
ERR3173130	1.34672	3.11678	0.43208696	2.31434894	Female
ERR3173132	1.77688	5.74892	0.30908066	3.23540138	Female
ERR3173134	0.4404	0.99782	0.44136217	2.26571299	Female

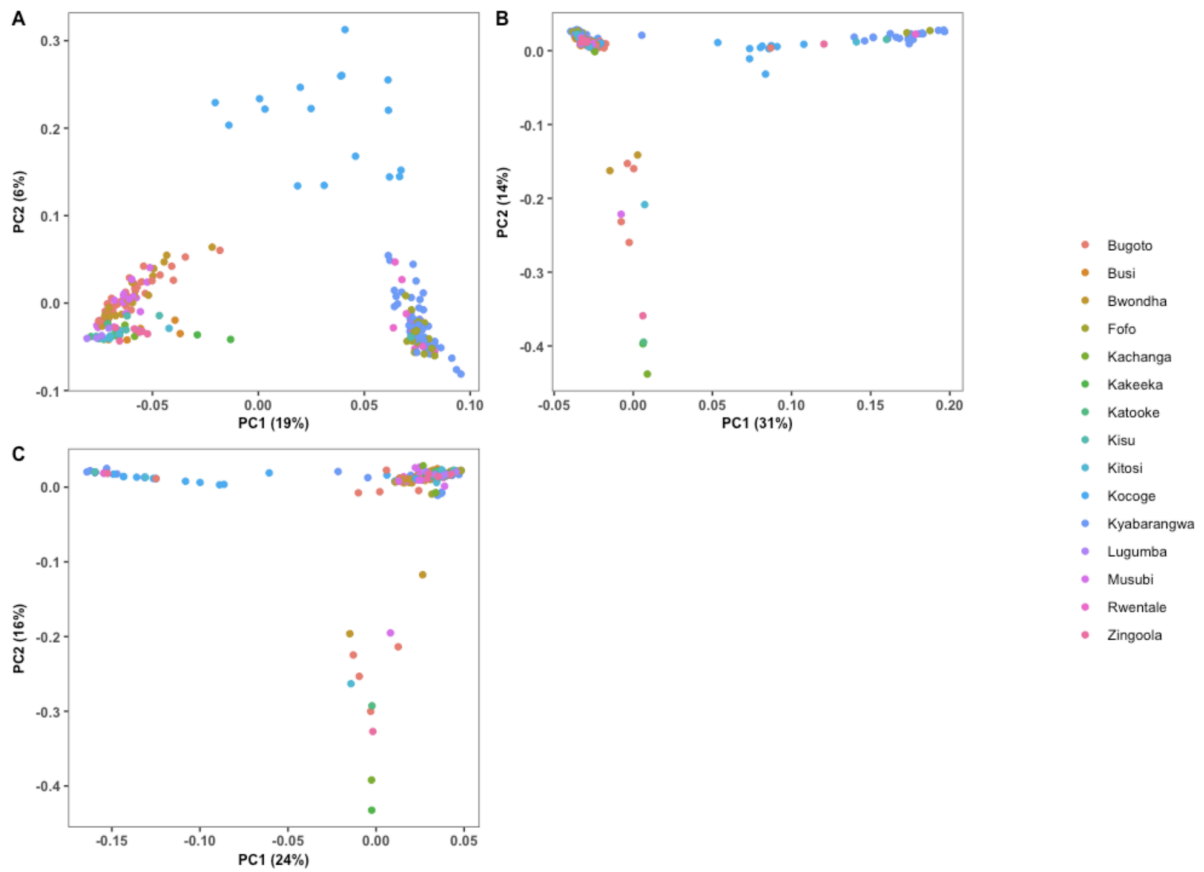
ERR3173136	0.39392	0.809	0.48692213	2.05371649	Female
ERR3173139	0.73584	0.7533	0.97682198	1.02372798	Male
ERR3173144	1.03888	1.30664	0.79507745	1.2577391	Male
ERR3173147	0.89136	1.81084	0.49223565	2.0315473	Female
ERR3173151	7.93076	9.16802	0.86504611	1.15600775	Male
ERR3173152	0.83248	2.0245	0.41120277	2.43189026	Female
ERR3173153	5.57	13.7099	0.40627576	2.46138241	Female
ERR3173165	2.42748	6.04944	0.40127351	2.49206585	Female
ERR3173166	8.62724	19.9575	0.4322806	2.31331225	Female
ERR3173170	17.021	16.4872	1.03237663	0.96863874	Male
ERR3173171	4.21808	11.6355	0.36251816	2.75848253	Female
ERR3173174	7.36152	18.4052	0.39996957	2.50019018	Female
ERR3173175	7.5362	16.1242	0.46738443	2.13956636	Female
ERR3173177	6.78284	16.5671	0.40941625	2.44250196	Female
ERR3173179	16.2832	14.8347	1.09764269	0.91104328	Male
ERR3173180	0.79324	2.62198	0.30253473	3.30540568	Female
ERR3173181	3.18168	7.55264	0.42126727	2.37378995	Female
ERR3173185	5.99268	15.3346	0.39079467	2.55888851	Female
ERR3173186	4.81072	5.9799	0.80448168	1.24303639	Male
ERR3173192	12.5936	14.0877	0.89394294	1.11863963	Male
ERR3173196	2.03776	4.94188	0.4123451	2.42515311	Female
ERR3173200	5.29948	13.9994	0.37855051	2.64165541	Female
ERR3173201	16.5325	15.5255	1.06486104	0.93908967	Male
ERR3173203	11.1608	11.2195	0.99476804	1.00525948	Male
ERR3173205	10.238	22.5633	0.45374568	2.20387771	Female
ERR3173206	9.57748	15.4846	0.61851646	1.61677184	Female
ERR3173208	18.6148	19.8798	0.93636757	1.06795668	Male
ERR3173209	18.1126	18.8624	0.96024896	1.0413966	Male
ERR3173213	12.9689	13.8701	0.9350257	1.06948932	Male
ERR3173216	17.8691	19.0772	0.9366731	1.06760833	Male
ERR3173217	8.27388	19.5093	0.42409928	2.35793848	Female
ERR3173221	2.80724	6.40354	0.43838877	2.28108035	Female
ERR3173225	6.9778	16.7711	0.41606096	2.40349394	Female
ERR3173226	5.30916	5.3857	0.98578829	1.01441659	Male
ERR3173227	23.6488	24.1282	0.98013113	1.02027164	Male
ERR3173230	3.18792	6.95866	0.45812268	2.1828214	Female
ERR3173232	9.7308	21.2536	0.45784244	2.18415752	Female

ERR3173234	7.39936	8.19044	0.90341422	1.10691195	Male
ERR3173237	16.9521	17.4838	0.96958899	1.03136485	Male
ERR3173239	19.3849	20.7042	0.93627863	1.06805813	Male
ERR3173242	5.80472	13.2198	0.43909288	2.27742251	Female
ERR3173243	8.191	19.2456	0.42560377	2.34960322	Female
ERR3173245	6.08016	6.49276	0.93645229	1.06786006	Male
ERR3173246	0.56596	0.89152	0.63482592	1.575235	Female
ERR3173247	10.4286	11.1378	0.93632495	1.06800529	Male
ERR3173248	12.0547	11.7294	1.02773373	0.97301467	Male
ERR3173250	15.84	15.9167	0.99518116	1.00484217	Male
ERR3173256	17.3001	17.521	0.98739227	1.01276871	Male
ERR3173259	17.3032	16.7115	1.03540676	0.96580401	Male
ERR3173260	17.1714	16.8841	1.01701601	0.98326869	Male
ERR3173261	7.18736	15.6615	0.45891901	2.17903375	Female
ERR3173262	5.40916	12.5245	0.4318863	2.31542421	Female
ERR539843	12.4837	12.6318	0.98827562	1.01186347	Male
ERR539845	4.88652	9.8937	0.49390218	2.02469242	Female
ERR539848	7.3668	14.7485	0.49949486	2.00202259	Female
Busi_1	21.7095	21.3002	1.01921578	0.9811465	Male
Busi_2	7.25236	14.2109	0.51033784	1.95948629	Female
Busi_3	6.87732	14.0603	0.48913039	2.04444464	Female
Busi_4	21.9363	22.3895	0.97975837	1.02065982	Male
Busi_5	9.76736	18.7567	0.52073979	1.9203449	Female
Busi_6	20.4972	29.4915	0.6950206	1.43880628	Female
Kachanga_1	8.24676	16.8317	0.48995407	2.04100762	Female
Kachanga_2	8.93664	16.1834	0.55221029	1.81090432	Female
Kachanga_3	25.4662	25.3884	1.00306439	0.99694497	Male
Kachanga_4	5.53036	11.0476	0.50059379	1.99762764	Female
Kachanga_5	20.1785	20.157	1.00106663	0.99893451	Male
Kachanga_6	10.855	22.7341	0.47747657	2.09434362	Female
Kakeeka_1	32.6474	32.2478	1.01239154	0.98776013	Male
Kakeeka_2	9.53524	17.8375	0.53456146	1.8706923	Female
Kakeeka_3	24.2916	25.8385	0.94013197	1.06368045	Male
Kakeeka_4	17.1567	24.26	0.70720115	1.41402484	Male
Kakeeka_5	12.2106	24.6191	0.49598076	2.01620723	Female
Kakeeka_6	19.0641	19.5863	0.97333851	1.0273918	Male
Katooke_1	15.9596	15.8619	1.00615941	0.99387829	Male

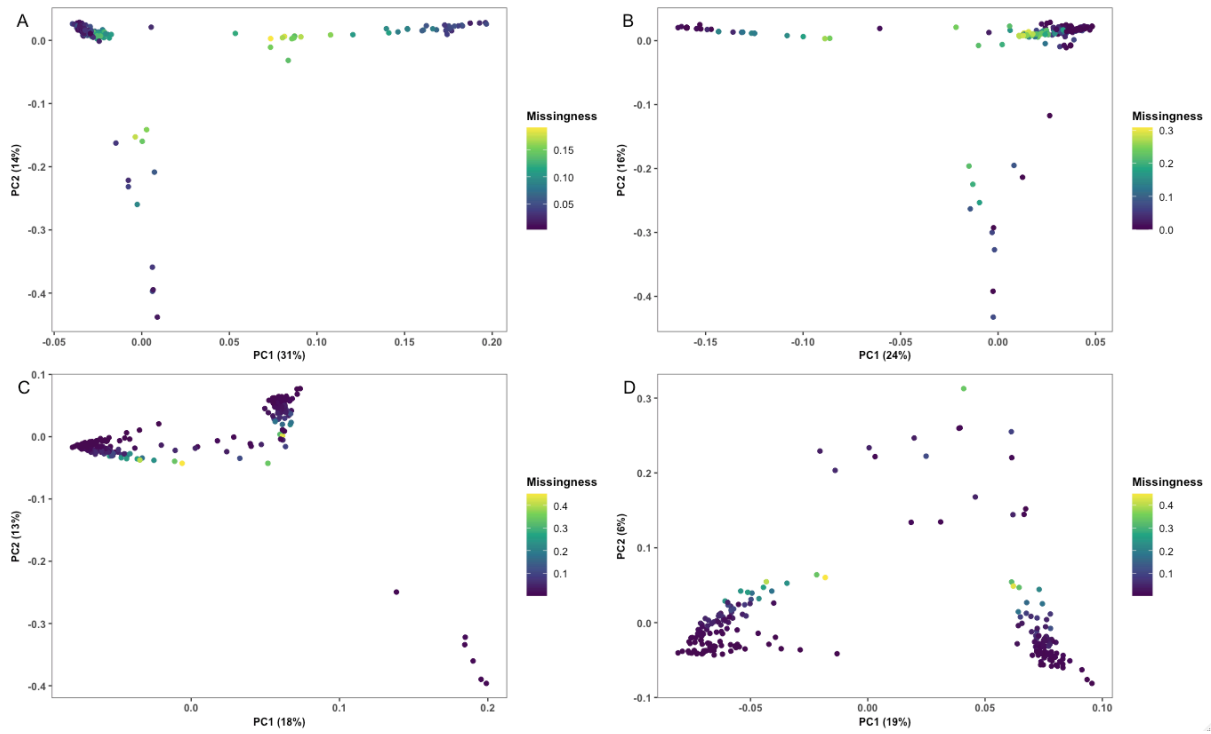
Katooke_2	13.3465	12.6815	1.05243859	0.9501742	Male
Katooke_3	15.1106	15.1495	0.99743226	1.00257435	Male
Katooke_4	24.5537	24.5491	1.00018738	0.99981266	Male
Katooke_5	8.89112	16.4275	0.54123391	1.84762999	Female
Katooke_6	18.8899	17.4473	1.08268328	0.92363115	Male
Kisu_1	21.3458	21.9538	0.97230548	1.02848336	Male
Kisu_2	9.41844	9.58356	0.98277049	1.01753157	Male
Kisu_3	16.7824	18.0506	0.92974195	1.07556726	Male
Kisu_4	4.19396	8.68354	0.48297814	2.07048708	Female
Kisu_5	31.4994	32.6419	0.96499897	1.03627053	Male
Kisu_6	20.5272	21.0061	0.97720186	1.02333002	Male
Kitosi_1	13.4565	27.9468	0.48150414	2.07682533	Female
Kitosi_2	13.3853	13.1813	1.01547647	0.9847594	Male
Kitosi_3	7.59804	15.6464	0.48560947	2.05926792	Female
Kitosi_4	7.2406	14.0469	0.51545893	1.94001878	Female
Kitosi_5	23.6258	25.6564	0.92085406	1.08594841	Male
Kitosi_6	13.1057	12.6019	1.0399781	0.96155871	Male
Lugumba_1	19.5756	21.8363	0.89647056	1.1154856	Male
Lugumba_2	19.9314	20.7404	0.960994	1.04058922	Male
Lugumba_3	8.24932	17.2043	0.47949175	2.0855416	Female
Lugumba_4	15.6096	16.579	0.94152844	1.06210281	Male
Lugumba_5	15.4859	32.0127	0.48374239	2.06721598	Female
Zingoola_1	6.62776	13.6142	0.48682699	2.05411783	Female
Zingoola_2	25.0023	25.5139	0.97994819	1.02046212	Male
Zingoola_3	34.3294	34.6441	0.9909162	1.00916707	Male
Zingoola_4	11.063	22.026	0.50227004	1.99096086	Female
Zingoola_5	34.6836	35.3401	0.98142337	1.01892825	Male
Zingoola_6	7.60516	14.8453	0.51229413	1.95200364	Female

Appendix Table 4.4: Genome-wide mean π for each Ugandan district.

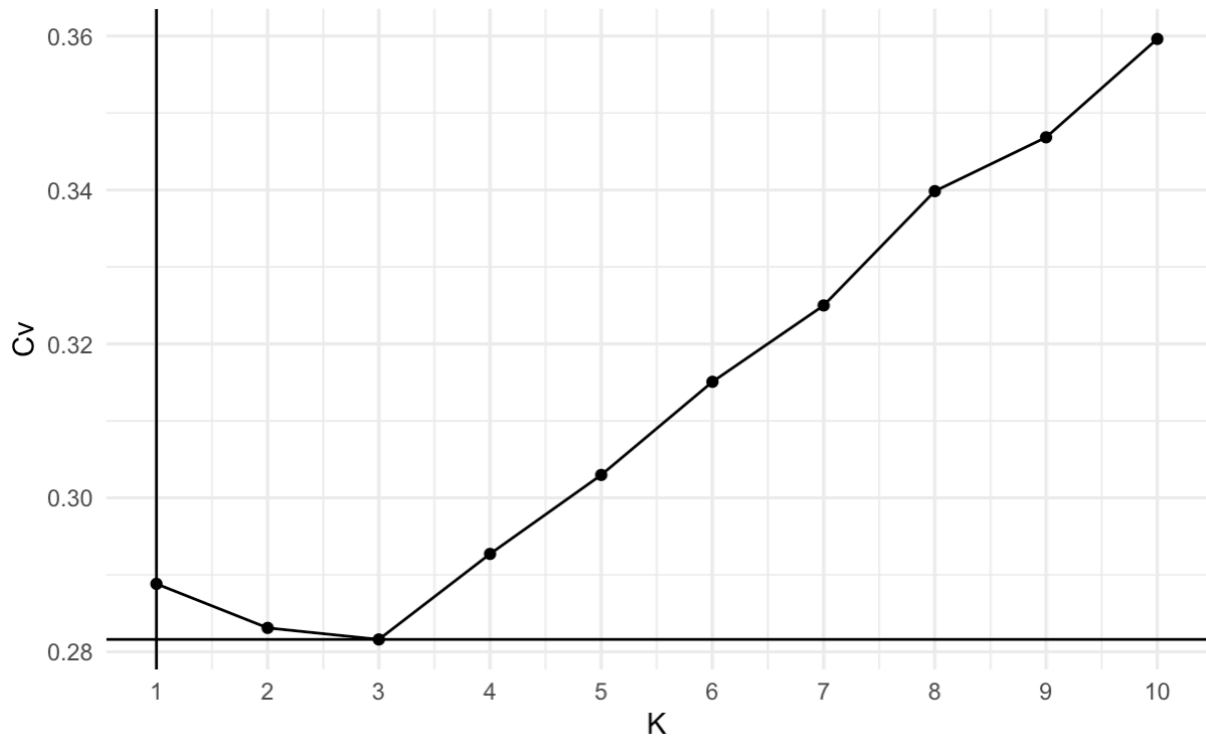
District	Mean π	99% Confidence interval
Hoima	0.00328	0.00326-0.00330
Koome Islands	0.00371	0.00369-0.00374
Tororo	0.00344	0.00342-0.00347
Mayuge	0.00339	0.00336-0.00341



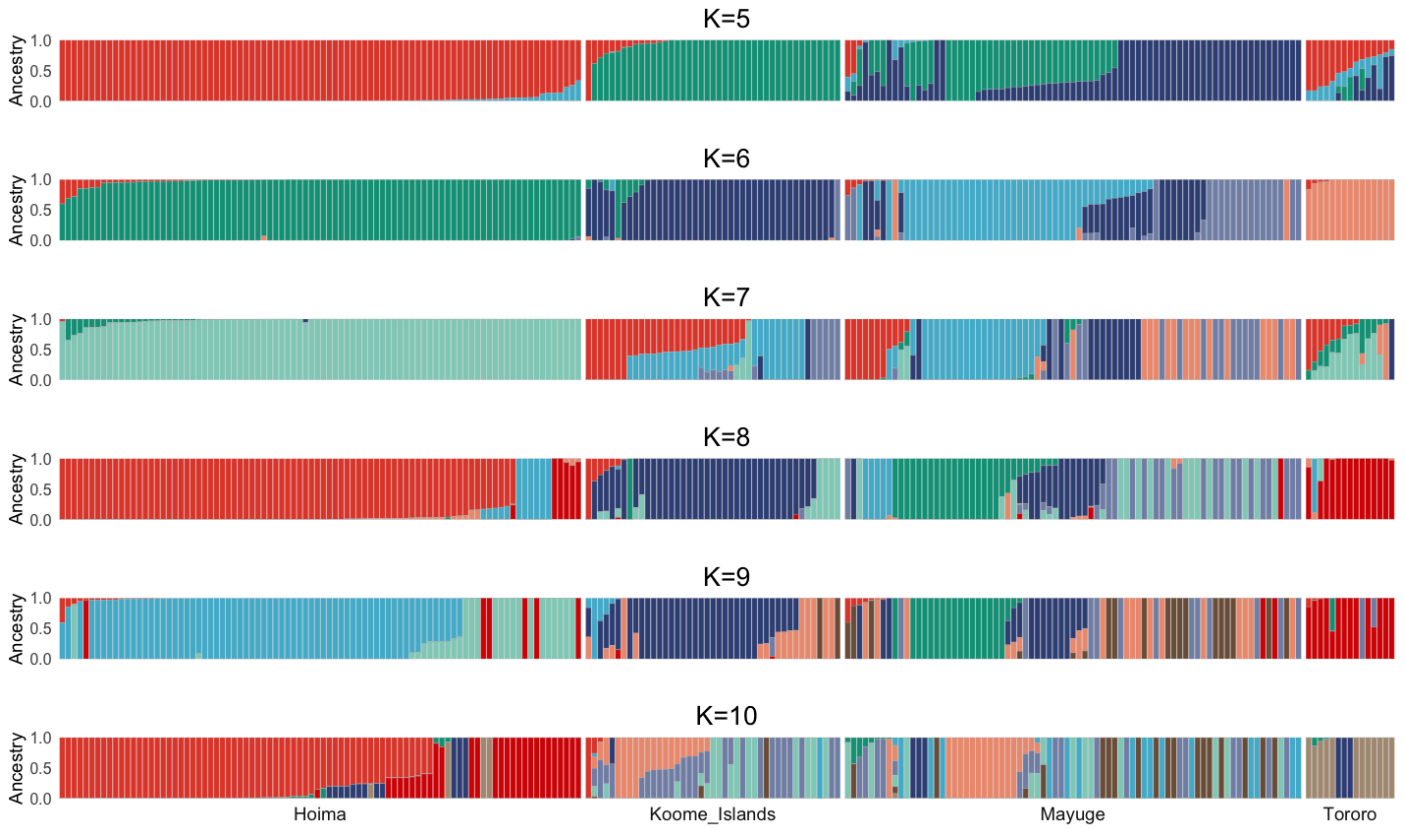
Appendix Figure 4.6: Population structure of *Schistosoma mansoni*. The PCA plots are from Uganda samples ($n=223$) (A); unlinked autosomal SNPs ($n=1,171,938$) (B); mitochondrial SNPs ($n=950$) (C); and *cox1* SNPs ($n=91$). Samples were coloured by sampling village.



Appendix Figure 4.7: Individual sampling missingness of *Schistosoma mansoni* samples. Principal component analysis (PCA) of (A) mitochondrial SNPs ($n=950$), (B) *cox1* SNPs ($n=91$), (C) 1,281,806 unlinked autosomal SNPs from all samples ($n=229$), (D) unlinked autosomal SNPs ($n=1,171,938$) from Ugandan samples. Samples were coloured by individual sample missingness.



Appendix Figure 4.8: Cross-validation error (CV) values generated using ADMIXTURE with K values ranging from 1-10.



Appendix Figure 4.9: Admixture plots depicting the ancestry proportions using ADMIXTURE. Theoretical K values (K=5-10) are displayed.

Appendix Figure 4.10: Material Transfer Agreement between LSHTM and the Medical Research Council/ Uganda Virus Research Institute and LSHTM Research Unit.



MATERIAL TRANSFER AGREEMENT (for the Supply of Non-Human Material)

This Agreement is made by and between:

a) **The London School of Hygiene and Tropical Medicine**, an organisation incorporated by Royal Charter, number RC000330, having its administrative office at Keppel Street, London, WC1E 7HT and operating through its branch office, **Medical Research Council/Uganda Virus research Institute and London School of Hygiene and Tropical Medicine Uganda Research Unit ("MRC/UVRI and LSHTM Uganda Research Unit")**, whose administrative offices are located at Plot 51-59 Nakiwogo Road, Entebbe, Uganda (the "Provider Institution")

and

b) **The London School of Hygiene & Tropical Medicine** whose administrative offices are located at Keppel Street, London WC1E 7HT, United Kingdom, an exempt charity within the meaning of Schedule 3 of the Charities Act 2011 ("the Recipient Institution")

hereinafter referred to as "the Parties" and each of them being "a Party"

BACKGROUND

- (A) The Recipient Institution is conducting a research project entitled "*Praziquantel for children under four: A Phase II PK/PD driven dose finding trial (PIP trial)*" as described in more detail at Schedule 1 ("the Research") under the direction of Amaya Bustinduy ("the Recipient Scientist") and wishes to access and utilise 350 FTA cards and Eppendorf tubes containing *Schistosoma mansoni* larval stages as more particularly described at Schedule 2 (the "Original Materials") for the purpose of the Research.
- (B) The Provider Institution is willing to supply the Materials to the Recipient Institution and the Recipient is willing to receive the Materials in accordance with the terms and conditions contained within this agreement (the "Agreement");

TERMS AND CONDITIONS

It is hereby agreed as follows:

1. Definitions:

1.1 Commercial Purposes: means-

- 1.1.1 The sale, lease, licence or other transfer of the Materials or Modifications to a for-profit organisation;
- 1.1.2 Use of the Materials or Modifications by an organisation, including Recipient Institution, to perform contract research, to screen compound libraries, to produce or manufacture products for general sale; and
- 1.1.3 the conduct of research activities that result in any sale, lease or transfer of the Materials or Modifications to a for-profit organisation.

Industrially sponsored academic research shall not be considered a use of the Materials or Modifications for Commercial Purposes unless any of the above conditions are met.

-
- 1.2 **Materials:** Original Materials, Progeny, Unmodified Derivatives and information related to the Materials. The Materials shall not include:
 - (a) Modifications, or
 - (b) other substances created by the Recipient Institution through use of the Materials which are not Modifications, Progeny or Unmodified Derivatives.
 - 1.3 **Modifications:** Substances created by the Recipient Institution which contain/incorporate the Materials.
 - 1.4 **Progeny:** Unmodified descendant from the Materials, such as virus from virus, cell from cell, or organism from organism.
 - 1.5 **Term:** the period of 3 (three) years starting on the date of execution of this Agreement.
 - 1.6 **Unmodified Derivatives:** Substances created by the Recipient Institution which constitute an unmodified functional subunit or product expressed by the Original Material. Some examples include: subclones of unmodified cell lines, purified or fractionated subsets of the Original Material, proteins expressed by DNA/RNA supplied by the Provider Institution, or monoclonal antibodies secreted by a hybridoma cell line.

2. Ownership and Use of Materials

- 2.1 LSHTM retains ownership of the Materials and any Materials contained or incorporated into any Modifications. Nothing in this Agreement shall prevent or impede the Provider Institution from being able to use the Materials for any purpose, including but not limited to distribution and licensing of the Materials to third parties, whether public, private or third sector, for any purpose.
- 2.2 The Recipient retains ownership of:
 - (a) Modifications (except that the Provider Institution retains ownership rights to the Materials contained therein); and
 - (b) Those substances created through the use of the Materials or Modifications but which are not Progeny, Unmodified Derivatives or Modifications.

If either 3(a) or 3(b) results from the collaborative efforts of the Provider Institution and the Recipient Institution, joint ownership may be negotiated.
- 2.3 The Provider Institution grants the Recipient Institution a non-exclusive licence to use the Materials solely for the Research under the direct supervision of the Recipient Scientist in the Recipient Scientist's laboratory.
- 2.4 The Recipient Institution shall not:
 - (a) Use the Materials on human subjects or for any clinical or diagnostic purposes; or
 - (b) Use the Materials in research which is subject to the provision of any rights in the Materials to a commercial third party without prior written consent from the Provider Institution; or
 - (c) Use the Materials directly or indirectly for Commercial Purposes without prior written consent from the Provide Institution such consent to be at the sole discretion of the Provider Institution and which may be subject to negotiated agreement of commercial licence terms; or
 - (d) Supply the Materials to any other party or permit its use within the Recipient Institution for any other purpose without the prior written consent of the Provider Institution; or
 - (e) Supply Modifications for Commercial Purposes without prior written consent of the Provider Institution;
 - (f) Reverse engineer the Materials; or
 - (g) Attempt to identify the structure, composition or properties of the Materials for any purpose whatsoever.
- 2.5 The Recipient Institution shall:
 - (a) Use the Materials in accordance with good laboratory practice and the highest standards of skill and care and shall ensure compliance with any applicable laws and regulations

LSHTM Non-Human Tissue Transfer V.1 March 2020

governing the transportation, keeping, use or disposal of the Materials.

- (b) Ensure that no-one other than the Recipient Scientist and the employees and students under the direct supervision of the Recipient Scientist have access to them; and
- (c) Refer to the Provider Institution any request for the Materials from anyone other than those persons working under the Recipient Scientist's direct supervision.

3 Confidentiality and Publication

3.1 The Recipient Institution agrees to keep confidential any of the Provider Institution's confidential information relating to the Materials and any confidential and proprietary information described as such at the point of disclosure and/or was marked as either "confidential" or "proprietary" (together the "Confidential Information"). The confidentiality obligations in this clause shall not apply where the Confidential Information:

- a) has become public knowledge, other than through an unauthorised disclosure by the Recipient Institution;
- b) was already known to the Recipient Institution, prior to disclosure by the Provider Institution;
- c) was disclosed to the Recipient Institution or the Recipient Scientist by a third party, whom to the Recipient Institution's knowledge, was not under any obligation of confidence to the Provider Institution;
- d) was released from confidential status by written authorisation of the Provider Institution;
- e) was independently developed by the Recipient Institution or Recipient Scientist without the knowledge of the Confidential Information provided by the Provider Institution as evidenced by contemporaneous written records; or
- f) is required to be disclosed by law or by requirement of a regulatory body or court order.

3.2 The Recipient Institution is free to publish the results of the Research provided that the Recipient Institution acknowledges the Provider Institution as the source of the Materials in any publication which mentions the Materials. The Recipient Institution shall provide copies of publications acknowledging use of the Materials to the Provider Institution. For the avoidance of doubt, the Recipient Institution shall not publish any Confidential Information of the Provider Institution without its prior written consent, including information contained within the Material provided.

4 Inventions

4.1 The Recipient Institution acknowledges that the Materials are or may be the subject of a patent application. Except as provided in this Agreement, no express or implied licenses or other rights are provided to the Recipient Institution under any patents, patent applications, trade secrets or other proprietary rights of the Provider Institution, including any altered forms of the Materials made by the Provider Institution. In particular, no express or implied licenses or other rights are provided to use the Materials, Modifications, or any related patents of the Provider Institution for Commercial Purposes.

4.2 The Recipient Institution and/or the Recipient Scientist shall have the right, without restriction, to distribute substances created by the Recipient Institution or Recipient Scientist through the use of the Materials only if those substances are not Progeny, Unmodified Derivatives, or Modifications.

- 4.3 If the Recipient Institution makes or observes any new discovery, use, Modifications, improvement or invention ("Invention") relating to or arising from the use of the Materials then the Recipient Institution shall notify the Provider Institution. The Recipient Scientist and the Recipient Institution shall not make or seek to make any commercial gain from an Invention unless an appropriate revenue sharing agreement has been agreed with the Provider Institution. The Recipient shall promptly notify the Provider Institution of any application for a patent or any other proprietary rights to protect an Invention. The Provider Institution will, at all times, retain the right to use an Invention for internal research purposes.

5 Liability and Indemnity

- 5.1 The Recipient Institution acknowledges that the Materials are experimental in nature and may have hazardous properties. The Provider Institution makes no representation or warranties of any kind, either express or implied including but not limited to warranties of merchantability or fitness for a particular purpose, or that the use of the Materials will not infringe any patent, copyright, trademark or other proprietary rights.
- 5.2 The Provider Institution confirms that the Material does not constitute "Relevant Material" as defined in the Human Tissue Act 2004 or "tissue" as defined in the Human Tissue (Scotland) Act 2006.
- 5.3 In no event shall the Provider Institution be liable for any use by the Recipient or Recipient Scientist of the Materials transferred under this Agreement. Recipient agrees to indemnify and hold harmless Provider Institution for any loss, claim, damage or liability, of whatsoever kind or nature, due to or arising from the use, handling, storage or disposal of the Materials by the Recipient, except when caused by the gross negligence or wilful misconduct of the Provider Institution.
- 5.4 Nothing in this Agreement limits or excludes either party's liability for (a) death or personal injury resulting from negligence; or (b) any fraud or for any sort of other liability which, by law, cannot be limited or excluded.
- 5.5 The liability of either Party for any breach of this Agreement, or arising in any other way out of the subject matter of this Agreement, will not extend to loss of business, or profit, or to any indirect or consequential damages or losses.

6 Termination

- 6.1 This Agreement will terminate on the earliest of the following dates: (a) when the Materials become generally available from third parties, or (b) on completion of the Recipient Scientist's current research with the Materials, or (c) on thirty (30) days' written notice by either party to the other, or (d) on expiration of the Term. The Term may be extended with the written agreement of the Provider Institution. Permission to extend the Term must be sought by the Recipient Scientist three (3) months before the expiry of the Term. The obligations of both parties in clauses 2, 3, 4 and 5 shall survive termination of this Agreement for whatever cause.
- 6.2 The Provider Institution may terminate this Agreement forthwith if the Recipient Institution is in material breach of any of the terms of this Agreement and, where the breach is capable of remedy, the Recipient Institution has failed to remedy the same within twenty-eight calendar days of service of a written notice from the Provider Institution specifying the breach and requiring it to be remedied.
- 6.3 Upon termination or expiry of this Agreement, the Recipient Institution shall cease all use of the Materials and, in accordance with the instructions of the Provider Institution, either return or destroy the Materials. The Materials may only be retained with the express written consent of the Provider Institution.

7 General

- 7.1 The rights and obligations of the Parties are personal and may not be assigned at any time without the prior written consent of the other Party which consent shall not be unreasonably withheld.
- 7.2 Materials are provided at no cost but the Recipient Institution agrees to pay any transfer, shipping or other associated costs in connection with the transfer of the Materials under this Agreement.
- 7.3 A person who is not a party to this Agreement shall not have any rights under or in connection with it.
- 7.4 This Agreement constitutes the entire agreement between the parties in respect of its subject matter and no statements or representations made by any Party have been relied upon by the other in entering into this Agreement.
- 7.5 This Agreement shall be governed and construed in accordance with the laws of England and Wales and the Parties agree to the exclusive jurisdiction of the English Courts.
- 7.6 This Agreement may be executed in one (1) or more counterparts, each of which shall be deemed an original, but all of which together shall constitute one and the same instrument. A signed copy of this Agreement delivered by e-mailed portable document format file or other means of electronic transmission shall be deemed to have the same legal effect as delivery of an original signed copy of this Agreement.

Accepted and Agreed on behalf of
**Medical Research Council/Uganda Virus
research Institute and London School of
Hygiene and Tropical Medicine Uganda
Research Unit**

Name: PONTIANO KALEEBU

Position: DIRECTOR

Signature:

Date: 16th JAN 2023

Accepted and Agreed on behalf of
**London School of Hygiene & Tropical
Medicine**

Name: Alex Hollander-Carney

Position: Head of Legal and Compliance

Signature:

Date 13th January 2023

Schedule 1

The Research

Project title: *"Praziquantel for children under four: A Phase II PK/PD driven dose finding trial (PIP trial)".*

Regulatory/Ethics Body	Approval Number	Time of approval
Uganda Virus Research Institute REC	GC/127/19/07/708	July 19, 2019
Uganda National Council for Science & Technology	HS 2650	August 30, 2019
National Drug Authority	CTC 0133/2020	July 27, 2020
LSHTM REC	14851 - 1	June 05, 2020

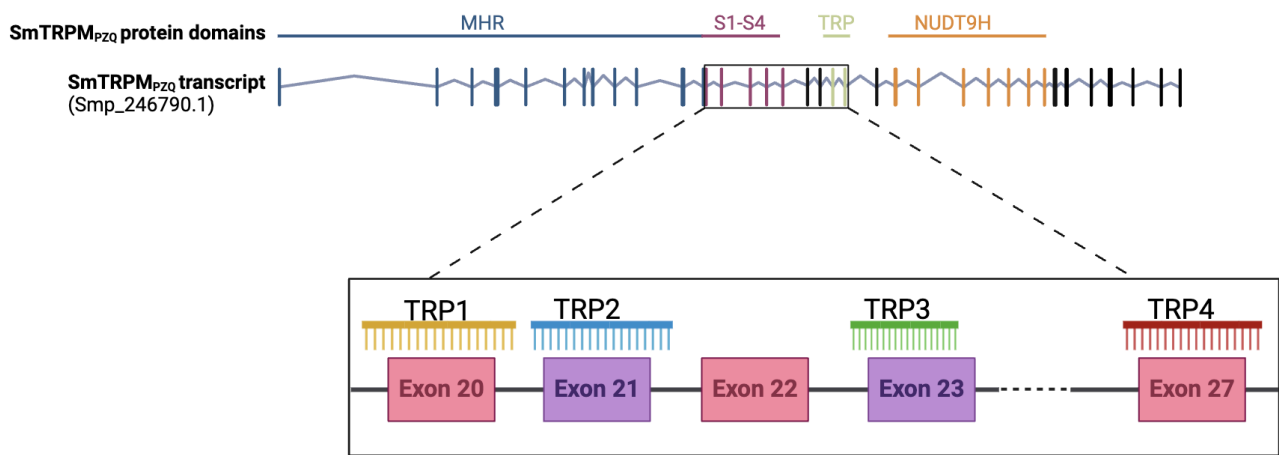
Schedule 2

The Material

350 FTA cards and Eppendorf tubes containing *Schistosoma mansoni* larval stages. 300 *Biomphalaria* intermediate snails.

The *Schistosoma mansoni* larval samples will be required for the duration of Shannan Summers' PhD project until January 2025. The remaining *Schistosoma mansoni* larval stages will be stored at the London School of Hygiene and Tropical Medicine. The scheduled shipment date will be March 2023.

The *Biomphalaria* intermediate snails will be maintained indefinitely at the London School of Hygiene and Tropical Medicine. They will not be destroyed. The scheduled date of shipment will be February/ March 2023.



Appendix Figure 5.1: Primer design for amplifying the PZQ binding site in SmTRPM_{PZQ} (Smp_246790.1). Figure created using Biorender.com.

Appendix Table 5.1: Primers designed for amplification of the exons encoding the PZQ binding site in SmTRPM_{PZQ} (Smp_246790.1).

Amplicon	Position	Forward primer	Reverse primer	Protein domain (exon)	Product size (bp)	Annealing temperature (°C)
TRP1	2738967-2739214	TCAGC GTTCCG GAAAA CGTTA C	TGATGT CCCCTC TGAGAC TCG	S1 (20)	247	65
TRP2	2739948-2740429	AACAC CATCG GATCT CTGCT	AGTCTC GCCGTT TTCGAT GA	S1/S2 (21)	481	63
TRP3	2,745,445-2745771	TGATCT AATCAT CTTCT CTCCC CT	TTGGTC CTAATGC AATATGA AAACT	S3/S4 (23)	327	65
TRP4	2,756,017-2,756,443	CCATC AGGAG AAACA GGCGT A	AAACGC AAATAAG TATCGTG GC	TRP (27)	426	64

Appendix Table 5.2: Primer sequences plus barcodes for amplicon sequencing.

Barcodes BC1-10 and BC21-30 were added to the 5' end of the forward primers.

BC11-BC20 and BC21-BC40 were added to the 5' end of the reverse primers. The forward primer and reverse primer barcodes used together are listed next to each other in the table.

Amplicon	Forward barcode name (Barcode)	Barcode + primer	Barcode name (reverse primer)	Barcode + primer
TRP1	BC1N (CTATCACG)	CTATCACGTC AGCGTTCGGA AAACGTTAC	BC11N (ATGGCTAG)	ATGGCTAGTG ATGTCCCCTC TGAGACTCG
	BC2N (TCCAGTGT)	TCCAGTGTTT AGCGTTCGGA AAACGTTAC	BC12N (GACTTGGT)	GACTTGGTTG ATGTCCCCTC TGAGACTCG
	BC3N (GATCAGTA)	GATCAGTATC AGCGTTCGGA AAACGTTAC	BC13N (TCGATCAC)	TCGATCACTG ATGTCCCCTC TGAGACTCG
	BC4N (AGTGTCGG)	AGTGTCGGTC AGCGTTCGGA AAACGTTAC	BC14N (ACACGTCA)	ACACGTCATG ATGTCCCCTC TGAGACTCG
	BC5N (GTAGCGCT)	GTAGCGCTTC AGCGTTCGGA AAACGTTAC	BC15N (CAATGTGC)	CAATGTGCTG ATGTCCCCTC TGAGACTCG
	BC6N (CATCTAAC)	CATCTAACTC AGCGTTCGGA AAACGTTAC	BC16N (GGGACTAC)	GGGACTACTG ATGTCCCCTC TGAGACTCG
	BC7N (TACAGATC)	TACAGATCTC AGCGTTCGGA AAACGTTAC	BC17N (ACGTA CTG)	ACGTA CTGTG ATGTCCCCTC TGAGACTCG
	BC8N (CGTCTTGT)	CGTCTTGTTT AGCGTTCGGA AAACGTTAC	BC18N (TGATTGCC)	TGATTGCCTG ATGTCCCCTC TGAGACTCG
	BC9N (TATGATCA)	TATGATCATCA GCGTTCGGAA AACGTTAC	BC19N (AACTCTAC)	AACTCTACTG ATGTCCCCTC TGAGACTCG
	BC10N (GGTAGCTT)	GGTAGCTTTT AGCGTTCGGA AAACGTTAC	BC20N (TGA CTCAA)	TGA CTCAATG ATGTCCCCTC TGAGACTCG
	BC21N (AACCAAGG)	AACCAAGGTC AGCGTTCGGA AAACGTTAC	BC31N (CGTAGGAA)	CGTAGGAATG ATGTCCCCTC TGAGACTCG
	BC22N	AAGGTACGTC	BC32N	GACATCTGTG

	(AAGGTACG)	AGCGTTCGGA AAACGTTAC	(GACATCTG)	ATGTCCCCTC TGAGACTCG
	BC23N (ACCTACCT)	ACCTACCTTC AGCGTTCGGA AAACGTTAC	BC33N (GCAATAGG)	GCAATAGGTG ATGTCCCCTC TGAGACTCG
	BC24N (ACTGGACT)	ACTGGACTTC AGCGTTCGGA AAACGTTAC	BC34N (GACTGT)	GACTGTGTTG ATGTCCCCTC TGAGACTCG
	BC25N (ATATGCCG)	ATATGCCGTC AGCGTTCGGA AAACGTTAC	BC35N (GTGAGTCT)	GTGAGTCTTG ATGTCCCCTC TGAGACTCG
	BC26N (CAACCATG)	CAACCATGTC AGCGTTCGGA AAACGTTAC	BC36N (TCACTCTG)	TCACTCTGTG ATGTCCCCTC TGAGACTCG
	BC27N (CTTCGAAG)	CTTCGAAGTC AGCGTTCGGA AAACGTTAC	BC37N (TCTCCAGT)	TCTCCAGTTG ATGTCCCCTC TGAGACTCG
	BC28N (CAGAAGTG)	CAGAAGTGTC AGCGTTCGGA AAACGTTAC	BC38N (TGGTTCCT)	TGGTTCCTTG ATGTCCCCTC TGAGACTCG
	BC29N (CAGTGACT)	CAGTGACTTC AGCGTTCGGA AAACGTTAC	BC39N (TGTGACTG)	TGTGACTGTG ATGTCCCCTC TGAGACTCG
	BC30N (CATGTGGT)	CATGTGGTTC AGCGTTCGGA AAACGTTAC	BC40N (GTCTACAG)	GTCTACAGTG ATGTCCCCTC TGAGACTCG
TRP2	BC1N (CTATCACG)	CTATCACGAA CACCATCGGA TCTCTGCT	BC11N (ATGGCTAG)	ATGGCTAGAG TCTCGCCGTT TTCGATGA
	BC2N (TCCAGTGT)	TCCAGTGTA CACCATCGGA TCTCTGCT	BC12N (GACTTGGT)	GACTTGGTAG TCTCGCCGTT TTCGATGA
	BC3N (GATCAGTA)	GATCAGTAAA CACCATCGGA TCTCTGCT	BC13N (TCGATCAC)	TCGATCACAG TCTCGCCGTT TTCGATGA
	BC4N (AGTGTCGG)	AGTGTCGGAA CACCATCGGA TCTCTGCT	BC14N (ACACGTCA)	ACACGTCAAG TCTCGCCGTT TTCGATGA
	BC5N (GTAGCGCT)	GTAGCGCTAA CACCATCGGA TCTCTGCT	BC15N (CAATGTGC)	CAATGTGCAG TCTCGCCGTT TTCGATGA

BC6N (CATCTAAC)	CATCTAACAA CACCATCGGA TCTCTGCT	BC16N (GGGACTAC)	GGGACTACAG TCTCGCCGTT TTCGATGA
BC7N (TACAGATC)	TACAGATCAA CACCATCGGA TCTCTGCT	BC17N (ACGTA CTG)	ACGTA CTGAG TCTCGCCGTT TTCGATGA
BC8N (CGTCTTGT)	CGTCTTG TAA CACCATCGGA TCTCTGCT	BC18N (TGATTGCC)	TGATTGCCAG TCTCGCCGTT TTCGATGA
BC9N (TATGATCA)	TATGATCAAAC ACCATCGGAT CTCTGCT	BC19N (AACTCTAC)	AACTCTACAG TCTCGCCGTT TTCGATGA
BC10N (GGTAGCTT)	GGTAGCTTAA CACCATCGGA TCTCTGCT	BC20N (TGA CTCAA)	TGA CTCAAAG TCTCGCCGTT TTCGATGA
BC21N (AACCAAGG)	AACCAAGGAA CACCATCGGA TCTCTGCT	BC31N (CGTAGGAA)	CGTAGGAAAG TCTCGCCGTT TTCGATGA
BC22N (AAGGTACG)	AAGGTACGAA CACCATCGGA TCTCTGCT	BC32N (GACATCTG)	GACATCTGAG TCTCGCCGTT TTCGATGA
BC23N (ACCTACCT)	ACCTACCTAA CACCATCGGA TCTCTGCT	BC33N (GCAATAGG)	GCAATAGGAG TCTCGCCGTT TTCGATGA
BC24N (ACTGGACT)	ACTGGACTAA CACCATCGGA TCTCTGCT	BC34N (GACACTGT)	GACACTGTAG TCTCGCCGTT TTCGATGA
BC25N (ATATGCCG)	ATATGCCGAA CACCATCGGA TCTCTGCT	BC35N (GTGAGTCT)	GTGAGTCTAG TCTCGCCGTT TTCGATGA
BC26N (CAACCATG)	CAACCATGAA CACCATCGGA TCTCTGCT	BC36N (TCACTCTG)	TCACTCTGAG TCTCGCCGTT TTCGATGA
BC27N (CTTCGAAG)	CTTCGAAGAA CACCATCGGA TCTCTGCT	BC37N (TCTCCAGT)	TCTCCAGTAG TCTCGCCGTT TTCGATGA
BC28N (CAGAAGTG)	CAGAAGTGAA CACCATCGGA TCTCTGCT	BC38N (TGGTTCCT)	TGGTTCCTAG TCTCGCCGTT TTCGATGA
BC29N (CAGTGA CT)	CAGTGA CTAA CACCATCGGA TCTCTGCT	BC39N (TGTGA CTG)	TGTGA CTGAG TCTCGCCGTT TTCGATGA

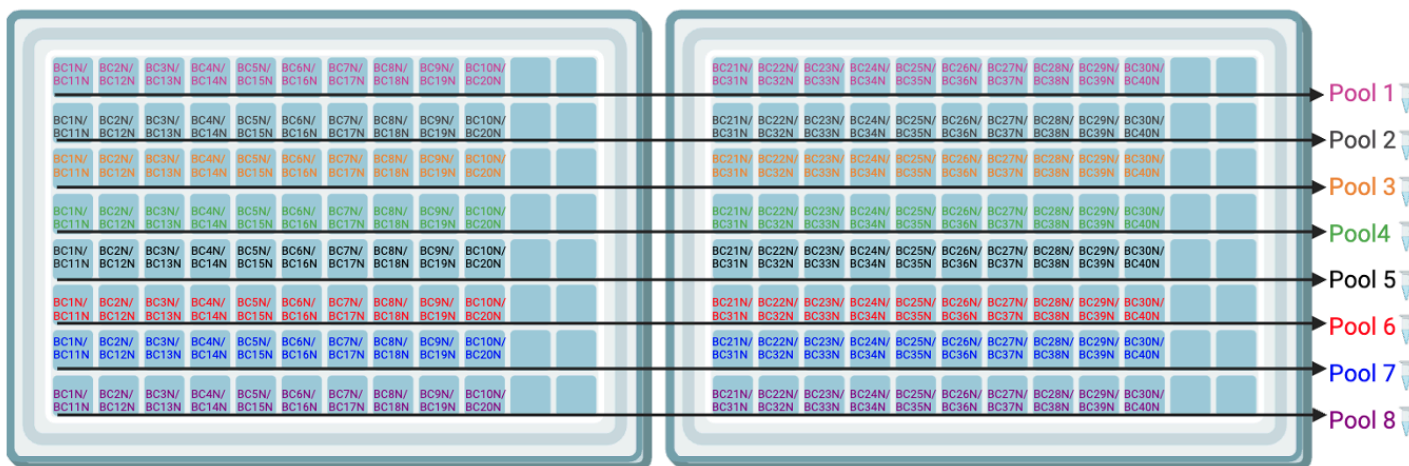
	BC30N (CATGTGGT)	CATGTGGTAA CACCATCGGA TCTCTGCT	BC40N (GTCTACAG)	GTCTACAGAG TCTCGCCGTT TTCGATGA
TRP3	BC1N (CTATCACG)	CTATCACGTG ATCTAATCATC TTCTCTCCCC T	BC11N (ATGGCTAG)	ATGGCTAGTT GGTCCTAATG CAATATGAAAA CT
	BC2N (TCCAGTGT)	TCCAGTGTTG ATCTAATCATC TTCTCTCCCC T	BC12N (GACTTGGT)	GACTTGGTTT GGTCCTAATG CAATATGAAAA CT
	BC3N (GATCAGTA)	GATCAGTATG ATCTAATCATC TTCTCTCCCC T	BC13N (TCGATCAC)	TCGATCACTT GGTCCTAATG CAATATGAAAA CT
	BC4N (AGTGTCGG)	AGTGTCGGTG ATCTAATCATC TTCTCTCCCC T	BC14N (ACACGTCA)	ACACGTCATT GGTCCTAATG CAATATGAAAA CT
	BC5N (GTAGCGCT)	GTAGCGCTTG ATCTAATCATC TTCTCTCCCC T	BC15N (CAATGTGC)	CAATGTGCTT GGTCCTAATG CAATATGAAAA CT
	BC6N (CATCTAAC)	CATCTAACTG ATCTAATCATC TTCTCTCCCC T	BC16N (GGGACTAC)	GGGACTACTT GGTCCTAATG CAATATGAAAA CT
	BC7N (TACAGATC)	TACAGATCTG ATCTAATCATC TTCTCTCCCC T	BC17N (ACGTA CTG)	ACGTA CTGTT GGTCCTAATG CAATATGAAAA CT
	BC8N (CGTCTTGT)	CGTCTTGTTG ATCTAATCATC TTCTCTCCCC T	BC18N (TGATTGCC)	TGATTGCCTT GGTCCTAATG CAATATGAAAA CT
	BC9N (TATGATCA)	TATGATCATGA TCTAATCATCT TCTCTCCCCT	BC19N (AACTCTAC)	AACTCTACTT GGTCCTAATG CAATATGAAAA CT
	BC10N (GGTAGCTT)	GGTAGCTTTG ATCTAATCATC TTCTCTCCCC T	BC20N (TGA CTCAA)	TGA CTCAATT GGTCCTAATG CAATATGAAAA CT
	BC21N	AACCAAGGTG	BC31N	CGTAGGAATT

	(AACCAAGG)	ATCTAATCATC TTCTCTCCCC T	(CGTAGGAA)	GGTCCTAATG CAATATGAAAA CT
	BC22N (AAGGTACG)	AAGGTACGTG ATCTAATCATC TTCTCTCCCC T	BC32N (GACATCTG)	GACATCTGTT GGTCCTAATG CAATATGAAAA CT
	BC23N (ACCTACCT)	ACCTACCTTG ATCTAATCATC TTCTCTCCCC T	BC33N (GCAATAGG)	GCAATAGGTT GGTCCTAATG CAATATGAAAA CT
	BC24N (ACTGGACT)	ACTGGACTTG ATCTAATCATC TTCTCTCCCC T	BC34N (GACACTGT)	GACACTGTTT GGTCCTAATG CAATATGAAAA CT
	BC25N (ATATGCCG)	ATATGCCGTG ATCTAATCATC TTCTCTCCCC T	BC35N (GTGAGTCT)	GTGAGTCTTT GGTCCTAATG CAATATGAAAA CT
	BC26N (CAACCATG)	CAACCATGTG ATCTAATCATC TTCTCTCCCC T	BC36N (TCACTCTG)	TCACTCTGTT GGTCCTAATG CAATATGAAAA CT
	BC27N (CTTCGAAG)	CTTCGAAGTG ATCTAATCATC TTCTCTCCCC T	BC37N (TCTCCAGT)	TCTCCAGTTT GGTCCTAATG CAATATGAAAA CT
	BC28N (CAGAAGTG)	CAGAAGTGTG ATCTAATCATC TTCTCTCCCC T	BC38N (TGGTTCCT)	TGGTTCCTTT GGTCCTAATG CAATATGAAAA CT
	BC29N (CAGTGACT)	CAGTGACTTG ATCTAATCATC TTCTCTCCCC T	BC39N (TGTGACTG)	TGTGACTGTT GGTCCTAATG CAATATGAAAA CT
	BC30N (CATGTGGT)	CATGTGGTTG ATCTAATCATC TTCTCTCCCC T	BC40N (GTCTACAG)	GTCTACAGTT GGTCCTAATG CAATATGAAAA CT
TRP4	BC1N (CTATCACG)	CTATCACGCC ATCAGGAGAA ACAGGCGTA	BC11N (ATGGCTAG)	ATGGCTAGAA ACGCAAATAA GTATCGTGCC
	BC2N (TCCAGTGT)	TCCAGTGTCC ATCAGGAGAA	BC12N (GACTTGGT)	GACTTGGTAA ACGCAAATAA

		ACAGGCGTA		GTATCGTGGC
	BC3N (GATCAGTA)	GATCAGTACC ATCAGGAGAA ACAGGCGTA	BC13N (TCGATCAC)	TCGATCACAA ACGCAAATAA GTATCGTGGC
	BC4N (AGTGTCGG)	AGTGTCGGCC ATCAGGAGAA ACAGGCGTA	BC14N (ACACGTCA)	ACACGTCAAA ACGCAAATAA GTATCGTGGC
	BC5N (GTAGCGCT)	GTAGCGCTCC ATCAGGAGAA ACAGGCGTA	BC15N (CAATGTGC)	CAATGTGCAA ACGCAAATAA GTATCGTGGC
	BC6N (CATCTAAC)	CATCTAACCC ATCAGGAGAA ACAGGCGTA	BC16N (GGGACTAC)	GGGACTACAA ACGCAAATAA GTATCGTGGC
	BC7N (TACAGATC)	TACAGATCCC ATCAGGAGAA ACAGGCGTA	BC17N (ACGTA CTG)	ACGTA CTGAA ACGCAAATAA GTATCGTGGC
	BC8N (CGTCTTGT)	CGTCTTGTCC ATCAGGAGAA ACAGGCGTA	BC18N (TGATTGCC)	TGATTGCCAA ACGCAAATAA GTATCGTGGC
	BC9N (TATGATCA)	TATGATCACCA TCAGGAGAAA CAGGCGTA	BC19N (AACTCTAC)	AACTCTACAA ACGCAAATAA GTATCGTGGC
	BC10N (GGTAGCTT)	GGTAGCTTCC ATCAGGAGAA ACAGGCGTA	BC20N (TGA CTCAA)	TGA CTCAAAA ACGCAAATAA GTATCGTGGC
	BC21N (AACCAAGG)	AACCAAGGCC ATCAGGAGAA ACAGGCGTA	BC31N (CGTAGGAA)	CGTAGGAAAA ACGCAAATAA GTATCGTGGC
	BC22N (AAGGTACG)	AAGGTACGCC ATCAGGAGAA ACAGGCGTA	BC32N (GACATCTG)	GACATCTGAA ACGCAAATAA GTATCGTGGC
	BC23N (ACCTACCT)	ACCTACCTCC ATCAGGAGAA ACAGGCGTA	BC33N (GCAATAGG)	GCAATAGGAA ACGCAAATAA GTATCGTGGC
	BC24N (ACTGGACT)	ACTGGACTCC ATCAGGAGAA ACAGGCGTA	BC34N (GACACTGT)	GACACTGTAA ACGCAAATAA GTATCGTGGC
	BC25N (ATATGCCG)	ATATGCCGCC ATCAGGAGAA ACAGGCGTA	BC35N (GTGAGTCT)	GTGAGTCTAA ACGCAAATAA GTATCGTGGC
	BC26N	CAACCATGCC	BC36N	TCACTCTGAA

	(CAACCATG)	ATCAGGAGAA ACAGGCGTA	(TCACTCTG)	ACGCAAATAA GTATCGTGCC
	BC27N (CTTCGAAG)	CTTCGAAGCC ATCAGGAGAA ACAGGCGTA	BC37N (TCTCCAGT)	TCTCCAGTAA ACGCAAATAA GTATCGTGCC
	BC28N (CAGAAGTG)	CAGAAGTGCC ATCAGGAGAA ACAGGCGTA	BC38N (TGGTTCCT)	TGGTTCCTAA ACGCAAATAA GTATCGTGCC
	BC29N (CAGTGACT)	CAGTGACTCC ATCAGGAGAA ACAGGCGTA	BC39N (TGTGACTG)	TGTGACTGAA ACGCAAATAA GTATCGTGCC
	BC30N (CATGTGGT)	CATGTGGTCC ATCAGGAGAA ACAGGCGTA	BC40N (GTCTACAG)	GTCTACAGAA ACGCAAATAA GTATCGTGCC

1) Pooling of target specific amplicons e.g. TRP1 with unique barcode combinations



2) Target specific amplicon pools quantified and normalised to 20 ng/ul



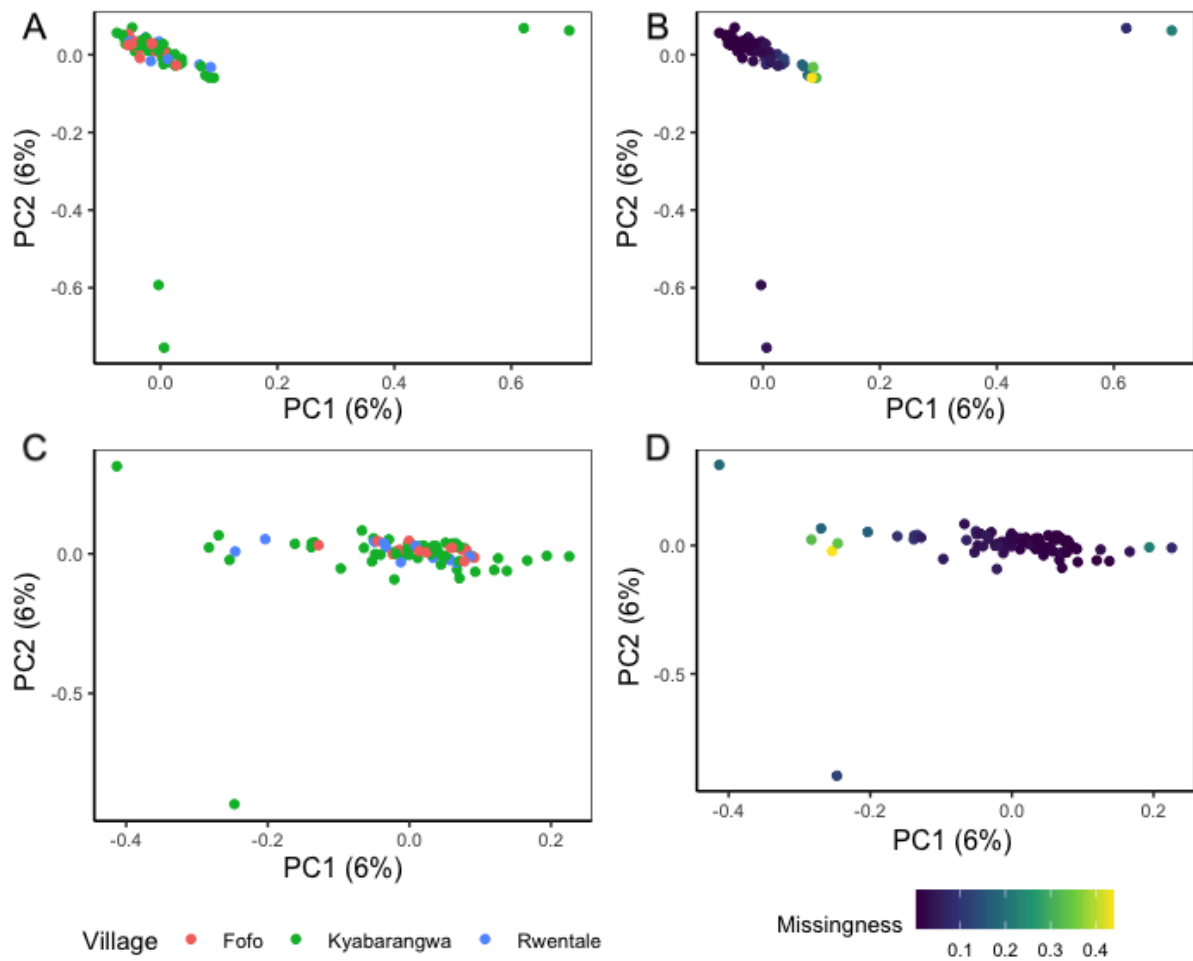
3) One of each target specific amplicon pool are pooled together



4) Amplicon pools sequenced on the Illumina MiSeq platform (2 x 250 bp)



Appendix Figure 5.2: Overview of amplicon pooling process. Initially, amplicons are grouped by target-specific regions (TRP1, TRP2, TRP3, and TRP4), each with unique barcode combinations. DNA from these target-specific pools is then purified using magnetic beads, and its concentration is quantified using Qubit. Subsequently, the purified pools are normalised to 20 ng/μl. Finally, one pool from each target-specific amplicon (e.g., Pool 1 of TRP1-4) is combined. The resulting amplicon pools are sequenced on the Illumina MiSeq platform (2 x 250 bp).



Appendix Figure 5.3: Population structure of Lake Albert miracidia. Principal component analysis of genetic differentiation between 88 *S. mansoni* miracidia sampled in this study. A and B represent principal components 1-4 coloured by village or individual sample missingness. C and D represent principal components 3 and 4 coloured by by village or individual sample missingness.

Appendix Table 5.3: Genome-wide mean nucleotide diversity (π) for each treatment time point stratified by treatment group.

Group	Mean π	99% Confidence interval
Standard pre-treatment	0.00312	0.00310-0.00314
Standard post-treatment	0.00294	0.00292-0.00295
Intensive pre-treatment	0.00315	0.00313-0.00317
Intensive post-treatment	0.00298	0.00296-0.00299

Appendix Table 5.4: Genome-wide mean genetic differentiation (F_{st}) comparisons between time point and treatment group.

Group	Mean F_{st}	99% CI
Standard Pre vs Post-treatment	0.00575	0.00566-0.00585
Intensive Pre vs Post-treatment	0.00562	0.00553-0.00572
Standard Pre vs Intensive Pre-treatment	0.00550	0.00541-0.00560
Standard Post vs Intensive Post-treatment	0.00582	0.00573-0.00591

Appendix Table 5.5: Genes encoding proteins present in the candidate regions of differentiation using genome-wide Fst.

Chromosome	Window start (bp)	Window end (bp)	Window size (kb)	Evidence	Gene IDs	Function/ name
SM_V10_1	22185000	22215000	30	Fst (Intensive Pre vs Post)	Smp_325980 Smp_093310 Smp_093320	Secreted protein E2F/DP family, putative, DNA binding, transcription regulation Nucleolar protein 10- rRNA processing
SM_V10_1	30940000	31045000	105	Fst (Intensive Pre vs Post)	Smp_347240 Smp_337620 Smp_160800 Smp_160810 Smp_160820 Smp_210750	BEACH domain-containing protein- mitochondrion BAH domain-containing protein- chromatin silencing complex DUF3480 domain-containing protein Putative amine oxidase- polyamine oxidase activity Protein kinase domain-containing protein- calcium ion transport across plasma membrane Peptidyl-prolyl cis-trans isomerase- DNA binding- rRNA processing
SM_V10_2	13330000	13400000	70	Fst (Intensive Pre vs Post)	Smp_161210 Smp_333810 Smp_317040 Smp_071830	G_PROTEIN_RECEP_ F1_2 domain-containing protein 6-phosphogluconate dehydrogenase, decarboxylating RNA-binding protein Transcription initiation factor IIA subunit 2- RNA polymerase II general transcription initiation factor activity
SM_V10_1	2050000	2070000	20	Fst	Smp_164480	Tubulin beta chain

				(Standard Pre vs Post)		
SM_V10_1	27600000	27640000	40	Fst (Standard Pre vs Post)	Smp_196950	One cut domain family member- DNA-binding transcription factor activity, RNA polymerase II-specific
SM_V10_2	25480000	25520000	40	Fst (Standard Pre vs Post)	Smp_012280	BAT2_N domain-containing protein
SM_V10_2	32140000	32175000	35	Fst (Standard Pre vs Post)	Smp_176850 Smp_176840 Smp_099690	Putative armc4 Putative hypoxia associated factor- mRNA processing and splicing Protein RER1- Involved in the retrieval of endoplasmic reticulum membrane proteins from the early Golgi compartment
SM_V10_3	6970000	7005000	35	Fst (Standard Pre vs Post)	Smp_029360	Amino acid transporter, putative
SM_V10_7	13200000	13375000	175	Fst (Standard Pre vs Post)	Smp_332340 Smp_318340 Smp_318350 Smp_166720	Uncharacterized transmembrane protein Uncharacterized protein Uncharacterized transmembrane protein Gnk2-homologous domain-containing protein
SM_V10_2	3300000	3325000	25	Fst (Standard Pre vs Intensive Post)	Smp_017230	Nicotinate phosphoribosyltransferase related pre-B cell enhancing factor
SM_V10_2	33140000	33175000	35	Fst (Standard Pre vs Intensive Post)	Smp_123390	Requim, req/dpf2, putative- Histone binding

SM_V10_3	11700000	11735000	35	Fst (Standard Pre vs Intensive Post)	Smp_080610 Smp_080620	NADH dehydrogenase [ubiquinone] 1 beta subcomplex subunit 11, mitochondrial XPG_I_2 domain-containing protein
SM_V10_3	15140000	15175000	35	Fst (Standard Pre vs Intensive Post)	Smp_074010 Smp_074000	DNA-(apurinic or apyrimidinic site) lyase, endonuclease activity Single-pass type I transmembrane protein
SM_V10_3	47865000	47890000	25	Fst (Standard Pre vs Intensive Post)	Smp_196810 Smp_172700 Smp_092490	Dihydropyrimidinase related protein-3 (M38 family) Serine/threonine kinase Putative nadh-plastoquinone oxidoreductase
SM_V10_4	27235000	27285000	50	Fst (Standard Pre vs Intensive Post)	Smp_053700 Smp_150890	Cytochrome b-c1 complex subunit 8 RBR-type E3 ubiquitin transferase

Appendix Table 5.6: Genes encoding proteins present in the candidate regions of selection using genome-wide XP-EHH.

Chromosome	Window start (bp)	Window end (bp)	Window size (kb)	Evidence	Gene IDs	Function/ name
SM_V10_1	55925000	55950000	25	XP-EHH (Standard Pre vs Post)	Smp_144550	Chromobox protein-related (Chromobox 1) (Heterochromatin 1)
SM_V10_1	59820000	59975000	155	XP-EHH (Standard Pre vs Post)	Smp_143240 Smp_247050 Smp_337310	Trafficking protein particle complex subunit 11 Uncharacterized protein Uncharacterized protein
SM_V10_2	32140000	32180000	40	XP-EHH (Standard Pre vs Post)	Smp_176850 Smp_176840 Smp_099690	Putative armc4 Putative hypoxia associated factor- mRNA processing and splicing Protein RER1- Involved in the retrieval of endoplasmic reticulum membrane proteins from the early Golgi compartment
SM_V10_5	9300000	9445000	145	XP-EHH (Standard Pre vs Post)	Smp_334490 Smp_334500 Smp_315870 Smp_330430 Smp_094630 Smp_094640	Cilia- and flagella-associated protein 91 Uncharacterized protein NADH dehydrogenase (Ubiquinone) complex I, assembly factor 6 Uncharacterized protein RRM domain-containing protein- RNA binding "Zinc finger protein, putative, DNA-binding transcription factor activity, RNA polymerase II-specific"
SM_V10_1	30800000	31040000	240	XP-EHH (Intensive Pre vs Post)	Smp_081260 Smp_246250 Smp_165980 Smp_210750 Smp_160800 Smp_160820 Smp_347770 Smp_347340 Smp_337620 Smp_160810	PH domain-containing protein Acidic fibroblast growth factor intracellular-binding protein DNA-directed RNA polymerase III subunit RPC6 Peptidyl-prolyl cis-trans isomerase, DNA binding-rRNA processing DUF3480

						<p>domain-containing protein Protein kinase domain-containing protein, calcium ion import across plasma membrane EGF-like domain-containing protein BEACH domain-containing protein- mitochondrion BAH domain-containing protein- chromatin silencing complex Putative amine oxidase- polyamine oxidase activity</p>
SM_V10_1	66835000	66920000	85	XP-EHH (Intensive Pre vs Post)	Smp_093630 Smp_158570 Smp_158560	<p>Mitochondrial carrier protein-related- Mitochondrial transporter mediating uptake of thiamine diphosphate into mitochondria Secreted protein Serine/threonine kinase, non-specific</p>
SM_V10_4	23180000	23415000	235	XP-EHH (Intensive Pre vs Post)	Smp_135500 Smp_135510 Smp_340460 Smp_024660	<p>Phosphodiesterase, membrane including synaptic membrane NAALADASE L peptidase (M28 family), Metallopeptidase Beta-1,4-galactosyltransfe rase, Catalyses the transfer of galactose onto proteins or lipids. Putative cell adhesion molecule, axon and plasma membrane</p>
SM_V10_5	8850000	9010000	160	XP-EHH (Intensive Pre vs Post)	Smp_344650 Smp_346180	<p>Ras-related protein Rab-3, Protein transport. Probably involved in vesicular traffic. protein-tyrosine-phosphat ase</p>
SM_V10_1	66800000	67020000	220	XP-EHH (Standard Pre vs Intensive Post)	Smp_213970 Smp_213960 Smp_158560 Smp_247270 Smp_067280 Smp_093630 Smp_158570	<p>Telomeric repeat-binding factor 2-interacting protein 1 Dentin sialophosphoprotein-like Serine/threonine kinase, non-specific</p>

						<p>Histone-lysine N-methyltransferase SMYD3 Dynamin-1-like protein, microtubule binding, peroxisome fission Mitochondrial thiamine pyrophosphate carrier, mediating uptake of thiamine diphosphate into mitochondria Secreted protein</p>
SM_V10_5	8850000	9010000	160	XP-EHH (Standard Pre vs Intensive Post)	Smp_344650 Smp_346180	<p>Ras-related protein Rab-3, Protein transport. Probably involved in vesicular traffic. protein-tyrosine-phosphatase</p>

Appendix Table 5.7: The mean coverage and distribution of SNPs and (indels) detected in each amplicon.

Amplicon	Mean coverage	Synonymous (n)	Non-synonymous (n)	Upstream gene variant (n)	Intronic (n)	Splice region (n)	Total
TRP1	669.29	0	1	0	4 (1)	0	5 (1)
TRP2	47.26	0	0	0	21 (1)	2	23 (1)
TRP3	438.84	0	1	0	0	0	1
TRP4	134.65	2	0	0	6 (1)	0	8 (1)

Appendix Table 5.8: The position and frequency of intronic SNPs.

Amplicon	Position	N ^a	Mutation	Genotype frequencies (%)			Alternate allele frequency (%)
				Homozygous (reference)	Heterozygous	Homozygous alternate	
TRP1	2739112	2	c.4167+48T >C	0.5	5.3	94.2	96.1
	2739139	2	c.4167+75G >A	98.5	1.5	0	0.9
	2739155	2	c.4167+91G >C	97.6	2.4	0	1.3
	2739189	2	c.4167+125 G>A	90.8	8.2	1	6.2
TRP2	2739978	2	c.4168-209T >C	98.9	1.1	0	0.6
	2739992	2	c.4168-209T >C	99.3	0	0.7	0.7
	2740047	2	c.4168-154T >C	99.4	0.3	0.3	0.9
	2740063	2	c.4168-138T >C	33.5	31.2	35.3	46.8
	2740070	2	c.4168-131C >T	99.3	0.7	0	0.6
	2740088	2	c.4168-113T >A	98.5	1.5	0	0.7
	2740153	2	c.4168-48G >C	98.9	0.7	0.4	1.9
	2740157	2	c.4168-44C> T	98.9	0.7	0.4	1.5
	2740181	2	c.4168-20T> C	80.6	16.2	3.2	11.3
	2740182	2	c.4168-19C> T	14.3	14.3	71.4	50.0
	2740186	2	c.4168-15T> C	95.5	4.5	0	2.2
	2740194	2	c.4168-7T> C	98.2	0.7	1.1	1.5
	2740336	2	c.4296+7A>	95.9	1.9	2.2	4.8

			C				
	2740353	2	c.4296+24T >C	98.8	1.2	0	0.6
	2740368	2	c.4296+39G >A	92.9	0.7	6.4	10.6
	2740378	2	c.4296+49G >A	92.9	0.7	6.4	10.6
	2740381	2	c.4296+52A >C	92.9	0.7	6.4	11.2
	2740385	2	c.4296+56T >C	95.9	1.9	2.2	5.2
	2740397	2	c.4296+68G >C	92.5	1.1	6.4	11.2
	2740398	2	c.4296+69A >C	92.5	1.1	6.4	11.2
	2740400	2	c.4296+71A >T	92.5	1.1	6.4	11.2
	2740402	2	c.4296+73G >T	92.5	1.1	6.4	11.4
	2740403	2	c.4296+74C >T	92.5	1.1	6.4	11.2
TRP4	2756075	2	c.4959-93A> G	97.7	1.8	0.5	1.1
	2756080	2	c.4959-88T> C	98.0	2.0	0	1.1
	2756105	2	c.4959-63C> T	98.0	2.0	0	1.1
	2756131	2	c.4959-37C> T	19.0	40.4	40.6	60.7
	2756158	2	c.4959-10A> G	43.0	39.4	17.6	37.5
	2756386	2	c.5158+19C >T	96.7	3.3	0	2.2

Appendix Table 5.9: The position and frequency of intronic indels. *associated with a homopolymer region.

Amplicon	Position	N ^a	Mutation	Genotype frequencies (%)			Alternate allele frequency (%)
				Homozygous (reference)	Heterozygous	Homozygous alternate	
TRP1	2739108	2	c.4167+45_4167+49delTA CTC	98.78	1.22	0	0.0061
TRP2	2740173 *	2	c.4168-27del T	64.29	32.14	3.57	0.0244
TRP4	2756123	2	c.4959-44del T	81.46	18.02	0.52	0.0953

Appendix Table 5.10: The position and frequency of non-synonymous and synonymous SNPs in the transmembrane region of SmTRPM_{PZQ} (Smp_246790.1).

Amplicon	Position	N ^a	Mutation	Genotype frequencies (%)			Alternate allele frequency (%)
				Homozygous (reference)	Heterozygous	Homozygous alternate	
TRP1	2739021	2	R1375H	96.9	3.1	0	0.02
TRP3	2745579	2	I1464V	99.3	0.7	0	0.05
TRP4	2756264	2	A1685A	98.0	2	0	0.01
TRP4	2756321	2	Q1704Q	97.7	1.7	0.5	0.01

References

1. Website [Internet]. Available from: <https://www.who.int/news-room/fact-sheets/detail/schistosomiasis>
2. World Health Organization. Ending the neglect to attain the Sustainable Development Goals: a strategic framework for integrated control and management of skin-related neglected tropical diseases. World Health Organization; 2022. 112 p.
3. Kincaid-Smith J, Tracey A, de Carvalho Augusto R, Bulla I, Holroyd N, Rognon A, et al. Morphological and genomic characterisation of the *Schistosoma* hybrid infecting humans in Europe reveals admixture between *Schistosoma haematobium* and *Schistosoma bovis*. *PLoS Negl Trop Dis*. 2021 Dec;15(12):e0010062.
4. Colley DG, Bustinduy AL, Evan Secor W, King CH. Human schistosomiasis. *Lancet*. 2014 Jun 28;383(9936):2253–64.
5. Rey O, Toulza E, Chaparro C, Allienne JF, Kincaid-Smith J, Mathieu-Begné E, et al. Diverging patterns of introgression from *Schistosoma bovis* across *S. haematobium* African lineages. *PLoS Pathog*. 2021 Feb 5;17(2):e1009313.
6. Lai YS, Biedermann P, Ekpo UF, Garba A, Mathieu E, Midzi N, et al. Spatial distribution of schistosomiasis and treatment needs in sub-Saharan Africa: a systematic review and geostatistical analysis. *Lancet Infect Dis*. 2015 Aug;15(8):927–40.
7. GBD 2017 DALYs and HALE Collaborators. Global, regional, and national disability-adjusted life-years (DALYs) for 359 diseases and injuries and healthy life expectancy (HALE) for 195 countries and territories, 1990–2017: a systematic analysis for the Global Burden of Disease Study 2017. *Lancet*. 2018 Nov 10;392(10159):1859–922.
8. Chabasse D, Bertrand G, Leroux JP, Gauthey N, Hocquet P. [Developmental bilharziasis caused by *Schistosoma mansoni* discovered 37 years after infestation]. *Bull Soc Pathol Exot Filiales*. 1985;78(5):643–7.
9. Vale N, Gouveia MJ, Rinaldi G, Brindley PJ, Gärtner F, Correia da Costa JM. Praziquantel for Schistosomiasis: Single-Drug Metabolism Revisited, Mode of Action, and Resistance. *Antimicrob Agents Chemother* [Internet]. 2017 May;61(5). Available from: <http://dx.doi.org/10.1128/AAC.02582-16>
10. Gryseels B, Polman K, Clerinx J, Kestens L. Human schistosomiasis. *Lancet*. 2006 Sep 23;368(9541):1106–18.
11. Ross AG, McManus DP, Farrar J, Hunstman RJ, Gray DJ, Li YS. Neuroschistosomiasis. *J Neurol*. 2012 Jan;259(1):22–32.
12. Website [Internet]. Available from: (<https://www.cdc.gov/dpdx/schistosomiasis/index.html>)
13. Attwood SW, Fatih FA, Mondal MMH, Alim MA, Fadjar S, Rajapakse RPVJ, et al. A DNA sequence-based study of the *Schistosoma indicum* (Trematoda: Digenea) group: population phylogeny, taxonomy and historical biogeography. *Parasitology*. 2007 Dec;134(Pt. 14):2009–20.
14. J. C, P. A, Russell J. Out of animals and back again: Schistosomiasis as a zoonosis in Africa. In: *Schistosomiasis*. InTech; 2012.

15. Lawton SP, Hirai H, Ironside JE, Johnston DA, Rollinson D. Genomes and geography: genomic insights into the evolution and phylogeography of the genus *Schistosoma*. *Parasit Vectors*. 2011 Jul 7;4:131.
16. Morgan JA, Dejong RJ, Snyder SD, Mkoji GM, Loker ES. *Schistosoma mansoni* and *Biomphalaria*: past history and future trends. *Parasitology*. 2001;123 Suppl:S211–28.
17. Agatsuma T, Iwagami M, Liu CX, Rajapakse RPVJ, Mondal MMH, Kitikoon V, et al. Affinities between Asian non-human *Schistosoma* species, the *S. indicum* group, and the African human schistosomes. *J Helminthol*. 2002 Mar;76(1):7–19.
18. Webster BL, Southgate VR, Littlewood DTJ. A revision of the interrelationships of *Schistosoma* including the recently described *Schistosoma guineensis*. *Int J Parasitol*. 2006 Jul;36(8):947–55.
19. Morgan JAT, DeJong RJ, Kazibwe F, Mkoji GM, Loker ES. A newly-identified lineage of *Schistosoma*. *Int J Parasitol*. 2003 Aug;33(9):977–85.
20. Snyder SD, Loker ES. Evolutionary relationships among the Schistosomatidae (Platyhelminthes: Digenea) and an Asian origin for *Schistosoma*. *J Parasitol*. 2000 Apr;86(2):283–8.
21. Kane RA, Southgate VR, Rollinson D, Littlewood DTJ, Lockyer AE, Pagès JR, et al. A phylogeny based on three mitochondrial genes supports the division of *Schistosoma intercalatum* into two separate species. *Parasitology*. 2003 Aug;127(Pt 2):131–7.
22. Lockyer AE, Olson PD, Ostergaard P, Rollinson D, Johnston DA, Attwood SW, et al. The phylogeny of the Schistosomatidae based on three genes with emphasis on the interrelationships of *Schistosoma Weinland*, 1858. *Parasitology*. 2003 Mar;126(Pt 3):203–24.
23. Agatsuma T. Origin and evolution of *Schistosoma japonicum*. *Parasitol Int*. 2003 Dec;52(4):335–40.
24. Attwood SW, Panasoponkul C, Upatham ES, Meng XH, Southgate VR. *Schistosoma ovuncatum* n. sp. (Digenea: Schistosomatidae) from northwest Thailand and the historical biogeography of Southeast Asian *Schistosoma Weinland*, 1858. *Syst Parasitol*. 2002 Jan;51(1):1–19.
25. McManus DP, Dunne DW, Sacko M, Utzinger J, Vennervald BJ, Zhou XN. Schistosomiasis. *Nature Reviews Disease Primers*. 2018 Aug 9;4(1):1–19.
26. Website [Internet]. Available from: <https://www.who.int/news-room/fact-sheets/detail/schistosomiasis>
27. Schistosomiasis [Internet]. 2019 [cited 2024 Feb 2]. Available from: <https://www.cdc.gov/dpdx/schistosomiasis/index.html>
28. Pearce EJ, MacDonald AS. The immunobiology of schistosomiasis. *Nat Rev Immunol*. 2002 Jul;2(7):499–511.
29. Fairfax K, Nascimento M, Huang SCC, Everts B, Pearce EJ. Th2 responses in schistosomiasis. *Semin Immunopathol*. 2012 Nov;34(6):863–71.
30. Olds GR, Dasarthy S. Recent Advances in Schistosomiasis. *Curr Infect Dis Rep*. 2001 Feb;3(1):59–67.

31. Ross AG, Vickers D, Olds GR, Shah SM, McManus DP. Katayama syndrome. *Lancet Infect Dis.* 2007 Mar;7(3):218–24.
32. Aula OP, McManus DP, Jones MK, Gordon CA. Schistosomiasis with a Focus on Africa. *Tropical Medicine and Infectious Disease.* 2021 Jun 22;6(3):109.
33. Cheever AW, Kamel IA, Elwi AM, Mosimann JE, Danner R, Sippel JE. *Schistosoma mansoni* and *S. haematobium* infections in Egypt. III. Extrahepatic pathology. *Am J Trop Med Hyg.* 1978 Jan;27(1 Pt 1):55–75.
34. Cheever AW. A quantitative post-mortem study of *Schistosomiasis mansoni* in man. *Am J Trop Med Hyg.* 1968 Jan;17(1):38–64.
35. Mohamed AR, al Karawi M, Yasawy MI. Schistosomal colonic disease. *Gut.* 1990 Apr;31(4):439–42.
36. Gryseels B, Polderman AM. Morbidity, due to schistosomiasis mansoni, and its control in Sub-Saharan Africa. *Parasitol Today.* 1991 Sep;7(9):244–8.
37. Gryseels B. Morbidity due to infection with *Schistosoma mansoni*: an update. *Trop Geogr Med.* 1992 Jul;44(3):189–200.
38. Homeida M, Ahmed S, Dafalla A, Suliman S, Eltom I, Nash T, et al. Morbidity associated with *Schistosoma mansoni* infection as determined by ultrasound: a study in Gezira, Sudan. *Am J Trop Med Hyg.* 1988 Aug;39(2):196–201.
39. Dessein AJ, Hillaire D, Elwali NE, Marquet S, Mohamed-Ali Q, Mirghani A, et al. Severe hepatic fibrosis in *Schistosoma mansoni* infection is controlled by a major locus that is closely linked to the interferon-gamma receptor gene. *Am J Hum Genet.* 1999 Sep;65(3):709–21.
40. Chen MG, Mott KE. Progress in Assessment of Morbidity Due to Schistosomiasis: Reviews of Recent Literature. 1989. 56 p.
41. Gryseels B. The relevance of schistosomiasis for public health. *Trop Med Parasitol.* 1989 Jun;40(2):134–42.
42. Schwartz DA. Helminths in the induction of cancer II. *Schistosoma haematobium* and bladder cancer. *Trop Geogr Med.* 1981 Mar;33(1):1–7.
43. Wamachi AN, Mayadev JS, Mungai PL, Magak PL, Ouma JH, Magambo JK, et al. Increased ratio of tumor necrosis factor- α to interleukin-10 production is associated with *Schistosoma haematobium*-induced urinary-tract morbidity. *J Infect Dis.* 2004 Dec 1;190(11):2020–30.
44. Bustinduy AL, Randriansolo B, Sturt AS, Kayuni SA, Leustcher PDC, Webster BL, et al. An update on female and male genital schistosomiasis and a call to integrate efforts to escalate diagnosis, treatment and awareness in endemic and non-endemic settings: The time is now. *Adv Parasitol.* 2022 Feb 17;115:1–44.
45. Sturt AS, Webb EL, Phiri CR, Mweene T, Chola N, van Dam GJ, et al. Genital self-sampling compared with cervicovaginal lavage for the diagnosis of female genital schistosomiasis in Zambian women: The BILHIV study. *PLoS Negl Trop Dis.* 2020 Jul;14(7):e0008337.
46. Sturt AS, Webb EL, Francis SC, Hayes RJ, Bustinduy AL. Beyond the barrier: Female Genital Schistosomiasis as a potential risk factor for HIV-1 acquisition. *Acta Trop.* 2020

Sep;209(105524):105524.

47. Rafferty H, Sturt AS, Phiri CR, Webb EL, Mudenda M, Mapani J, et al. Association between cervical dysplasia and female genital schistosomiasis diagnosed by genital PCR in Zambian women. *BMC Infect Dis.* 2021 Jul 17;21(1):691.
48. McCullough FS, Gayral P, Duncan J, Christie JD. Molluscicides in schistosomiasis control. *Bull World Health Organ.* 1980;58(5):681–9.
49. WHO guideline on control and elimination of human schistosomiasis. World Health Organization; 2022. 144 p.
50. Yang GJ, Sun LP, Hong QB, Zhu HR, Yang K, Gao Q, et al. Optimizing molluscicide treatment strategies in different control stages of schistosomiasis in the People's Republic of China. *Parasit Vectors.* 2012 Nov 14;5:260.
51. Tanaka H, Tsuji M. From discovery to eradication of schistosomiasis in Japan: 1847-1996. *Int J Parasitol.* 1997 Dec;27(12):1465–80.
52. Rollinson D, Knopp S, Levitz S, Stothard JR, Tchuem Tchuenté LA, Garba A, et al. Time to set the agenda for schistosomiasis elimination. *Acta Trop.* 2013 Nov;128(2):423–40.
53. Ekabo OA, Farnsworth NR, Henderson TO, Mao G, Mukherjee R. Antifungal and molluscicidal saponins from *Serjania salzmanniana*. *J Nat Prod.* 1996 Apr;59(4):431–5.
54. Assessment of toxicity of *Moringa oleifera* flower extract to *Biomphalaria glabrata*, *Schistosoma mansoni* and *Artemia salina*. *Chemosphere.* 2015 Aug 1;132:188–92.
55. Grimes JET, Croll D, Harrison WE, Utzinger J, Freeman MC, Templeton MR. The roles of water, sanitation and hygiene in reducing schistosomiasis: a review. *Parasit Vectors.* 2015 Mar 13;8(1):1–16.
56. Esrey SA, Potash JB, Roberts L, Shiff C. Effects of improved water supply and sanitation on ascariasis, diarrhoea, dracunculiasis, hookworm infection, schistosomiasis, and trachoma. *Bull World Health Organ.* 1991;69(5):609–21.
57. Helminth control in school-age children: a guide for managers of control programmes -- Second edition [Internet]. World Health Organization; 2011 [cited 2024 Feb 18]. Available from: <https://www.who.int/publications/i/item/9789241548267>
58. Aagaard-Hansen J, Mwangi JR, Bruun B. Social science perspectives on schistosomiasis control in Africa: past trends and future directions. *Parasitology.* 2009 Nov;136(13):1747–58.
59. Cioli D, Pica-Mattoccia L, Archer S. Antischistosomal drugs: past, present ... and future? *Pharmacol Ther.* 1995;68(1):35–85.
60. Bustinduy AL, Wright S, Joekes EC, Kabatereine NB, Reinhard-Rupp J, King CH, et al. One hundred years of neglect in paediatric schistosomiasis. *Parasitology.* 2017 Oct;144(12):1613–23.
61. Christopherson JB. Intravenous injections of antimony tartaratum in bilharziosis. *Br Med J.* 1918 Dec 14;2(3024):652–3.
62. Jordan P. From katayama to the Dakhla Oasis: the beginning of epidemiology and control of bilharzia. *Acta Trop.* 2000 Oct 23;77(1):9–40.

63. Cioli D, Knopf PM. A study of the mode of action of hycanthonne against *Schistosoma mansoni* in vivo and in vitro. *Am J Trop Med Hyg.* 1980 Mar;29(2):220–6.
64. Rosi D, Peruzzotti G, Dennis EW, Berberian DA, Freele H, Archer S. A New, Active Metabolite of “Miracil D.” *Nature.* 1965 Dec;208(5014):1005–6.
65. Davis A. Antischistosomal drugs and clinical practice. 1993; Available from: <https://www.cabidigitallibrary.org/doi/full/10.5555/19940801348>
66. Coura JR, Amaral RS. Epidemiological and control aspects of schistosomiasis in Brazilian endemic areas. *Mem Inst Oswaldo Cruz.* 2004 Oct 13;99(5 Suppl 1):13–9.
67. Foster R. A review of clinical experience with oxamniquine. *Trans R Soc Trop Med Hyg.* 1987;81(1):55–9.
68. Pica-Mattoccia L, Dias LC, Cioli D. Genetic complementation analysis of two independently isolated hycanthonne-resistant strains of *Schistosoma mansoni*. *Mem Inst Oswaldo Cruz.* 1992;87 Suppl 4:211–4.
69. Cioli D, Pica-Mattoccia L, Moroni R. *Schistosoma mansoni*: hycanthonne/oxamniquine resistance is controlled by a single autosomal recessive gene. *Exp Parasitol.* 1992 Dec;75(4):425–32.
70. Cioli D, Pica-Mattoccia L, Archer S. Resistance of schistosomes to hycanthonne and oxamniquine. *Mem Inst Oswaldo Cruz.* 1989 Oct;84 Suppl 1:38–45.
71. Groll E. Praziquantel. Garattini S, Goldin A, Hawking F, Kopin IJ, Schnitzer RJ, editors. *Adv Pharmacol Chemother.* 1984;20:219–38.
72. Gönner R, Andrews P. Praziquantel, a new broad-spectrum antischistosomal agent. *Z Parasitenkd.* 1977 Jul 21;52(2):129–50.
73. Froberg H, Schulze Schencking M. Toxicological profile of praziquantel, a new drug against cestode and schistosome infections, as compared to some other schistosomicides. *Arzneimittelforschung.* 1981;31(3a):555–65.
74. Davis A, Wegner DH. Multicentre trials of praziquantel in human schistosomiasis: design and techniques. *Bull World Health Organ.* 1979;57(5):767–71.
75. Froberg H. Results of toxicological studies on praziquantel. *Arzneimittelforschung.* 1984;34(9B):1137–44.
76. Rugel AR, Guzman MA, Taylor AB, Chevalier FD, Tarpley RS, McHardy SF, et al. Why does oxamniquine kill *Schistosoma mansoni* and not *S. haematobium* and *S. japonicum*? *Int J Parasitol Drugs Drug Resist.* 2020 Aug;13:8–15.
77. da Rocha Pitta MG, da Rocha Pitta MG, de Melo Rêgo MJB, Galdino SL. The evolution of drugs on schistosoma treatment: looking to the past to improve the future. *Mini Rev Med Chem.* 2013 Apr;13(4):493–508.
78. Davis A, Biles JE, Ulrich AM. Initial experiences with praziquantel in the treatment of human infections due to *Schistosoma haematobium*. *Bull World Health Organ.* 1979;57(5):773–9.
79. King CH, Muchiri EM, Mungai P, Ouma JH, Kadzo H, Magak P, et al. Randomized comparison of low-dose versus standard-dose praziquantel therapy in treatment of urinary tract morbidity due to *Schistosoma haematobium* infection. *Am J Trop Med Hyg.*

2002 Jun;66(6):725–30.

80. Bustinduy AL, Waterhouse D, de Sousa-Figueiredo JC, Roberts SA, Atuhaire A, Van Dam GJ, et al. Population Pharmacokinetics and Pharmacodynamics of Praziquantel in Ugandan Children with Intestinal Schistosomiasis: Higher Dosages Are Required for Maximal Efficacy. *MBio* [Internet]. 2016 Aug 9;7(4). Available from: <http://dx.doi.org/10.1128/mBio.00227-16>
81. Doenhoff MJ, Hagan P, Cioli D, Southgate V, Pica-Mattoccia L, Botros S, et al. Praziquantel: its use in control of schistosomiasis in sub-Saharan Africa and current research needs. *Parasitology*. 2009 Nov;136(13):1825–35.
82. Kokaliaris C, Garba A, Matuska M, Bronzan RN, Colley DG, Dorkenoo AM, et al. Effect of preventive chemotherapy with praziquantel on schistosomiasis among school-aged children in sub-Saharan Africa: a spatiotemporal modelling study. *Lancet Infect Dis*. 2022 Jan;22(1):136–49.
83. Fenwick A, Webster JP, Bosque-Oliva E, Blair L, Fleming FM, Zhang Y, et al. The Schistosomiasis Control Initiative (SCI): rationale, development and implementation from 2002-2008. *Parasitology*. 2009 Nov;136(13):1719–30.
84. Webster JP, Koukounari A, Lamberton PHL, Stothard JR, Fenwick A. Evaluation and application of potential schistosome-associated morbidity markers within large-scale mass chemotherapy programmes. *Parasitology*. 2009 Nov;136(13):1789–99.
85. Koukounari A, Fenwick A, Whawell S, Kabatereine NB, Kazibwe F, Tukahebwa EM, et al. Morbidity indicators of *Schistosoma mansoni*: relationship between infection and anemia in Ugandan schoolchildren before and after praziquantel and albendazole chemotherapy. *Am J Trop Med Hyg*. 2006;75(2):278–86.
86. Koukounari A, Gabrielli AF, Toure S, Bosque-Oliva E, Zhang Y, Sellin B, et al. *Schistosoma haematobium* infection and morbidity before and after large-scale administration of praziquantel in Burkina Faso. *J Infect Dis*. 2007 Sep 1;196(5):659–69.
87. Summary of global update on preventive chemotherapy implementation in 2015. *Wkly Epidemiol Rec*. 2016 Sep 30;91(39):456–9.
88. Mazigo HD. Participatory integrated control strategies and elimination of schistosomiasis in sub-Saharan Africa. *Lancet Glob Health*. 2019 Aug;7(8):e998–9.
89. World Health Organisation. Report of a meeting to review the results of studies on the treatment of schistosomiasis in preschool-age children. In 2010 [cited 2024 Aug 30]. Available from: https://apps.who.int/iris/bitstream/handle/10665/44639/9789241501880_eng.pdf
90. Helminthiasis ST. Prevention and control of schistosomiasis and soil-transmitted helminthiasis : report of a WHO expert committee. 2002;
91. Jordan P, Webbe G, Sturrock RF. *Human Schistosomiasis*. Oxford University Press, USA; 1993. 486 p.
92. Mutapi F. Changing policy and practice in the control of pediatric schistosomiasis. *Pediatrics*. 2015 Mar;135(3):536–44.
93. Stothard JR, Sousa-Figueiredo JC de, Betson M, Adriko M, Arinaitwe M, Rowell C, et al. *Schistosoma mansoni* Infections in young children: when are schistosome antigens in

- urine, eggs in stool and antibodies to eggs first detectable? *PLoS Negl Trop Dis*. 2011 Jan 4;5(1):e938.
94. Stothard JR, Gabrielli AF. Schistosomiasis in African infants and preschool children: to treat or not to treat? *Trends Parasitol*. 2007 Mar;23(3):83–6.
 95. Stothard JR, Sousa-Figueiredo JC, Betson M, Bustinduy A, Reinhard-Rupp J. Schistosomiasis in African infants and preschool children: let them now be treated! *Trends Parasitol*. 2013 Apr;29(4):197–205.
 96. The pediatric praziquantel consortium [Internet]. [cited 2024 Aug 30]. Available from: <https://www.pediatricpraziquantelconsortium.org/>
 97. Sousa-Figueiredo JC, Pleasant J, Day M, Betson M, Rollinson D, Montresor A, et al. Treatment of intestinal schistosomiasis in Ugandan preschool children: best diagnosis, treatment efficacy and side-effects, and an extended praziquantel dosing pole. *Int Health*. 2010 Jun;2(2):103–13.
 98. Elgharably A, Gomaa AI, Crossey MM, Norsworthy PJ, Waked I, Taylor-Robinson SD. Hepatitis C in Egypt - past, present, and future. *Int J Gen Med*. 2017;10:1–6.
 99. WHO guideline on control and elimination of human schistosomiasis. Geneva: World Health Organization; 2022.
 100. Díaz AV, Walker M, Webster JP. Reaching the World Health Organization elimination targets for schistosomiasis: the importance of a One Health perspective. *Philos Trans R Soc Lond B Biol Sci*. 2023 Oct 9;378(1887):20220274.
 101. Odogwu SE, Ramamurthy NK, Kabatereine NB, Kazibwe F, Tukahebwa E, Webster JP, et al. *Schistosoma mansoni* in infants (aged < 3 years) along the Ugandan shoreline of Lake Victoria. *Ann Trop Med Parasitol*. 2006 Jun;100(4):315–26.
 102. Sousa-Figueiredo JC, Betson M, Atuhaire A, Arinaitwe M, Navaratnam AMD, Kabatereine NB, et al. Performance and safety of praziquantel for treatment of intestinal schistosomiasis in infants and preschool children. *PLoS Negl Trop Dis*. 2012 Oct 18;6(10):e1864.
 103. Mandour ME, el Turabi H, Homeida MM, el Sadig T, Ali HM, Bennett JL, et al. Pharmacokinetics of praziquantel in healthy volunteers and patients with schistosomiasis. *Trans R Soc Trop Med Hyg*. 1990 May;84(3):389–93.
 104. el Guiniady MA, el Touny MA, Abdel-Bary MA, Abdel-Fatah SA, Metwally A. Clinical and pharmacokinetic study of praziquantel in Egyptian schistosomiasis patients with and without liver cell failure. *Am J Trop Med Hyg*. 1994 Dec;51(6):809–18.
 105. Olliaro P, Delgado-Romero P, Keiser J. The little we know about the pharmacokinetics and pharmacodynamics of praziquantel (racemate and R-enantiomer). *J Antimicrob Chemother*. 2014 Apr;69(4):863–70.
 106. Park SK, Gunaratne GS, Chulkov EG, Moehring F, McCusker P, Dosa PI, et al. The anthelmintic drug praziquantel activates a schistosome transient receptor potential channel. *J Biol Chem*. 2019 Dec 6;294(49):18873–80.
 107. Doenhoff MJ, Cioli D, Utzinger J. Praziquantel: mechanisms of action, resistance and new derivatives for schistosomiasis. *Curr Opin Infect Dis*. 2008 Dec;21(6):659–67.
 108. Brindley PJ, Sher A. The chemotherapeutic effect of praziquantel against *Schistosoma*

- mansoni is dependent on host antibody response. *J Immunol.* 1987 Jul 1;139(1):215–20.
109. Cavalcanti MG, Cunha AFA, Peralta JM. The advances in molecular and New Point-of-care (POC) diagnosis of schistosomiasis pre- and post-praziquantel use: In the pursuit of more reliable approaches for low endemic and non-endemic areas. *Front Immunol.* 2019 May 28;10:858.
110. Kittur N, Castleman JD, Campbell CH, King CH, Colley DG. Comparison of *Schistosoma mansoni* prevalence and intensity of infection, as determined by the circulating cathodic antigen urine assay or by the Kato-Katz fecal assay: A systematic review. *Am J Trop Med Hyg.* 2016 Mar;94(3):605–10.
111. Corstjens PLAM, de Dood CJ, Knopp S, Clements MN, Ortu G, Umulisa I, et al. Circulating anodic antigen (CAA): A highly sensitive diagnostic biomarker to detect active *Schistosoma* infections-improvement and use during SCORE. *Am J Trop Med Hyg.* 2020 Jul;103(1_Suppl):50–7.
112. Edition 5th. need to know about ADME [Internet]. Available from: https://www.evotec.com/uploads/download-files/Downloadable_Publications/Cyprotex-Guides/Cyprotex-ADME-Guide-5th-Edition.pdf
113. Castro N, Medina R, Sotelo J, Jung H. Bioavailability of praziquantel increases with concomitant administration of food. *Antimicrob Agents Chemother.* 2000 Oct;44(10):2903–4.
114. Andrews P, Thomas H, Pohlke R, Seubert J. Praziquantel. *Med Res Rev.* 1983 Apr;3(2):147–200.
115. Kabatereine NB, Kemijumbi J, Ouma JH, Kariuki HC, Richter J, Kadzo H, et al. Epidemiology and morbidity of *Schistosoma mansoni* infection in a fishing community along Lake Albert in Uganda. *Trans R Soc Trop Med Hyg.* 2004 Dec;98(12):711–8.
116. Bustinduy AL, Sousa-Figueiredo JC, Adriko M, Betson M, Fenwick A, Kabatereine N, et al. Fecal occult blood and fecal calprotectin as point-of-care markers of intestinal morbidity in Ugandan children with *Schistosoma mansoni* infection. *PLoS Negl Trop Dis.* 2013 Nov;7(11):e2542.
117. Leopold G, Ungethüm W, Groll E, Diekmann HW, Nowak H, Wegner DH. Clinical pharmacology in normal volunteers of praziquantel, a new drug against schistosomes and cestodes. An example of a complex study covering both tolerance and pharmacokinetics. *Eur J Clin Pharmacol.* 1978 Dec 1;14(4):281–91.
118. Webb EL, Edielu A, Wu HW, Kabatereine NB, Tukahebwa EM, Mubangizi A, et al. The praziquantel in preschoolers (PIP) trial: study protocol for a phase II PK/PD-driven randomised controlled trial of praziquantel in children under 4 years of age. *Trials.* 2021 Sep 6;22(1):601.
119. Katz N, Chaves A, Pellegrino J. A simple device for quantitative stool thick-smear technique in *Schistosomiasis mansoni*. *Rev Inst Med Trop Sao Paulo.* 1972 Nov-Dec;14(6):397–400.
120. World Health Organization. Preventive Chemotherapy in Human Helminthiasis: Coordinated Use of Anthelmintic Drugs in Control Interventions : a Manual for Health Professionals and Programme Managers. World Health Organization; 2006. 62 p.

121. Organization WH, Others. Assessing the efficacy of anthelmintic drugs against schistosomiasis and soil-transmitted helminthiases. 2013; Available from: https://apps.who.int/iris/bitstream/handle/10665/79019/9789241564557_eng.pdf
122. Casacuberta-Partal M, Hoekstra PT, Kornelis D, van Lieshout L, van Dam GJ. An innovative and user-friendly scoring system for standardised quantitative interpretation of the urine-based point-of-care strip test (POC-CCA) for the diagnosis of intestinal schistosomiasis: a proof-of-concept study. *Acta Trop*. 2019 Nov;199:105150.
123. Corstjens PLAM, De Dood CJ, Kornelis D, Fat EMTK, Wilson RA, Kariuki TM, et al. Tools for diagnosis, monitoring and screening of *Schistosoma* infections utilizing lateral-flow based assays and upconverting phosphor labels. *Parasitology*. 2014 Dec;141(14):1841–55.
124. Yoshida K, Bartel A. Tableone: create “table 1” to describe baseline characteristics with or without propensity score weights, version 0.13. 2, R studio package. Inc : Vienna, Austria. 2022;
125. Team RC. R: A language and environment for statistical computing. R Foundation for Statistical Computing. (No Title) [Internet]. 2013; Available from: <https://cir.nii.ac.jp/crid/1370857669939307264>
126. Sabah AA, Fletcher C, Webbe G, Doenhoff MJ. *Schistosoma mansoni*: chemotherapy of infections of different ages. *Exp Parasitol*. 1986 Jun;61(3):294–303.
127. Cioli D, Pica-Mattoccia L, Basso A, Guidi A. Schistosomiasis control: praziquantel forever? *Mol Biochem Parasitol*. 2014 Jun;195(1):23–9.
128. Lamberton PHL, Kabatereine NB, Oguttu DW, Fenwick A, Webster JP. Sensitivity and specificity of multiple Kato-Katz thick smears and a circulating cathodic antigen test for *Schistosoma mansoni* diagnosis pre- and post-repeated-praziquantel treatment. *PLoS Negl Trop Dis*. 2014 Sep;8(9):e3139.
129. Casacuberta-Partal M, Beenakker M, de Dood CJ, Hoekstra PT, Kroon L, Kornelis D, et al. Specificity of the Point-of-care urine strip test for *Schistosoma* circulating cathodic antigen (POC-CCA) tested in non-endemic pregnant women and young children. *Am J Trop Med Hyg*. 2021 Feb 1;104(4):1412–7.
130. Peralta JM, Cavalcanti MG. Is POC-CCA a truly reliable test for schistosomiasis diagnosis in low endemic areas? The trace results controversy. *PLoS Negl Trop Dis*. 2018 Nov;12(11):e0006813.
131. Bärenbold O, Garba A, Colley DG, Fleming FM, Haggag AA, Ramzy RMR, et al. Translating preventive chemotherapy prevalence thresholds for *Schistosoma mansoni* from the Kato-Katz technique into the point-of-care circulating cathodic antigen diagnostic test. *PLoS Negl Trop Dis*. 2018 Dec;12(12):e0006941.
132. Clark J, Moses A, Nankasi A, Faust CL, Adriko M, Ajambo D, et al. Translating from egg- to antigen-based indicators for *Schistosoma mansoni* elimination targets: A Bayesian latent class analysis study. *Front Trop Dis*. 2022 Feb 18;3:825721.
133. Clark J, Moses A, Nankasi A, Faust CL, Moses A, Ajambo D, et al. Reconciling egg- and antigen-based estimates of *Schistosoma mansoni* clearance and reinfection: A modeling study. *Clin Infect Dis*. 2022 May 3;74(9):1557–63.
134. Colley DG, King CH, Kittur N, Ramzy RMR, Secor WE, Fredericks-James M, et al.

- Evaluation, validation, and recognition of the Point-of-care circulating cathodic antigen, urine-based assay for mapping *Schistosoma mansoni* infections. *Am J Trop Med Hyg.* 2020 Jul;103(1_Suppl):42–9.
135. Colley DG, Ramzy RMR, Maganga J, Kinung’hi S, Odiero MR, Musuva RM, et al. The POC-CCA assay for detection of *Schistosoma mansoni* infection needs standardization in production and proper quality control to be reliable. *Acta Trop.* 2023 Feb;238(106795):106795.
136. Viana AG, Gazzinelli-Guimarães PH, Castro VN de, Santos YL de OD, Ruas ACL, Bezerra FS de M, et al. Discrepancy between batches and impact on the sensitivity of point-of-care circulating cathodic antigen tests for *Schistosoma mansoni* infection. *Acta Trop.* 2019 Sep;197(105049):105049.
137. van Lieshout L, de Jonge N, Bassily S, Mansour MM, Deelder AM. Assessment of cure in schistosomiasis patients after chemotherapy with praziquantel by quantitation of circulating anodic antigen (CAA) in urine. *Am J Trop Med Hyg.* 1991 Mar;44(3):323–8.
138. Knopp S, Corstjens PLAM, Koukounari A, Cercamondi CI, Ame SM, Ali SM, et al. Sensitivity and specificity of a urine circulating anodic antigen test for the diagnosis of *Schistosoma haematobium* in low endemic settings. *PLoS Negl Trop Dis.* 2015 May;9(5):e0003752.
139. van Dam GJ, Odermatt P, Acosta L, Bergquist R, de Dood CJ, Cornelis D, et al. Evaluation of banked urine samples for the detection of circulating anodic and cathodic antigens in *Schistosoma mekongi* and *S. japonicum* infections: a proof-of-concept study. *Acta Trop.* 2015 Jan;141(Pt B):198–203.
140. van Dam GJ, Xu J, Bergquist R, de Dood CJ, Utzinger J, Qin ZQ, et al. An ultra-sensitive assay targeting the circulating anodic antigen for the diagnosis of *Schistosoma japonicum* in a low-endemic area, People’s Republic of China. *Acta Trop.* 2015 Jan;141(Pt B):190–7.
141. Vonghachack Y, Sayasone S, Khieu V, Bergquist R, van Dam GJ, Hoekstra PT, et al. Comparison of novel and standard diagnostic tools for the detection of *Schistosoma mekongi* infection in Lao People’s Democratic Republic and Cambodia. *Infect Dis Poverty.* 2017 Aug 10;6(1):127.
142. Clements MN, Corstjens PLAM, Binder S, Campbell CH Jr, de Dood CJ, Fenwick A, et al. Latent class analysis to evaluate performance of point-of-care CCA for low-intensity *Schistosoma mansoni* infections in Burundi. *Parasit Vectors.* 2018 Feb 23;11(1):111.
143. Weerakoon KGAD, Gobert GN, Cai P, McManus DP. Advances in the diagnosis of human schistosomiasis. *Clin Microbiol Rev.* 2015 Oct;28(4):939–67.
144. Plaisier AP, Alley ES, Boatman BA, Van Oortmarssen GJ, Remme H, De Vlas SJ, et al. Irreversible effects of ivermectin on adult parasites in onchocerciasis patients in the Onchocerciasis Control Programme in West Africa. *J Infect Dis.* 1995 Jul;172(1):204–10.
145. Kim JS, Oh DS, Ahn KS, Shin SS. Effects of kimchi extract and temperature on embryostasis of *Ascaris suum* eggs. *Korean J Parasitol.* 2012 Mar;50(1):83–7.
146. Utzinger J, Booth M, N’Goran EK, Müller I, Tanner M, Lengeler C. Relative contribution of day-to-day and intra-specimen variation in faecal egg counts of *Schistosoma mansoni* before and after treatment with praziquantel. *Parasitology.* 2001 May;122(Pt 5):537–44.

147. Engels D, Sinzinkayo E, Gryseels B. Day-to-day egg count fluctuation in *Schistosoma mansoni* infection and its operational implications. *Am J Trop Med Hyg.* 1996 Apr;54(4):319–24.
148. Colley DG, Andros TS, Campbell CH Jr. Schistosomiasis is more prevalent than previously thought: what does it mean for public health goals, policies, strategies, guidelines and intervention programs? *Infect Dis Poverty.* 2017 Mar 22;6(1):63.
149. Haggag AA, Rabiee A, Abd Elaziz KM, Campbell CH, Colley DG, Ramzy RMR. Thirty-day daily comparisons of Kato-Katz and CCA assays of 45 Egyptian children in areas with very low prevalence of *Schistosoma mansoni*. *Am J Trop Med Hyg.* 2019 Mar;100(3):578–83.
150. Crellen T, Allan F, David S, Durrant C, Huckvale T, Holroyd N, et al. Whole genome resequencing of the human parasite *Schistosoma mansoni* reveals population history and effects of selection. *Sci Rep.* 2016 Feb 16;6:20954.
151. Vianney TJ, Berger DJ, Doyle SR, Sankaranarayanan G, Serubanja J, Nakawungu PK, et al. Genome-wide analysis of *Schistosoma mansoni* reveals limited population structure and possible praziquantel drug selection pressure within Ugandan hot-spot communities. *PLoS Negl Trop Dis.* 2022 Aug;16(8):e0010188.
152. Berger DJ, Crellen T, Lamberton PHL, Allan F, Tracey A, Noonan JD, et al. Whole-genome sequencing of *Schistosoma mansoni* reveals extensive diversity with limited selection despite mass drug administration. *Nat Commun.* 2021 Aug 6;12(1):4776.
153. Berger DJ, Park SK, Crellen T, Vianney TJ, Kabatereine NB, Cotton JA, et al. Extensive transmission and variation in a functional receptor for praziquantel resistance in endemic *Schistosoma mansoni* [Internet]. *bioRxiv.* 2024. p. 2024.08.29.610291. Available from: <https://www.biorxiv.org/content/10.1101/2024.08.29.610291v1>
154. Gower CM, Gouvras AN, Lamberton PHL, Deol A, Shrivastava J, Mutombo PN, et al. Population genetic structure of *Schistosoma mansoni* and *Schistosoma haematobium* from across six sub-Saharan African countries: implications for epidemiology, evolution and control. *Acta Trop.* 2013 Nov;128(2):261–74.
155. Berger DJ, Léger E, Sankaranarayanan G, Sène M, Diouf ND, Rabone M, et al. Genomic evidence of contemporary hybridization between *Schistosoma* species. *PLoS Pathog.* 2022 Aug;18(8):e1010706.
156. Djuikwo-Teukeng FF, Kouam Simo A, Allienne JF, Rey O, Njyou Ngapagna A, Tchuem-Tchuente LA, et al. Population genetic structure of *Schistosoma bovis* in Cameroon. *Parasit Vectors.* 2019 Jan 24;12(1):56.
157. Angora EK, Allienne JF, Rey O, Menan H, Touré AO, Coulibaly JT, et al. High prevalence of *Schistosoma haematobium* × *Schistosoma bovis* hybrids in schoolchildren in Côte d'Ivoire. *Parasitology.* 2020 Mar;147(3):287–94.
158. Angora EK, Vangraefschepe A, Allienne JF, Menan H, Coulibaly JT, Meité A, et al. Population genetic structure of *Schistosoma haematobium* and *Schistosoma haematobium* × *Schistosoma bovis* hybrids among school-aged children in Côte d'Ivoire. *Parasite.* 2022 May 3;29:23.
159. Van den Broeck F, Maes GE, Larmuseau MHD, Rollinson D, Sy I, Faye D, et al. Reconstructing Colonization Dynamics of the Human Parasite *Schistosoma mansoni*

- following Anthropogenic Environmental Changes in Northwest Senegal. *PLoS Negl Trop Dis*. 2015 Aug;9(8):e0003998.
160. Webster BL, Webster JP, Gouvras AN, Garba A, Lamine MS, Diaw OT, et al. DNA “barcoding” of *Schistosoma mansoni* across sub-Saharan Africa supports substantial within locality diversity and geographical separation of genotypes. *Acta Trop*. 2013 Nov;128(2):250–60.
 161. Betson M, Sousa-Figueiredo JC, Kabatereine NB, Stothard JR. New insights into the molecular epidemiology and population genetics of *Schistosoma mansoni* in Ugandan pre-school children and mothers. *PLoS Negl Trop Dis*. 2013 Dec 12;7(12):e2561.
 162. Curtis J, Sorensen RE, Page LK, Minchella DJ. Microsatellite loci in the human blood fluke *Schistosoma mansoni* and their utility for other schistosome species: PRIMER NOTE. *Mol Ecol Notes*. 2001 Sep;1(3):143–5.
 163. Durand P, Sire C, Théron A. Isolation of microsatellite markers in the digenetic trematode *Schistosoma mansoni* from Guadeloupe island. *Mol Ecol*. 2000 Jul;9(7):997–8.
 164. Golan R, Gower CM, Emery AM, Rollinson D, Webster JP. Isolation and characterization of the first polymorphic microsatellite markers for *Schistosoma haematobium* and their application in multiplex reactions of larval stages. *Mol Ecol Resour*. 2008 May;8(3):647–9.
 165. Stothard JR, Webster BL, Weber T, Nyakaana S, Webster JP, Kazibwe F, et al. Molecular epidemiology of *Schistosoma mansoni* in Uganda: DNA barcoding reveals substantial genetic diversity within Lake Albert and Lake Victoria populations. *Parasitology*. 2009 Nov;136(13):1813–24.
 166. Morgan JAT, Dejong RJ, Adeoye GO, Ansa EDO, Barbosa CS, Brémond P, et al. Origin and diversification of the human parasite *Schistosoma mansoni*: PHYLOGEOGRAPHY OF *SCHISTOSOMA MANSONI*. *Mol Ecol*. 2005 Oct;14(12):3889–902.
 167. Platt RN 2nd, Le Clerc’h W, Chevalier FD, McDew-White M, LoVerde PT, Ramiro de Assis R, et al. Genomic analysis of a parasite invasion: Colonization of the Americas by the blood fluke *Schistosoma mansoni*. *Mol Ecol*. 2022 Apr;31(8):2242–63.
 168. Agola LE, Steinauer ML, Mburu DN, Mungai BN, Mwangi IN, Magoma GN, et al. Genetic diversity and population structure of *Schistosoma mansoni* within human infrapopulations in Mwea, central Kenya assessed by microsatellite markers. *Acta Trop*. 2009 Sep;111(3):219–25.
 169. Steinauer ML, Hanelt B, Agola LE, Mkoji GM, Loker ES. Genetic structure of *Schistosoma mansoni* in western Kenya: The effects of geography and host sharing. *Int J Parasitol*. 2009 Oct;39(12):1353–62.
 170. Van den Broeck F, Meurs L, Raeymaekers JAM, Boon N, Dieye TN, Volckaert FAM, et al. Inbreeding within human *Schistosoma mansoni*: do host-specific factors shape the genetic composition of parasite populations? *Heredity (Edinb)*. 2014 Jul;113(1):32–41.
 171. Huyse T, Van den Broeck F, Jombart T, Webster BL, Diaw O, Volckaert FAM, et al. Regular treatments of praziquantel do not impact on the genetic make-up of *Schistosoma mansoni* in Northern Senegal. *Infect Genet Evol*. 2013 Aug;18:100–5.
 172. Rey O, Webster BL, Huyse T, Rollinson D, Van den Broeck F, Kincaid-Smith J, et al.

- Population genetics of African *Schistosoma* species. *Infect Genet Evol.* 2021 Apr;89:104727.
173. Ending the neglect to attain the Sustainable Development Goals: A road map for neglected tropical diseases 2021–2030 [Internet]. World Health Organization; 2021 [cited 2024 Jun 3]. Available from: <https://www.who.int/publications/i/item/9789240010352>
 174. Buddenberg SK, Tracey A, Berger DJ, Lu Z, Doyle SR, Fu B, et al. Assembled chromosomes of the blood fluke *Schistosoma mansoni* provide insight into the evolution of its ZW sex-determination system [Internet]. *bioRxiv*. bioRxiv; 2021. Available from: <http://biorxiv.org/lookup/doi/10.1101/2021.08.13.456314>
 175. Buddenberg SK, Lu Z, Sankaranarayanan G, Doyle SR, Berriman M. The stage- and sex-specific transcriptome of the human parasite *Schistosoma mansoni*. *Sci Data*. 2023 Nov 7;10(1):775.
 176. Le Clec'h W, Chevalier FD, McDew-White M, Allan F, Webster BL, Gouvras AN, et al. Whole genome amplification and exome sequencing of archived schistosome miracidia. *Parasitology*. 2018 Nov;145(13):1739–47.
 177. Doyle SR, Sankaranarayanan G, Allan F, Berger D, Jimenez Castro PD, Collins JB, et al. Evaluation of DNA extraction methods on individual helminth egg and larval stages for whole-genome sequencing. *Front Genet*. 2019 Sep 20;10:826.
 178. Platt RN, McDew-White M, Le Clec'h W, Chevalier FD, Allan F, Emery AM, et al. Ancient Hybridization and Adaptive Introgression of an Invadolysin Gene in Schistosome Parasites. *Mol Biol Evol*. 2019 Oct 1;36(10):2127–42.
 179. Gawad C, Koh W, Quake SR. Single-cell genome sequencing: current state of the science. *Nat Rev Genet*. 2016 Mar;17(3):175–88.
 180. Ellis P, Moore L, Sanders MA, Butler TM, Brunner SF, Lee-Six H, et al. Reliable detection of somatic mutations in solid tissues by laser-capture microdissection and low-input DNA sequencing. *Nat Protoc*. 2020 Dec 14;16(2):841–71.
 181. Pitchford RJ, Visser PS. A simple and rapid technique for quantitative estimation of helminth eggs in human and animal excreta with special reference to *Schistosoma* sp. *Trans R Soc Trop Med Hyg*. 1975;69(3):318–22.
 182. Gower CM, Shrivastava J, Lamberton PHL, Rollinson D, Webster BL, Emery A, et al. Development and application of an ethically and epidemiologically advantageous assay for the multi-locus microsatellite analysis of *Schistosoma mansoni*. *Parasitology*. 2007 Apr;134(Pt 4):523–36.
 183. Moore L, Leongamornlert D, Coorens THH, Sanders MA, Ellis P, Dentro SC, et al. The mutational landscape of normal human endometrial epithelium. *Nature*. 2020 Apr 22;580(7805):640–6.
 184. Lee-Six H, Olafsson S, Ellis P, Osborne RJ, Sanders MA, Moore L, et al. The landscape of somatic mutation in normal colorectal epithelial cells. *Nature*. 2019 Oct 23;574(7779):532–7.
 185. McIntyre J, Morrison A, Maitland K, Berger D, Price DRG, Dougan S, et al. Chromosomal genome assembly resolves drug resistance loci in the parasitic nematode *Teladorsagia circumcincta* [Internet]. *bioRxiv*. 2024 [cited 2024 Aug 11]. p.

2024.07.22.603261. Available from:
<https://www.biorxiv.org/content/10.1101/2024.07.22.603261v1>

186. Howe KL, Bolt BJ, Cain S, Chan J, Chen WJ, Davis P, et al. WormBase 2016: expanding to enable helminth genomic research. *Nucleic Acids Res.* 2016 Jan 4;44(D1):D774–80.
187. Howe KL, Bolt BJ, Shafie M, Kersey P, Berriman M. WormBase ParaSite - a comprehensive resource for helminth genomics. *Mol Biochem Parasitol.* 2017 Jul;215:2–10.
188. Tarasov A, Vilella AJ, Cuppen E, Nijman IJ, Prins P. Sambamba: fast processing of NGS alignment formats. *Bioinformatics.* 2015 Jun 15;31(12):2032–4.
189. Barnett DW, Garrison EK, Quinlan AR, Strömberg MP, Marth GT. BamTools: a C++ API and toolkit for analyzing and managing BAM files. *Bioinformatics.* 2011 Jun 15;27(12):1691–2.
190. Quinlan AR, Hall IM. BEDTools: a flexible suite of utilities for comparing genomic features. *Bioinformatics.* 2010 Mar 15;26(6):841–2.
191. Li H, Handsaker B, Wysoker A, Fennell T, Ruan J, Homer N, et al. The Sequence Alignment/Map format and SAMtools. *Bioinformatics.* 2009 Aug 15;25(16):2078–9.
192. Wood DE, Lu J, Langmead B. Improved metagenomic analysis with Kraken 2. *Genome Biol.* 2019 Nov 28;20(1):257.
193. Ewels P, Magnusson M, Lundin S, Käller M. MultiQC: summarize analysis results for multiple tools and samples in a single report. *Bioinformatics.* 2016 Oct 1;32(19):3047–8.
194. Wickham H, Averick M, Bryan J, Chang W, McGowan L, François R, et al. Welcome to the tidyverse. *J Open Source Softw.* 2019 Nov 21;4(43):1686.
195. Csardi G NT. The igraph software package for complex network research. *InterJournal.* 2006;Complex Systems:1695.
196. Minh BQ, Schmidt HA, Chernomor O, Schrempf D, Woodhams MD, von Haeseler A, et al. IQ-TREE 2: New Models and Efficient Methods for Phylogenetic Inference in the Genomic Era. *Mol Biol Evol.* 2020 Feb 3;37(5):1530–4.
197. Letunic I, Bork P. Interactive Tree of Life (iTOL) v6: recent updates to the phylogenetic tree display and annotation tool. *Nucleic Acids Res.* 2024 Apr 13;52(W1):W78–82.
198. Korunes KL, Samuk K. pixy: Unbiased estimation of nucleotide diversity and divergence in the presence of missing data. *Mol Ecol Resour.* 2021 May;21(4):1359–68.
199. Alexander DH, Novembre J, Lange K. Fast model-based estimation of ancestry in unrelated individuals. *Genome Res.* 2009 Sep;19(9):1655–64.
200. Buddenborg SK, Tracey A, Berger DJ, Lu Z, Doyle SR, Fu B, et al. Assembled chromosomes of the blood fluke *Schistosoma mansoni* provide insight into the evolution of its ZW sex-determination system. *bioRxiv [Internet].* 2021; Available from: <https://www.biorxiv.org/content/10.1101/2021.08.13.456314.abstract>
201. Brann T, Beltramini A, Chaparro C, Berriman M, Doyle SR, Protasio AV. Subtelomeric plasticity contributes to gene family expansion in the human parasitic flatworm *Schistosoma mansoni*. *BMC Genomics.* 2024 Feb 27;25(1):217.

202. Rowel C, Fred B, Betson M, Sousa-Figueiredo JC, Kabatereine NB, Stothard JR. Environmental epidemiology of intestinal schistosomiasis in Uganda: population dynamics of *Biomphalaria* (gastropoda: planorbidae) in Lake Albert and Lake Victoria with observations on natural infections with digenetic trematodes. *Biomed Res Int*. 2015 Feb 1;2015:717261.
203. Andrus PS, Stothard JR, Wade CM. Seasonal patterns of *Schistosoma mansoni* infection within *Biomphalaria* snails at the Ugandan shorelines of Lake Albert and Lake Victoria. *PLoS Negl Trop Dis*. 2023 Aug;17(8):e0011506.
204. Adriko M, Standley CJ, Tinkitina B, Mwesigwa G, Kristensen TK, Stothard JR, et al. Compatibility of Ugandan *Schistosoma mansoni* isolates with *Biomphalaria* snail species from Lake Albert and Lake Victoria. *Acta Trop*. 2013 Nov;128(2):303–8.
205. Kazibwe F, Makanga B, Rubaire-Akiiki C, Ouma J, Kariuki C, Kabatereine NB, et al. Ecology of *Biomphalaria* (Gastropoda: Planorbidae) in Lake Albert, Western Uganda: snail distributions, infection with schistosomes and temporal associations with environmental dynamics. *Hydrobiologia*. 2006 Sep;568(1):433–44.
206. Crellen T, Walker M, Lamberton PHL, Kabatereine NB, Tukahebwa EM, Cotton JA, et al. Reduced efficacy of praziquantel against *Schistosoma mansoni* is associated with multiple rounds of mass drug administration. *Clin Infect Dis*. 2016 Nov 1;63(9):1151–9.
207. Anderson RM. Determinants of infection in human schistosomiasis. *Baillière's clinical tropical medicine and communicable diseases*. 1987;2(2):279–300.
208. Lichtenberg F, Rollinson D, Simpson A. Consequences of infections with schistosomes. 1987;185–232.
209. Catalano S, Léger E, Fall CB, Borlase A, Diop SD, Berger D, et al. Multihost transmission of *Schistosoma mansoni* in Senegal, 2015–2018. *Emerg Infect Dis*. 2020 Jun;26(6):1234–42.
210. Agola LE, Mburu DN, DeJong RJ, Mungai BN, Muluvi GM, Njagi ENM, et al. Microsatellite typing reveals strong genetic structure of *Schistosoma mansoni* from localities in Kenya. *Infect Genet Evol*. 2006 Nov;6(6):484–90.
211. Monrad J, Christensen NO, Nansen P, Johansen MV, Lindberg R. Acquired resistance against *Schistosoma bovis* after single or repeated low-level primary infections in goats. *Res Vet Sci*. 1995 Jan;58(1):42–5.
212. Theron A, Sire C, Rognon A, Prugnolle F, Durand P. Molecular ecology of *Schistosoma mansoni* transmission inferred from the genetic composition of larval and adult infrapopulations within intermediate and definitive hosts. *Parasitology*. 2004 Nov;129(Pt 5):571–85.
213. Bradley DJ, Sturrock RF, Williams PN. The circumstantial epidemiology of *Schistosoma haematobium* in Lango district, Uganda. *East Afr Med J*. 1967 May;44(5):193–204.
214. Haldar K, Bhattacharjee S, Safeukui I. Drug resistance in *Plasmodium*. *Nat Rev Microbiol*. 2018 Mar;16(3):156–70.
215. Wolstenholme AJ, Fairweather I, Prichard R, von Samson-Himmelstjerna G, Sangster NC. Drug resistance in veterinary helminths. *Trends Parasitol*. 2004 Oct;20(10):469–76.
216. Kaplan RM, Vidyashankar AN. An inconvenient truth: global worming and anthelmintic

- resistance. *Vet Parasitol.* 2012 May 4;186(1-2):70–8.
217. Doyle SR, Laing R, Bartley D, Morrison A, Holroyd N, Maitland K, et al. Genomic landscape of drug response reveals mediators of anthelmintic resistance. *Cell Rep.* 2022 Oct 18;41(3):111522.
218. Montresor A, Mupfasoni D, Mikhailov A, Mwinzi P, Lucianez A, Jamsheed M, et al. The global progress of soil-transmitted helminthiasis control in 2020 and World Health Organization targets for 2030. *PLoS Negl Trop Dis.* 2020 Aug;14(8):e0008505.
219. Kabatereine NB, Tukahebwa E, Kazibwe F, Namwangye H, Zaramba S, Brooker S, et al. Progress towards countrywide control of schistosomiasis and soil-transmitted helminthiasis in Uganda. *Trans R Soc Trop Med Hyg.* 2006 Mar;100(3):208–15.
220. Fleming FM, Fenwick A, Tukahebwa EM, Lubanga RGN, Namwangye H, Zaramba S, et al. Process evaluation of schistosomiasis control in Uganda, 2003 to 2006: perceptions, attitudes and constraints of a national programme. *Parasitology.* 2009 Nov;136(13):1759–69.
221. Norton AJ, Gower CM, Lamberton PHL, Webster BL, Lwambo NJS, Blair L, et al. Genetic consequences of mass human chemotherapy for *Schistosoma mansoni*: population structure pre- and post-praziquantel treatment in Tanzania. *Am J Trop Med Hyg.* 2010 Oct 10;83(4):951–7.
222. Gryseels B, Mbaye A, De Vlas SJ, Stelma FF, Guissé F, Van Lieshout L, et al. Are poor responses to praziquantel for the treatment of *Schistosoma mansoni* infections in Senegal due to resistance? An overview of the evidence. *Trop Med Int Health.* 2001 Nov;6(11):864–73.
223. Ismail M, Metwally A, Farghaly A, Bruce J, Tao LF, Bennett JL. Characterization of isolates of *Schistosoma mansoni* from Egyptian villagers that tolerate high doses of praziquantel. *Am J Trop Med Hyg.* 1996 Aug;55(2):214–8.
224. Melman SD, Steinauer ML, Cunningham C, Kubatko LS, Mwangi IN, Wynn NB, et al. Reduced susceptibility to praziquantel among naturally occurring Kenyan isolates of *Schistosoma mansoni*. *PLoS Negl Trop Dis.* 2009 Aug 18;3(8):e504.
225. Fallon PG, Doenhoff MJ. Drug-resistant schistosomiasis: resistance to praziquantel and oxamniquine induced in *Schistosoma mansoni* in mice is drug specific. *Am J Trop Med Hyg.* 1994 Jul;51(1):83–8.
226. Ismail MM, Taha SA, Farghaly AM, el-Azony AS. Laboratory induced resistance to praziquantel in experimental schistosomiasis. *J Egypt Soc Parasitol.* 1994 Dec;24(3):685–95.
227. Le Clec'h W, Chevalier FD, Mattos ACA, Strickland A, Diaz R, McDew-White M, et al. Genetic analysis of praziquantel response in schistosome parasites implicates a transient receptor potential channel. *Sci Transl Med.* 2021 Dec 22;13(625):eabj9114.
228. Park SK, Friedrich L, Yahya NA, Rohr CM, Chulkov EG, Maillard D, et al. Mechanism of praziquantel action at a parasitic flatworm ion channel. *Sci Transl Med.* 2021 Dec 22;13(625):eabj5832.
229. Chevalier FD, Le Clec'h W, Berriman M, Anderson TJC. A single locus determines praziquantel response in *Schistosoma mansoni*. *Antimicrob Agents Chemother.* 2024 Mar 6;68(3):e0143223.

230. Chibwana FD, Tumwebaze I, Mahulu A, Sands AF, Albrecht C. Assessing the diversity and distribution of potential intermediate hosts snails for urogenital schistosomiasis: *Bulinus* spp. (Gastropoda: Planorbidae) of Lake Victoria. *Parasit Vectors*. 2020 Aug 14;13(1):418.
231. Cotton JA, Doyle SR. A genetic TRP down the channel to praziquantel resistance. *Trends Parasitol*. 2022 May;38(5):351–2.
232. Manichaikul A, Mychaleckyj JC, Rich SS, Daly K, Sale M, Chen WM. Robust relationship inference in genome-wide association studies. *Bioinformatics*. 2010 Oct 5;26(22):2867–73.
233. Campos M, Phelan J, Spadar A, Collins E, Gonçalves A, Pelloquin B, et al. High-throughput barcoding method for the genetic surveillance of insecticide resistance and species identification in *Anopheles gambiae* complex malaria vectors. *Sci Rep*. 2022 Aug 16;12(1):1–11.
234. Bolger AM, Lohse M, Usadel B. Trimmomatic: a flexible trimmer for Illumina sequence data. *Bioinformatics*. 2014 Aug 1;30(15):2114–20.
235. Faust CL, Crotti M, Moses A, Oguttu D, Wamboko A, Adriko M, et al. Two-year longitudinal survey reveals high genetic diversity of *Schistosoma mansoni* with adult worms surviving praziquantel treatment at the start of mass drug administration in Uganda. *Parasit Vectors*. 2019 Dec 27;12(1):607.
236. Aemero M, Boissier J, Climent D, Moné H, Mouahid G, Berhe N, et al. Genetic diversity, multiplicity of infection and population structure of *Schistosoma mansoni* isolates from human hosts in Ethiopia. *BMC Genet*. 2015 Dec 3;16(1):137.
237. Gower CM, Gehre F, Marques SR, Lamberton PHL, Lwambo NJ, Webster JP. Phenotypic and genotypic monitoring of *Schistosoma mansoni* in Tanzanian schoolchildren five years into a preventative chemotherapy national control programme. *Parasit Vectors*. 2017 Dec 2;10(1):593.
238. Steinauer ML, Christie MR, Blouin MS, Agola LE, Mwangi IN, Maina GM, et al. Non-invasive sampling of schistosomes from humans requires correcting for family structure. *PLoS Negl Trop Dis*. 2013 Sep 19;7(9):e2456.
239. Gower CM, Gabrielli AF, Sacko M, Dembelé R, Golan R, Emery AM, et al. Population genetics of *Schistosoma haematobium*: development of novel microsatellite markers and their application to schistosomiasis control in Mali. *Parasitology*. 2011 Jul;138(8):978–94.
240. Neves MI, Webster JP, Walker M. Estimating helminth burdens using sibship reconstruction. *Parasit Vectors*. 2019 Sep 16;12(1):441.
241. Kohn AB, Anderson PA, Roberts-Misterly JM, Greenberg RM. Schistosome calcium channel beta subunits. Unusual modulatory effects and potential role in the action of the antischistosomal drug praziquantel. *J Biol Chem*. 2001 Oct 5;276(40):36873–6.
242. Greenberg RM. Are Ca²⁺ channels targets of praziquantel action? *Int J Parasitol*. 2005 Jan;35(1):1–9.
243. Pica-Mattoccia L, Valle C, Basso A, Troiani AR, Vigorosi F, Liberti P, et al. Cytochalasin D abolishes the schistosomicidal activity of praziquantel. *Exp Parasitol*. 2007 Apr 1;115(4):344–51.

244. Nogi T, Zhang D, Chan JD, Marchant JS. A novel biological activity of praziquantel requiring voltage-operated Ca²⁺ channel beta subunits: subversion of flatworm regenerative polarity. *PLoS Negl Trop Dis*. 2009 Jun 23;3(6):e464.
245. Kohn AB, Roberts-Misterly JM, Anderson PAV, Khan N, Greenberg RM. Specific sites in the Beta Interaction Domain of a schistosome Ca²⁺ channel beta subunit are key to its role in sensitivity to the anti-schistosomal drug praziquantel. *Parasitology*. 2003 Oct;127(Pt 4):349–56.
246. Valle C, Troiani AR, Festucci A, Pica-Mattoccia L, Liberti P, Wolstenholme A, et al. Sequence and level of endogenous expression of calcium channel β subunits in *Schistosoma mansoni* displaying different susceptibilities to praziquantel. *Mol Biochem Parasitol*. 2003 Aug 31;130(2):111–5.
247. Chan JD, Cupit PM, Gunaratne GS, McCorvy JD, Yang Y, Stoltz K, et al. The anthelmintic praziquantel is a human serotonergic G-protein-coupled receptor ligand. *Nat Commun*. 2017 Dec 5;8(1):1910.
248. Blanton RE, Blank WA, Costa JM, Carmo TM, Reis EA, Silva LK, et al. *Schistosoma mansoni* population structure and persistence after praziquantel treatment in two villages of Bahia, Brazil. *Int J Parasitol*. 2011 Aug 15;41(10):1093–9.
249. Lelo AE, Mburu DN, Magoma GN, Mungai BN, Kihara JH, Mwangi IN, et al. No apparent reduction in schistosome burden or genetic diversity following four years of school-based mass drug administration in mwea, central kenya, a heavy transmission area. *PLoS Negl Trop Dis*. 2014 Oct;8(10):e3221.
250. French MD, Churcher TS, Basáñez MG, Norton AJ, Lwambo NJS, Webster JP. Reductions in genetic diversity of *Schistosoma mansoni* populations under chemotherapeutic pressure: the effect of sampling approach and parasite population definition. *Acta Trop*. 2013 Nov;128(2):196–205.
251. Marchant J. TRP Tracker [Internet]. [cited 2024 Sep 18]. Available from: <https://www.trptracker.live/>
252. Rohr CM, Sprague DJ, Park SK, Malcolm NJ, Marchant JS. Natural variation in the binding pocket of a parasitic flatworm TRPM channel resolves the basis for praziquantel sensitivity. *Proc Natl Acad Sci U S A*. 2023 Jan 3;120(1):e2217732120.
253. Marchant JS. Progress interrogating TRPMPZQ as the target of praziquantel. *PLoS Negl Trop Dis*. 2024 Feb;18(2):e0011929.
254. Gardner JMF, Mansour NR, Bell AS, Helmbly H, Bickle Q. The discovery of a novel series of compounds with single-dose efficacy against juvenile and adult *Schistosoma* species. *PLoS Negl Trop Dis*. 2021 Jul;15(7):e0009490.
255. Moss S, Mańko E, Vasileva H, Da Silva ET, Goncalves A, Osborne A, et al. Population dynamics and drug resistance mutations in *Plasmodium falciparum* on the Bijagós Archipelago, Guinea-Bissau. *Sci Rep*. 2023 Apr 18;13(1):6311.
256. Anopheles gambiae 1000 Genomes Consortium, Data analysis group, Partner working group, Sample collections-Angola:, Burkina Faso:, Cameroon:, et al. Genetic diversity of the African malaria vector *Anopheles gambiae*. *Nature*. 2017 Dec 7;552(7683):96–100.
257. Phelan JE, O’Sullivan DM, Machado D, Ramos J, Oppong YEA, Campino S, et al. Integrating informatics tools and portable sequencing technology for rapid detection of

resistance to anti-tuberculous drugs. *Genome Med.* 2019 Jun 24;11(1):41.